1996-03

A water tunnel investigation of the influence of Reynolds number on the high-incidence flow over double-delta wings

Fritzelas, Anastasios E.

Monterey, California. Naval Postgraduate School

NAVAL POSTGRADUATE SCHOOL
Monterey, California

THESIS

A WATER TUNNEL INVESTIGATION OF THE INFLUENCE OF REYNOLDS NUMBER ON THE HIGH-INCIDENCE FLOW OVER DOUBLE-DELTA WINGS

by

Anastasios E. Fritzelas

March 1996

Thesis Advisor: M.F. Platzer

Approved for public release; distribution is unlimited.

DISCLAIMER NOTICE

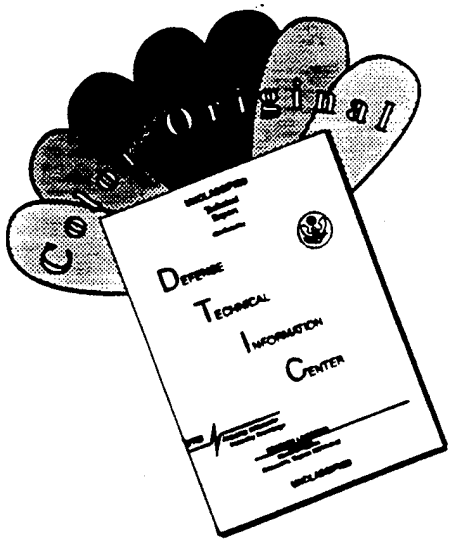

THIS DOCUMENT IS BEST QUALITY AVAILABLE. THE COPY FURNISHED TO DTIC CONTAINED A SIGNIFICANT NUMBER OF COLOR PAGES WHICH DO NOT REPRODUCE LEGIBLY ON BLACK AND WHITE MICROFICHE.

REPORT DOCUMENTATION PAGE		Form Approved OMB No. 0704

1. AGENCY USE ONLY *(Leave blank)*	2. REPORT DATE March 1996	3. REPORT TYPE AND DATES COVERED Master's Thesis

4. TITLE AND SUBTITLE : A WATER TUNNEL INVESTIGATION OF THE INFLUENCE OF REYNOLDS NUMBER ON THE HIGH-INCIDENCE FLOW OVER DOUBLE-DELTA WINGS	5. FUNDING NUMBERS
6. AUTHOR: Anastasios E. Fritzelas	
7. PERFORMING ORGANIZATION NAME(S) AND ADDRESS(ES) Naval Postgraduate School Monterey CA 93943-5000	8. PERFORMING ORGANIZATION REPORT NUMBER
9. SPONSORING/MONITORING AGENCY NAME(S) AND ADDRESS(ES)	10. SPONSORING/MONITORING AGENCY REPORT NUMBER

11. SUPPLEMENTARY NOTES The views expressed in this thesis are those of the author and do not reflect the official policy or position of the Department of Defense or the U.S. Government.

12a. DISTRIBUTION/AVAILABILITY STATEMENT Approved for public release; distribution unlimited.	12b. DISTRIBUTION CODE

13. ABSTRACT *(maximum 200 words)* : There are several disagreements in the published literature on vortex interaction and bursting data obtained in various wind and water tunnel tests of double-delta wings at high angle of attack (AOA). Therefore a test program was carried out in the Naval Postgraduate School water tunnel using a 76/40 deg. baseline double-delta wing model to investigate the effect of Reynolds number.The program consisted of : (i) Flow visualisation studies at tunnel speeds of 0,2-0,6 and 1,0 ft/sec in the 0-30 deg. AOA range to determine the influence of flow Reynolds number on vortex trajectory/interaction and breakdown , (ii) Laser Doppler Velocimetry studies of the flowfield to gain a better understanding of the vortex structure and verify the flow visualisation results . Comparison of the test results at these tunnel speeds (corresponding to nominal flow Reynolds number of 15,000, 45,000, and 75,000 indicates a change in the vortical flowfield structure. The strake and wing vortices do not coil up and the breakdown occurs earlier as the tunnel speed is increased.The trends in the interaction and bursting data at higher tunnel speeds appear to be in better agreement with previous wind tunnel data.

14. SUBJECT TERMS REYNOLDS NUMBER EFFECTS ON VORTICAL FLOW OVER DOUBLE-DELTA WINGS			15. NUMBER OF PAGES 202
			16. PRICE CODE
17. SECURITY CLASSIFICATION OF REPORT Unclassified	18. SECURITY CLASSIFICATION OF THIS PAGE Unclassified	19. SECURITY CLASSIFICATION OF ABSTRACT Unclassified	20. LIMITATION OF ABSTRACT UL

NSN 7540-01-280-5500
Prescribed by ANSI Std. 239-18

Standard Form 298 (Rev. 2-89)

Approved for public release; distribution is unlimited.

A WATER TUNNEL INVESTIGATION OF THE INFLUENCE OF REYNOLDS NUMBER ON THE HIGH-INCIDENCE FLOW OVER DOUBLE-DELTA WINGS

Anastasios E. Fritzelas
Lieutenant, Hellenic Navy
B.S., Hellenic Naval Academy, 1986

Submitted in partial fulfillment
of the requirements for the degree of

MASTER OF SCIENCE IN AERONAUTICAL ENGINEERING

from the

NAVAL POSTGRADUATE SCHOOL
March 1996

Author: 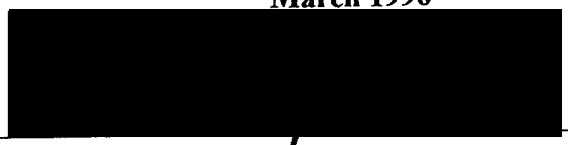
Anastasios E. Fritzelas

Approved by: 
M.F. Platzer, Thesis Advisor


S.K. Hebbar, Second Reader


D. Collins, Chairman
Department of Aeronautics and Astronautics

ABSTRACT

There are several disagreements in the published literature on vortex interaction and bursting data obtained in various wind and water tunnel tests of double-delta wings at high angle of attack (AOA).Therefore a test program was carried out in the Naval Postgraduate School water tunnel using a 76/40 deg. baseline double - delta wing model to investigate the effect of Reynolds number.The program consisted of : (i) Flow visualisation studies at tunnel speeds of 0.2, 0.6 and 1.0 ft/sec in the 0-30 deg. AOA range to determine the influence of flow Reynolds number on vortex trajectory/interaction and breakdown. (ii) Laser Doppler Velocimetry studies of the flowfield to gain a better understanding of the vortex structure and verify the flow visualisation results.Comparison of the test results at these tunnel speeds (corresponding to nominal flow Reynolds number of 15,000, 45,000, and 75,000) indicates a change in the vortical flowfield structure.The strake and wing vortices do not coil up and the breakdown occurs earlier as the tunnel speed is increased.The trends in the interaction and bursting data at higher tunnel speeds appear to be in better agreement with previous wind tunnel data.

TABLE OF CONTENTS

ACKNOWLEDGMENT

This thesis was a part of a research program on double-delta wings supported by the NAWC, Warminster and by the Naval Postgraduate School.My gratitude goes to my thesis advisor M.F. Platzer, for his guidance, encouragement and patience throughout the course of this research.Also, thanks to professor S.K. Hebbar, who acted as co-advisor during the first quarter of this three quarter project, for his help and interest.

I would like also to thank the many people at the Naval Postgraduate School who provided the services and expertise necessary to accomplish this research, and helped me gain knowledge and experience in the Aeronautical Engineering field.

Finally, I would like to express my deepest gratitude and appreciation to my wife Konstantina, for her encouragement in support of my efforts.

I. INTRODUCTION

A. BACKGROUND

The first flight of a powered, heavier-than-air aircraft was, of course, made by Orville Wright on December 17, 1903. In the decades following this historic event, aircraft types of amazing variety were built in the continual quest for better fighting machines as well as transport vehicles.

Fighter aircraft usually reflect the latest in design refinements because they require high performance and maneuverability characteristics, such as speed in various flight conditions, rate of climb and ceiling, roll rate, turning radius and climb capability while in a turn, range and endurance.These desirable characteristics for a successful fighter aircraft have not changed very much over the years, although they have been more precisely defined.

A little more than a quarter of a century separated the endings of World Wars I and II. During this time, the maximum speed of propeller - driven fighter aircraft increased from 134 miles per hour for the SPAD-XIII to 437 miles per hour for the North-American P-51D [Ref. 1]. Integration of the jet engine resulted in a quantum increase in the capability and performance of fighter aircraft and by 1955 maximum speeds had reached 1,500 miles per hour.Further increases in the capability of jet fighters and their engines have continued to the present [Ref. 2], albeit at a slower pace than that which characterized the first 10 years following the end of World War II.

As jet propulsion opened the prospects of flight in the high-subsonic, transonic and supersonic regimes the classic shape of the early aircraft had to fundamentally alter.In 1936 Busemann in Germany first suggested the use of wing sweep.A variation on the swept wing

theme is the delta wing first proposed by Alexander Lippisch in the same period.This wing derives its name from the Greek letter Δ, which describes the planform shape.

First of the pioneer jet fighters was the German Messerschmitt " ME-262 ", which made its initial flight on March 25, 1942 and was the first aircraft that used an 18,5 deg. leading edge sweepback.Follow-on Messerschmitt fighter aircraft, including one with about 40 deg. of wing sweep were studied when termination of hostilities put an end to all German aircraft development.

After World War II, Mikoyan and Gurevich in the U.S.S.R. designed the first swept-wing fighter in 1946 (Fig.1).In the U.S. the first swept-wing subsonic jet fighter was the North American " F - 86 Sabre " (Fig . 2) which made its first flight on October 1, 1947.Both designs were based on captured German data.

In the 1950's further studies showed that delta wings have an additional advantage at high angles of attack where the leading edge vortex flows reduce pre-stall buffet levels and provide a more gradual loss of lift.Delta winged aircraft were designed by the U.S.S.R. " Mig - 21 ", Sweden " Saab - 210 ", France "Mirage - III " and the U.S. " Convair - XF 92 / F 102 ."

In the 1960's most of the new concepts had been explored, and the days of rapid design and construction of new prototypes were at an end, mostly because of the great complexity and associated high development cost of any new fighter.In the U.S. only three new fighters were produced the " Mc Donnell - F 4 " (Fig. 3), the " Northrop F-5 " and the " General Dynamics F-111 " (Fig. 4) which is the first production aircraft in the world to have a variable-sweep wing.

Contemporary designs such as the " Mc Donnell - Douglas F - 15 Eagle ", the " F - 18 Hornet " (Fig. 5), and the " General Dynamics F - 16 " (Fig. 6), use delta wing planforms. Therefore there is still interest in exploring the vortical flows over such planforms and how they

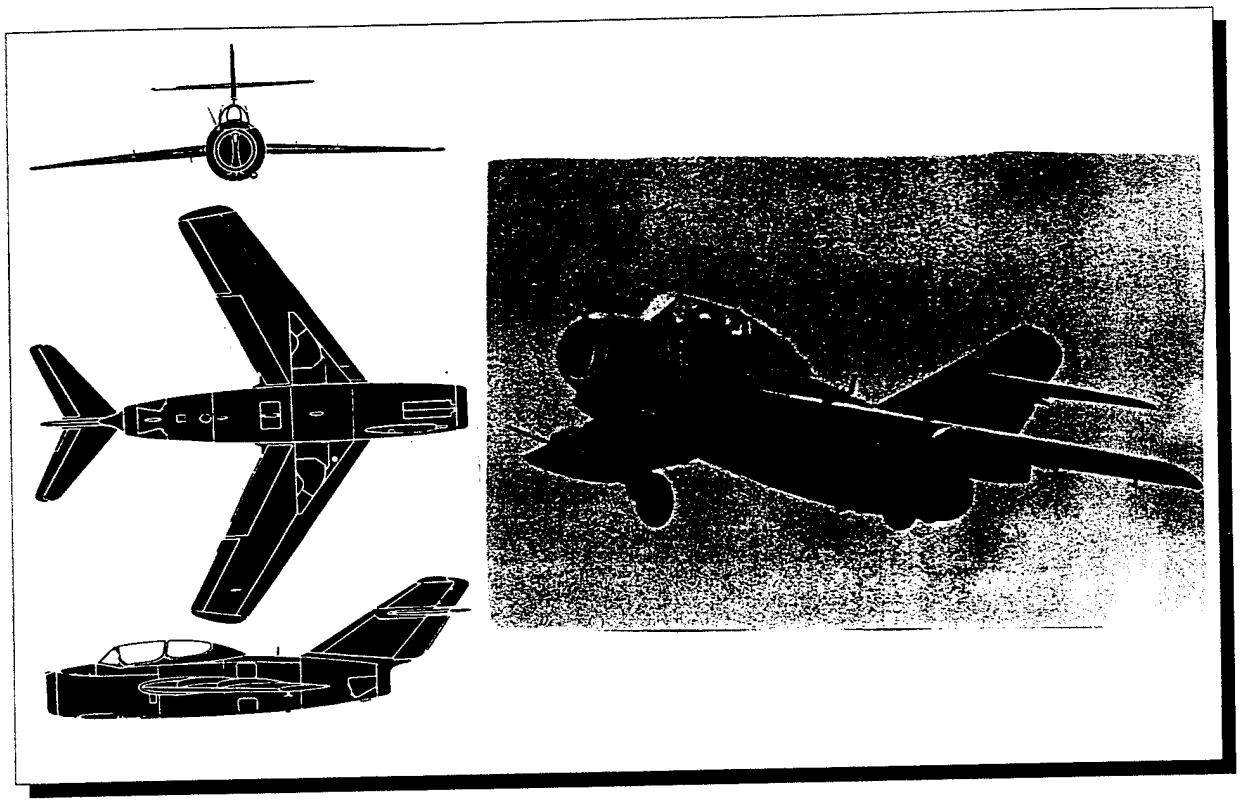

Fig. 1: Mikoyan - Gurevich Mig - 15 UTI

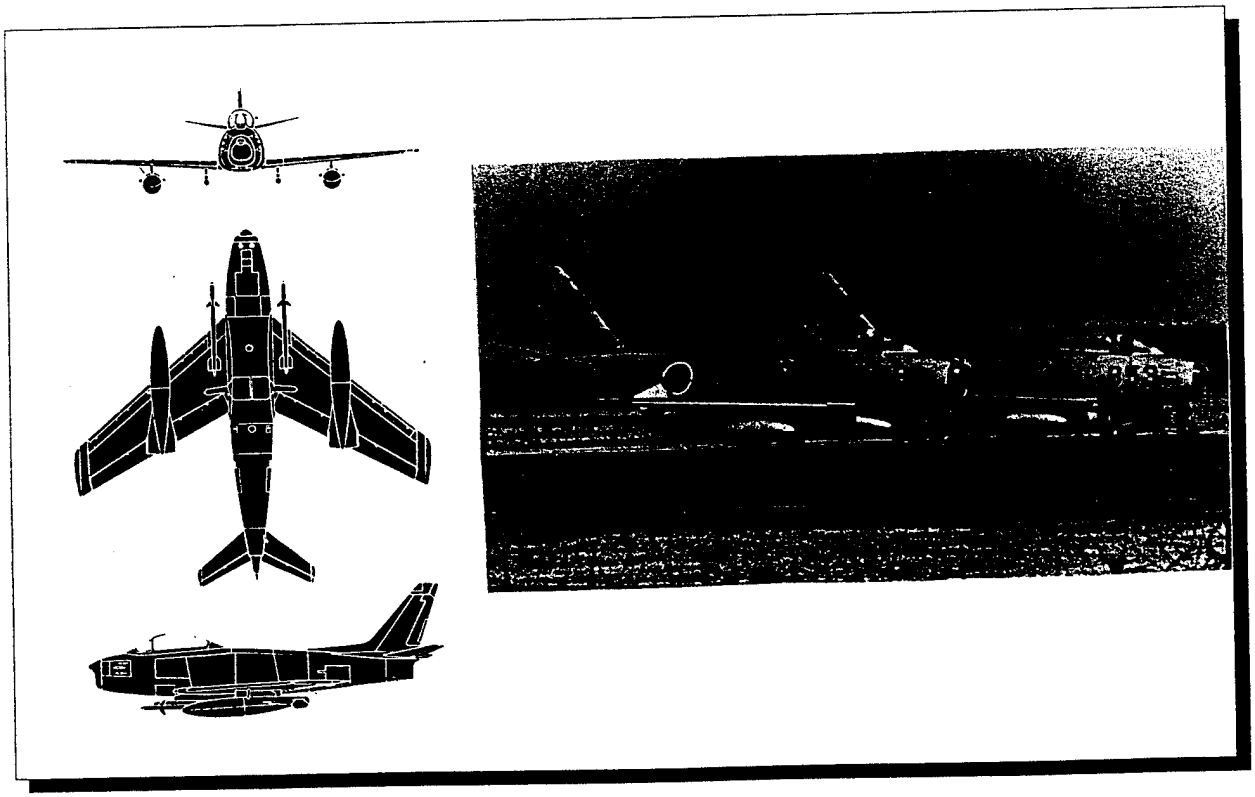

Fig. 2: North American F - 86 Sabre Midget

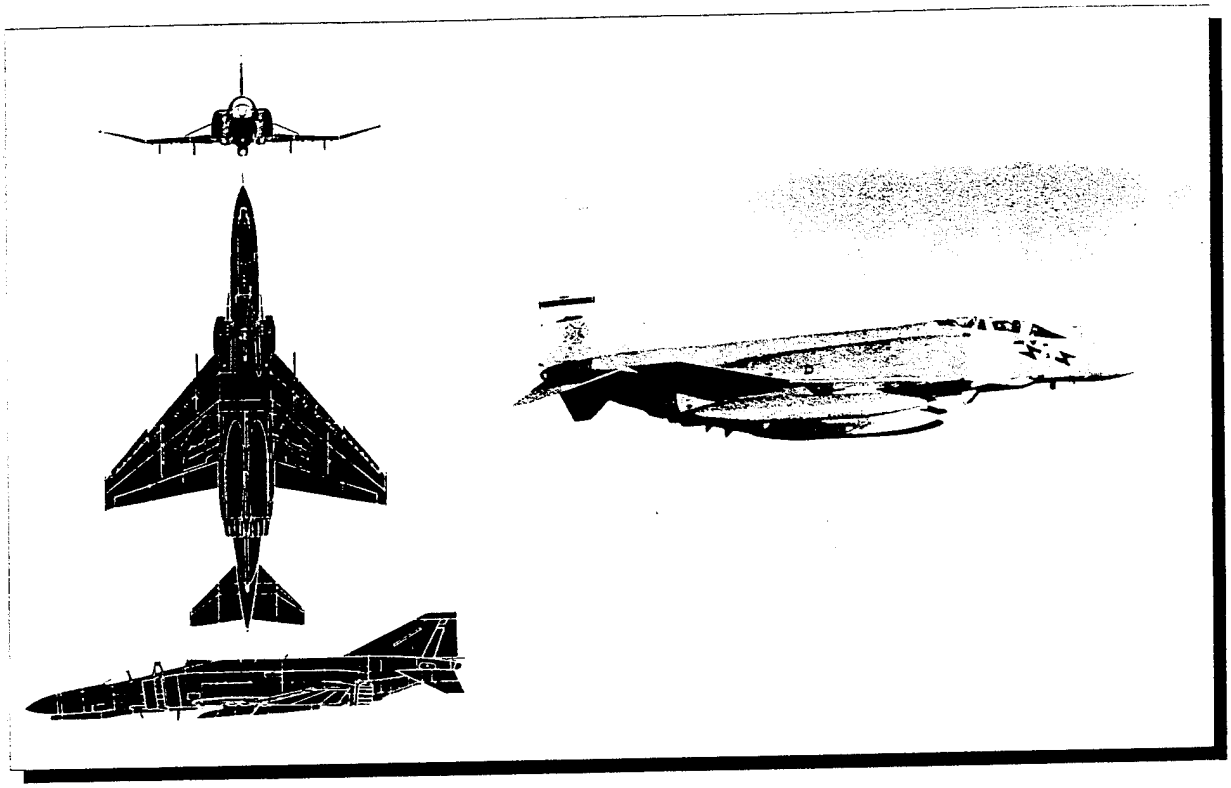

Fig. 3: McDonnell Douglas F - 4 Phantom II

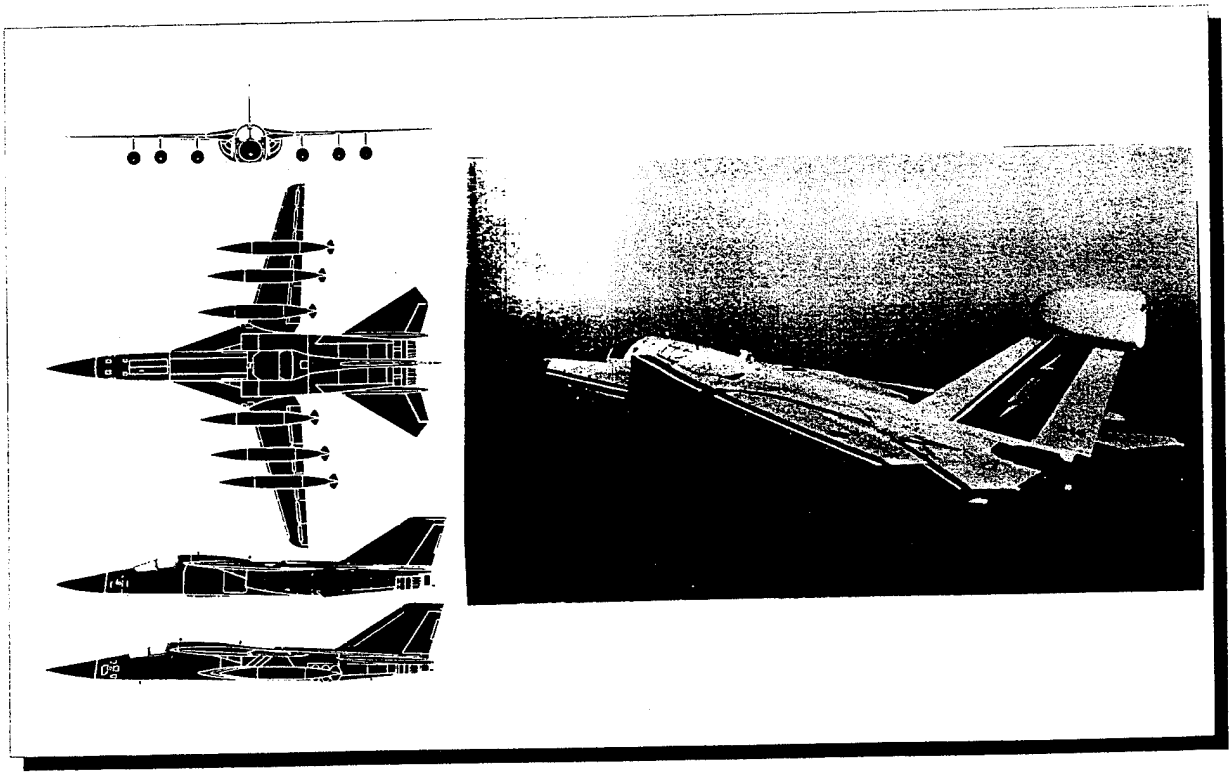

Fig. 4: General Dynamics F - 111

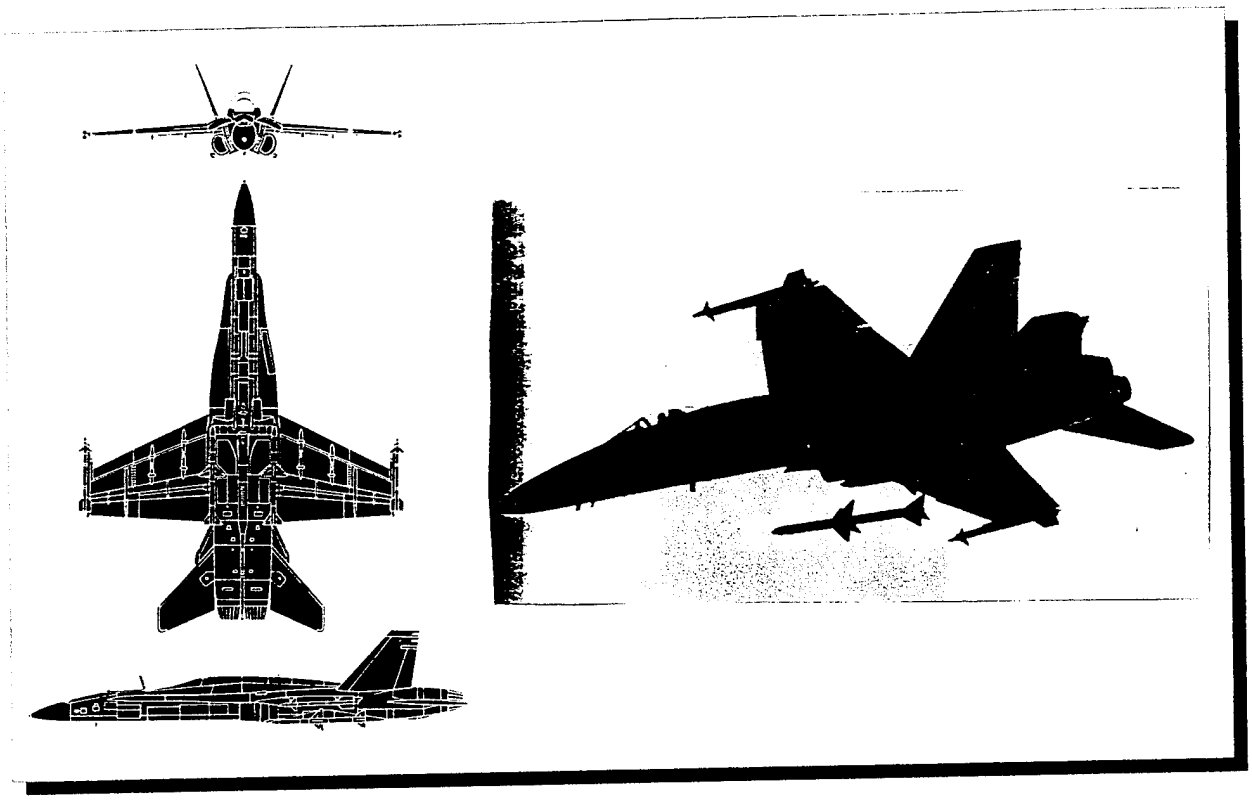

Fig. 5 McDonnell Douglas / Northrop F / A - 18 Hornet

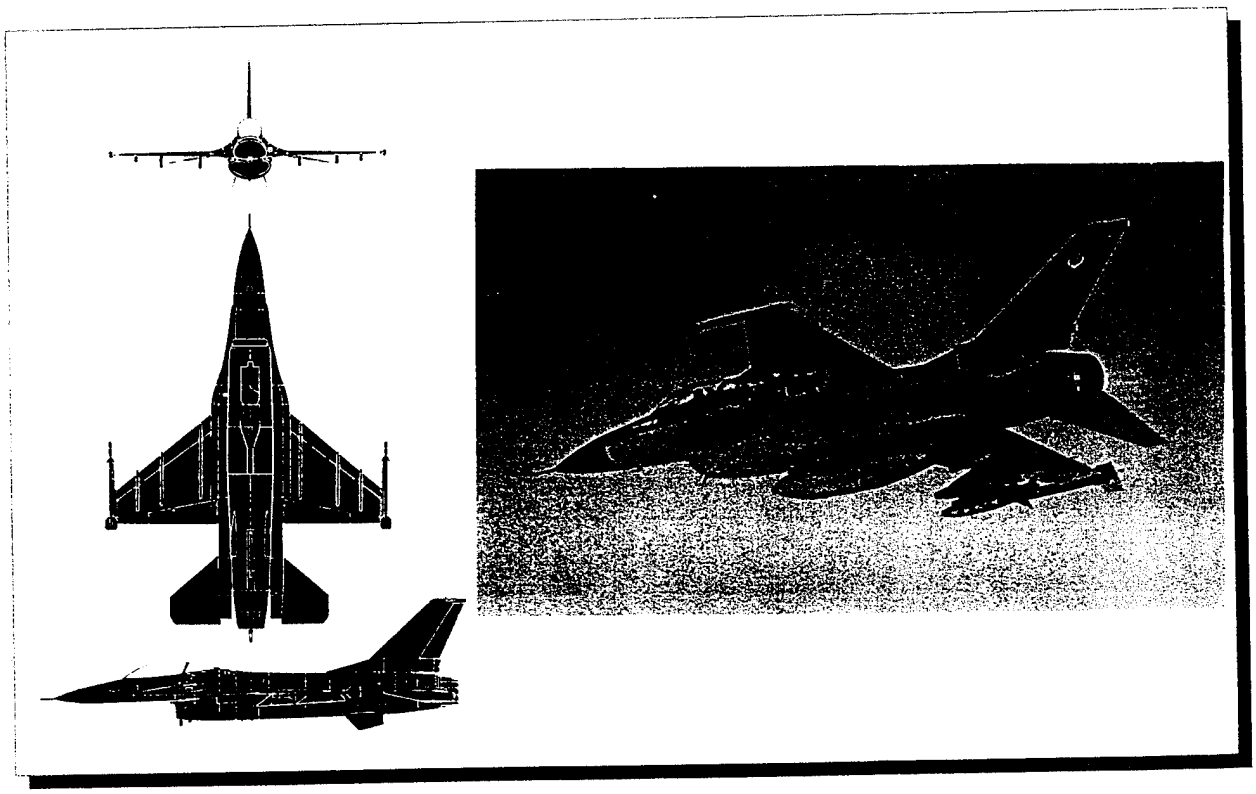

Fig. 6 General Dynamics F - 16 Fighting Falcon

can be controlled to provide additional lift and subsequently higher maneuverability at extremely high angles of attack.

B. AERODYNAMICS OF DELTA AND DOUBLE- DELTA WINGS

A primary purpose of the fighter aircraft is to destroy other aircraft, either in offensive or defensive modes of operation, or to pose such a compelling threat that enemy air operations are effectively curtailed.To perform its intended function, the fighter must be able to reach a favorable position for inflicting crippling damage on the enemy.Therefore fighter aircraft designers constantly try to increase the limits of the operating envelope.An important ingredient inherent in a successful fighter aircraft is the manner in which it handles.

Delta wing designs are characterized by the formation of leading edge vortex flows (Fig. 7) that reduce pre-stall buffet levels and provide a gradual loss of lift above the angle of attack for maximum lift coefficient.Disadvantages are the low wing loading and poor maneuverability at low speed flight [Ref. 3].

Modern designs have in addition a highly swept area ahead of the main wing called strake or leading edge extension (L E X).These are called double-delta wing configurations.

Most recently, increased interest in high angle of attack maneuvering called for providing and improving new concepts for vortex control.At high angles of attack, the flow does not attach to the wing surface.The maximum lift angle of attack for an airfoil is about 15 degrees, but a 70 degrees swept wing shows increasing lift to an angle of attack of 40 degrees [Ref. 4].This enhanced lift is primarily a result of the leading edge vortices of the delta wing.Generally, the vortex generated lift may be as much as 30 % of the total lift and becomes even more significant as angle of attack increases beyond the limits of a conventional wing [Ref. 5].

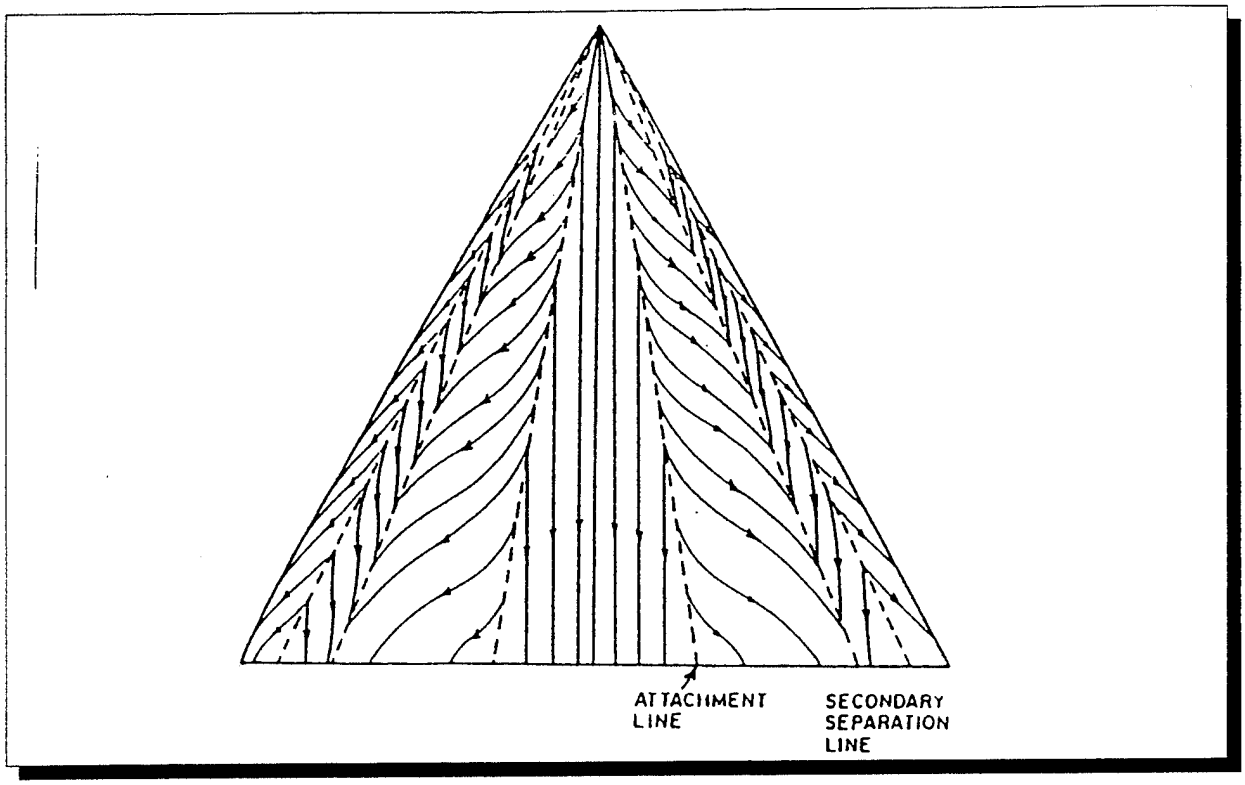

Fig. 7: Surface flow pattern over a single delta - wing

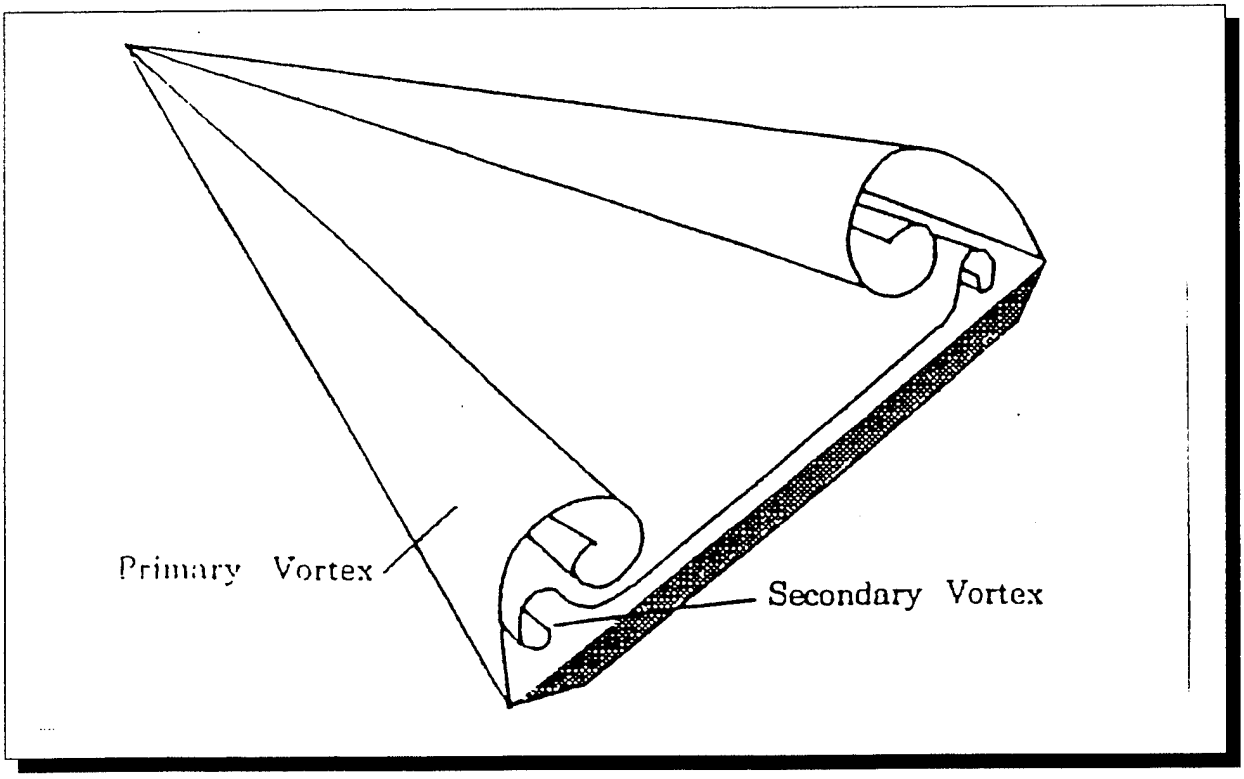

Fig. 8: Typical vortex structure over a delta wing at AOA

The aerodynamic phenomenon of a delta wing planform has been under study since the 1950's and basically can be described as the formation of two leading edge vortices, their development and subsequent breakdown (burst) [Ref. 6].These leading edge vortices are in general symmetric and are generated on wings with sweep angles greater than 45 degrees as the wing pitches up (Fig. 8) [Ref. 7].

At moderate angle of attack the flow attaches to the surface and then turns toward the swept leading edge.A primary vortex is generated and its size is on the order of the half span.It causes the flow over the upper surface to accelerate producing extra lift, called vortex lift.

At high angle of attack the core flow of the primary vortex suddenly stagnates and expands in size.This phenomenon is called vortex breakdown or bursting.The location of the burst point is influenced by the shape of the leading edge, wing sweep and angle of attack [Ref. 8].

The double-delta wing configuration is a particular strake and wing combination with geometric characteristics similar to a single delta wing.The leading edge of the wing has a discontinuity or kink at which the sweep angle changes abruptly to a lower angle.The flow pattern over a double-delta wing is more complicated than the flow over a single delta wing (Fig. 9).

The highly swept strake is an additional lifting surface above which a stable vortex is formed.This strake vortex persists over the wing and induces a strong outflow, which energizes the boundary layer on the upper surface of the wing and keeps it attached to a higher angle of attack than in the case of a wing without a strake.Therefore, strakes increase the lift efficiency of delta wings at high angles of attack.At the strake / wing leading edge kink or juncture, a wing vortex originates that increases in size and strength with distance downstream from the kink.The strake and wing vortices have the same direction of rotation and their trajectories entwine due to

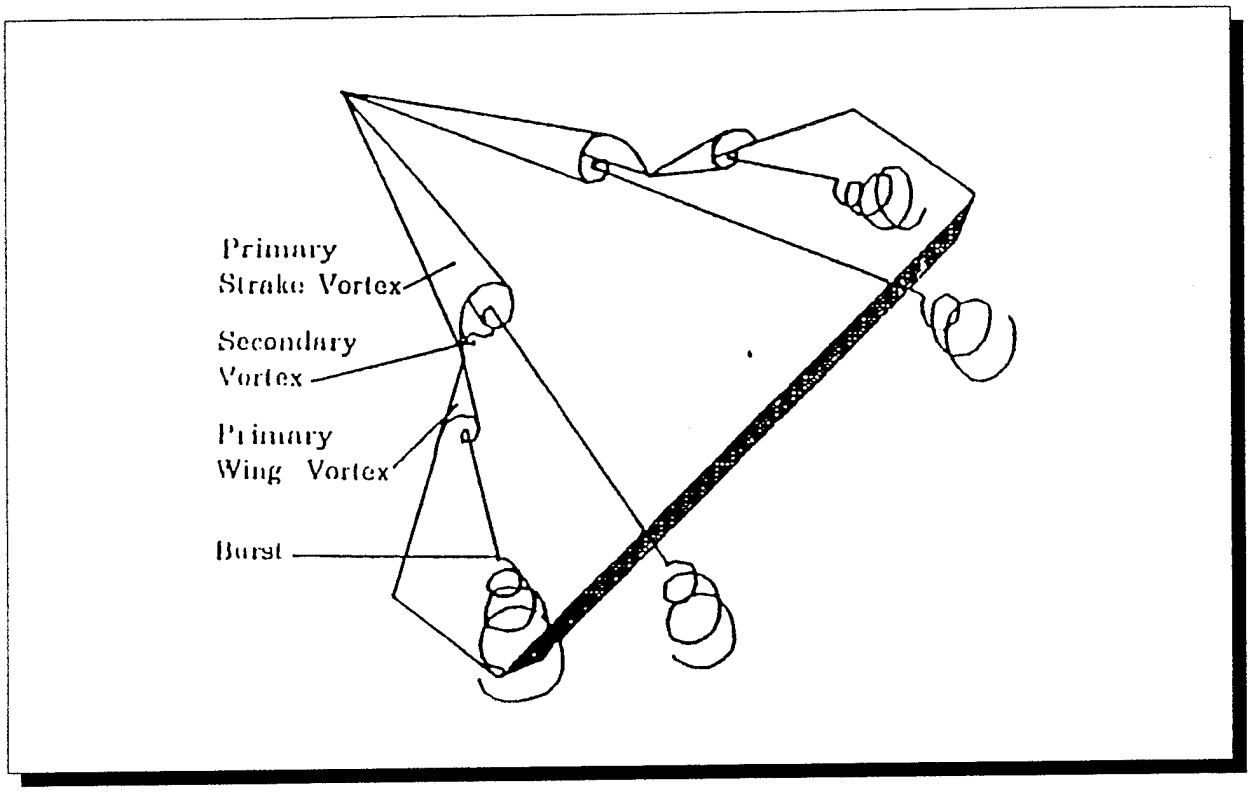

Fig. 9: Double-delta wing vortex burst phenomenon

interaction.A limit to these effects is reached once the angle of attack attains values where vortex breakdown occurs over the wing.

Experimental data on the structure of the subsonic flow over strake / wing configurations is available from several studies carried out in water and wind tunnels on models that are mostly double-delta wings.The results of these studies are used to validate numerical solutions.The experiments indicate that the interaction process and breakdown of the strake and wing vortices depend on the angle of attack, the shape of the leading edge cross section and the leading edge kink angle.The latter angle is the difference between the leading edge sweep of the strake and the leading edge sweep of the wing.In general, the cross-over point of the interacting strake and wing vortices moves upstream with increasing angle of attack and decreasing leading edge kink angle. The majority of the experimental and numerical studies were carried out on double-delta wings

with strake leading edge sweep angles between 76 and 80 degrees and wing sweep angles near 60 degrees.These sweep angle combinations are required for high speed aircraft configurations to achieve sufficient supersonic cruise performance.

C. MOTIVE OF THIS THESIS STUDY

For highly maneuverable aircraft, strake / wing configurations are employed which feature wing leading edge sweep angles less than 60 degrees to increase wing area and low speed performance.A 76 / 40 degrees planform is representative of such a type of aircraft [Ref. 7]. Experimental data for double-delta wings that have a 40 degrees swept wing are rather limited. Experimental studies by Brennenstuhl [Ref. 10], Graves [Ref. 11], Thompson [Ref. 12], and Verhaagen [Ref. 13] provide qualitative insight into the effect of the angle of attack on the crossflow structure, the interaction and breakdown of the strake and wing vortices, and the forces and moments.However, no surface pressures or flowfield data are presented in these references. The unsteady aerodynamics of a pitching double-delta wing were investigated by Cunnigham and Den Boer [Ref. 14], and more recently by Hebbar et al. [Ref. 15].As far as numerical solutions are concerned, solutions of the Navier-Stokes equations for the flow over a double-delta wing with a 40 degrees swept wing were computed by Kern [Ref. 7], Hsu and Liu [Ref. 16], and Ekaterinaris et al.[Ref. 17].The solutions predict the interaction and breakdown of the strake and wing vortices as well as the surface pressure levels reasonably well at low angles of attack.

For a more detailed validation of numerical solutions, additional experimental data are needed on the effect of angle of attack, sideslip and Reynolds number on the vortex flowfield and induced wing surface pressures.

The objective of the present study was to establish an extensive database to investigate the Reynolds number effect on the vortical flow over a 76 / 40 degrees double-delta wing model.It consisted of extensive flow visualization studies in the Naval Postgraduate School Water Tunnel facility using dye-injection technique and Laser Doppler Velocimetry measurements, with a primary focus on the vortex core trajectories, interaction and breakdown characteristics on the leeward surface at varying angles of attack from 0 degrees up to 30 degrees.

II. EXPERIMENTAL FACILITIES AND EQUIPMENT

A. THE NAVAL POSTGRADUATE SCHOOL (N.P.S.) WATER TUNNEL

The experiments were performed in the Naval Postgraduate School flow visualization water tunnel facility [Ref. 18].This water tunnel was the first one designed by Eidetics International Inc., Torrance, California, and installed at N.P.S. in late 1988 (Fig. 10).It is a closed circuit facility appropriate for studying a wide range of aerodynamic and fluid dynamic phenomena.

The key design features of the water tunnel are high flow quality, horizontal orientation and continuous operation.The flow rate of circulation of water is up to 900 gallons per minute which corresponds to a flow velocity of about 1 ft / sec.

Horizontal orientation facilitates model access, and enables models to be readily changed without draining the water from the tunnel.The top cover of the water tunnel test section is removable for easy access to the model even when the tunnel is running.The facility is operated as a continuous flow channel, and the water level is adjusted to be approximately 2 inches below the top of the test section.The entire circuit is constructed of non - corrosive materials supported by a structural steel framework.

The test section is constructed primarily of tempered glass to provide thermal stability, scratch resistance and maximum viewing of the model.It is 60 inches long, 15 inches wide and 20 inches high.In order to compensate for boundary layer growth and to maintain uniform flow velocity throughout, the side walls of the test section have slight divergence.Simultaneous viewing of the model flowfield is possible from the bottom, both sides and the rear.The latter feature is specially advantageous when studying flow structures in the cross-flow plane.

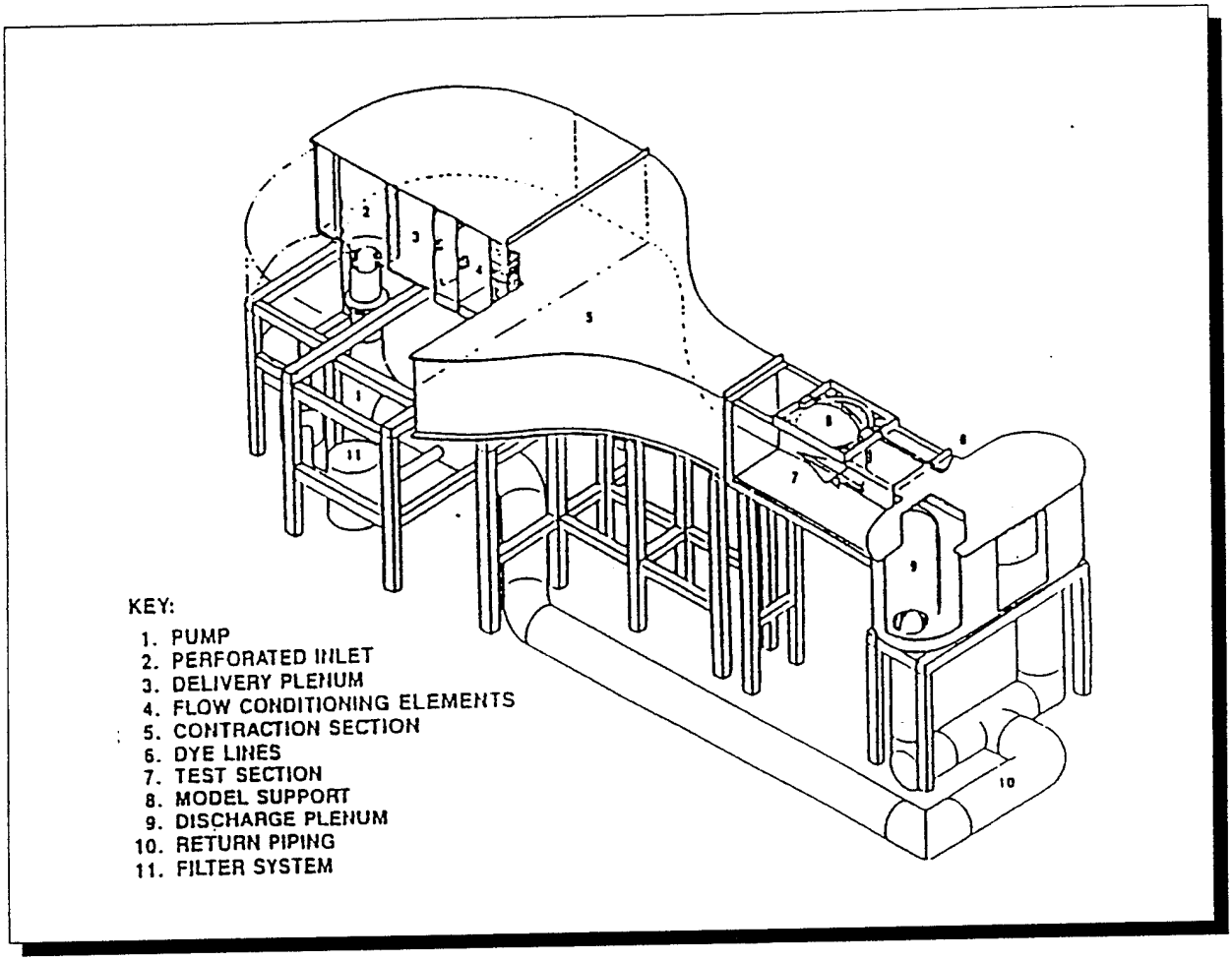

Fig. 10: Water tunnel facility at NPS

There is enough space underneath the test section for convenient viewing and set-up space for either direct or indirect (with a mirror) visual access for photography and video tape recording through the bottom glass window of the test section.

The test section flow velocity is variable from 0 up to 1.0 ft / sec.

The level of flow quality over the range of the test section velocity is presented in Table 1.

Mean flow angularity	< +- 1% in pitch and yaw
Turbulence intensity level (R M S)	< +- 1%
Velocity uniformity	< +- 2%

Table 1. Flow quality in the test section

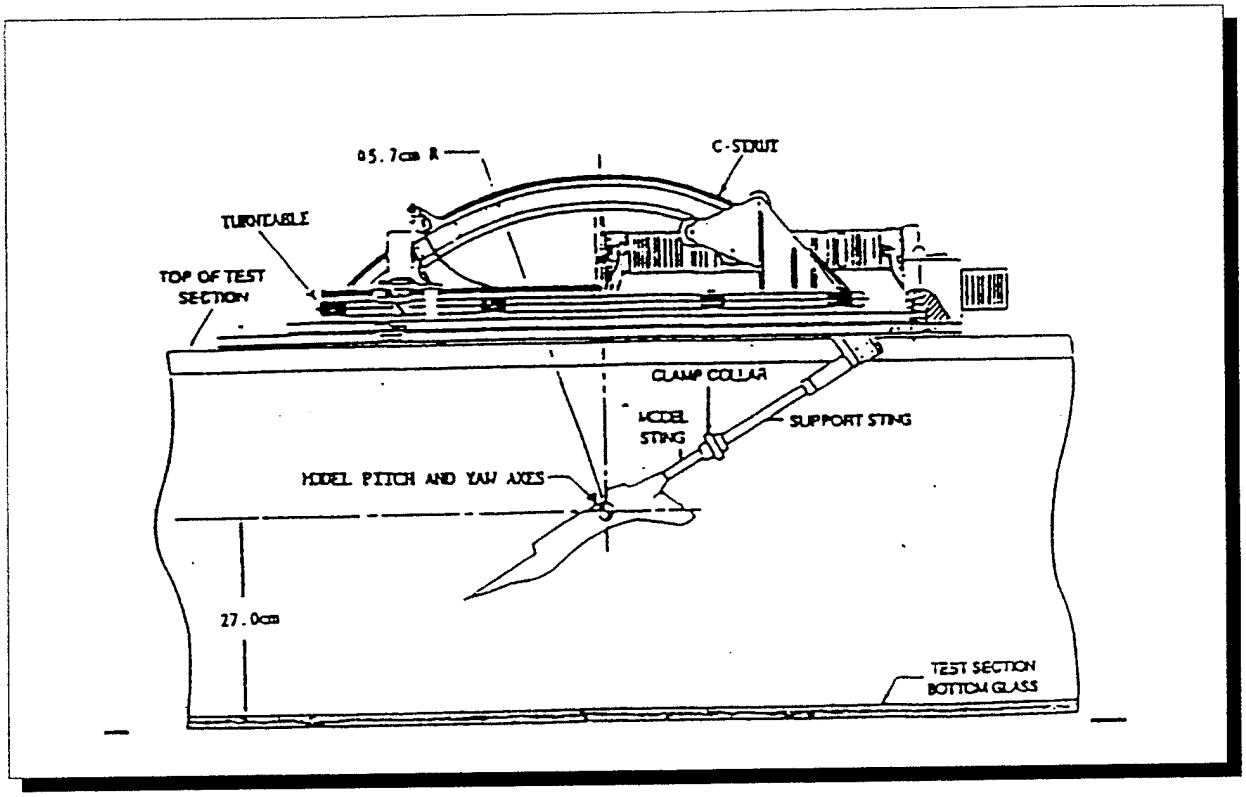

Fig. 11: Model support system of the NPS water tunnel

A pressurized six-color dye system designed to use water-soluble food coloring is provided for flow visualization.Individually routed lines connect the dye canisters to the model support system.A small compressor and a pressure regulator are used for pressurization and controlling of the pressure level.In order to regulate the dye emission each dye line is equipped with a flow control valve.Unfortunately, dye ejection rates cannot be measured quantitatively. Another way to control dye emission would be the pressurization level of the canisters, but this is not convenient and still does not solve the problem of measuring dye ejection rates.

The model support system shown in (Fig. 11) is mounted on top of the test section, and the model is usually sting - mounted upside-down in the test section.The system is designed for high angle of attack aerodynamic research studies, with change in angle of attack and sideslip capability through the following ranges :

A . O . A . α = -10 deg to 110 deg
Sideslip β = -20 deg to 20 deg

Angle of attack is set by pitching the model in the vertical plane on a C-strut arrangement and sideslip angles are achieved by rotating the model support assembly on a turntable.

The attitude control system consists of two servo motors which provide independent control of model pitch and yaw, with separate actuation switches and high / low rate control switches through a remote control for ease of operation and observation.The high pitch rate and low pitch rate correspond to 4.8 deg / sec and 2.2 deg / sec, respectively.

B. DOUBLE - DELTA WING TEST MODEL

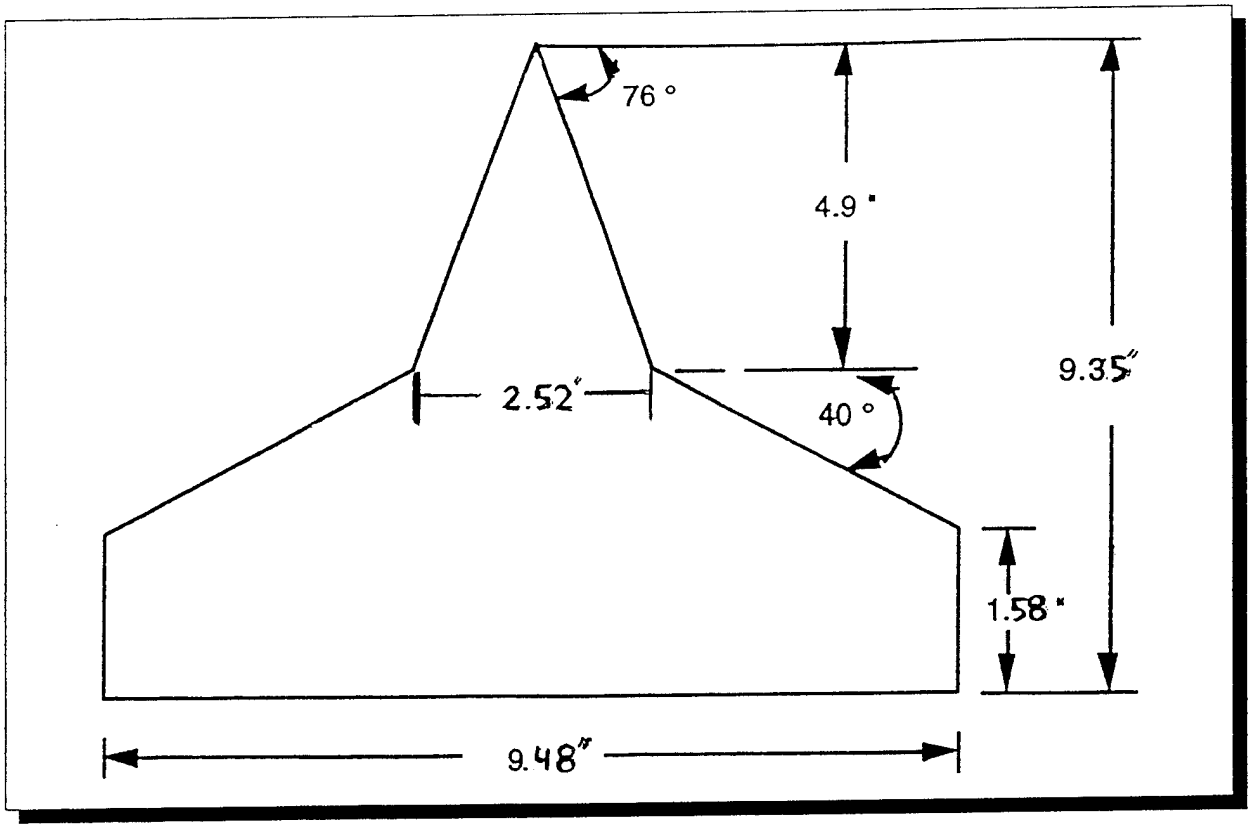

Fig. 12: Double-delta wing baseline model

The model of the double-delta wing that was used during the experiments is the "baseline" model shown in Fig. 12.It has a 76 degree sweep strake and a 40 degree sweep wing, both with sharp, 20 degree beveled leading edges and flat top surfaces.It is 0.25 inches thick and is constructed of plexiglas.The centerline chord is 9.35 inches and the planform area is 38.4 square inches.The upper surface of the model is marked with grid lines 0.25 x 0.25 inches that make the vortex burst point location and core trajectory easily identifiable.

C. DYE TUBE INSTALLATION

On the lower surface of the model six dye tubes were installed.They were made of brass and had a diameter of 26 / 1000 of an inch inside and 64 / 1000 of an inch outside.The tubes were secured at certain positions with the help of heavy duty electrical tape which made changing of their exact location permissible without leaving residues and therefore without causing very much trouble.A general view of the dye tube system is shown in Fig's. 13 and 14.Two of the brass tube tips were installed close to the apex, two close to the juncture or kink and two in the middle between the kink and the wing tip.

Both the location of the dye injection and the injection rate are very important in obtaining a good flow visualization of the model flowfield.The right location for the tip of the dye tubes was determined by moving around the tubes and observing the dye streamlines at different angles of attack.Satisfactory results were obtained when the tips of the brass tubes were sitting squarely on the flat surface (Fig. 13).

In order to improve the quality of the flow visualization different colors were injected at the three locations : red for the apex, green for the juncture or kink and blue for the center of the

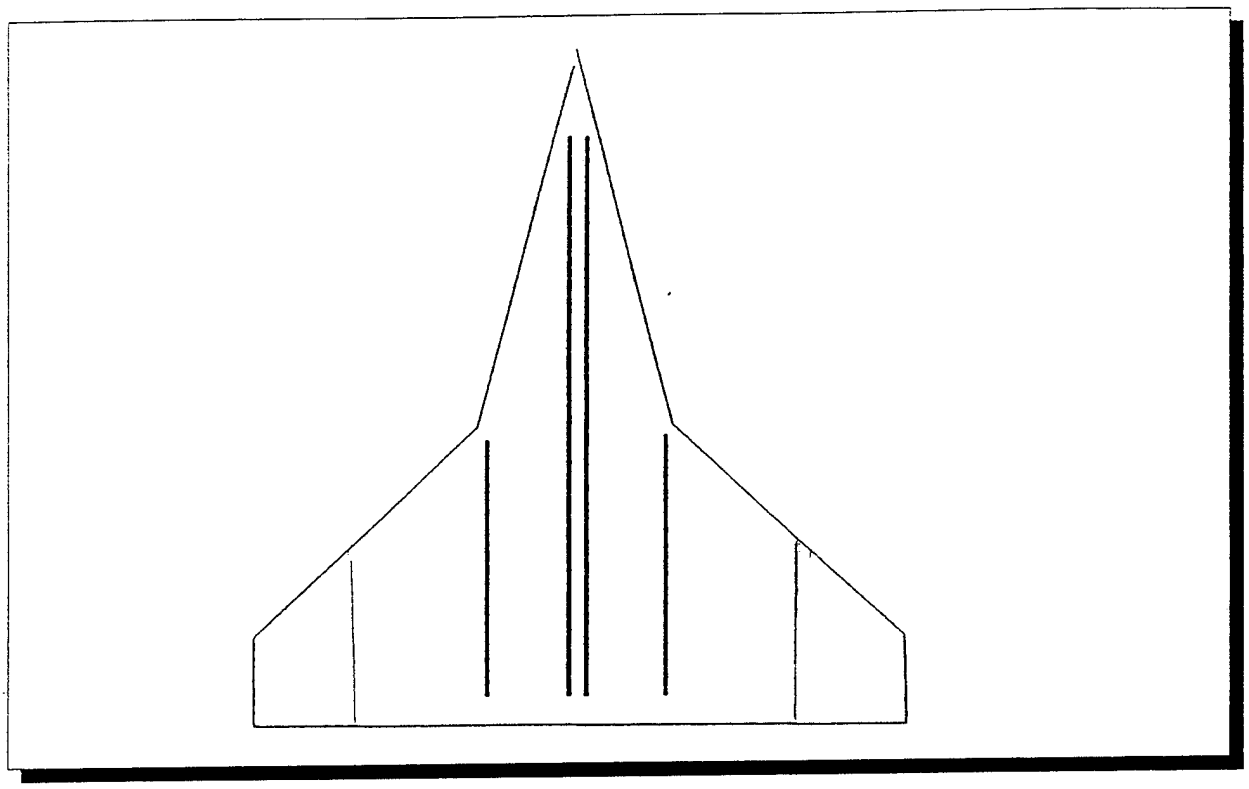

Fig. 13: The position 1 of the dye tubes

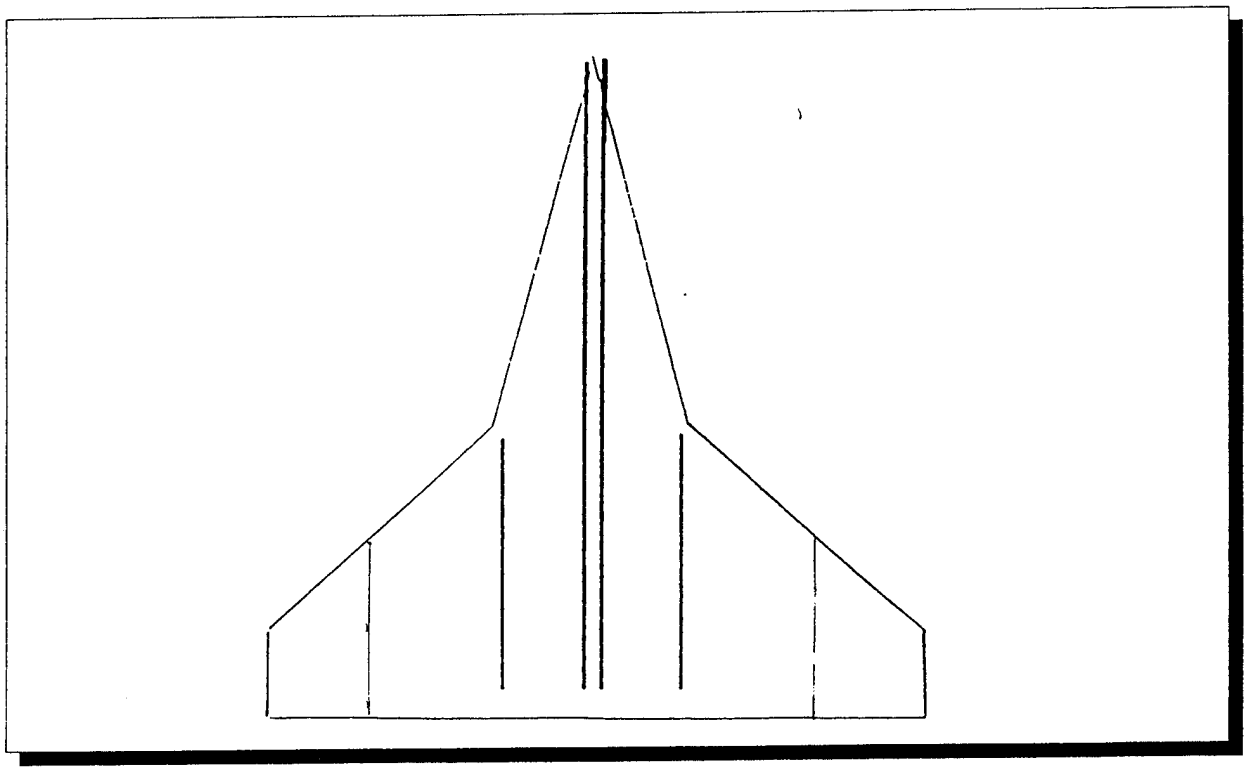

Fig. 14: The position 2 of the dye tubes

wing leading edge.The behaviour of the vortices generated by the apex or the kink can thus easily be distinguished and analyzed.

D. MODEL MOUNTING

A very important consideration for the visualization of the flow field is symmetry of the vortex cores and vortex burst locations.Therefore, it is extremely important to mount the model horizontally in the water tunnel with zero pitch, zero roll and zero yaw.Details on the mounting of the model are given in Ref. 9.

The model sting was secured to the sting holder of the model support system and then introduced into the test section.The centerline of the model was aligned with the free stream (tunnel centerline), to ensure zero pitch angle.To justify zero roll angle the height of both the left and right wing tip from the bottom of the test section must be equal.To assure zero yaw the model apex was set at equal distance from either sidewall of the test section.In addition, three parallel lines were drawn on the tunnel glass wall to check that the model reference line was parallel to these lines.

Another way to adjust the position of the model developed with increasing experience on the operation of the water tunnel.At some point during the course of emptying and refilling the tunnel the water level is exactly even with the model and sting when they are in the horizontal position.At this point one is able to check if the model is exactly parallel to the water line which means that both roll and pitch are zero.To verify that yaw is also zero equal distance from the apex of the model to either sidewall of the test section has to be measured, as it was previously mentioned.

E. PHOTOGRAPHIC AND VIDEO - RECORDING EQUIPMENT

Two 35 - mm automatic cameras were used for taking pictures.One Minolta 5000 i Maxima and one Olympus OM - 10.

The video recordings were done with the help of one U-matic Sony Video Camera.

In order to achieve appropriate lighting of the model 3 Smith-Victor 600 Watt photographic lights were used.

F. LASER DOPPLER VELOCIMETRY (L.D.V.) EQUIPMENT

The Laser system used to take velocity measurements is an Argon-Ion Laser system [Ref. 19] made by " T. S. I . - Incorporated " (Fig. 15) and consists of :

a) A Colorburst Multicolor Beam Separator Model 9201

b) A two - component Fiberoptic Probe system

c) Two I F A - 550 Signal Processors

d) An automatic traverse system capable of moving in all directions

(X- axis , Y - axis , Z - axis)

e) A personal computer with the Flow Information Display (F I N D)

software.

The Model 9201 Colorburst Multicolor Beam Separator converts an argon-ion laser beam to perform Laser Doppler Velocimetry (L D V).The conversion produces three pairs of shifted and unshifted beams : two green beams at 514.5 nanometers, two blue beams at 488.0 nanometers, and two violet beams at 476.5 nanometers.The Colorburst Separator is designed for many L D V applications.In this case it is used for one component velocity measurements.

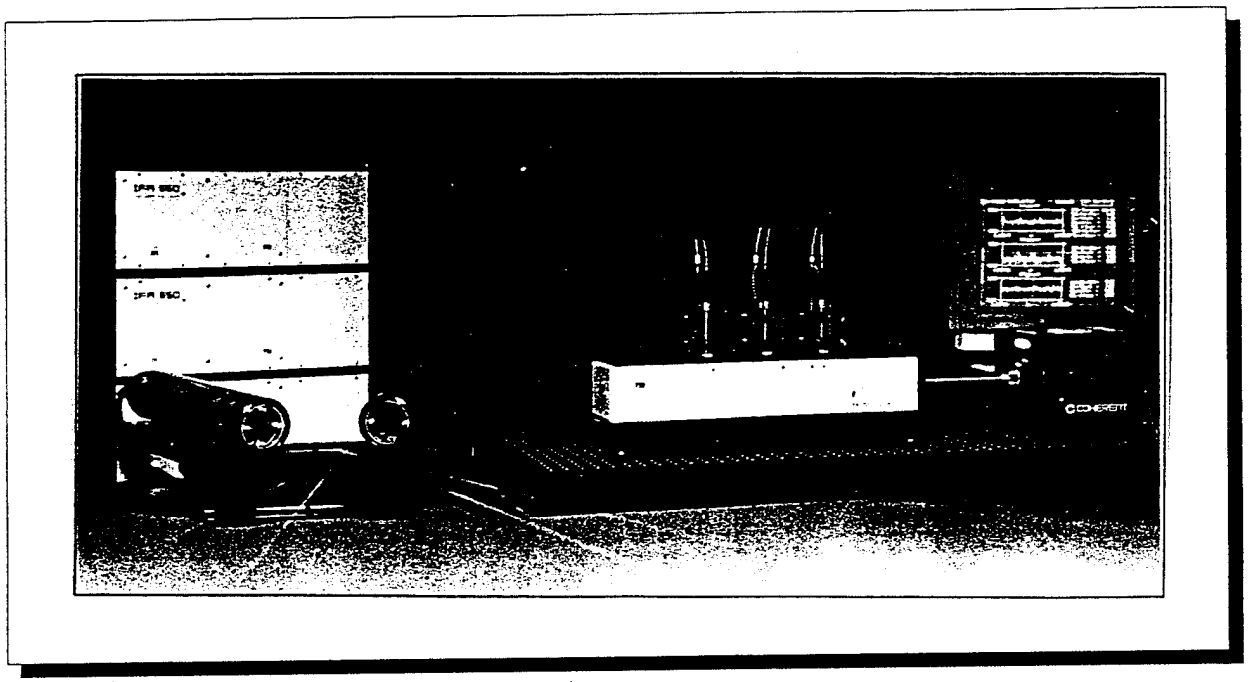

Fig. 15: Argon-Ion Laser system

The two-component, Fiberoptic Probe system is able to measure two components of velocity.Measurements of one component of velocity in a given flow is possible by crossing two laser beams at a single point in the flow and measuring the amount of light scattered by the movement of particles.The change in frequency, or Doppler shift, of this scattered light, as observed by a stationary detector, is used to calculate the flow velocity.

The I F A.-.550 Signal Processor extracts frequency information from cyclical analog signals that are mixed with noise.It offers very simple, very fast, high resolution processing.For best performance, medium to high data density must be present in the measurement application. The processor can make measurements wherever the data rate ensures one valid measurement before the velocity changes more than 10 or 15 %.

The automatic traverse system is capable of manually moving in all three directions X, Y, Z by remote control.It can also follow a certain traverse control program when used in

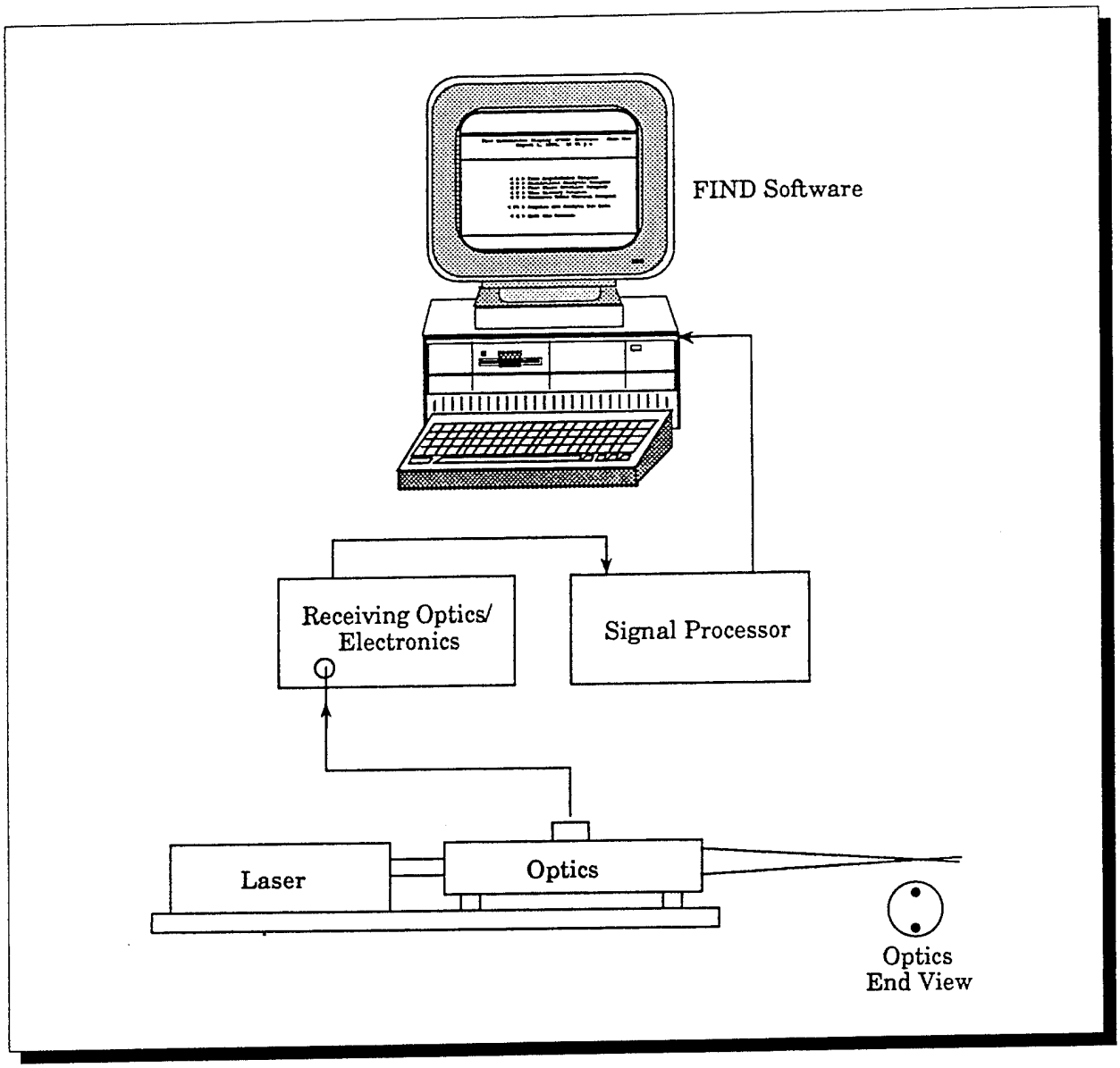

Fig. 16: FIND Software

a computer-controlled operation.The remote control has a slow / fast option and a jog / run option as well.The accuracy of the position is in the range of hundreds of a millimeter.

The Flow Information Display (F I N D) is a data analysis software package that is part of T S I's integrated L D V systems (Fig. 16).It is a user-oriented, DOS-based software designed to make L D V measurements easy and accurate.F I N D performs all hardware interfacing functions and runs software diagnostics to make sure the hardware is operating correctly.On the other hand,

it provides complete flow statistics for every measurement point.It calculates and displays all basic flow statistics, including mean velocity, standard deviation, and turbulence intensity.Data are displayed in the form of profile plots and histograms.

III. EXPERIMENTAL PROCEDURE

A. EXPERIMENTAL PROGRAM

Experimental investigations by Verhaagen [Ref. 13], Thompson [Ref. 12] Olsen and Nelson [Ref. 20], Graves [Ref. 11], and Hebbar et al. [Ref. 15], provide qualitative insight into the effect of angle of attack on the interaction and breakdown of the strake and wing vortices, the crossflow structures, the forces and moments, the surface pressure distribution and the velocity field. Solutions of the Navier-Stokes equations for the fully laminar flow about a 76 / 40 deg. double-delta wing have been computed by Kern [Ref. 7]. It should be pointed out that the flow Reynolds number varied considerably in these studies : 0.5 to 1.5 million in the wind tunnel tests [Ref. 21], 0.02 million in the water tunnel tests [Ref. 22], and 1 million in the numerical simulation [Ref. 9].

There are several disagreements in the interaction and bursting data from the wind tunnel tests, water tunnel tests and numerical predictions. The water tunnel data of Hebbar et al.,[Ref. 15, 22], indicate that, with increasing angle of attack, the interaction moves upstream until the angle of attack is large enough to cause the bursting of the strake vortex even before the interaction and subsequent destabilization of the wing vortex. These observations are in general agreement with those reported in Ref. 11 and 20. The angle of attack range for coiling-up of the vortices is narrow (10 ~ 20 deg.) and the vortex cores maintain their separate identity without merging into a single vortex even at higher angles of attack. This latter finding is in direct contrast to that reported in Ref. 12, 13 and 21. The wind tunnel data of Verhaagen [Ref. 21] imply that the strake vortex cores and the vortex cores generated at the kink hardly interact at 10 degrees angle of attack. Both these implications contradict the water tunnel data of Hebbar et al. The numerical solutions

of Kern [Ref. 7] show vortex interaction, leading to merging at higher angles of attack.But they also reveal an unusual wing vortex structure midway down the leading edge of the wing suggesting a second (torn) wing vortex.

It is therefore clear that additional experimental data, particularly on the effect of the Reynolds number on the vortex flow field, is needed for a more detailed validation of numerical solutions as well as to understand the apparent discrepancies between the water tunnel data, wind tunnel data and the numerical simulations.

In order to provide answers to some of these discrepancies a static flow visualization program was carried out in the Naval Postgraduate School water tunnel using a 76 / 40 deg. baseline double-delta wing model.To determine the influence of flow Reynolds number on vortex trajectories / interaction and vortex breakdown tunnel speeds of 0.2, 0.6 and 1.0 ft / sec were used.The angle of attack varied from 0 up to 30 degrees as follows : " 0 , 5 , 10 , 15 , 20, 22.5 , 25 , 30 ."

Both still picture photography and videotape recording were used for documentation of the flow visualization of the model in topview and sideview.In addition Laser Doppler Velocimetry measurements were taken to provide quantitative results of the flow over the model.

B. TEST PROCEDURE

The test procedure is outlined below :

1) Mount the model in the test section, and connect the dye tubes to the dye lines.Check the position of the model with the help of all reference markings to verify that zero pitch, roll, and yaw initial conditions agree with the readings of the sting control system.

2) Set up the lighting arrangement and adjust the lamp location to get the best possible lighting of the model.

3) Set up the 35-mm cameras and the video camera for recording the flow visualization data.

4) Turn on the water tunnel and run it at 0.2 ft / sec.

5) Fill each of the canisters with dye of the appropriate color red, green and blue accordingly.

6) Pressurize the dye injection system with the help of the air compressor and adjust the pressure at 5 lbs / sq in.

7) Check that the dye injection system operates adequately.

8) Operate the pitch and yaw controls to bring the model in the desired test condition.

9) Turn on each dye control knob and fine tune it to get the optimum dye injection rate for flow visualization purposes.

10) Observe the vortical flow patterns for the model test condition and make notes on the flow visualization.

11) Record the flow visualization data on video tapes and take pictures of sideview and topview of the model . Be careful : pictures of both views must be taken simultaneously with the help of remote control shutters for the cameras.

12) Turn off the dye control knob and set up the next condition for the model (water flow velocity and angle of attack).Repeat items 9 to 11 according to the requirements of the experimental program.

For the Laser Doppler Velocimetry measurements proceed as follows :

1) Turn on all the components required to operate the laser system.

2) Check the position of the model in the tunnel and bring it to the desired test position.

3) Turn on the water tunnel and run it at 0.2 ft / sec.

4) Align the laser beams with respect to the tip of the strake of the test model. Zero the readings of the counter of the traverse position so that this position becomes the new relative home of the system.

5) Move the traverse to the point where the measurement will be taken.

6) Set the computer program to analyze the data of the laser and make notes of the results.

7) Proceed to the next point to collect the data.Change the flow conditions if necessary by increasing or decreasing the water tunnel speed, or by moving the sting and changing the angle of attack of the model. Repeat item 6.

C. DATA ACQUISITION AND REDUCTION

The flow visualization data were acquired with the help of :

a) Direct visual observation of the flow field.

b) Two 35-mm cameras taking pictures simultaneously by remote control shutters of the sideview from the starboard side and top view of the vortical flow field originating at the apex and the kink of the model for different angles of attack and water flow velocities.

c) A video-camera was also used to record the flow phenomenon for later playback during the data reduction phase.

Laser Doppler Velocimetry measurements were taken with the help of an argon-ion laser system.Several surveys were executed following vertical to centerline of the model paths in the X-direction.Measurements of velocity at certain points at specific angles of attack and water tunnel velocity were taken to find the exact burst point of the strake and kink vortices.Point to point measurements were also taken at certain model conditions (angle of attack setting), while changing the velocity of the water tunnel, in order to understand how the flowfield is changing with respect to the Reynolds number.

The data reduction consisted of :

1) Measuring the vortex core location in the X-direction (parallel to the centerline of the model), Y-direction (outboard of the model centerline), and Z-direction (perpendicular to the X-Y plane), and plotting vortex core trajectories at different angles of attack and water tunnel flow velocities for static conditions.

2) Measuring the burst location of the strake vortex and plotting it as a function of water tunnel flow velocity (Reynolds number) at different angles of attack.

3) Making tables of point to point flow field Laser Doppler Velocimetry measurements and comparing results as water tunnel flow velocity changes at different angle of attack settings.

In order to verify the symmetry of the vortex core trajectories and burst location, flow visualization analysis as well as Laser Doppler Velocimetry measurements were done in both positive and negative Y-direction.

The vortex core trajectories and burst locations were visually determined from direct observation, videotape playback and photographs with utmost care and consistency and scaled for non-dimensionalization using the centerline chord length of the model " C ".

Based on the L D V measurements it was possible to identify the vortex trajectories by conducting surveys in the Y-direction at different Z-direction positions.Vortex burst locations were identified based on the data from the flow visualization by trial and error measurements at different points in the flow field in an effort to determine a point with zero velocity and high turbulence.A vortex burst point is characterized by the fact that when moving away from it in any direction non-zero velocity must be observed.

There may be some degree of imprecision in the flow visualization data due to the difficulty in locating the trajectory and burst point location, especially at high angles of attack and high water tunnel flow velocities.On the other hand, L D V measurements are more precise. However, because they are point to point measurements it is very difficult to cover the entire flow field.

At last, it should be noted that during the experiments, the vortex burst location changed position constantly up to + / - 0.75 inches (about 8 % of the centerline chord).The vortex core coordinates and burst locations according to flow visualization and L D V measurements are listed in " Appendix B " and "Appendix C " respectively.

D. METHOD OF PHOTOGRAPHY AND VIDEO - RECORDING

The equipment used for data acquisition consisted of two 35-mm cameras, and one U-matic Sony Video-camera.In an effort to achieve appropriate lighting for the model, eliminating all possible shadows and areas of low visibility three Smith-Victor 600 Watt photographic lights were used.Two of them were placed at a distance of one to three feet at 45 degrees angle from the test section and the third one was placed parallel to the centerline of the model under the

water tunnel test section and close to the beginning of the glass section.The lighting set up for both sideview and topview is illustrated in Fig. 17.

An angle of attack scale was fixed to the rear side wall of the water tunnel test section to help in reading the instantaneous angle of attack in the sideview photographs and video-recordings.

An Olympus OM-10 camera positioned in front of the test section at the same height level with the model, when in horizontal position, was used for sideview photography with 35-mm Black and White or Color Kodak ASA-400 film.A Minolta 5000i Maxima camera positioned at the bottom of the test section was used for topview photography with the same kind of film.Both

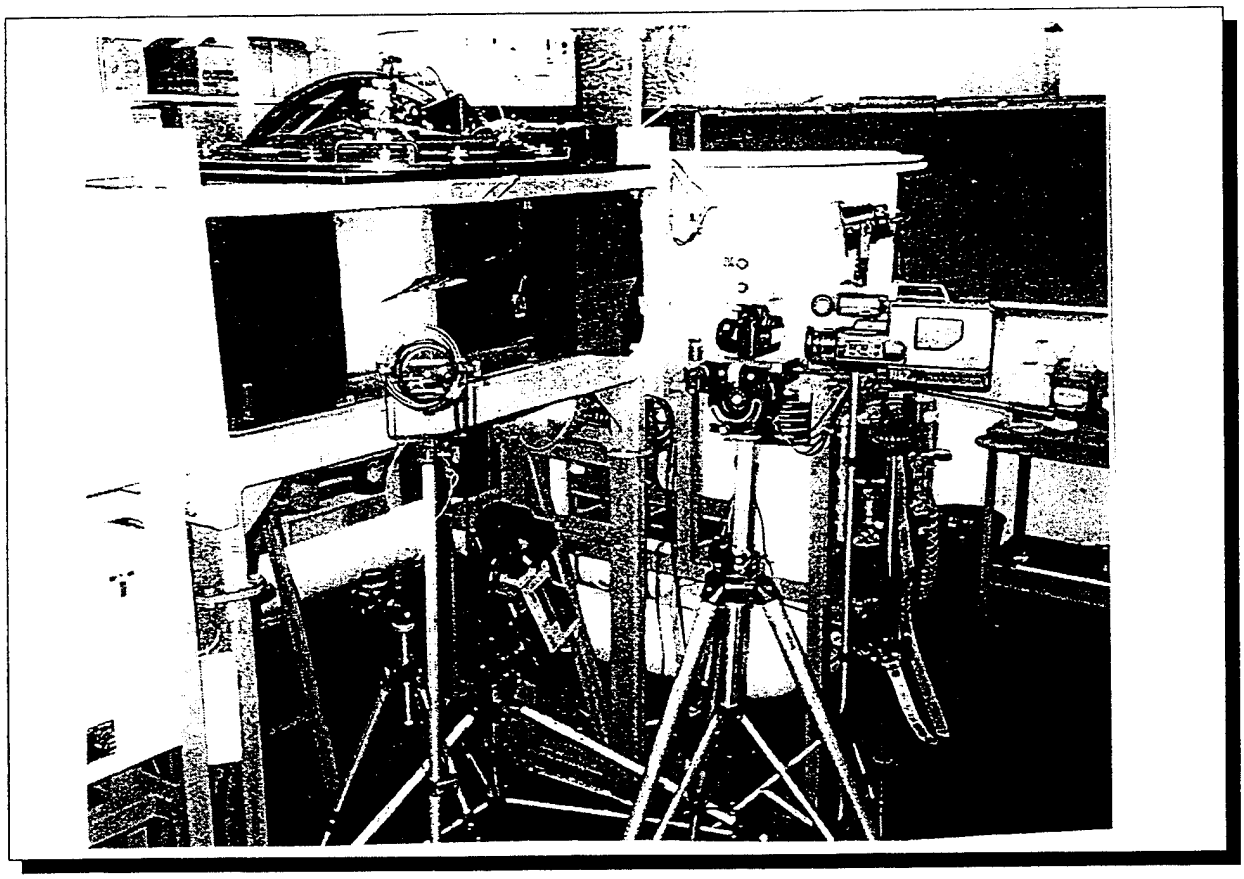

Fig. 17: Video-camera, 35-mm camera

cameras were focused manually based on a central and lighting set-up position the model would get during the experimental procedure.The camera at the bottom of the test section was operated using a remote control shutter release because of the necessity of simultaneous photography.

The Sony Video-camera was used for both sideview and topview recordings conducted one after the other.

E. METHOD OF L.D.V. MEASUREMENTS

The equipment used for conducting LDV measurements consisted of an Argon-Ion Laser system with a two-component Fiberoptic Probe, a Signal Processor, a traverse system and a personal computer.The experimental set-up enables the user to measure only one component at a time either in the X or Z direction of a velocity vector in a given flow.

The position of the traverse table is parallel to the water tunnel test section centerline.The Fiberoptic Probe system is aligned so that the two-laser-beam plane is parallel to the bottom of the water tunnel test section.Therefore it was possible to take velocity measurements in the X-direction, the direction of the water flow in the tunnel.This means that in every measurement we were able to estimate only the X-component of the velocity vector and not the Y- or Z-component.The set-up of the Laser system is illustrated in Fig. 18.

The LDV measurements are point measurements and the flowfield we have to investigate has numerous points.For this reason we decided to limit the number of different flow conditions to only one angle of attack and vary only the flow velocity from 0.2 to 0.6 to 1.0 ft / sec.The angle of attack that was selected is 15 degrees because it was in the middle of the range we

explored and would probably be the most representative for the vortex flowfield change with velocity.

The following method in collecting velocity data was adopted :

a) Position the model at 15 degrees angle of attack.Align the system with respect to the nose of the model which is the reference point with zero coordinates (0,0,0).Then move the probe in the X-direction in order to verify that it is parallel to the model's centerchord.

b) Conduct LDV measurements at random points with symmetric coordinates to verify the symmetry of the flowfield as well as the correct alignment of the system.

c) Try to estimate the burst point location of the strake and wing vortices in different flow velocities by trial and error.When at the correct point record zero or reverse velocity readings. Then try to move the system in any possible direction, as little as possible.This must result in increased velocity measurements.

d) Map a flowfield cross-section by measuring velocity changes for a specified water flow velocity of 0.6 ft / sec, at certain X locations, for example 38.62% and 62.73% of the model center-chord when measured from the tail of the model.In the Y-direction take measurements in one-millimeter intervals while in the Z-direction every two or three millimeters away from the surface of the model.

e) Identify zero or reverse flow velocity regions of the wing area from 120 mm to 225 mm in the X-direction, measured from the nose of the model.Measure three millimeters from the surface of the model in the Z-direction and every ten millimeters in the Y-direction.

f) Finally identify vortex burst locations using dye injection in parallel with LDV at water flow velocity of 0.2 - 0.6 - 1.0 ft / sec and verify that flow visualization results are is in total agreement with actual velocity fluctuations.

All LDV measurements with associated tables and figures are listed in " Appendix C ".

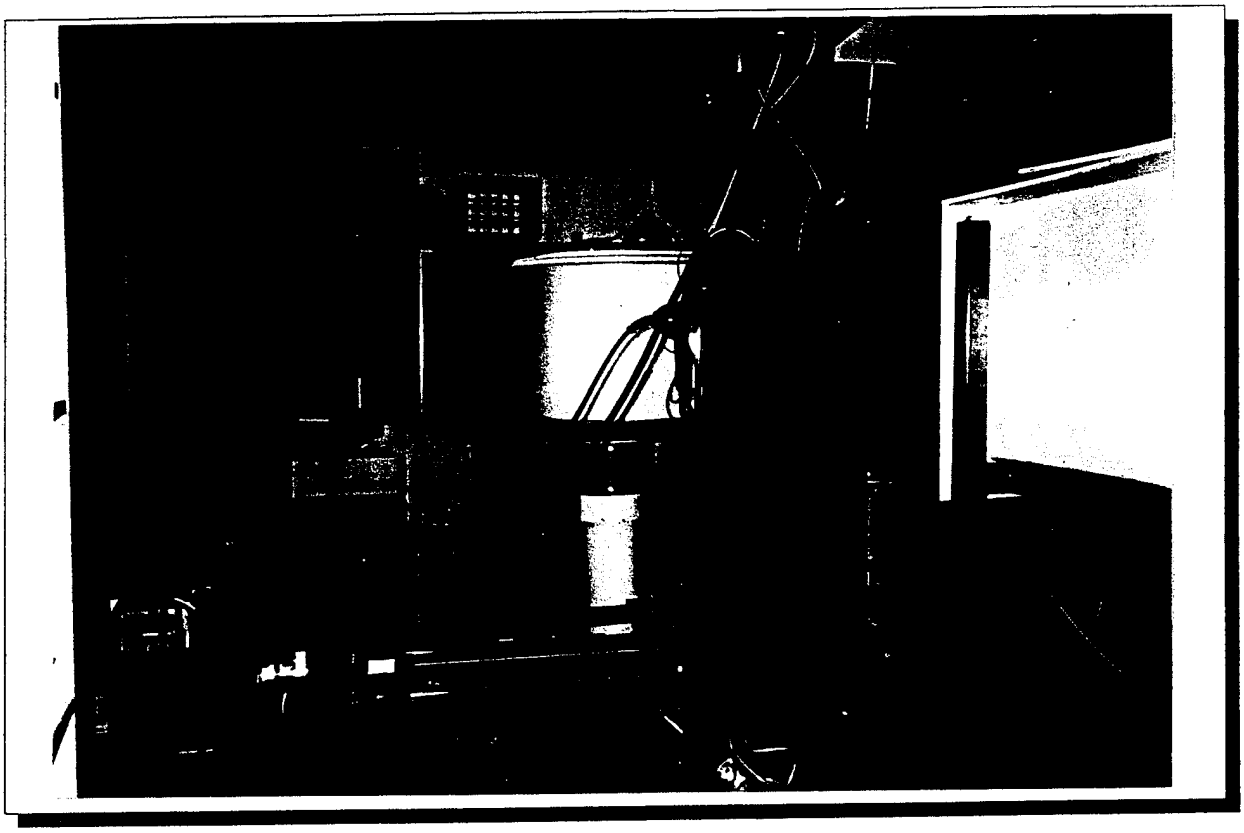

Fig. 18: Laser system experimental set-up

VI. RESULTS AND DISCUSSION

A. FLOW VISUALIZATION RESULTS

A large amount of flow visualization data was collected during the experiment using several rolls of 35 mm Black and White, and Color film along with videotape recording of the flow over the model both in sideview and topview.The reduced data was analyzed in an effort to explain the Reynolds number effect on the vortex core trajectories and interactions as well as on the breakdown (bursting) of the vortices for static conditions with zero sideslip.

Selected photographs of the model at all angles of attack (5 to 30 deg.), and all water tunnel speeds (0.2 - 0.6 - 1.0 ft / sec) are presented in " Appendix A " (Fig. 19 - 39) to highlight the flow characteristics.The experimental data on vortex core trajectory and breakdown extracted from all the flow visualization are presented in tables and graphs in " Appendix B " (Tables 3 - 44, Fig. 40 - 95).Every graph represents a sideview or a topview of the model and every table contains the coordinates of the vortex trajectories.

A careful observation of the vortex cores (either direct observation or video playback) indicates that at a water tunnel flow velocity of 0.2 ft / sec the vortex trajectories and breakdown locations are unstable, moving usually in opposite directions (right side strake vortex moves forward as left side moves rearward with respect to an imaginary center point).As the water tunnel flow velocity is increased to 0.6 ft / sec or 1.0 ft / sec the vortices seem to be more stable.The vortex core trajectories and breakdown locations continue to move in a similar way but over a smaller distance.All changes return to an intermediate stable position much faster as flow velocity is increased.

At a water tunnel flow velocity of 0.2 ft / sec (Fig. 19 - 25) the strake and wing vortex appear to interact with each other very early, just about 5 % after the kink of the model, coiling up for angles of attack less than 25 degrees.If the angle of attack is equal to or greater than 25 degrees (Fig. 24 , 25) the strake vortex breakdown occurs prior to the interaction.At the higher water tunnel flow velocity of 0.6 - 1.0 ft / sec (Fig. 26 - 39) the strake and wing vortex hardly interact at any angle of attack.

The strake vortex trajectory moves outboard (away from the center-chord) as the velocity is increased from 0.2 to 0.6 ft / sec at every angle of attack, except at the 5 degree setting.Further increase from 0.6 to 1.0 ft / sec has a minor effect on the trajectory, which is characterized by the same tendency to move outboard.The wing vortex trajectory behaves in a similar manner, i.e. moves outboard as the flow velocity is increased from 0.6 to 1.0 ft / sec.On the other hand, if we examine the strake and wing vortex trajectories with respect to their distance from the model surface, it can be said that the distance is decreased as the flow velocity is increased.After thorough examination of the vortex core trajectories in the range of 5 up to 20 degrees angle of attack we can conclude that the strake and wing vortices are attracted to each other.

As far as the breakdown location of the vortices is concerned, the following can be identified : At 0.2 ft /sec and while the strake and wing vortex interact, with their trajectories coiling up (Fig. 19 - 25), the wing vortex bursts after the strake vortex.As the water tunnel flow velocity is increased to 0.6 - 1.0 ft / sec (Fig. 26 - 39), the wing vortex bursts earlier than the strake vortex.

Careful observation of the experimental data leads to the conclusion that the breakdown locations of the strake and wing vortices move forward (in the direction of the nose) as the flow

velocity is increased.This is very clear for lower angles of attack (5 to 10 deg.) and when comparing the vortex flow at 0.2 ft / sec to the one at 0.6 ft / sec (Fig. 19, 20, 26, 27).For 5 degrees angle of attack and 0.2 ft / sec the breakdown location remains outside of the wing surface, barely reaching the trailing edge at 10 degrees angle of attack and 0.2 ft / sec.For 10 degrees angle of attack and 0.6 ft / sec it is well inside the wing surface.The same behavior is observed for the vortex breakdown locations throughout the whole range of angle of attack and water tunnel flow velocity (Reynolds number) settings.This is documented in the pictures, tables and graphs presented in the Appendices (Fig. 19 - 39, 39 - 95, Tables 3 - 44).

In general, it is suggested that at low water tunnel flow velocity (0.2 ft / sec) flow visualization results are in agreement with those reported by Hebbar et al., [Ref. 15, 22], but at higher velocity (0.6 - 1.0 ft / sec) the results are more similar to the wind tunnel results of Verhaagen [Ref. 13, 21].It is therefore believed that the difference in the flow Reynolds number is responsible for previously observed discrepancies.

B. L. D. V. RESULTS

In order to gain a better understanding of the vortex structure and to verify the flow visualization results LDV measurements were carried out.To this end numerous one-component flow velocity data were collected which can be categorized as follows:

a) flow velocity distribution of both strake vortices in a cross-section perpendicular to the model surface (Fig. 96 - 103, Table 45).

b) flow velocity distribution of the strake and wing vortices in a cross-section perpendicular to the model surface (Fig. 104 - 114, Table 46).

c) regions of zero or reverse flow of the model wing area as water tunnel flow velocity is increased from 0.2 ft / sec to 1.0 ft / sec (Fig. 115 - 117, Table 47).

In study cases (a) and (b) the flow velocity was 0.6 ft / sec and the angle of attack 15 deg.The same angle of attack was used in case study (c) as well.During the course of the experiments the whole process was repeated to verify that the collected data are correct.

In case study (a) (Fig. 96 - 103, Table 45) it was found that the vortex flowfield is completely symmetric, making it possible to restrict the data collection to half of the model surface and flowfield only.

In study cases (a) and (b) (Fig. 96 - 103, 104 -114, Tables 45, 46) the interval used in the Y-direction between point measurements was one (1) mm.Although this interval appears to be very small at first sight, it was found that a coarser distribution would not allow an adequate resolution of the velocity gradients.Furthermore, attention was paid to the repeatability of the measurements at a given point.

The graphical representation of the measured velocity profiles induced by the two vortices is given in " Appendix C ".This is possible for only the strake vortex (Fig. 96 - 103, Table 45), or a combination of the strake vortex and the associated wing vortex (Fig. 104 - 114, Table 46).For example, it is estimated that, at small distance in the Z-direction from the model surface and along the projection of a vortex core trajectory in the X-direction on it, the flow velocity is very low (Fig. 96, 104).In contrast, as the distance in the Z-direction is increased to a certain point, probably close to the vortex core location, sharp flow velocity peaks are observed (Fig. 99, 107, 108).These peaks level off as distance from the model surface is increased.

From case study (b), where a strake vortex and an associated wing vortex are investigated, the graphical representation implies that the strake vortex is stronger than the wing vortex (Fig . 106, 107, 108), because the velocity profile shows a higher peak in the area where the strake vortex is expected to be.It can also be identified which of the vortex cores is closer to the model surface and that is in our case the wing vortex core (Fig. 106, 107, 108).The way the two vortices interact, and in this case they do not appear to do so, can also be investigated.Bear in mind that we are looking only at one cross-section.

In case study (c) areas of the wing, three (3) mm from the model surface, where zero or reverse flow velocity is measured, are visualized.Graphs of the model, with these areas highlighted, at 0.2 - 0.6 - 1.0 ft / sec are listed in " Appendix C " (Fig. 115 - 117).As the water tunnel flow velocity is increased, the Reynolds number effect on the flowfield can be estimated This area of the wing in which zero or reverse flow velocity is observed is significant at 0.2 ft / sec (Fig. 115), decreasing at 0.6 ft / sec (Fig. 116) around the wing's leading edge, and at 1.0 ft / sec (Fig. 117) hardly any point is found having such characteristics.

At last, by trial and error point to point LDV measurements, the breakdown location of the strake and wing vortices was found.According to the results, the vortex breakdown location moves forward towards the nose of the model as flow velocity is increased.

C. COMPARISON OF FLOW VISUALIZATION RESULTS AND LDV MEASUREMENTS

One of the most important aspects of this study is to examine whether the flow visualization results agree with the LDV measurements.During the course of this study

experimental data were collected at first by the flow visualization method and later as a second and possibly more reliable method LDV was used.After carefully analyzing and comparing the data it can be asserted that they agree in general, presenting only a substantial difference of 5-10% that has been expected and is within acceptable limits.

The strake vortex trajectory, as predicted by the flow visualization method, appears to pass through the same location in the cross-section analyzed by LDV.The same seems to be the case for the strake-wing vortex combination.

The strake and wing vortex breakdown locations estimated from photographs and video-recordings, when compared to the breakdown location estimated by LDV measurements, suggest an uncertainty in the same range of 5-10 %.

It has to be noted that the flow visualization analysis is based on subjective estimations, and it is accepted that these estimations may be slightly different, according to the skill and the personal understanding of the investigator.Do not forget that the vortex flowfield is very dynamic, fluctuating continuously, especially at low flow velocity.On the other hand, LDV measurements are much more precise but initial alignment problems may be the cause of some inconsistency.

Another experimental procedure was adopted towards the end of the data collection, when dye-injection was used in parallel with the LDV measurements.Despite the fact that the data collection was not very extensive, the dye injection did not affect the LDV measurement quality. No significant fluctuation in the data collected, with or without dye injection, was recognized.By combining the two methods, it became possible to determine a vortex core, a breakdown location or a reverse flow region.It was amazing to see how well the LDV velocity measurements confirmed the flow visualization interpretations.

In conclusion, it can be said that there are no significant discrepancies between the flow visualization and the LDV method.What appears as a minor discrepancy is probably deceptive and is caused by the unavoidable measurement uncertainty or flowfield fluctuation.

D. EXPERIMENTAL LIMITATIONS

1. Reynolds Number

In this study the Reynolds number effect on the vortex flowfield over a double-delta wing is investigated.The Reynolds number is a dimensionless parameter, defined as :

$$Re = [V * c] / \nu \quad , \text{where}$$

V = tunnel speed, c = centerchord of the model and ν = water kinematic viscosity .

It is difficult to vary the kinematic viscocity or the test model dimensions, therefore we vary the water tunnel flow velocity from 0.2 ft / sec to 1.0 ft / sec which is the maximum attainable.

Since c = 0.78 ft and $\nu = 1{,}076 * 10^{-5}$ ft^2 / sec we can calculate the flow Reynolds number shown in Table 2.

Water Tunnel Velocity in ft / sec	Nominal Reynolds Number
0.2	15,000
0.6	45,000
1	75,000

Table 2. Reynolds number range

2. Flow Visualization

All flow visualization data have been non-dimensionalized, expressed in percentages and tabulated according to the angle of attack and tunnel speed where they correspond.In the X-direction non-dimensionalization is done with respect to the centerchord of the model and all distances are measured from the tail of the model.In the Y- and Z- direction non-dimensionalization is done with respect to the halfspan, and all distances in the Y- direction are measured from the centerchord outboards, and in the Z- direction away from the model surface.

It is very important to summarize interesting factors that affect the flow visualization data quality :

The angle of attack of the model and the water tunnel flow velocity are set according to the readings on the control panel, which means that there may be some difference with the actual settings.

The position of the dye-tubes affects the vortex core trajectory and interaction, especially at low angle of attack and water tunnel flow velocity.

Dye injection rates are critical, because they appear to change significantly the flow visualization results of the vortex interaction by altering the trajectories.

The position of the photographic equipment may cause offset problems, and simultaneous photography of both the sideview and topview is necessary in order to achieve satisfactory correspondence to each other.

At higher velocity, another problem is the difficulty to pinpoint the exact breakdown location of the wing vortices, especially at high angle of attack.

Finally, flow visualization studies were conducted with Reynolds number varying from 15,000 to 75,000 which is a very limited range, but further investigation is limited by the water tunnel performance.

3. L.D.V. Measurements

It is very important to refer to the fact that no dye was used during the LDV measurements in an effort to avoid disturbing the flowfield.From the bulk of the data collected it can be appreciated that further exploration of the flowfield, at different angle of attack or flow velocity, is quite time consuming.

It is very important to refer to some interesting factors that affect the LDV data quality :

First of all, correct alignment of the traverse and probe system is necessary.Once the system has been aligned, the position of the system relative to the point (0, 0, 0) should not be altered, because this may cause discrepancies in the collected data due to a slight change of the coordinates of each point.It has to be noted that precise alignment of the system is very important, and has to be checked at both the nose and tail of the model, especially in the Y-direction (perpendicular to the center-chord).

Also the data collection rate must be sufficient so that the velocity measurements can be done quickly and reliably.

During the course of the experiments the whole process was repeated to verify that the collected data are correct.

Finally, the LDV technique was used only in one cross-section, at one water tunnel velocity and one angle of attack setting.This is very significant because it limits, up to a point, the formulation of general conclusions.

V. CONCLUSIONS AND RECOMMENDATIONS

A study of the vortical flow over a baseline double-delta wing model was conducted in the NPS water tunnel at three nominal flow Reynolds numbers of 15000, 45000, and 75000.A flow visualization with the dye-injection method was performed which was further enhanced by LDV measurements.

The primary focus of this investigation was to determine the influence of flow Reynolds number on vortex trajectory / interaction and breakdown, and to gain a better understanding of the vortical flowfield.

The following conclusions are drawn from the results of the experimental investigation :

1) The strake and wing vortex trajectories tend to move outboards in the Y-direction (away from the centerchord), and closer to the model surface as the flow Reynolds number is increased.

2) Previously recorded discrepancies between results from water and wind tunnel experiments can be attributed to the difference in the flow Reynolds number.

3) The vortex breakdown location is characterized by a forward movement towards the nose of the model, as the flow Reynolds number is increased.

4) The LDV data reveal an increase of the flow velocity in the core of a vortex in the X-direction of about 60% over the undisturbed water tunnel flow velocity.Along the projection of the core trajectory on the model surface and at a small distance in the Z-direction a decrease in the flow velocity is observed of about 35% below the undisturbed water tunnel flow velocity.

From the experimental results the following recommendations can be expressed :

1) Continue LDV measurements to complete a sufficient data base, by examining the synthesis of the vortical flowfield at different angles of attack and water tunnel flow velocity.

2) Extend experimentation on the Reynolds number effect on the vortical flowfield by performing wind tunnel tests where higher velocities can be investigated.

3) Study other double-delta wing models in order to verify similarity in the vortical flowfield behavior in respect to a Reynolds number change.

4) Improve the Laser system by increasing its ability to conduct two or even three velocity component measurements, to gain a better understanding of the vortical flowfield.

LIST OF REFERENCES

1) L.K. Loftin, " Quest for performance, The Evolution of Modern aircraft ", NASA, 1985.

2) D. Wood, " Janes World Aircraft Recognition Handbook ", London, 1982.

3) R., Whitford, " Design for Air Combat ", Janes Publishing Co. Ltd. London, 1987.

4) M. Lee, M.C. Ho, " Vortex Dynamics of Delta Wings ", Spring-Verlag, 1989.

5) N.J. Wood and L. Roberts, " Control of Vortical Lift on Delta Wings by Tangential Leading Edge Blowing ", Journal of Aircraft, Vol. 25, No. 3, 1988.

6) John J. Bertin, Michael L. Smith, " Aerodynamics for Engineers ", Prentice Hall, Second Edition, 1989.

7) S.B. Kern, and " Vortex Flow Control Using Fillets on a Double-Delta Wing ", Journal of Aircraft, Vol. 30, No. 6, 1993.

8) M.W. Walters, " Flowfield of Bursting Vortices over Moderately Swept Delta Wings ",HTP-5 Workshopon Vortical Flow Breakdown and Structural Interactions, Nasa LaRC, 1991.

9) O.V. Cavazos, " A Flow Visualization of Lex Generated Vortices on a Scale Model F/A-18 at High A.O.A. ", Master's Thesis, NPS, Monterey CA, 1990.

10) U. Brennenstuhl, " Experimentelle und theoretische Untersuchungen uber die Wirbelbildung an Doppeldeltafluegeln ", Braunschweig, 1985.

11) T.V. Graves, " Aerodynamic Performance of Strake Wing Configurations ", High-Angle-of-Attack Technology Vol.I, NASA CP-3149, Part 1, pp.173-204, May 1992.

12) D.H. Thompson, " A Visualisation Study of the Vortex Flow Around Double-Delta Wings ", ARL-AERO-R-615, Melbourne, 1985.

13) N.G. Verhaagen, " An Experimental Investigation of the Vortex Flow over Delta and Double-Delta Wings at Low Speed ", TUD Report LR-372, Delft, 1983.

14) A.M. Cunningham, R.G. Den Boer, " Low Speed Aerodynamics of a Pitching Straked Wing at High Incidence-Part II : Harmonic Analysis " , Journal of Aircraft, Vol. 27, No. 1, 1990.

15) S.K. Hebbar, M.F. Platzer, Li F.M., " A Visualization Study of the Vortical Flowfield over a Double-Delta Wing in Dynamic Motion ", AIAA 93-3425-CP, Monterey, 1993.

16) C.H. Hsu, C.H. Liu, " Upwind Navier-Stokes Solutions for Leading Edge Vortex Flows ", AIAA 89-0265, Nevada, 1989.

17) J.A. Ekaterinaris, R.L. Courtley, L.B. Schiff, M.F. Pflatzer, " Numerical Investigation of the Flow over a Double-Delta Wing at High Incidence ", AIAA 91-0753, Nevada, 1991 and AIAA Journal Vol. 32, No. 3, pp. 457 - 463, 1995.

18) " User's Manual, Flow Visualization Water Tunnel Operation for Model 1520, Eidetic International Inc., California, 1988.

19) " Laser System User's Manual ", TSI - Incorporated .

20) P. Olsen, R. Nelson, " Vortex Interaction over Double-Delta Wings at High Angles of Attack ", AIAA 89-2191, 1989.

21) N.G. Verhaagen, L.N. Jenkins, S.B. Kern, A.E. Washburn, " A Study of the Vortex Flow over a 76 / 40 deg. Double-Delta Wing ", AIAA 95-0650, 1995.

22) S.K. Hebbar, M.F. Platzer, A.M. Alkhozam, " Investigation into the Effects of Juncture Fillets on the Vortical Flow over a Cropped Double-Delta Wing ", AIAA 94-0626, 1994, and AIAA 95-0649, 1995.

APPENDIX A

(PHOTOGRAPHS)

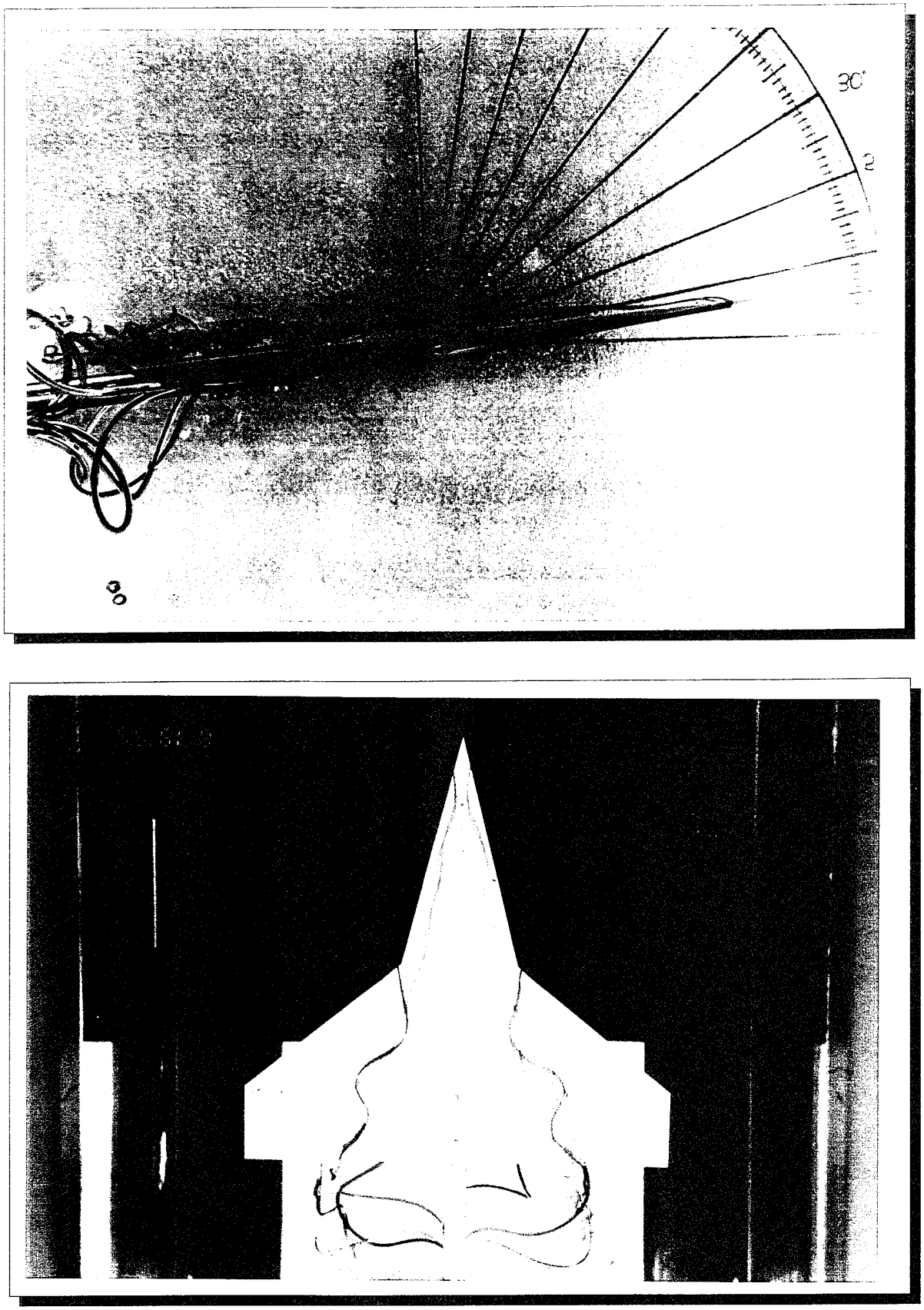

Fig . 19 : Model Sideview - Topview at 5 deg. AOA and V = 0.2 ft / sec .

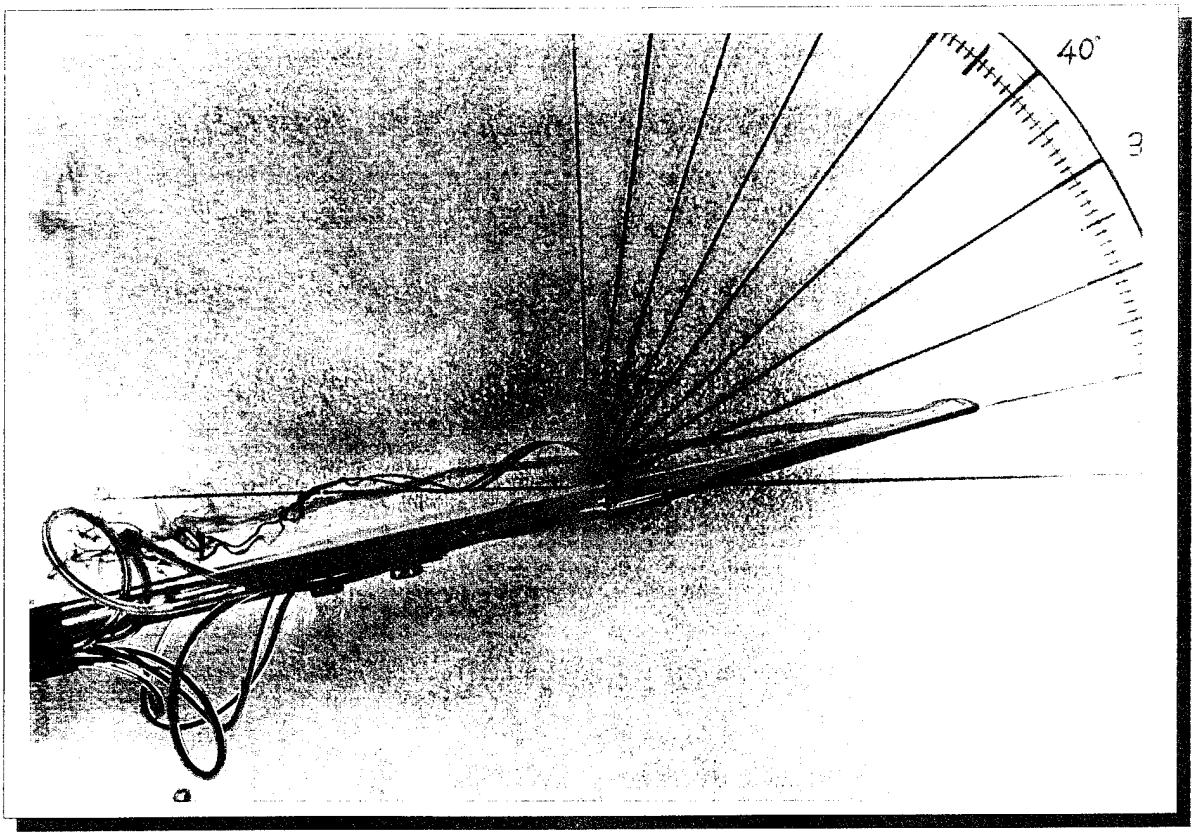

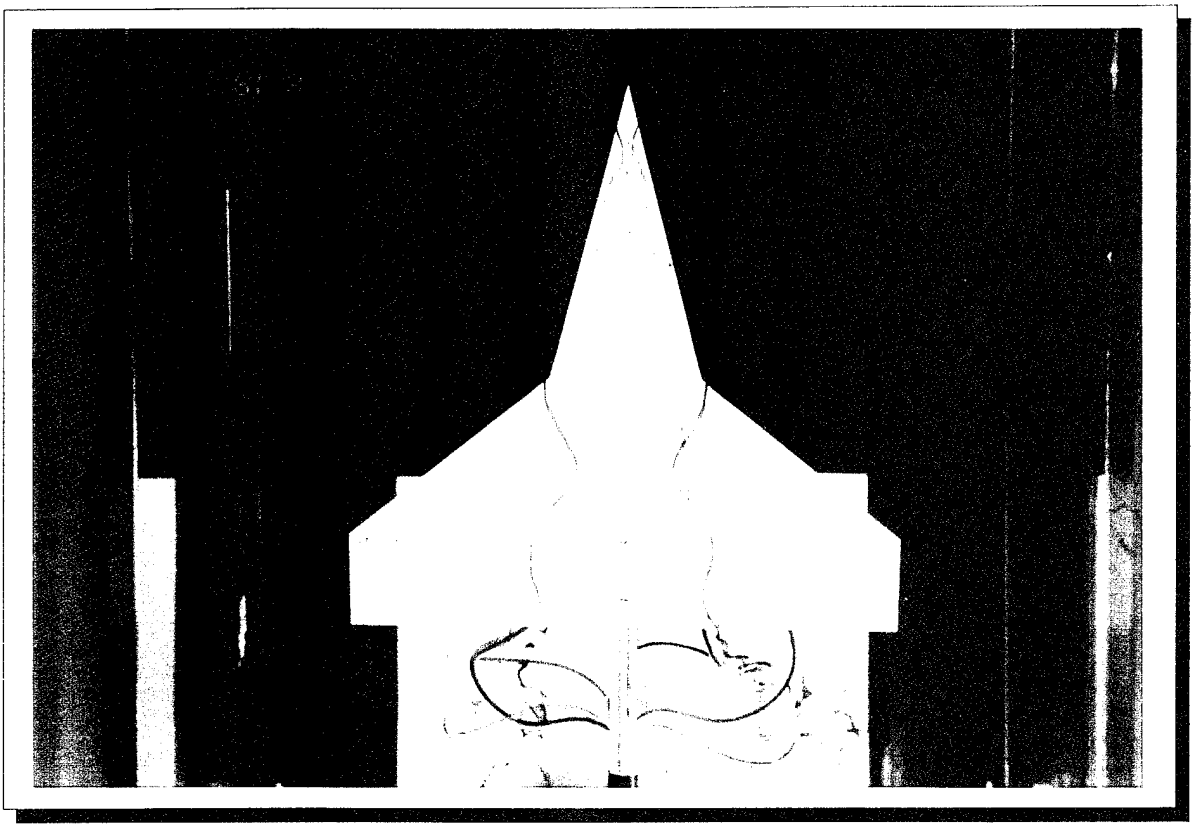

Fig . 20 : Model Sideview - Topview at 10 deg. AOA and V = 0.2 ft / sec .

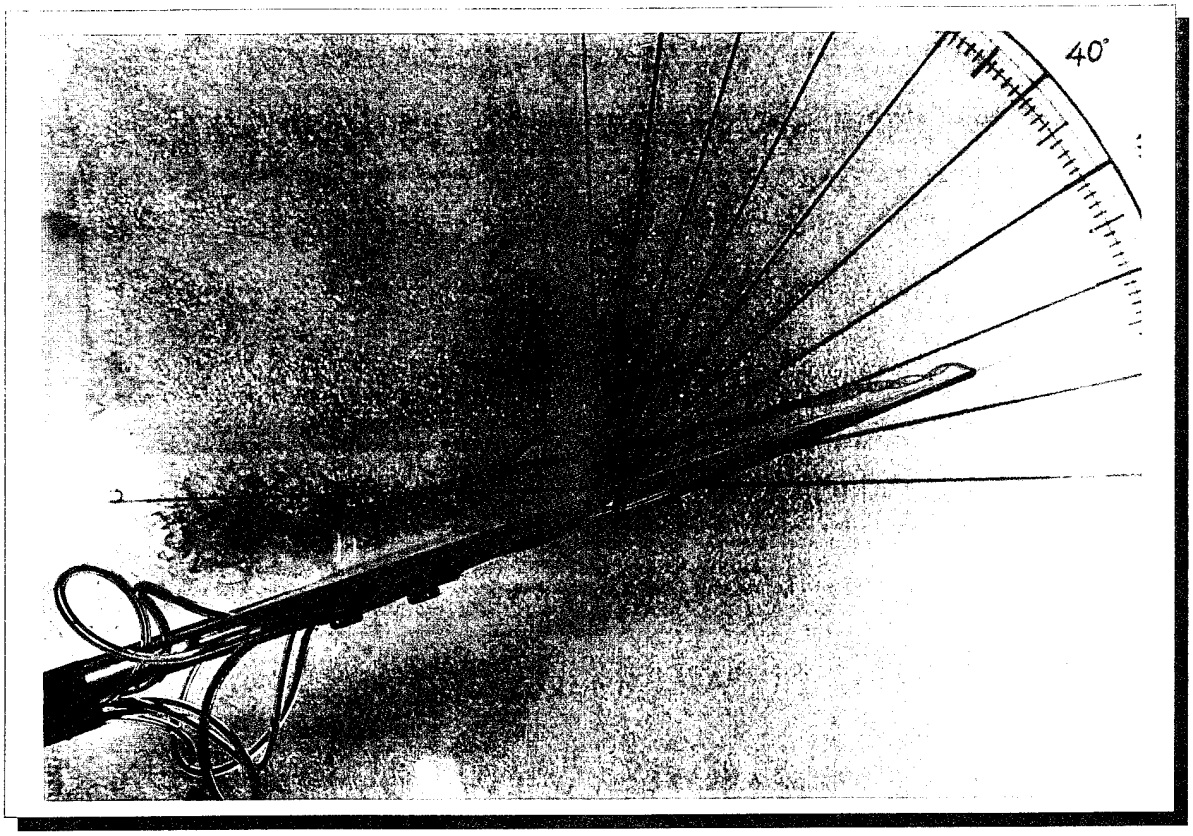

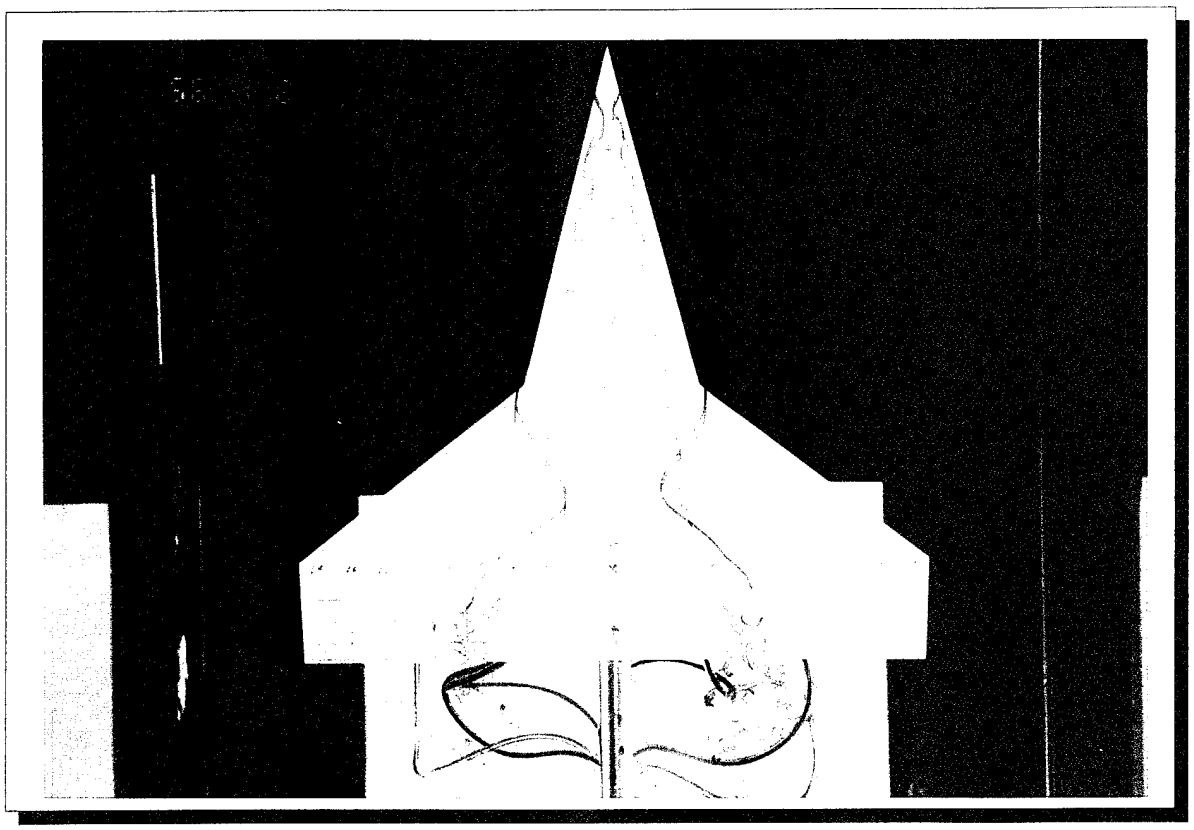

Fig . 21 : Model Sideview - Topview at 15 deg. AOA and V = 0.2 ft / sec .

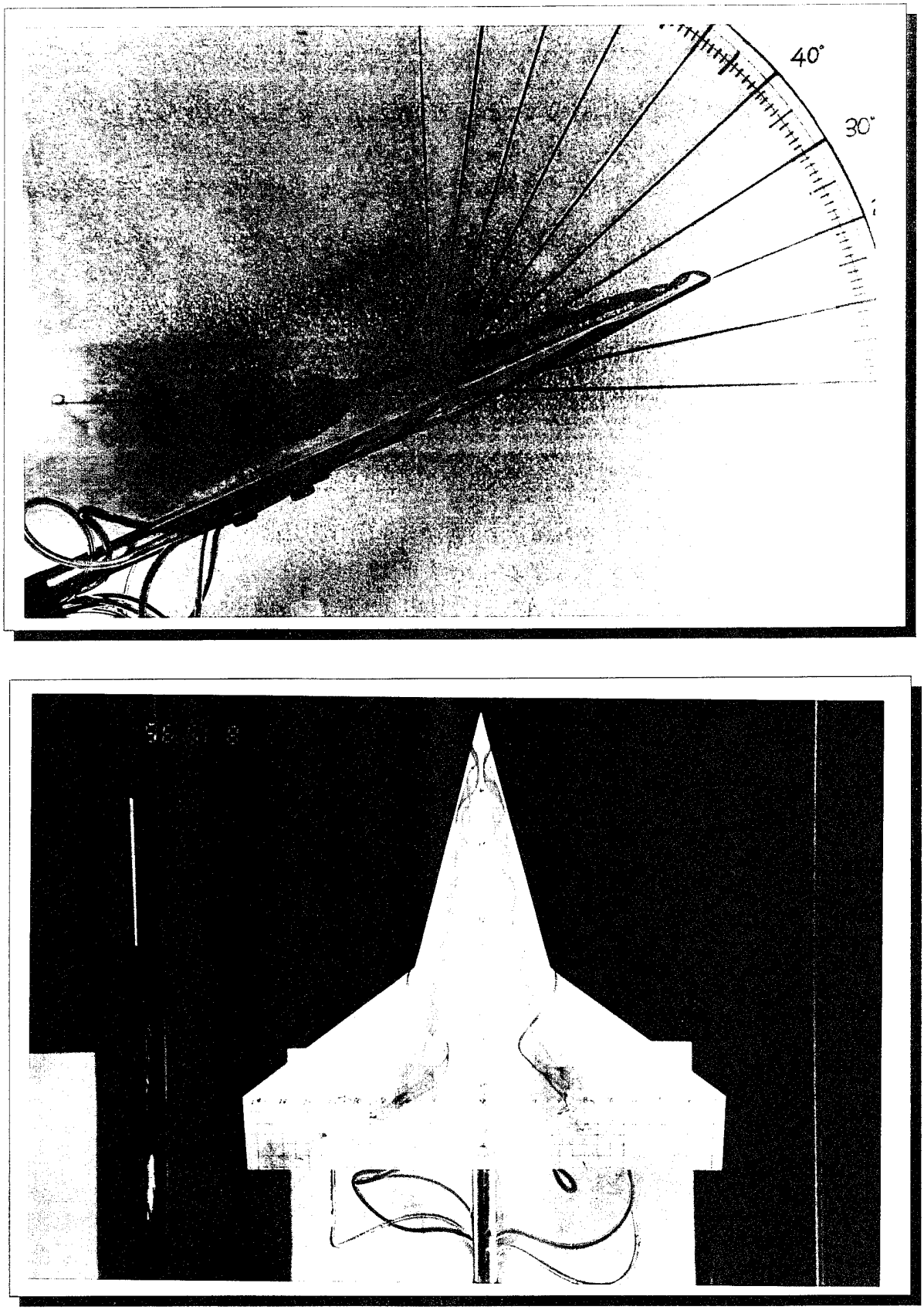

Fig . 22 : Model Sideview - Topview at 20 deg. AOA and V = 0.2 ft / sec .

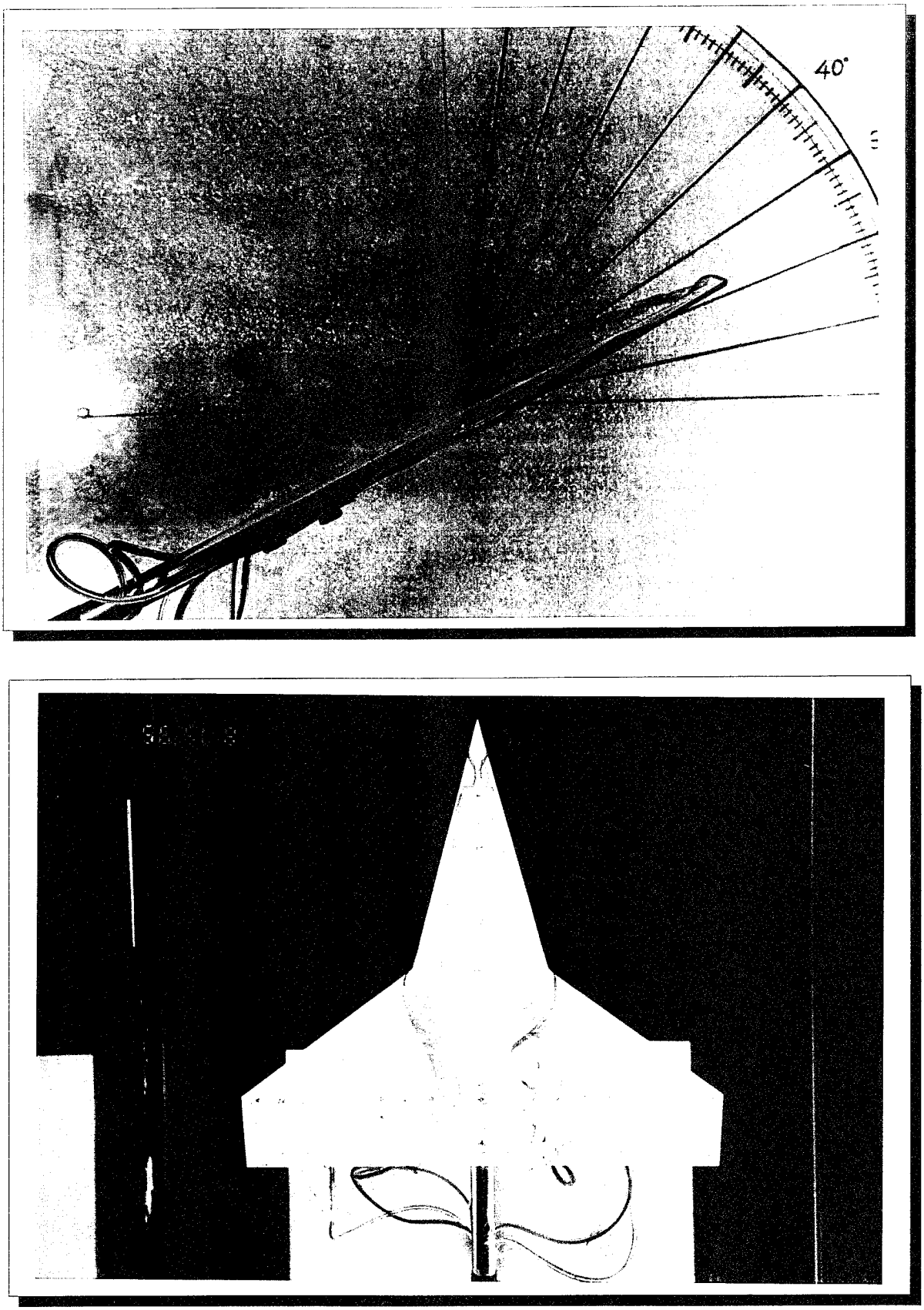

Fig . 23 : Model Sideview - Topview at 22.5 deg AOA and V = 0.2 ft / sec .

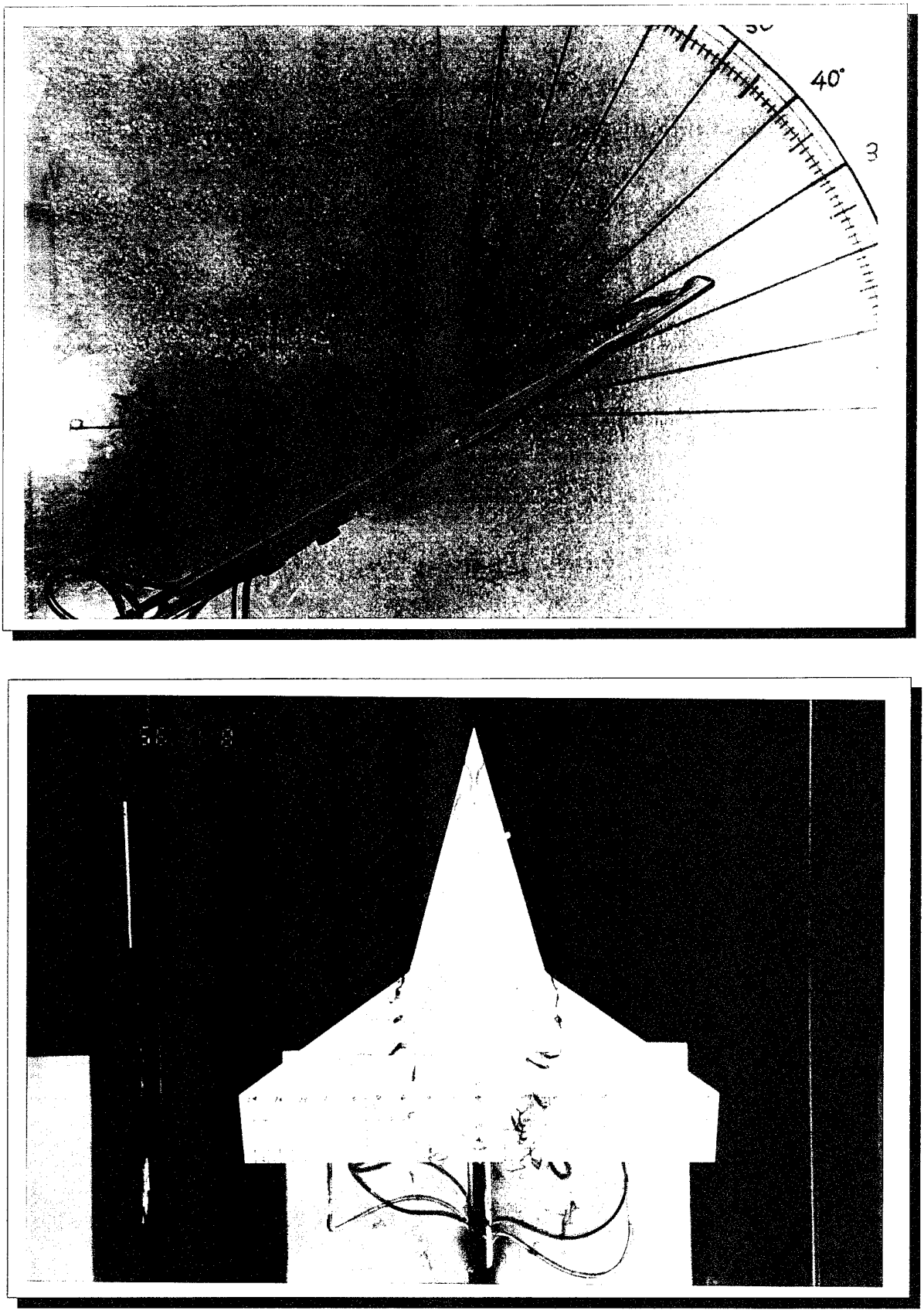

Fig . 24 : Model Sideview - Topview at 25 deg. AOA and V = 0.2 ft / sec .

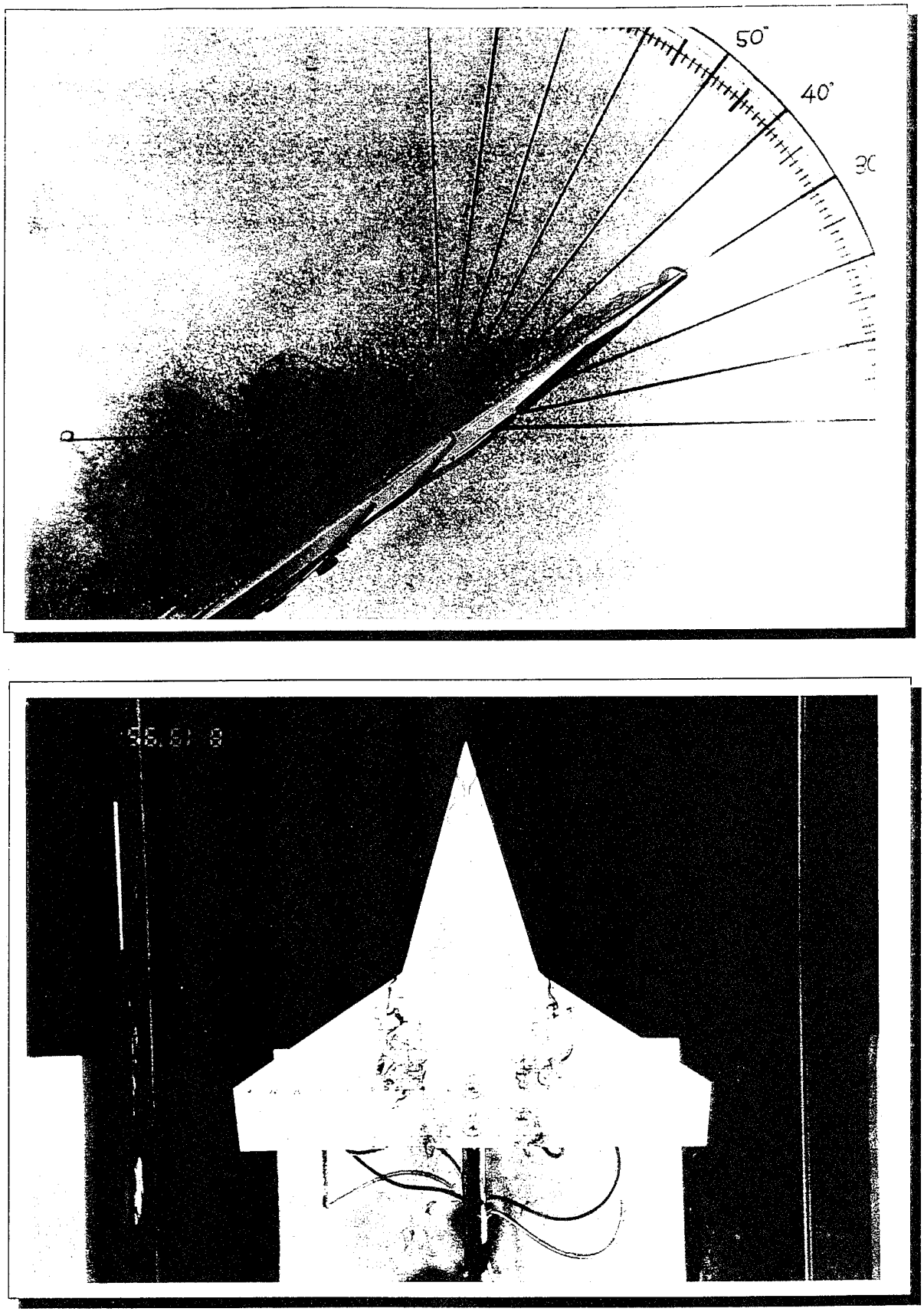

Fig . 25 : Model Sideview - Topview at 30 deg. AOA and V = 0.2 ft / sec .

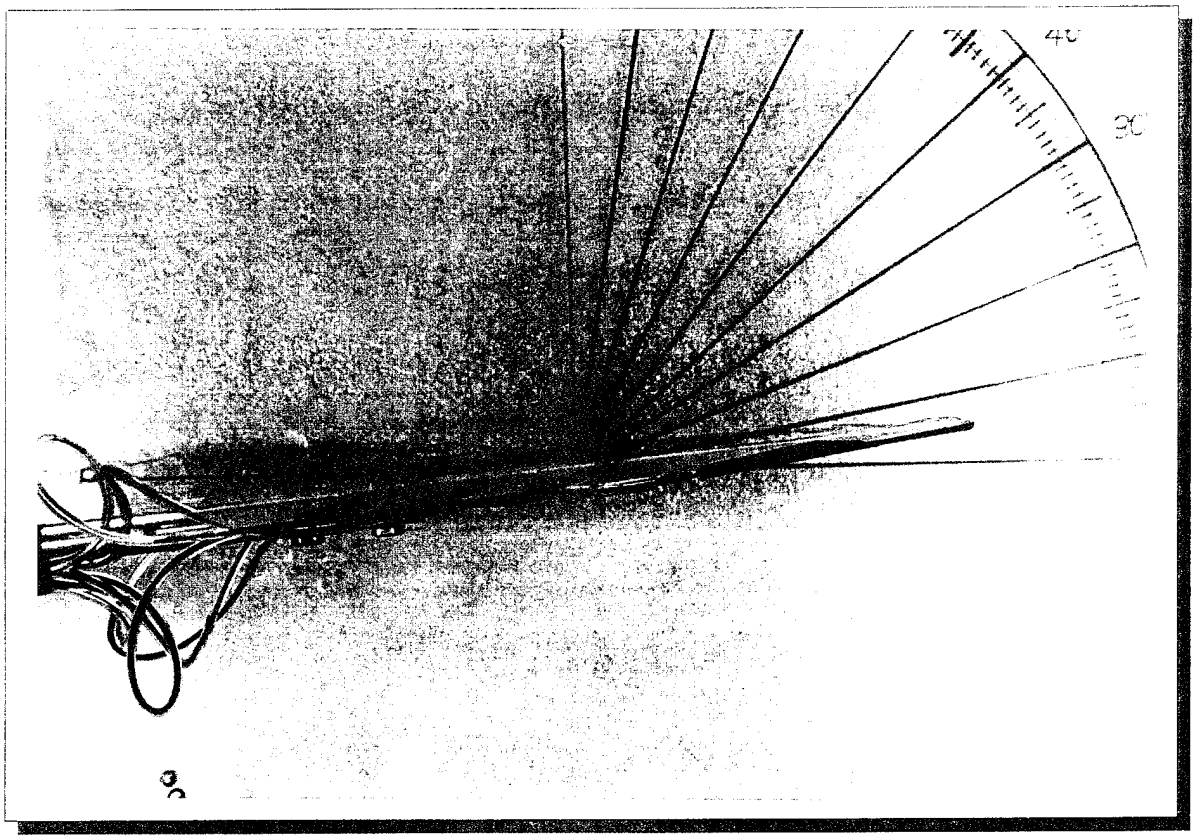

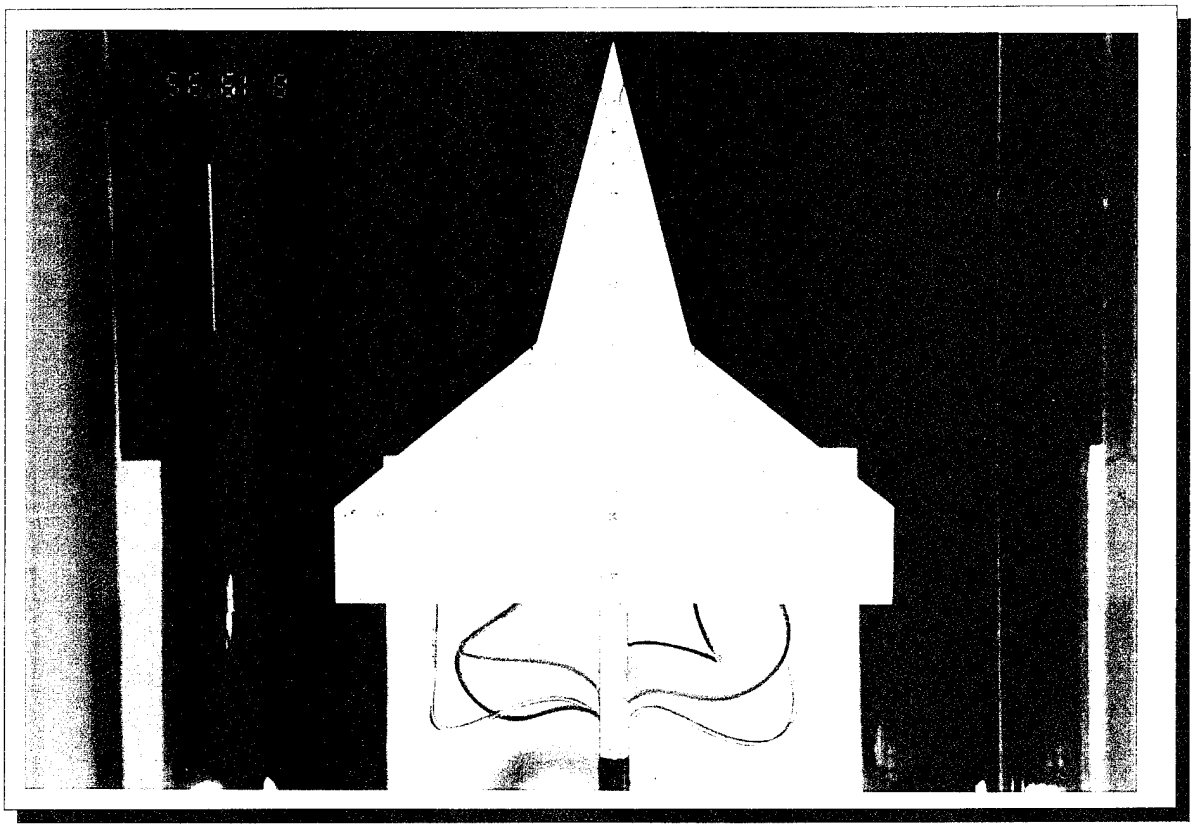

Fig . 26 : Model Sideview - Topview at 5 deg. AOA and V = 0.6 ft / sec .

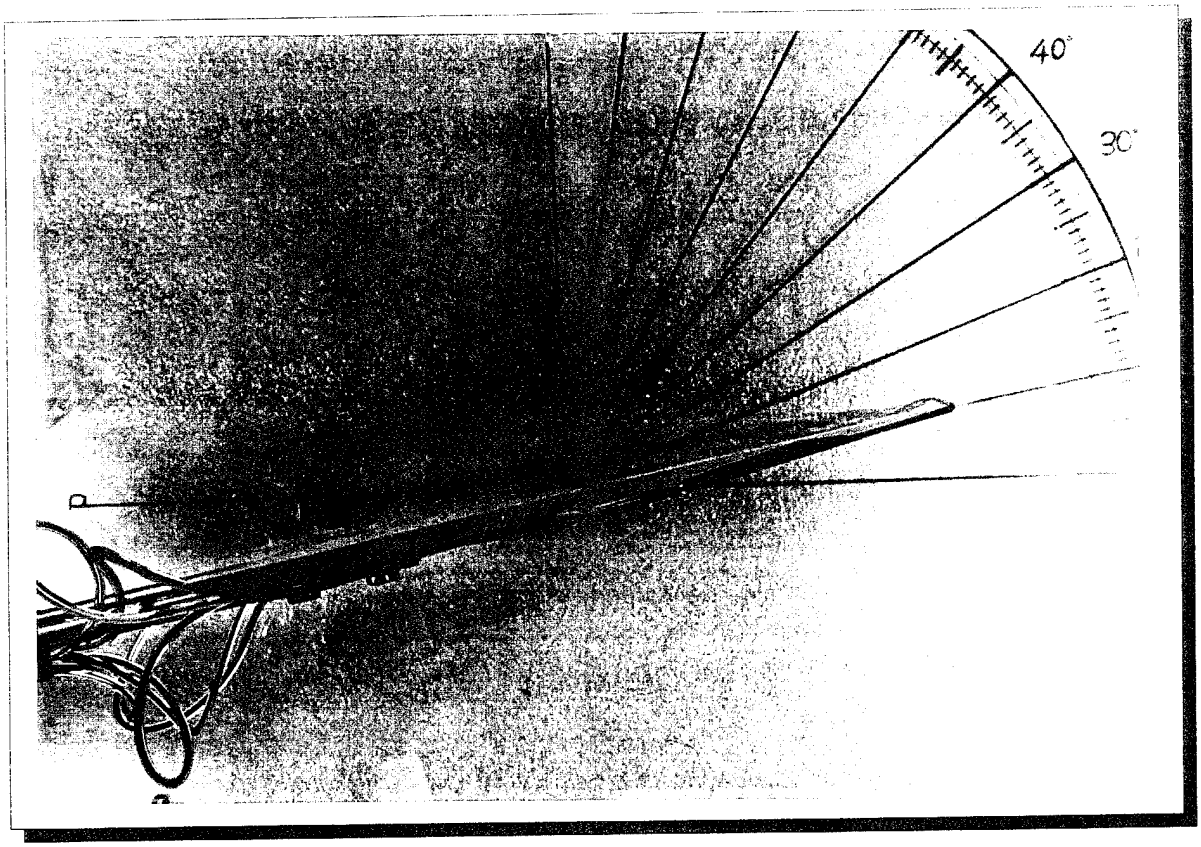

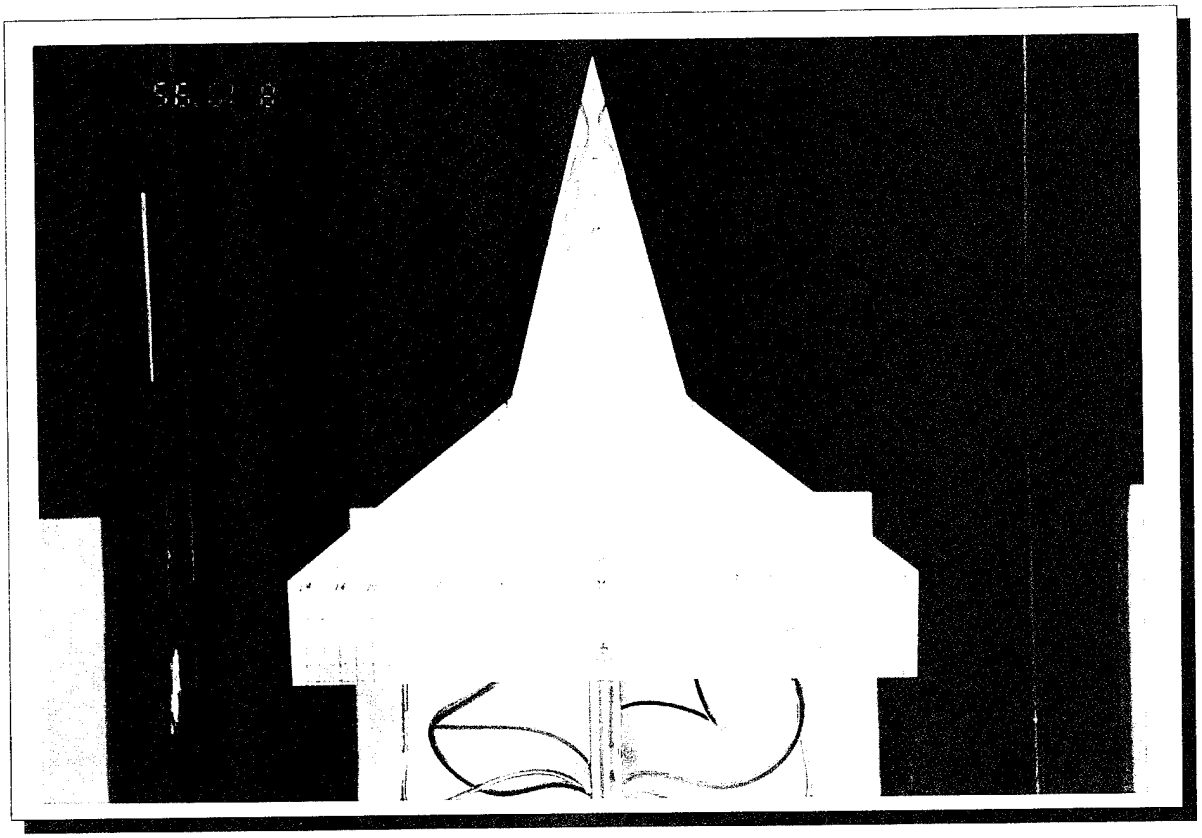

Fig . 27 : Model Sideview - Topview at 10 deg. AOA and V = 0.6 ft / sec .

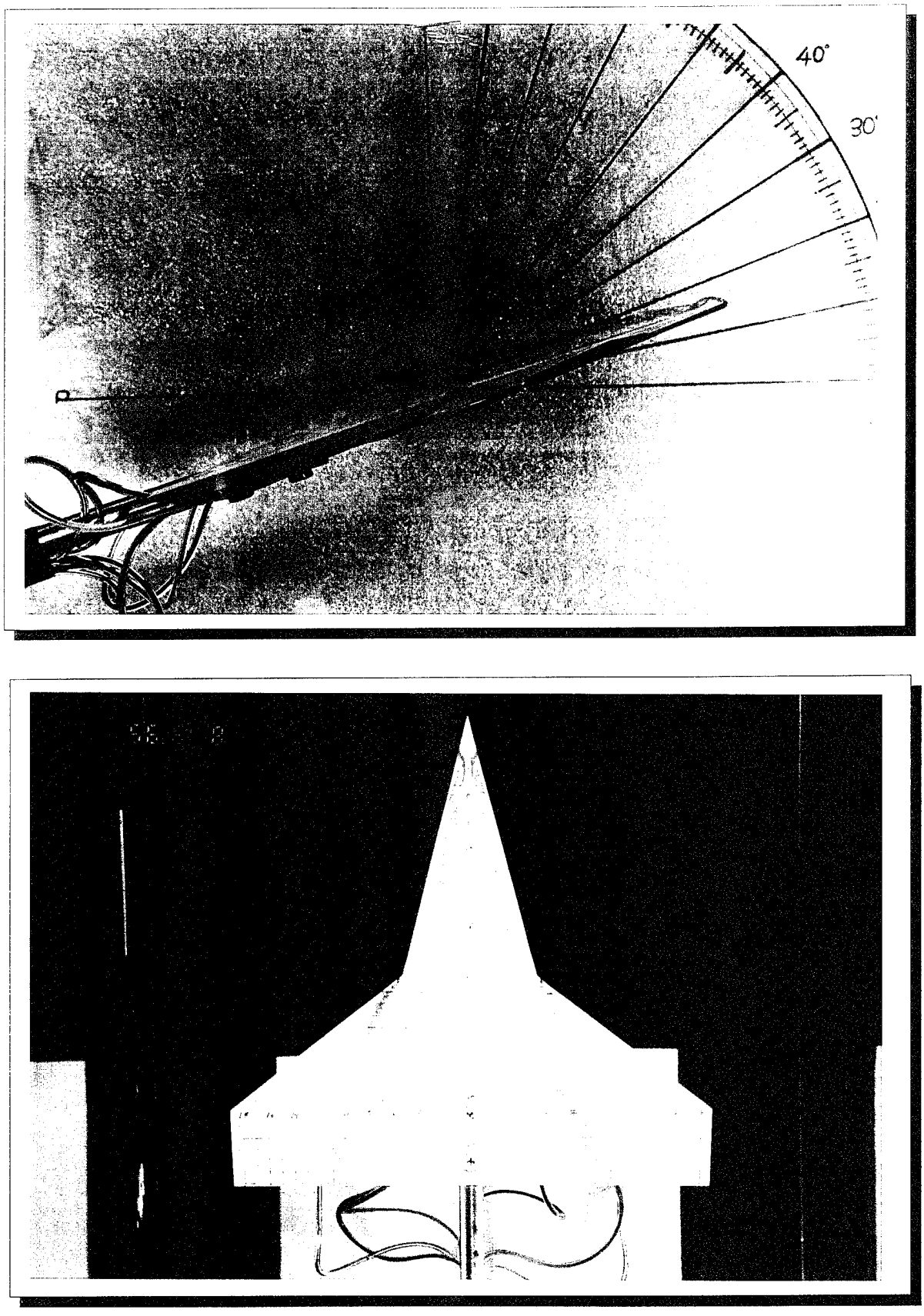

Fig . 28 : Model Sideview - Topview at 15 deg. AOA and V = 0.6 ft / sec .

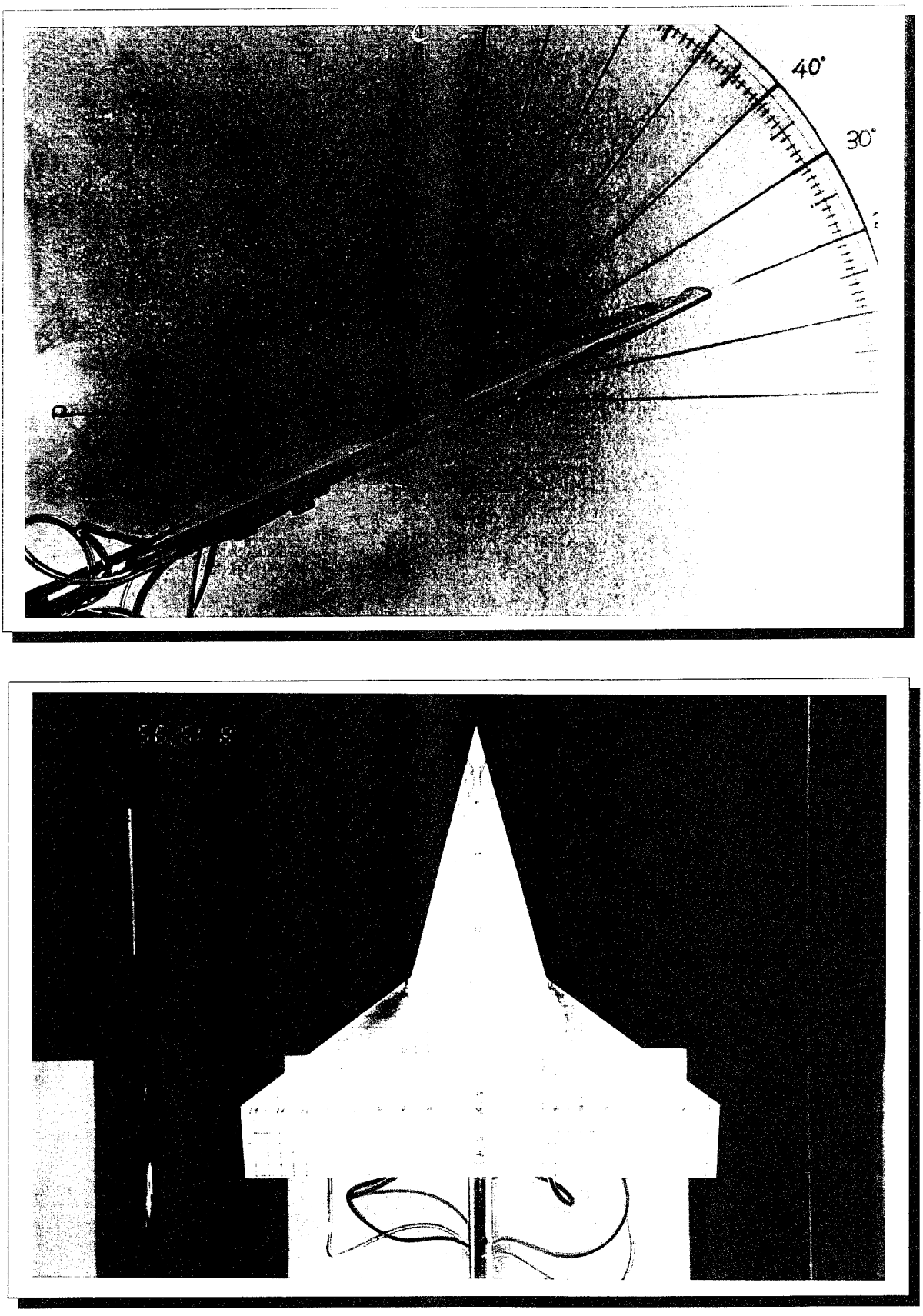

Fig . 29 : Model Sideview - Topview at 20 deg. AOA and V = 0.6 ft / sec .

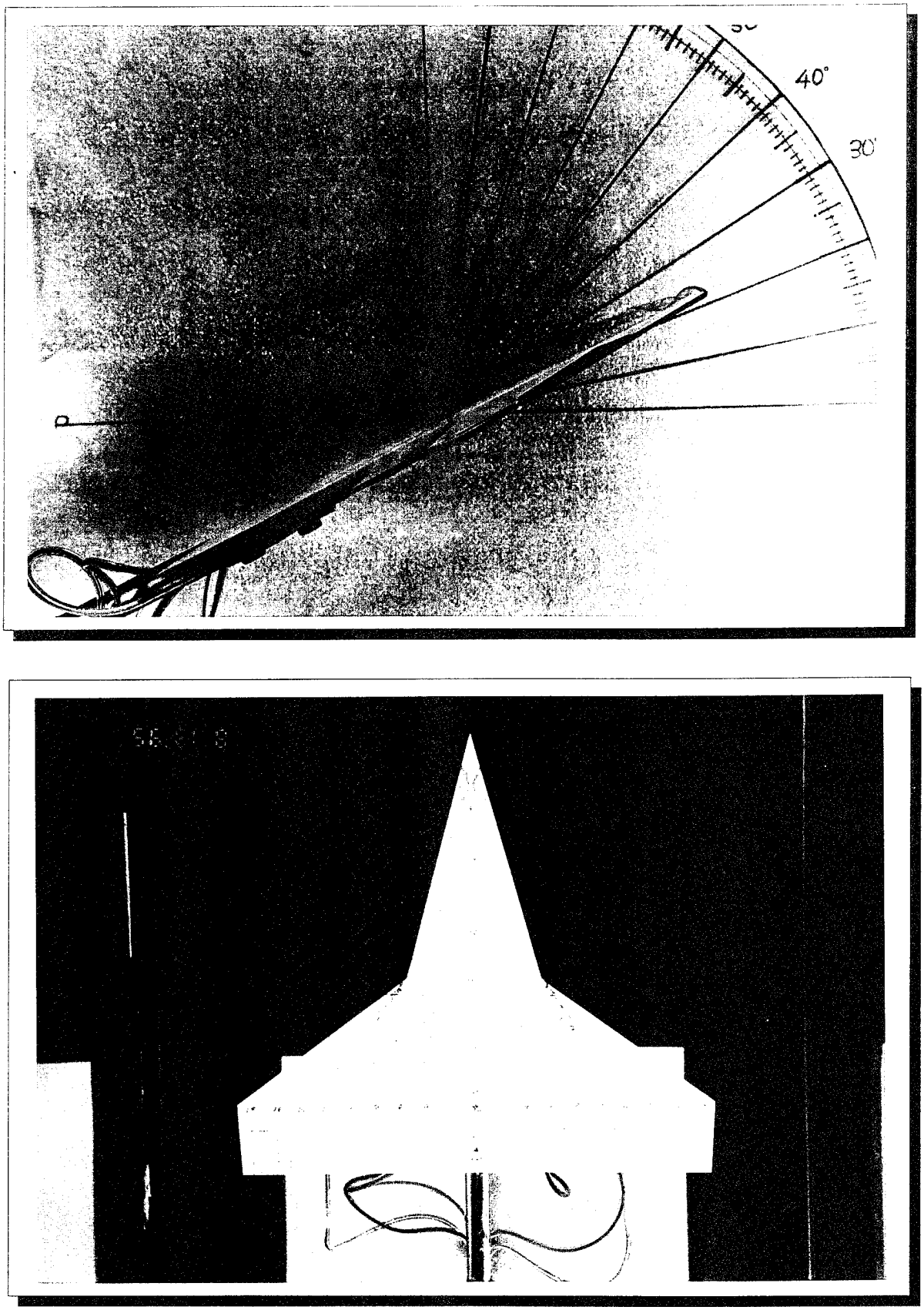

Fig . 30 : Model Sideview - Topview at 22.5 deg. AOA and V = 0.6 ft / sec .

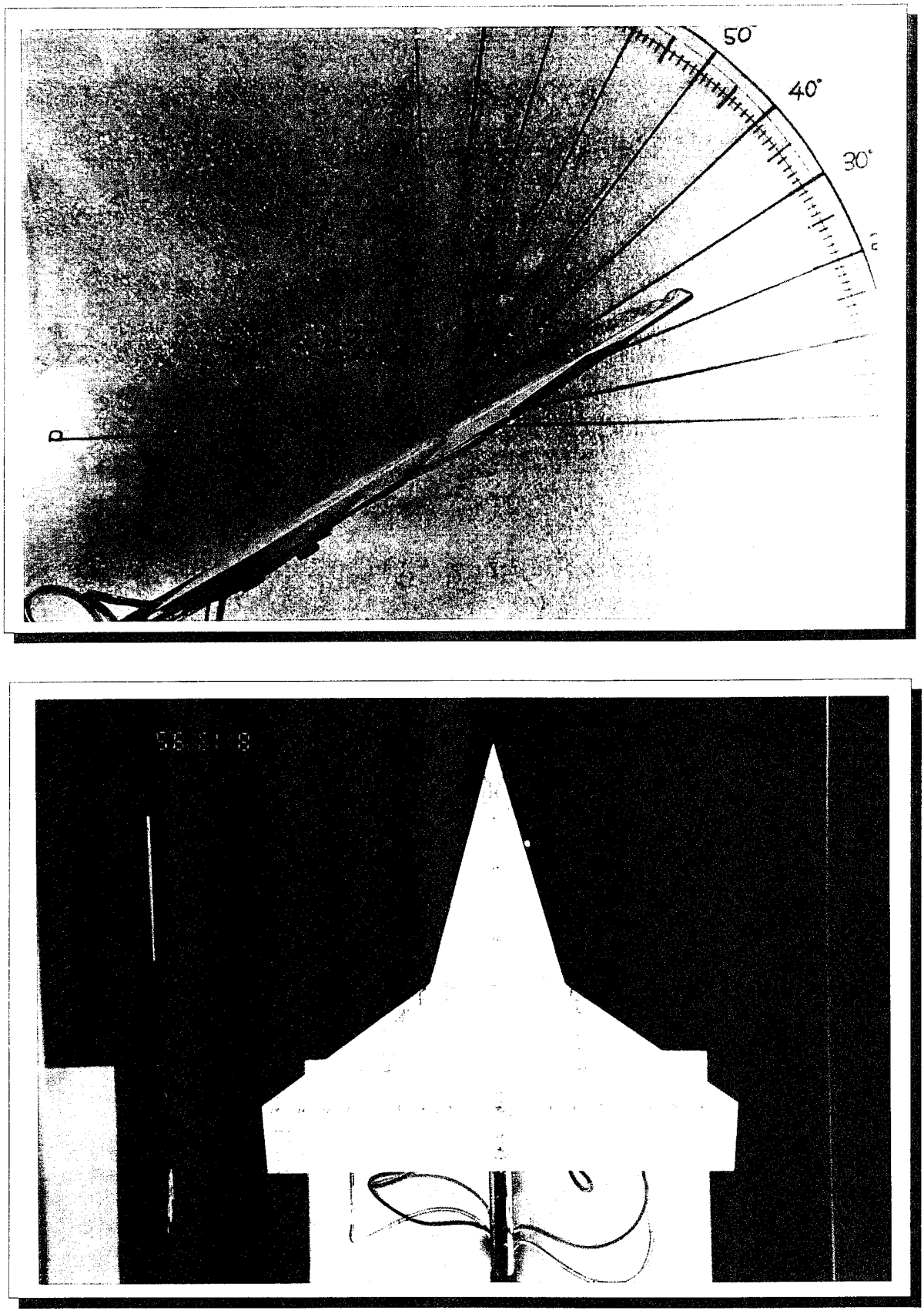

Fig . 31 : Model Sideview - Topview at 25 deg. AOA and V = 0.6 ft / sec .

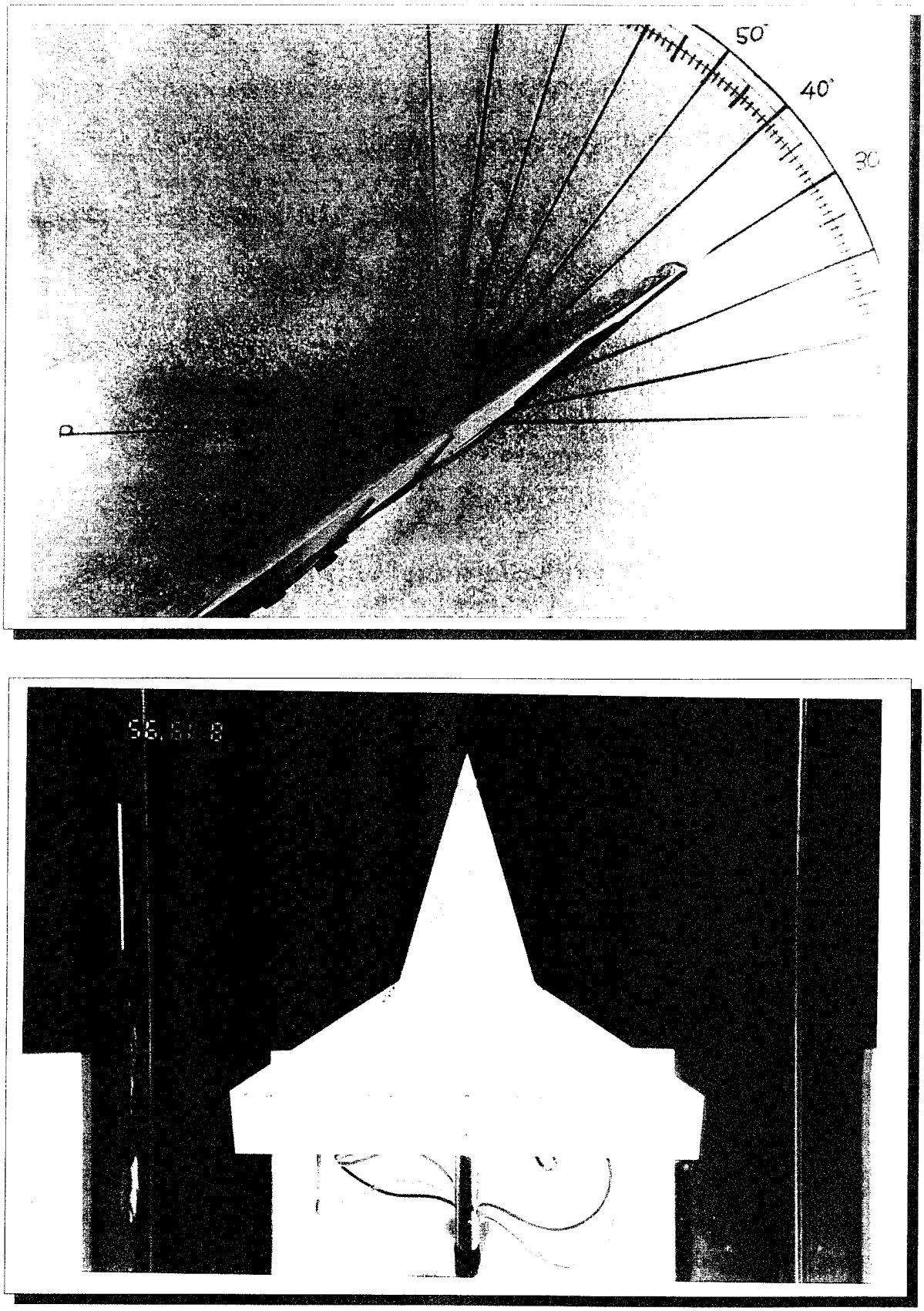

Fig . 32 : Model Sideview - Topview at 30 deg. AOA and V = 0.6 ft / sec .

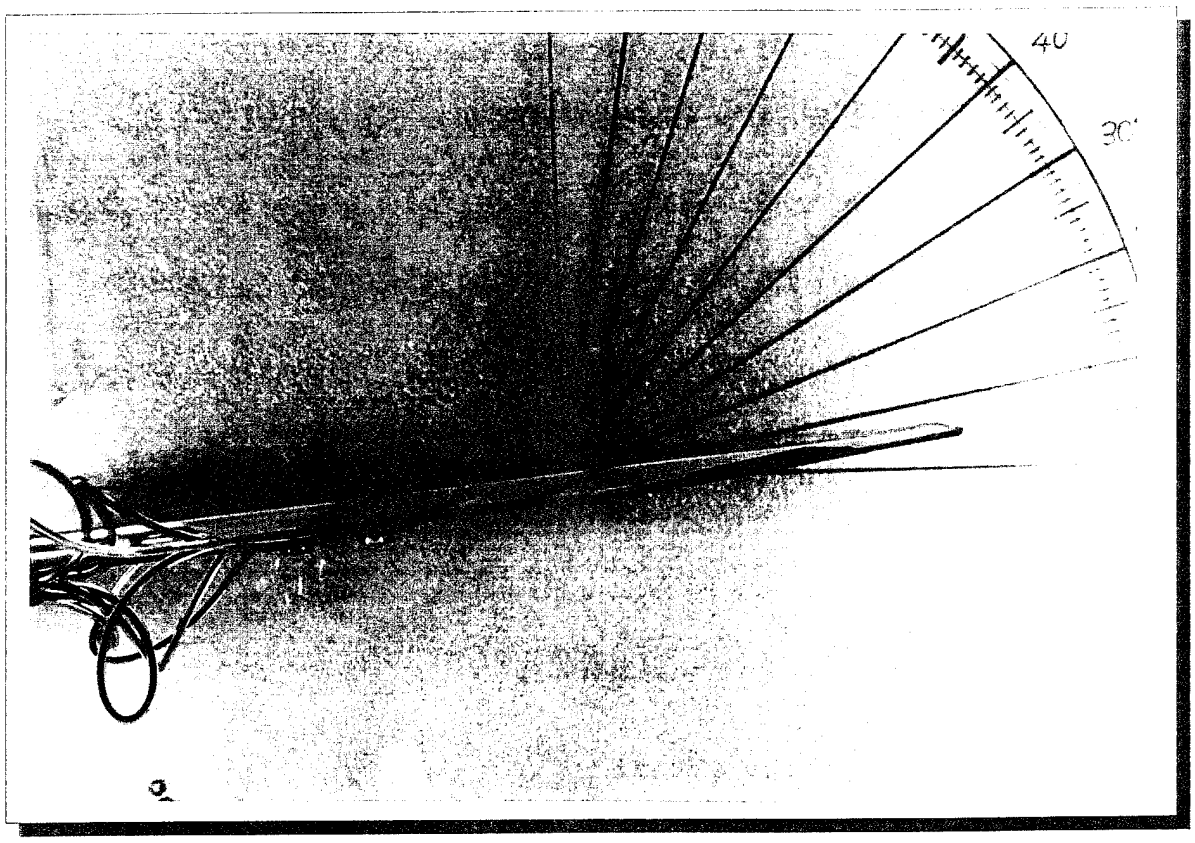

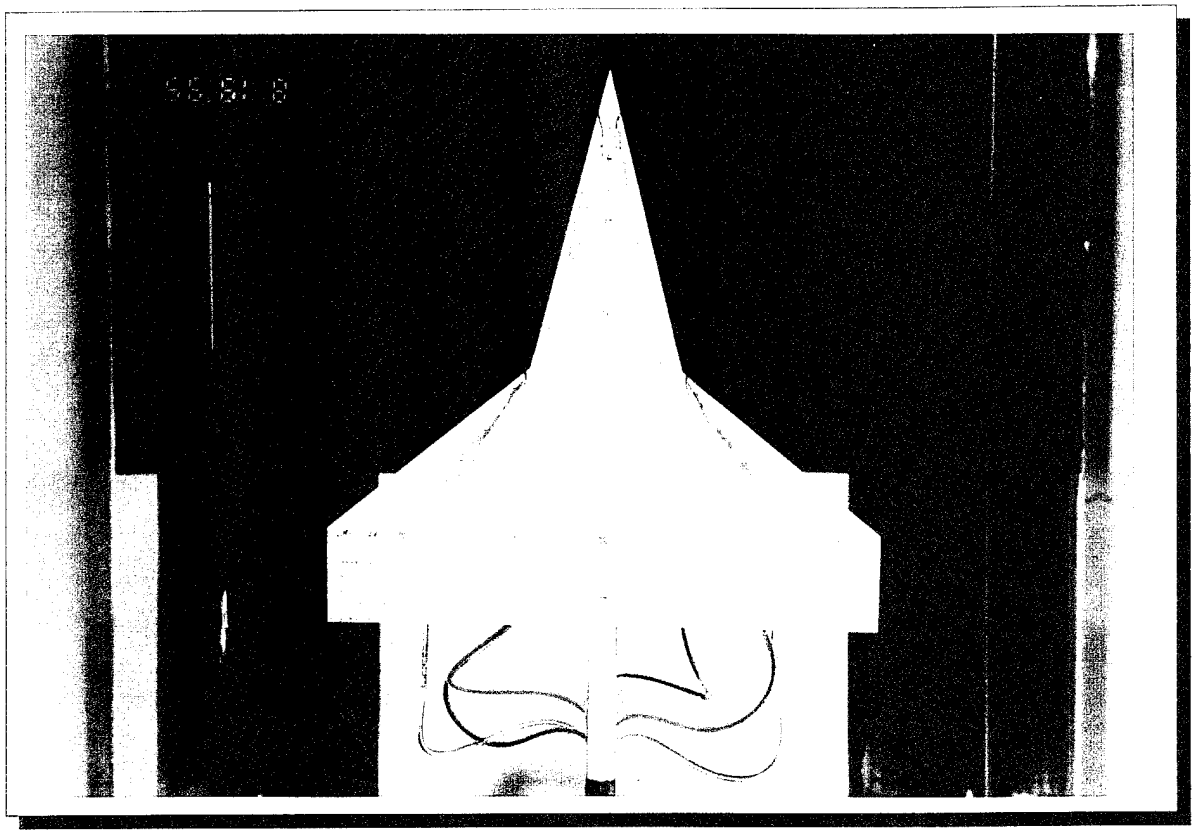

Fig . 33 : Model Sideview - Topview at 5 deg. AOA and V = 1.0 ft / sec .

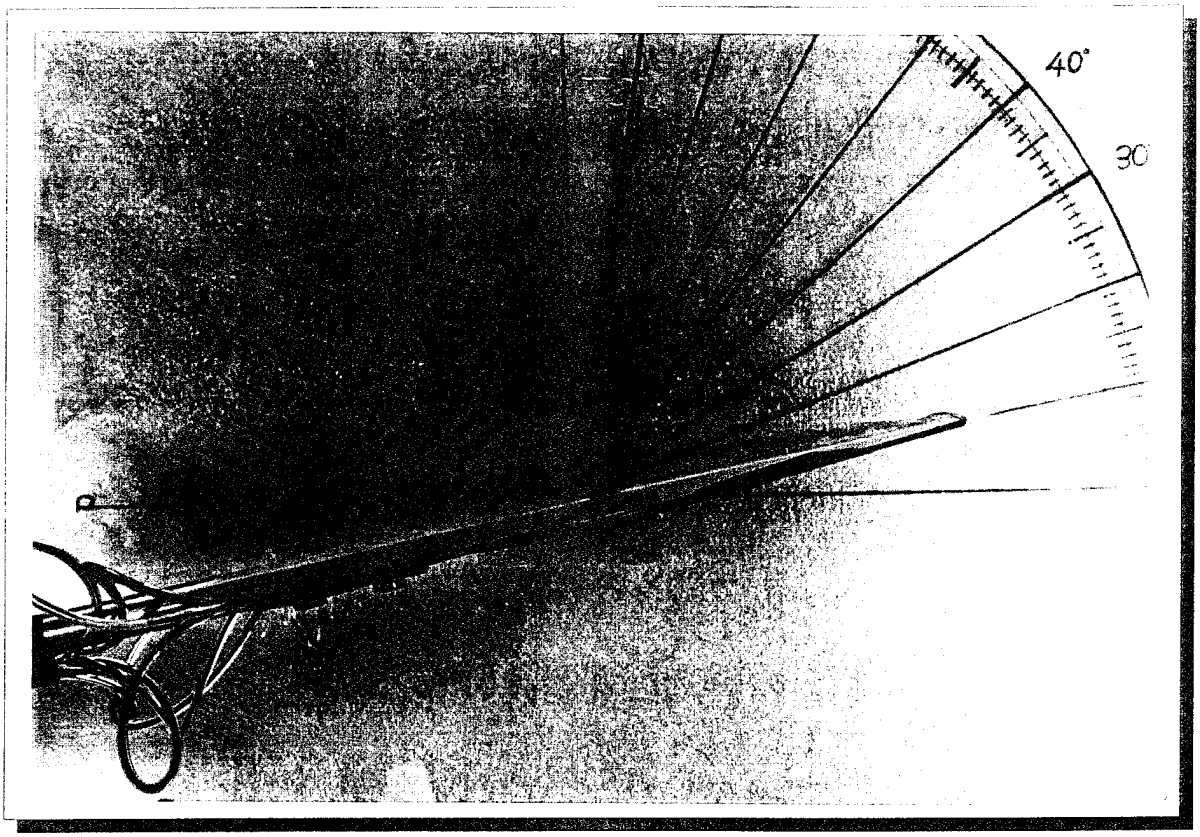

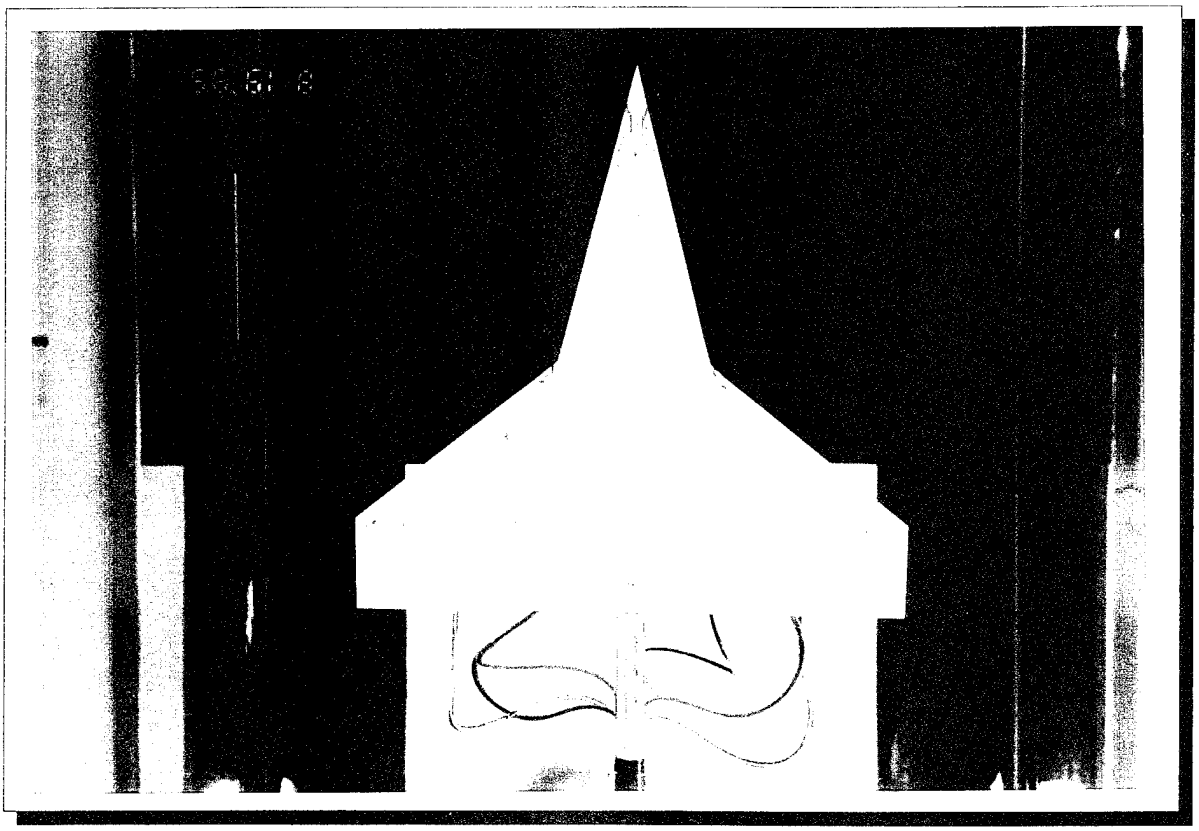

Fig . 34 : Model Sideview - Topview at 10 deg. AOA and V = 1.0 ft / sec .

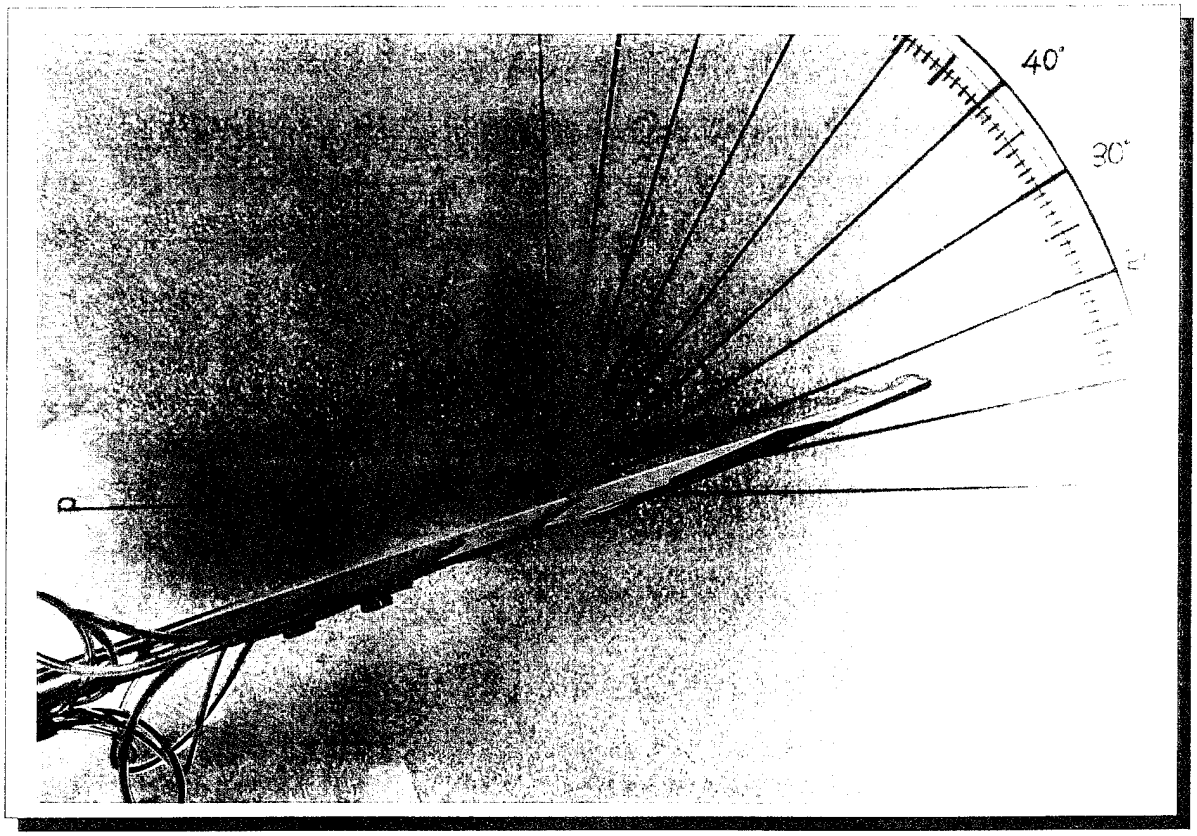

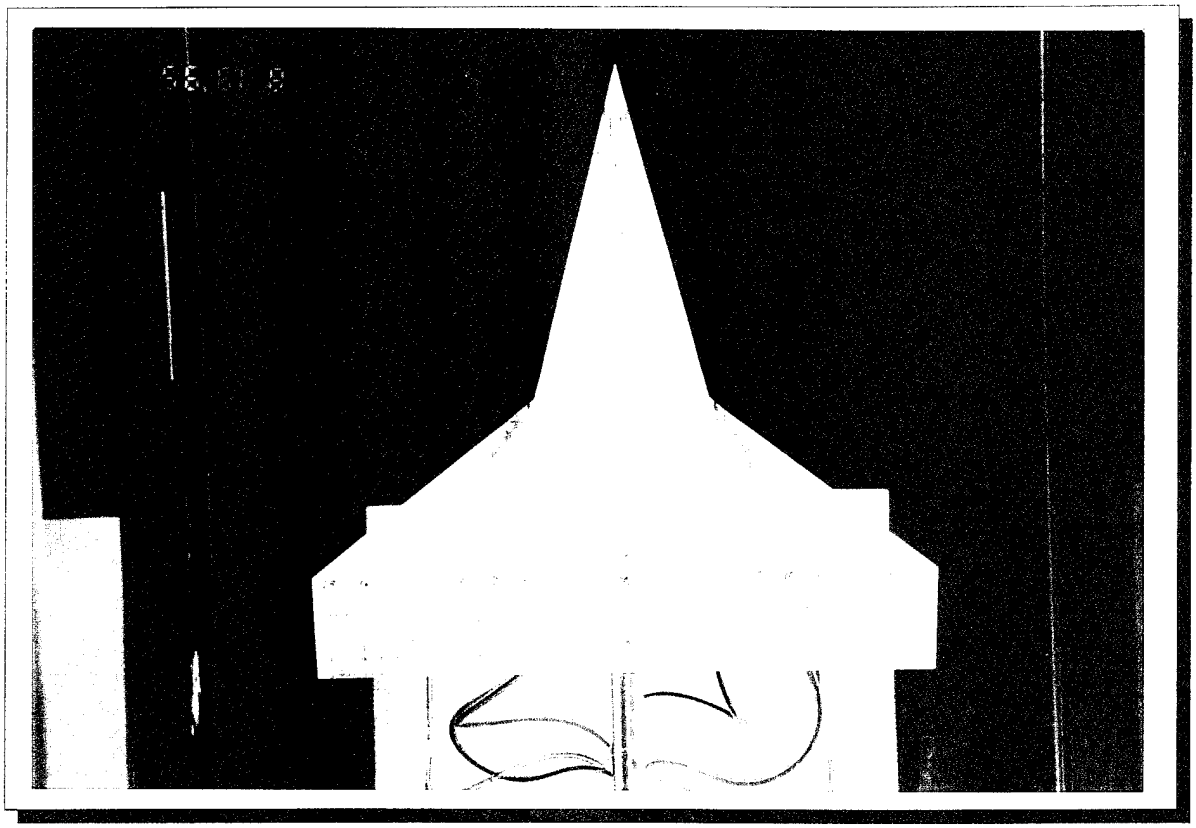

Fig . 35 : Model Sideview - Topview at 15 deg. AOA and V = 1.0 ft / sec .

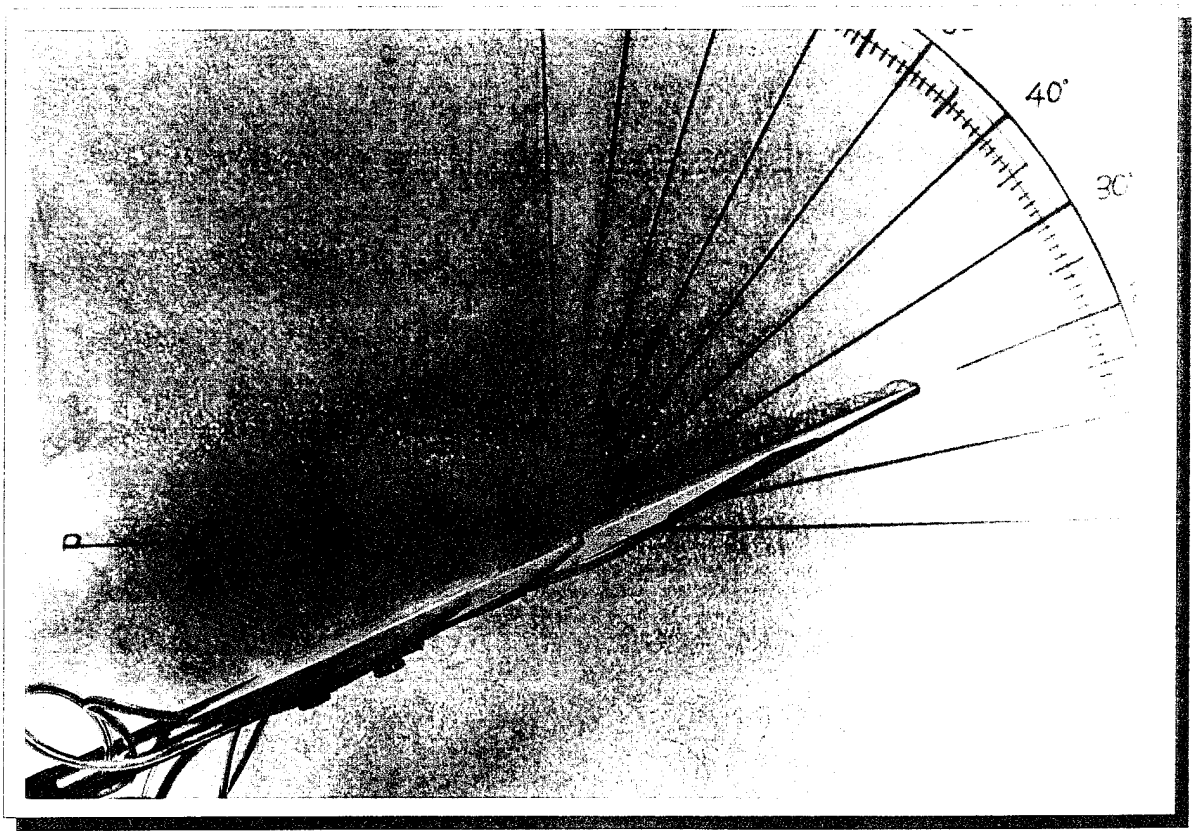

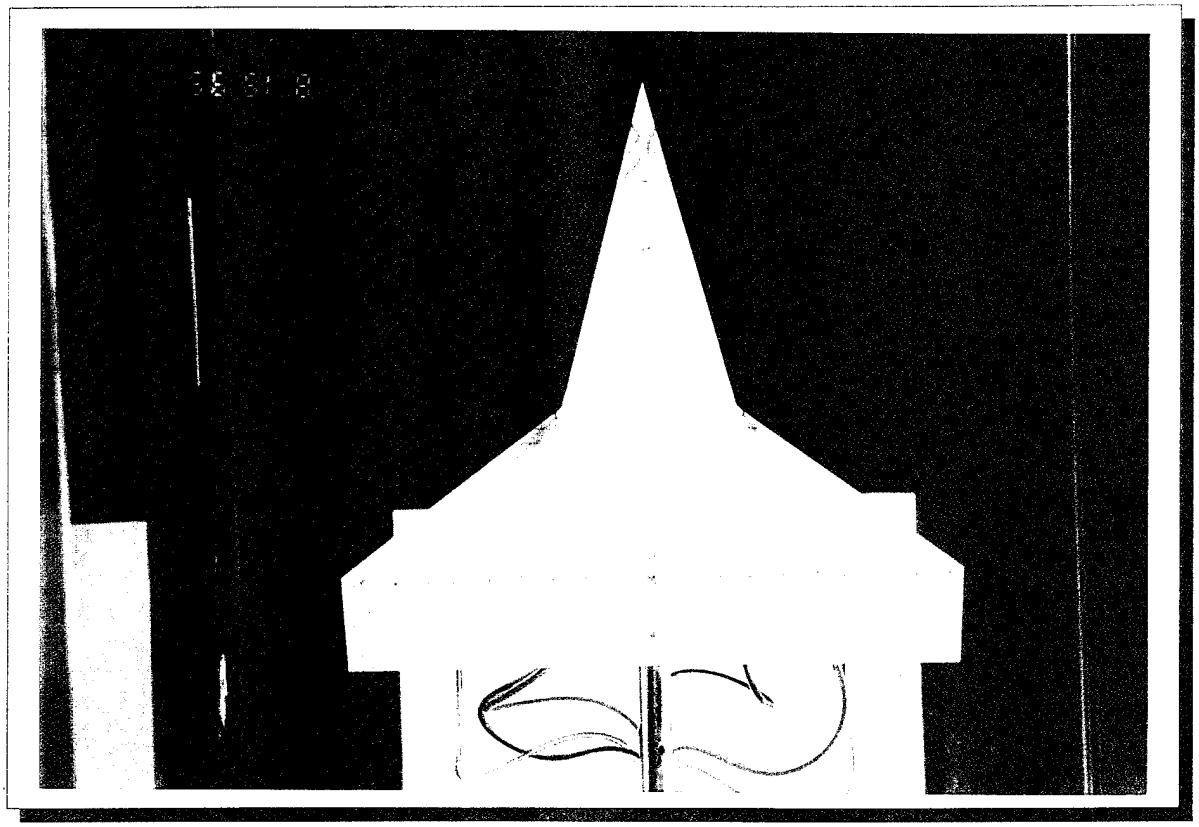

Fig . 36 : Model Sideview - Topview at 20 deg. AOA and V = 1.0 ft / sec .

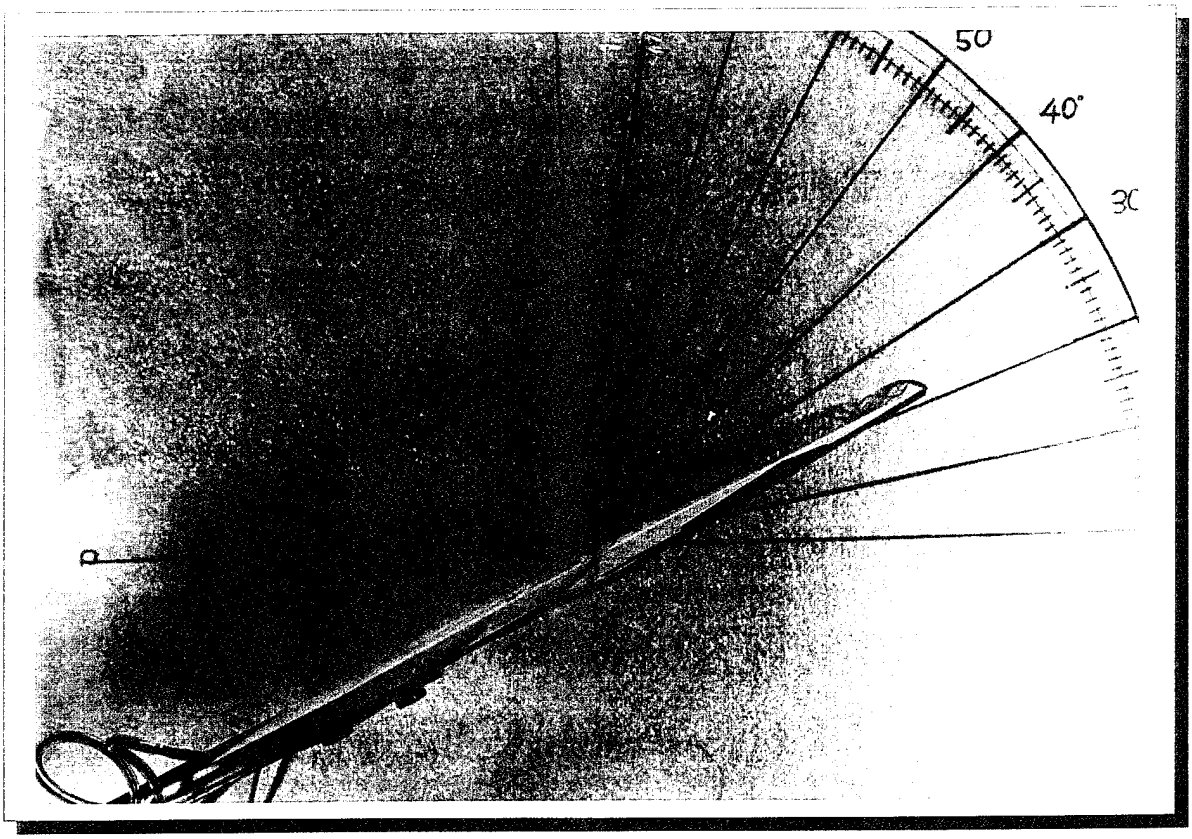

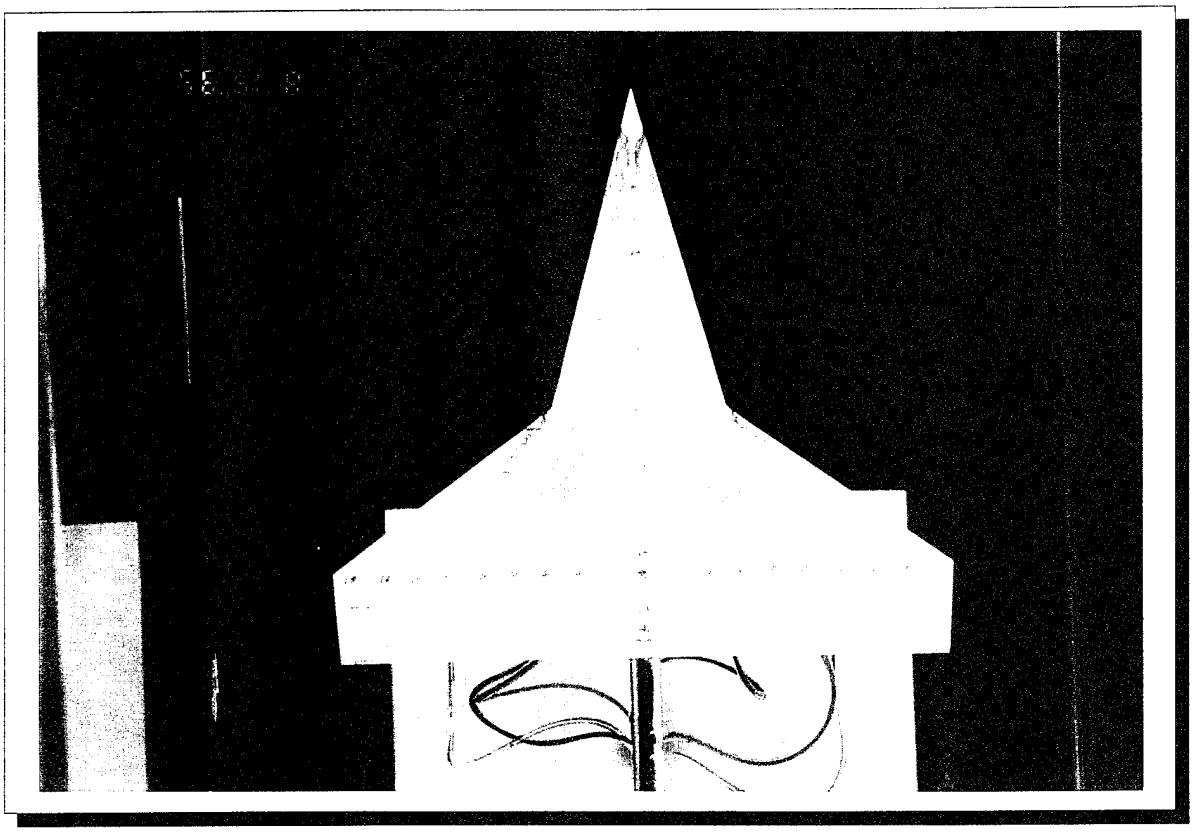

Fig . 37 : Model Sideview - Topview at 22.5 deg. AOA and V = 1.0 ft / sec .

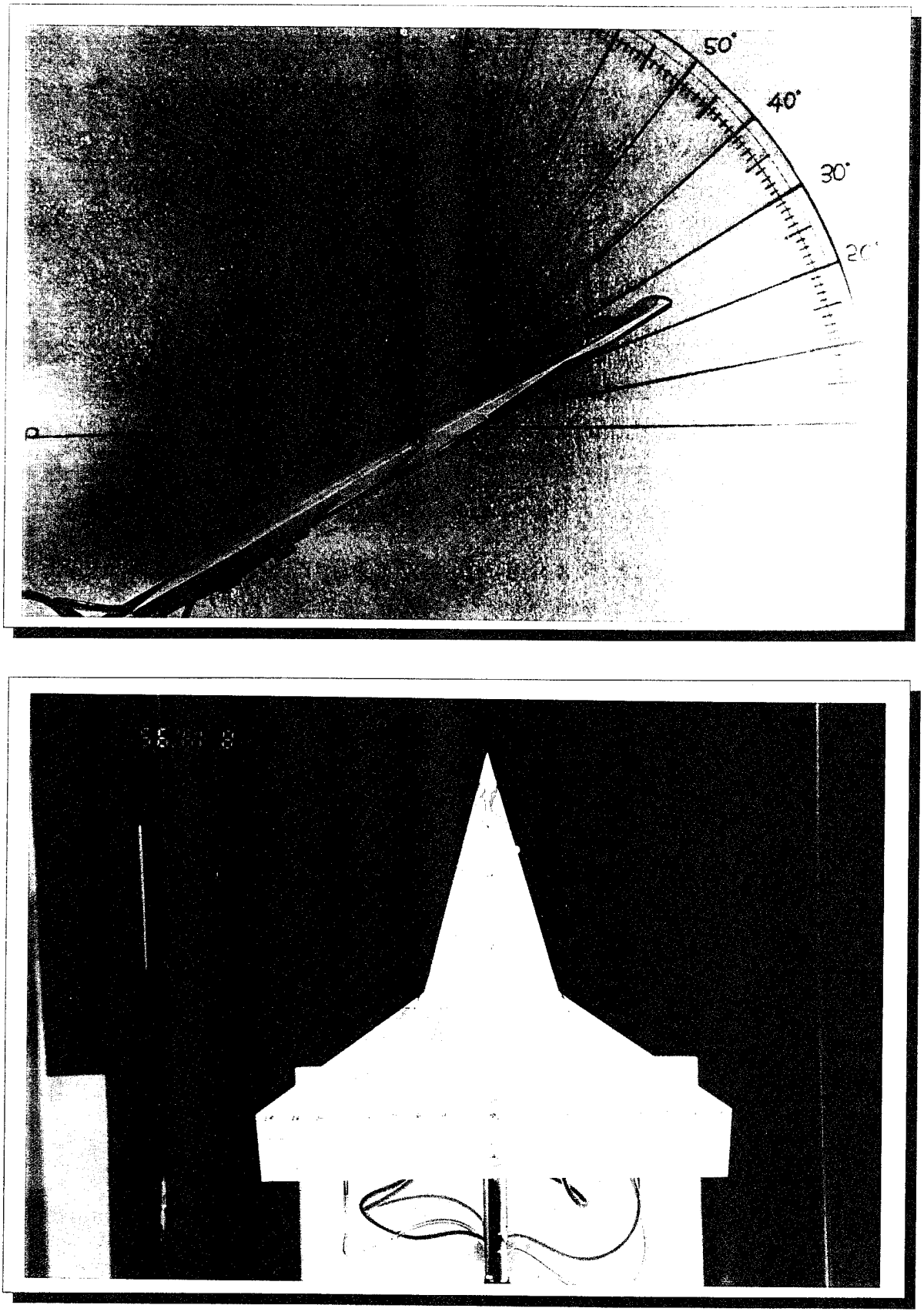

Fig . 38 : Model Sideview - Topview at 25 deg. AOA and V = 1.0 ft / sec .

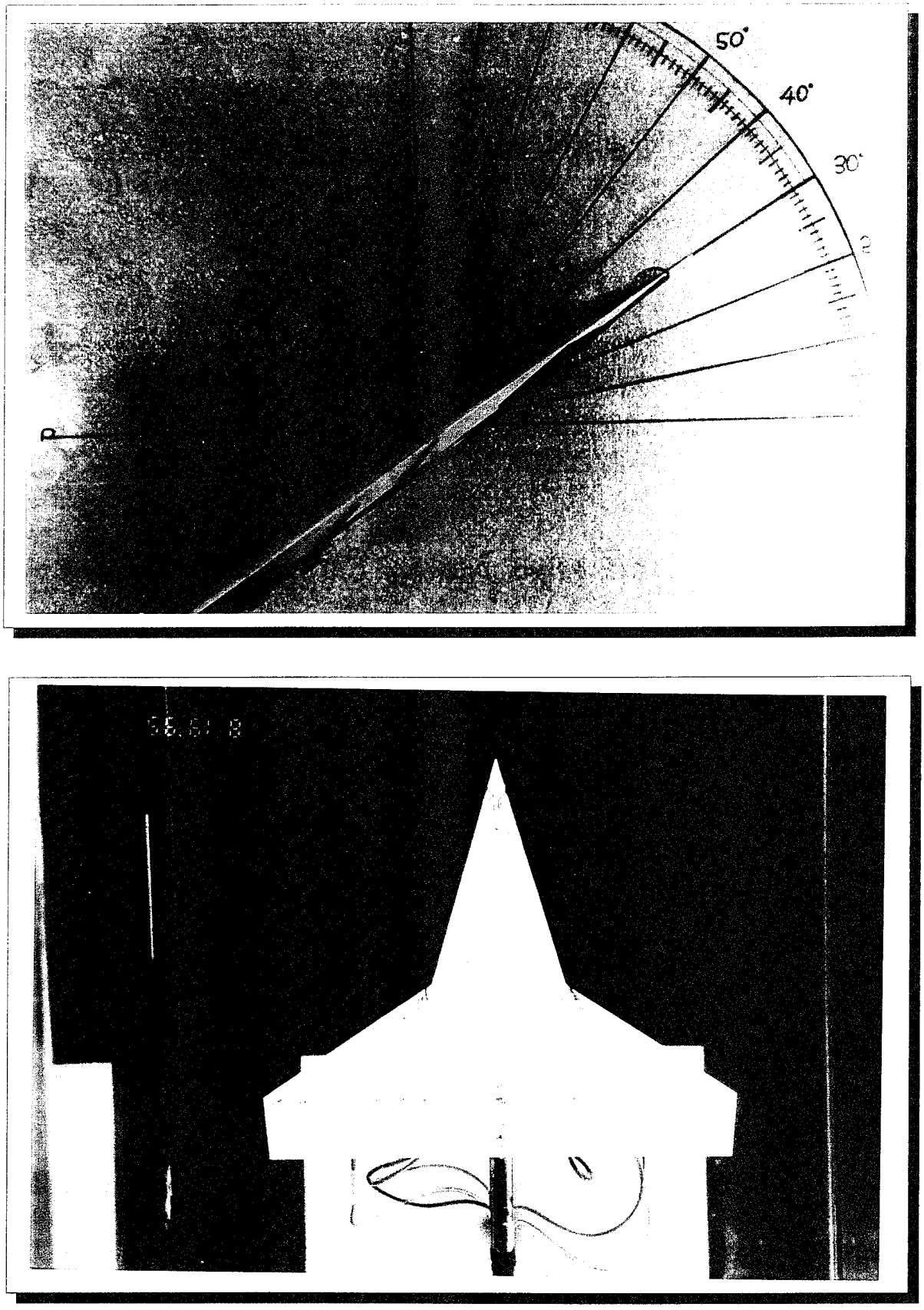

Fig . 39 : Model Sideview - Topview at 30 deg. AOA and V = 1.0 ft / sec .

APPENDIX - B

EXPERIMENTAL RESULTS

(TABLES AND GRAPHS)

Table 3: Strake Vortex core trajectory in % , V = 0.2 ft/sec - AOA = 5 deg .

X/C	Y/S	X/C	Z/S
0	60.19	0	5.26
6.93	61.55	64.38	1.5
13.86	47.88	70.06	0.75
20.79	47.19	75.74	1.5
27.72	40.35	95.43	0
34.65	30.78		
41.58	24.62		
48.52	19.83		
55.45	17.78		
62.38	13.68		
69.31	10.26		
76.24	11.63		
83.17	4.1		
90.1	1.37		
95.3	2.32		

Table 4: Wing Vortex core trajectory in % , V = 0.2 ft/sec - AOA = 5 deg .

X/C	Y/S	X/C	Z/S
0	62.92	0	1.05
6.93	47.88	3.79	1.09
13.86	49.24	7.57	1.13
20.79	52.66	11.36	5.26
27.72	28.73	15.15	0.75
34.65	25.31	18.93	5.26
41.59	29.41	22.72	0.75
46.09	30.78	26.51	3.76
		30.3	3.76
		34.08	5.26
		41.66	4.51
		45.44	2.25

Table 5: Strake Vortex core trajectory in % , V = 0.2 ft/sec - AOA = 10 deg .

X/C	Y/S	X/C	Z/S
0	43.69	0	12.28
7.19	36.65	96	0
14.39	31.01		
21.58	24.67		
28.77	23.96		
35.96	21.85		
43.16	20.44		
50.35	17.62		
57.54	15.5		
64.74	14.09		
71.93	10.57		
79.12	7.05		
86.32	7.05		
93.51	1.41		

Table 6: Wing Vortex core trajectory in % , V = 0.2 ft/sec - AOA = 10 deg .

X/C	Y/S	X/C	Z/S
0	36.65	1.65	6.55
7.19	29.6	6.19	5.73
14.39	33.83	10.31	9.82
21.58	29.6	14.44	14.73
28.77	19.03	18.57	14.73
35.96	21.85	23.11	11.46
43.16	30.3	26.82	6.55
		30.95	6.55
		35.07	9.82
		39.2	12.28
		43.32	9
		47.45	0

Table 7: Strake Vortex core trajectory in % , V = 0.2 ft/sec - AOA = 15 deg .

X/C	Y/S	X/C	Z/S
4.25	36.74	4.03	19.39
9.12	31.95	22.18	13.22
15.2	24.49	95.44	0
21.28	22.9		
27.35	19.7		
33.43	19.7		
39.51	16.51		
45.59	15.97		
51.67	14.38		
57.75	13.31		
63.83	9.58		
69.91	7.99		
75.99	7.45		
82.07	4.26		
88.14	2.13		
94.22	3.2		

Table 8: Wing Vortex core trajectory in % , V = 0.2 ft/sec - AOA = 15 deg .

X/C	Y/S	X/C	Z/S
10.2	44.57	10	13.22
17	39.29	26.4	7.93
23.8	28.15	30	8.37
30.6	15.25	34	13.22
37.4	21.11	38	16.75
44.2	28.74	42	14.1
		46	4.41

Table 9: Strake Vortex core trajectory in % , V = 0.2 ft/sec - AOA = 20 deg .

X/C	Y/S	X/C	Z/S
23.01	25.87	25.9	19.85
29.59	24.15	36.35	15.79
36.16	20.7	95.88	0
42.74	18.97		
49.31	16.67		
55.89	14.37		
62.46	12.65		
69.04	10.92		
75.61	8.62		
82.19	7.47		
88.76	4.6		
95.34	2.53		

Table 10: Wing Vortex core trajectory in % , V = 0.2 ft/sec - AOA = 20 deg .

X/C	Y/S	X/C	Z/S
16.75	32.2	16.84	13.54
20.01	28.17	26.06	9.48
23.45	22.42	28.07	8.57
26.8	16.67	30.07	8.57
30.15	15.52	32.08	10.38
33.5	20.12	34.08	13.09
36.85	25.3	36.09	15.79
40.2	29.32	38.09	18.95
43.55	30.47	40.1	19.85
45.56	30.47	42.1	18.95
		44.11	16.24
		46.11	4.51
		46.92	0

Table 11: Strake Vortex core trajectory in % , V = 0.2 ft/sec - AOA = 22.5 deg .

X/C	Y/S	X/C	Z/S
33.55	23.17	33.03	15.39
38.71	21.34	47.66	11.87
45.16	17.68	95.33	0
51.62	16.46		
58.06	14.02		
64.52	12.19		
70.97	9.15		
77.42	6.1		
83.88	6.1		
90.33	3.66		

Table 12: Wing Vortex core trajetory in % , V = 0.2 ft/sec - AOA = 22.5 deg .

X/C	Y/S	X/C	Z/S
21.29	20.73	22.7	9.42
22.58	12.19	24.78	11.05
25.81	10.37	26.83	9.83
29.03	12.19	28.9	10.64
32.26	18.29	30.96	15.15
35.49	26.22	33.02	20.06
38.71	31.1	35.09	22.93
41.94	32.32	37.15	23.34
45.16	32.32	39.22	22.93
46.13	30.49	41.28	21.29
		43.34	18.42
		45.41	10.64
		47.47	0

Table 13: Strake Vortex core trajectory in % , V = 0.2 ft/sec , AOA = 25 deg .

X/C	Y/S	X/C	Z/S
47.16	17.98	47.02	12.26
48.54	16.82	95.81	0
52.01	15.08		
55.48	13.92		
58.95	12.76		
62.41	11.6		
65.88	11.02		
69.35	9.86		
72.82	8.7		
76.28	9.28		
79.75	6.96		
83.22	5.8		
86.69	5.22		
90.15	2.32		
93.62	1.74		
95.01	2.32		

Table 14: Wing Vortex core trajectory in % , V = 0.2 ft/sec - AOA = 25 deg .

X/C	Y/S	X/C	Z/S
27.74	34.8	28.35	27.34
31.21	34.22	30.37	28.14
34.67	33.64	32.4	28.14
38.14	31.9	34.42	29.75
41.61	32.48	36.45	27.34
46.46	30.16	38.47	20.5
		40.5	19.3
		42.52	10.45
		44.55	7.24
		46.57	3.22
		47.38	0

Table 15: Strake Vortex core trajectory in % , V = 0.2 ft/sec - AOA = 30 deg .

X/C	Y/S	X/C	Z/S
60.07	13.5	60.88	11.46
63.6	11.04	67.55	8.81
67.14	11.04	95.77	0
70.67	9.82		
74.2	7.97		
77.74	7.36		
81.27	5.52		
84.8	4.91		
88.34	1.23		
95.4	2.45		

Table 16: Wing Vortex core trajectory in % , V= 0.2 ft/sec - AOA = 30 deg .

X/C	Y/S	X/C	Z/S
41	33	41.22	7.49
40.2	33	44.1	6.17
44.22	31.35	45.34	4.85
47.03	28.6	47.4	0

Table 17: Strake Vortex trajectory in % , V = 0.6 ft/sec - AOA = 5 deg .

X/C	Y/S	X/C	Z/S
0	35.57	0	14.01
6.67	36.24	95.14	0
13.33	35.57		
20	34.9		
26.66	31.54		
33.33	28.86		
40	24.83		
46.66	20.13		
53.33	17.45		
59.99	14.76		
66.66	11.41		
73.32	10.07		
79.99	8.05		
86.66	4.03		
93.32	2.95		

Table 18: Wing Vortex core trajectory in % , V = 0.6 ft/sec - AOA = 5 deg .

X/C	Y/S	X/C	Z/S
20	53.69	19.32	4.79
26.66	53.02	44.27	1.99
30	48.32	46.29	1.6
33.33	42.95	47.49	0
36.66	37.58		
40	36.24		
43.33	30.87		
45.66	30.2		

Table 19: Strake Vortex core trajectory in % , V = 0.6 ft/sec - AOA = 10 deg .

X/C	Y/S	X/C	Z/S
13.73	49.98	13.76	18.18
17.91	40.46	95.18	0
23.88	33.32		
29.85	30.94		
35.82	26.18		
41.79	23.2		
47.76	19.04		
53.73	15.47		
59.7	16.06		
65.67	12.49		
71.64	10.11		
77.61	7.73		
83.58	5.35		
89.55	2.38		
95.52	1.78		

Table 20: Wing Vortex core trajectory in % , V = 0.6 ft/sec - AOA = 10 deg .

X/C	Y/S	X/C	Z/S
17.31	57.71	17.72	9.99
17.91	57.12	24.73	8.18
20.89	55.33	28.85	7.27
23.88	52.95	30.91	7.27
26.86	50.57	32.98	6.82
29.85	47.6	35.04	6.82
32.83	44.62	37.1	6.82
35.82	41.05	39.16	6.36
38.8	37.48	41.22	6.36
41.79	33.91	43.28	5.45
46.57	29.75	45.34	4.54
		47.4	0

Table 21: Strake Vortex core trajectory in % , V = 0.6 ft/sec - AOA = 15 deg .

X/C	Y/S	X/C	Z/S
17.55	44.24	19.87	13.13
21.95	36.36	95.58	0
28.21	29.09		
34.48	24.85		
40.75	22.42		
47.02	19.39		
53.29	17.57		
59.56	14.54		
65.83	12.73		
72.1	10.3		
78.37	8.48		
84.64	6.67		
90.91	1.21		

Table 22: Wing Vortex core trajectory in % , V = 0.6 ft/sec - AOA = 15 deg .

X/C	Y/S	X/C	Z/S
29.47	39.39	28.77	12.05
31.35	40	32.42	11.65
34.48	39.39	34.44	11.25
37.62	38.18	36.47	10.04
40.75	36.36	38.49	9.24
43.89	32.72	40.52	7.23
45.77	30.91	42.55	5.62
		44.57	3.21
		46.6	1.2
		47.4	0

Table 23: Strake Vortex core trajectory in % , V = 0.6 ft/sec - AOA = 20 deg .

X/C	Y/S	X/C	Y/S
32.5	27.88	35.4	13.16
39	22.42	95.14	0
45.5	18.79		
52	16.36		
58.5	13.94		
65	12.12		
71.5	9.7		
78	7.27		
84.5	4.85		
91	1.21		

Table 24: Wing Vortex core trajectory in % , V = 0.6 ft/sec - AOA = 20 deg .

X/C	Y/S	X/C	Z/S
35	39.39	33.95	7.02
38.5	38.78	40.9	6.14
42	36.97	42.94	4.83
45.5	31.51	44.99	4.83
46.2	29.69	47.03	1.75
		47.44	0

Table 25: Strake Vortex core trajectory in % , V = 0.6 ft/sec - AOA = 22.5 deg .

X/C	Y/S	X/C	Z/S
44.31	19.51	44.32	10.4
45.75	17.68	95.42	0
49.02	16.46		
52.29	15.24		
55.56	14.63		
58.82	14.02		
62.09	12.19		
65.36	11.58		
68.63	10.37		
71.9	8.54		
75.16	7.93		
78.43	7.32		
81.7	5.49		
84.97	4.27		
88.24	1.83		
91.5	2.44		
95.42	2.68		

Table 26: Wing Vortex core trajectory in % , V = 0.6 ft/sec - AOA = 22.5 deg .

X/C	Y/S	X/C	Z/S
40.47	39.02	40.9	5.63
42.6	35.36	44.55	4.77
46.15	29.27	46.57	3.9
		47.38	0

Table 27: Strake Vortex core trajectory in % , V = 0.6 ft/sec - AOA = 25 deg .

X/C	Y/S	X/C	Z/S
53.45	18.88	54.87	8.72
54.74	17.11	93.51	2.61
57.96	15.93	95.26	0
61.18	14.16		
64.4	12.98		
67.62	11.8		
70.84	10.62		
74.06	9.44		
77.28	8.26		
80.5	6.49		
83.72	5.9		
86.94	4.72		
90.16	2.95		
93.38	2.36		
95.31	2.6		

Table 28: Wing Vortex core trajectory in % , V = 0.6 ft/sec -AOA = 25 deg .

X/C	Y/S	X/C	Z/S
39.93	33.64	40.6	5.67
43.79	31.9	46	4.36
45.72	30.16	46.8	3.05
		47.2	0

Table 29: Strake Vortex core trajectory in % , V = 0.6 ft/sec - AOA = 30 deg .

X/C	Y/S	X/C	Z/S
65.81	13.5	66.23	6.96
66.55	12.27	93.42	2.61
70.24	11.66	95.18	0
73.94	9.82		
77.64	8.59		
81.33	7.36		
85.03	6.13		
88.73	4.29		
92.42	1.84		
95.01	2.45		

Table 30: Wing Vortex core trajectory in % , V = 0.6 ft/sec - AOA = 30 deg .

X/C	Y/S	X/C	Z/S
40.67	35.58	40.18	3.91
45.84	30.67	44.2	3.48
		46.21	3.48
		46.81	3.04
		47.01	0

Table 31: Strake Vortex core trajectory in % , V = 1.0 ft/sec - AOA = 5 deg .

X/C	Y/S	X/C	Z/S
0	38.76	0	9.26
6.96	37.4	92.58	2.2
13.92	36.72	94.82	0
20.88	33.32		
27.84	33.32		
34.8	28.56		
41.76	24.48		
48.72	20.4		
55.68	17.68		
62.64	12.92		
69.6	12.24		
76.56	9.52		
83.52	6.8		
90.48	3.4		
95	2.72		

Table 32: Wing Vortex core trajectory in % , V = 1.0 ft/sec - AOA = 5 deg .

X/C	Y/S	X/C	Z/S
26.93	54.4	26.8	3.7
30.3	48.96	45.35	2.2
33.67	43.52	47	0
37.04	38.08		
40.4	36.72		
43.77	31.28		
46.8	28.56		

Table 33: Strake Vortex core trajectory in % , V = 1.0 ft/sec - AOA = 10 deg .

X/C	Y/S	X/C	Z/S
16.66	42.84	16.85	9.67
21.27	36.72	91.78	1.76
28.36	31.96	95.11	0
35.45	27.2		
42.54	23.12		
49.63	19.72		
56.72	17		
63.81	14.28		
70.9	11.56		
77.99	8.16		
85.08	6.12		
92.17	2.04		

Table 34: Wing Vortex core trajectory in % , V = 1.0 ft/sec - AOA = 10 deg .

X/C	Y/S	X/C	Z/S
21.98	55.76	21.92	11.87
24.81	53.72	38.57	5.72
28.36	51	46.89	0
31.9	47.6		
35.45	42.16		
38.99	36.72		
42.54	35.36		
46.08	29.92		

Table 35: Strake Vortex core trajectory in % , V = 1.0 ft/sec - AOA = 15 deg .

X/C	Y/S	X/C	Z/S
20.09	38.56	20.22	8.72
25.51	32.53	92.76	1.74
31.88	28.32	95.17	0
38.26	24.7		
44.64	21.69		
51.02	19.28		
57.39	16.27		
63.77	14.46		
70.15	12.65		
76.52	10.24		
82.9	7.23		
89.28	3.61		
95.02	2.65		

Table 36: Wing Vortex core trajectory in % ,V = 1.0 ft/sec - AOA = 15 deg .

X/C	Y/S	X/C	Z/S
31.88	43.98	32.32	7.41
35.07	42.17	46.68	1.74
38.26	39.76	47.08	0
41.45	36.15		
46.55	28.92		

Table 37: Strake Vortex core trajectory in % , V = 1.0 ft/sec - AOA = 20 deg .

X/C	Y/S	X/C	Z/S
36.04	25.15	36.34	0
39.31	23.93	92.5	2.62
42.59	22.09	95.15	7.43
45.86	20.24		
49.14	19.02		
52.42	18.4		
55.69	17.18		
58.97	15.95		
62.24	14.72		
65.52	12.88		
68.8	11.66		
72.07	10.43		
75.35	9.82		
78.62	8.59		
81.9	6.13		
85.18	4.91		
88.45	4.29		
91.73	2.45		
95	2.7		

Table 38: Wing Vortex core trajectory in % , V = 1.0 ft/sec - AOA = 20 deg .

X/C	Y/S	X/C	Z/S
36.69	40.49	37.68	3.93
39.31	36.81	42.55	3.49
42.59	32.51	44.57	2.62
46.52	28.83	46.6	1.31
		47	0

Table 39: Strake Vortex core trajectory in % , V = 1.0 ft/sec - AOA = 22.5 deg .

X/C	Y/S	X/C	Z/S
44.11	21.34	43.81	6.58
47.5	18.9	93.81	2.63
50.89	17.68	95.14	0
54.29	16.46		
57.68	15.24		
61.07	14.02		
64.47	12.8		
67.86	11.58		
71.25	10.97		
74.65	9.76		
78.04	8.54		
81.43	7.32		
84.82	6.1		
88.22	4.27		
91.61	2.44		
95	2.68		

Table 40: Wing Vortex core trajectory in % , V = 1.0 ft/sec - AOA = 22.5 deg .

X/C	Y/S	X/C	Z/S
40.47	33.92	39.77	10.09
42.6	32.77	41.78	8.78
46.15	29.32	42.18	5.26
		44.19	3.07
		46.19	1.75
		47	0

Table 41: Strake Vortex core trajectory in % , V = 1.0 ft/sec - AOA = 25 deg .

X/C	Y/S	X/C	Z/S
48.72	19.51	49.01	7.81
52.2	18.29	92.77	2.6
55.68	17.07	95	0
59.16	15.85		
62.64	14.63		
66.12	13.41		
69.6	12.19		
73.08	9.76		
76.56	8.54		
80.04	7.32		
83.52	6.1		
87	4.27		
90.48	2.44		
93.96	2.44		
95	2.68		

Table 42: Wing Vortex core trajectory in % , V = 1.0 ft/sec - AOA = 25 deg .

X/C	Y/S	X/C	Z/S
39.48	38.41	39.5	7.81
42.3	34.15	41.47	6.51
46.53	29.27	43.45	5.21
		45.42	3.47
		47	0

Table 43: Strake Vortex core trajectory in % , V = 1.0 ft/sec - AOA = 30 deg .

X/C	Y/S	X/C	Z/S
66.8	11.25	66.74	6.12
70.51	10	92.72	3.49
74.22	8.75	95.15	0
77.93	7.5		
81.64	6.25		
85.35	5		
89.06	3.13		
92.77	2.5		
95	2.75		

Table 44: Wing Vortex core trajectory in % , V = 1.0 ft/sec - AOA = 30 deg .

X/C	Y/S	X/C	Z/S
41.6	37.52	42	4.81
44	32.48	46	3.06
46.4	29.12	46.8	1.31
		47	0

Fig.40:Sideview of Strake and Wing Vortex at 5 deg. AOA and V=0.2 ft/s

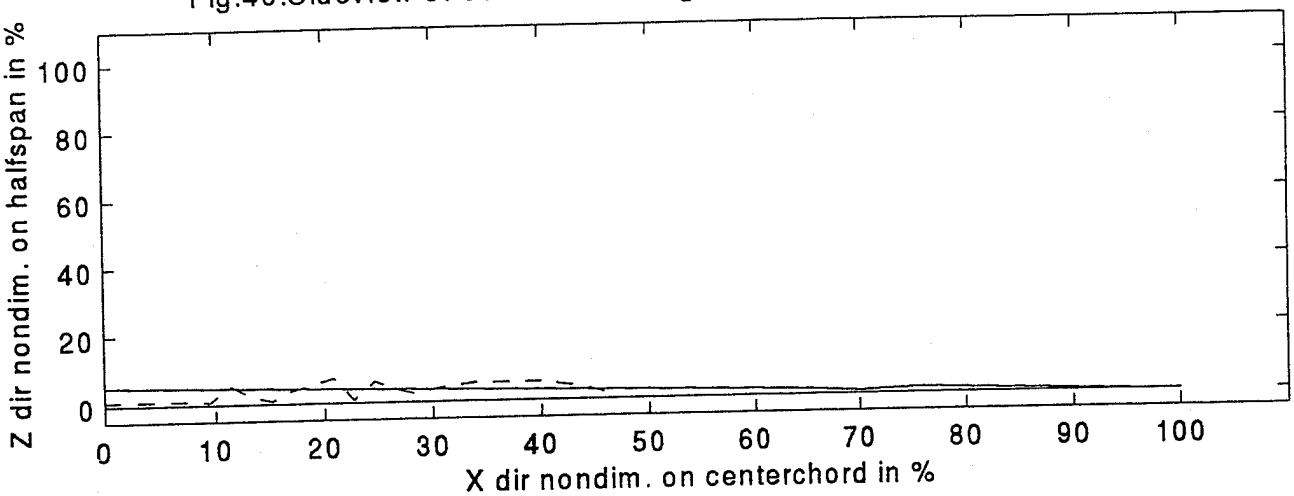

Fig.41:Topview of Strake and Wing Vortex at 5 deg. AOA and V=0.2 ft/s

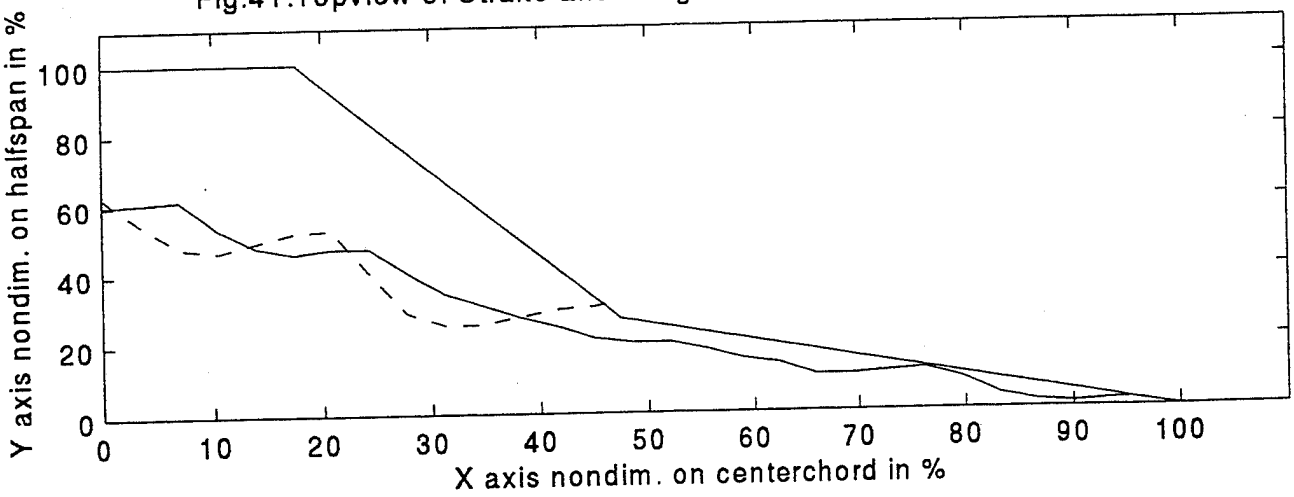

Fig.42:Sideview of Strake and Wing Vortex at 10 deg. AOA and V=0.2 ft/s

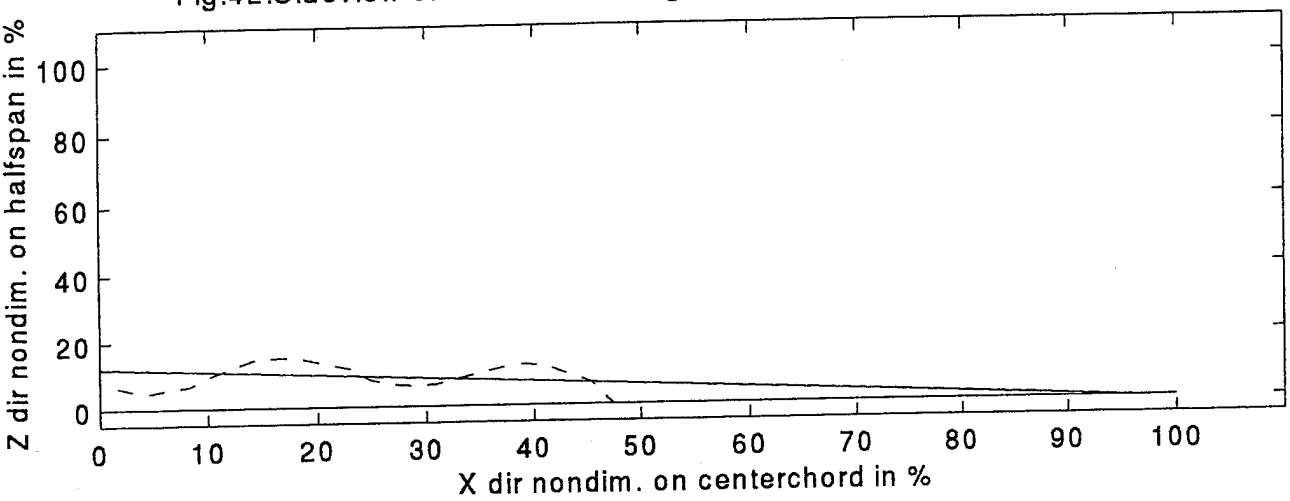

Fig.43:Topview of Strake and Wing Vortex at 10 deg. AOA and V=0.2 ft/s

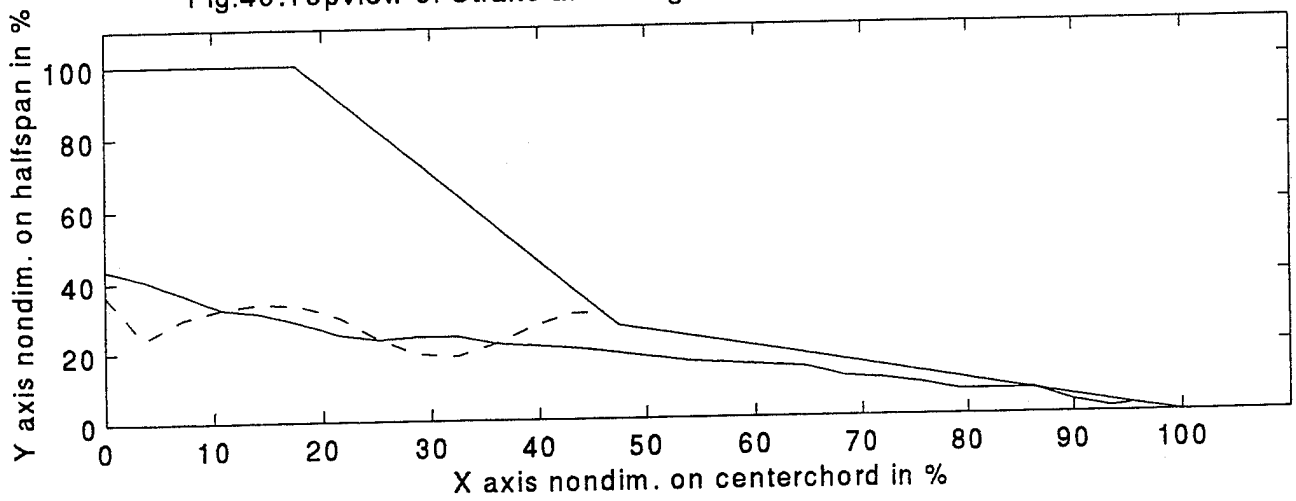

Fig.44:Sideview of Strake and Wing Vortex at 15 deg. AOA and V=0.2 ft/s

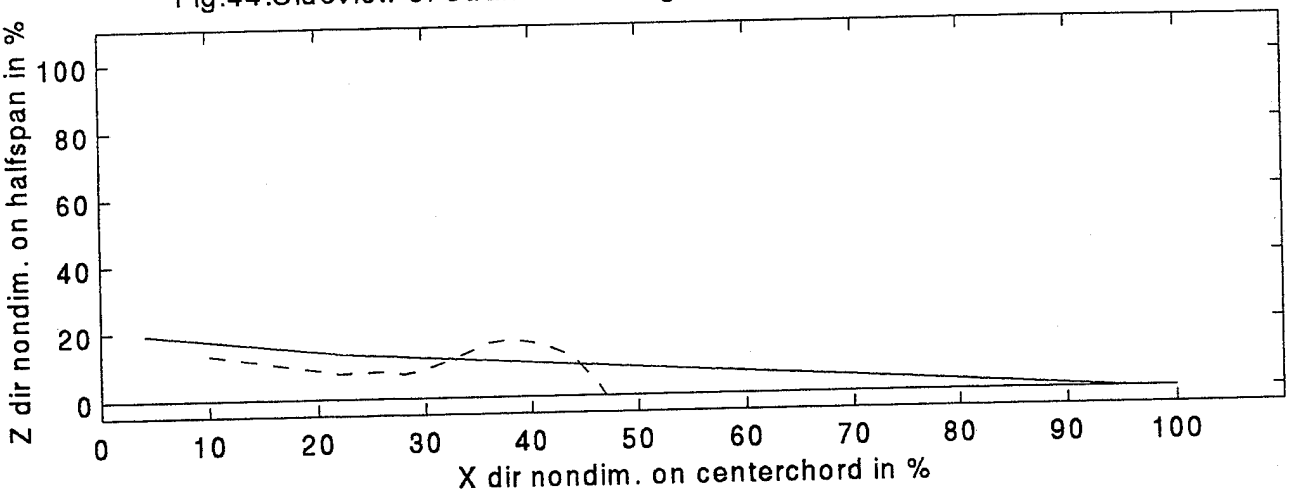

Fig.45:Topview of Strake and Wing Vortex at 15 deg. AOA and V=0.2 ft/s

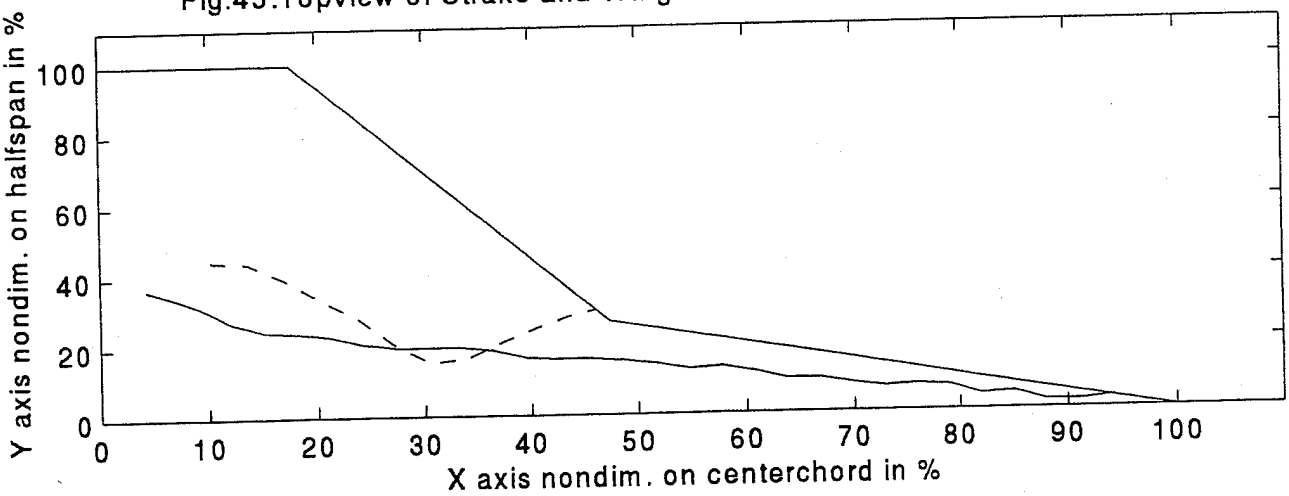

Fig.46:Sideview of Strake and Wing Vortex at 20 deg. AOA and V=0.2 ft/s

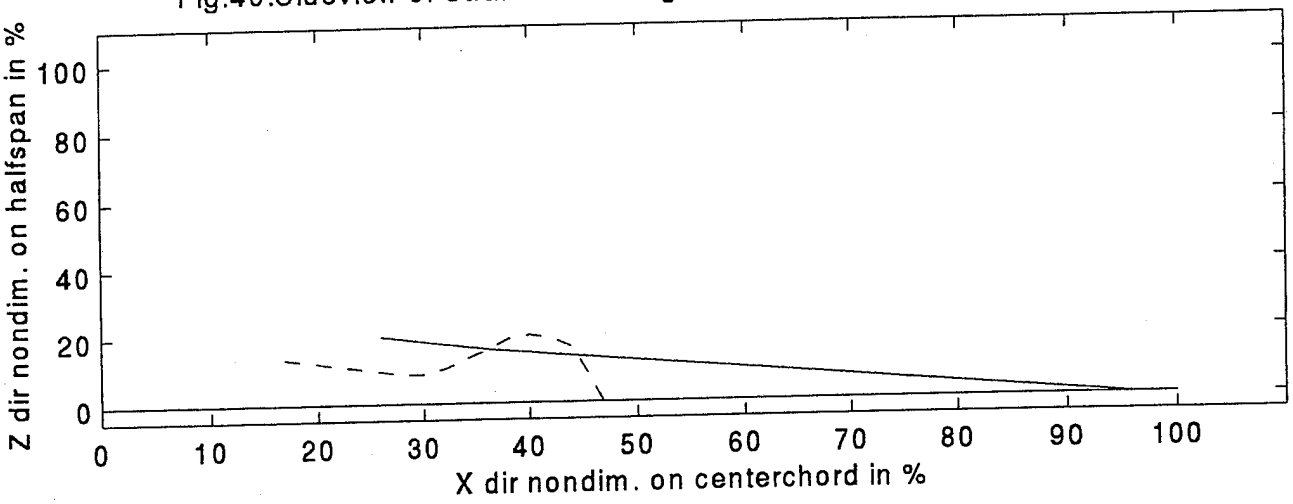

Fig.47:Topview of Strake and Wing Vortex at 20 deg. AOA and V=0.2 ft/s

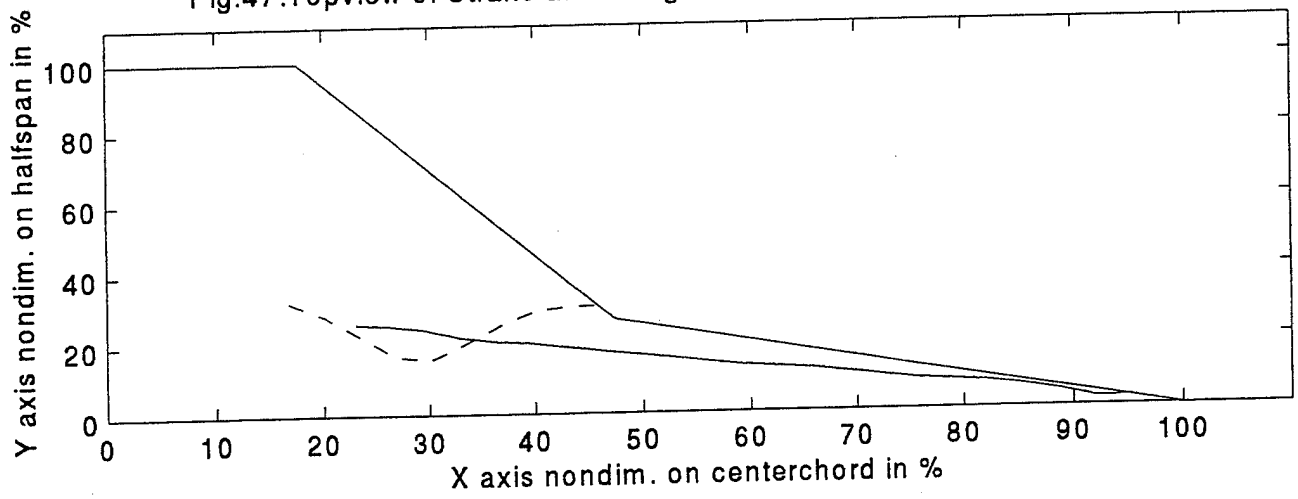

Fig.48:Sideview of Strake and Wing Vortex at 22.5 deg. AOA and V=0.2 ft/s

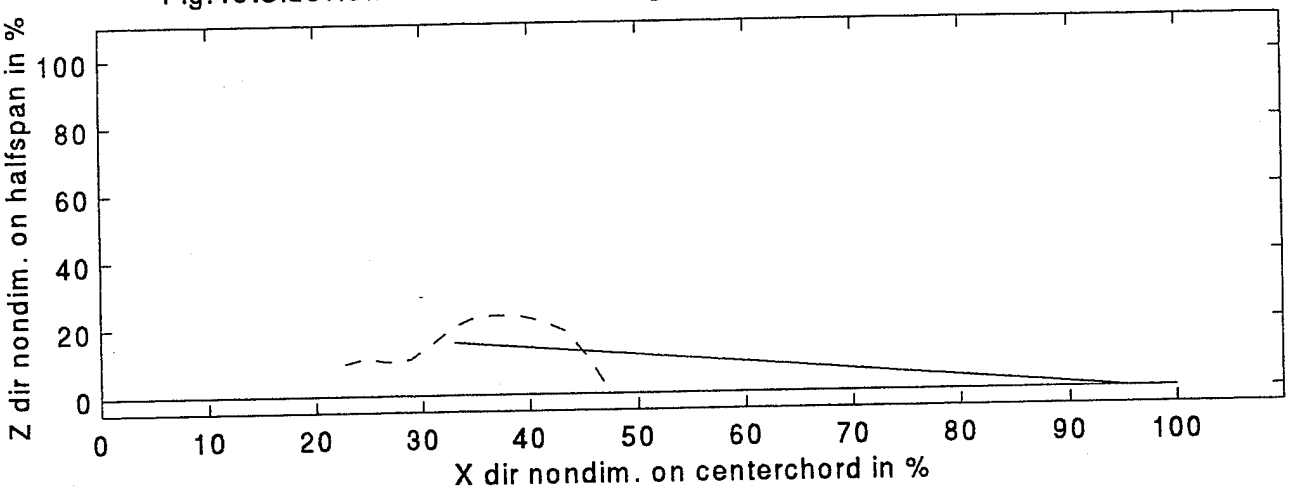

Fig.49:Topview of Strake and Wing Vortex at 22.5 deg. AOA and V=0.2 ft/s

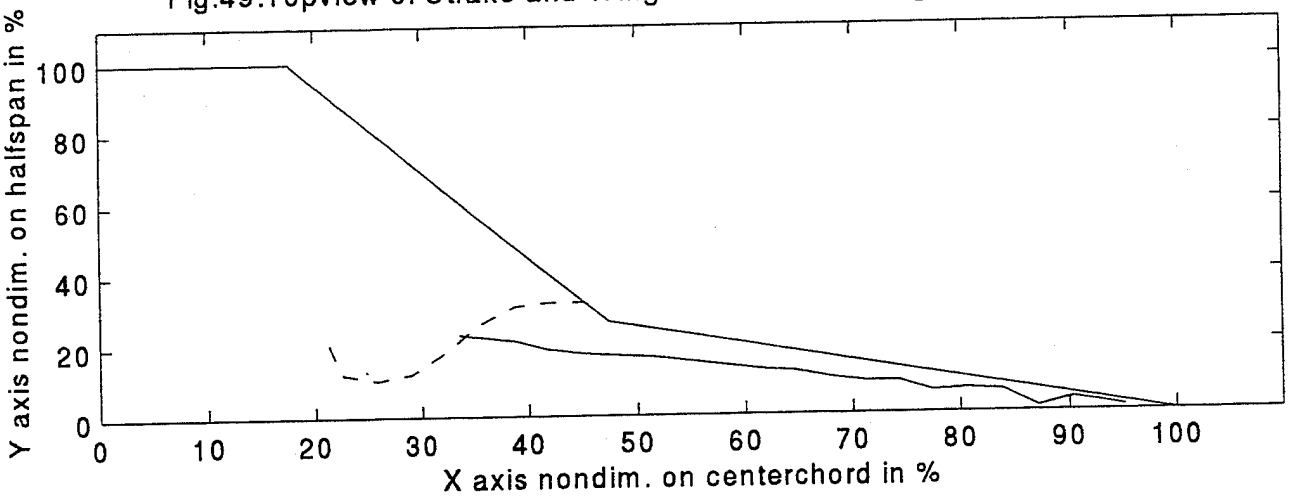

Fig.50:Sideview of Strake and Wing Vortex at 25 deg. AOA and V=0.2 ft/s

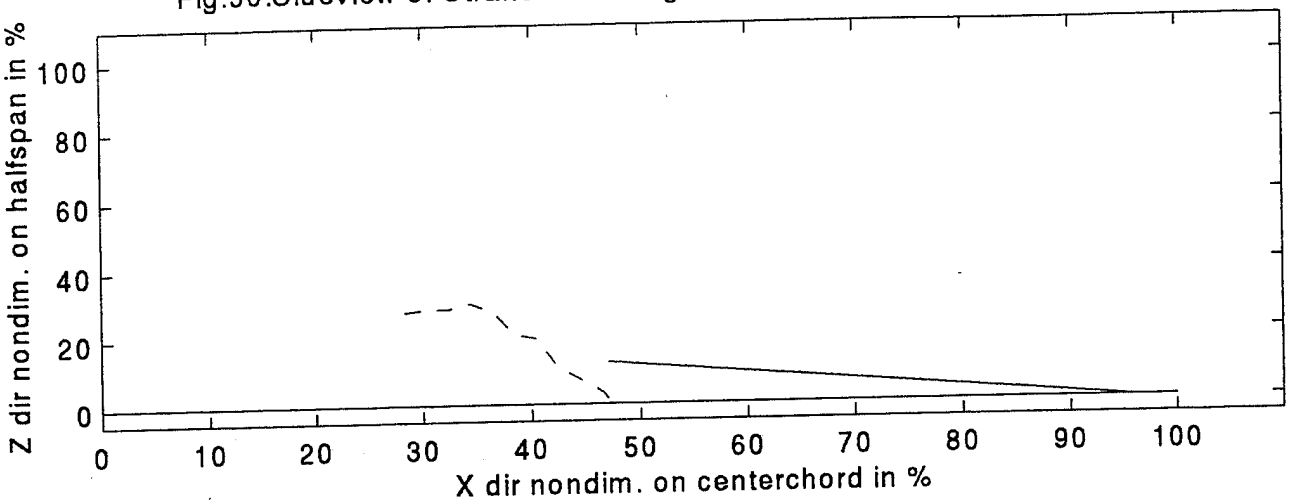

Fig.51:Topview of Strake and Wing Vortex at 25 deg. AOA and V=0.2 ft/s

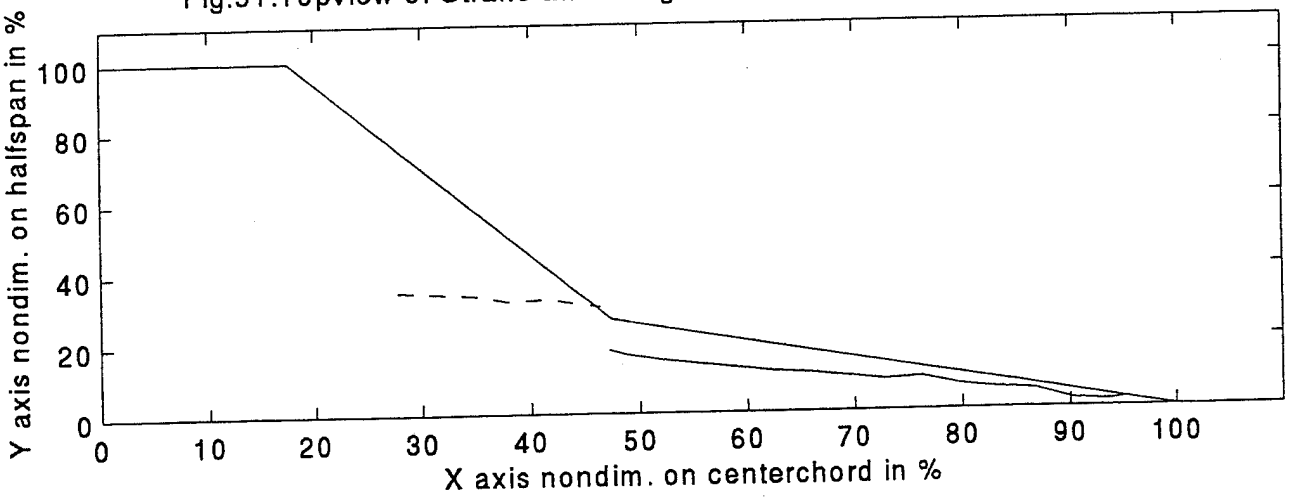

Fig.52:Sideview of Strake and Wing Vortex at 30 deg. AOA and V=0.2 ft/s

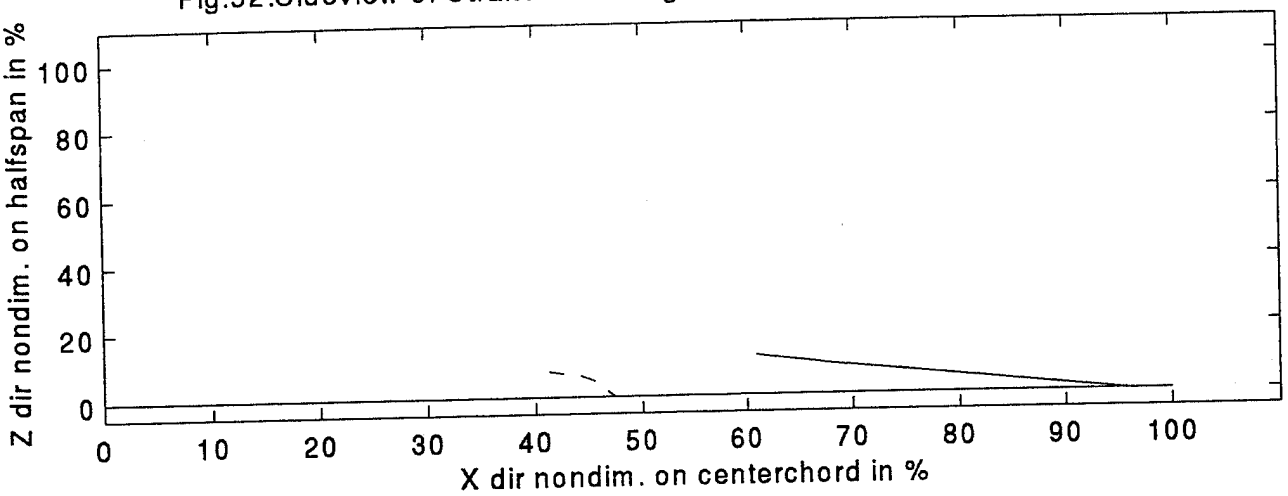

Fig.53:Topview of Strake and Wing Vortex at 30 deg. AOA and V=0.2 ft/s

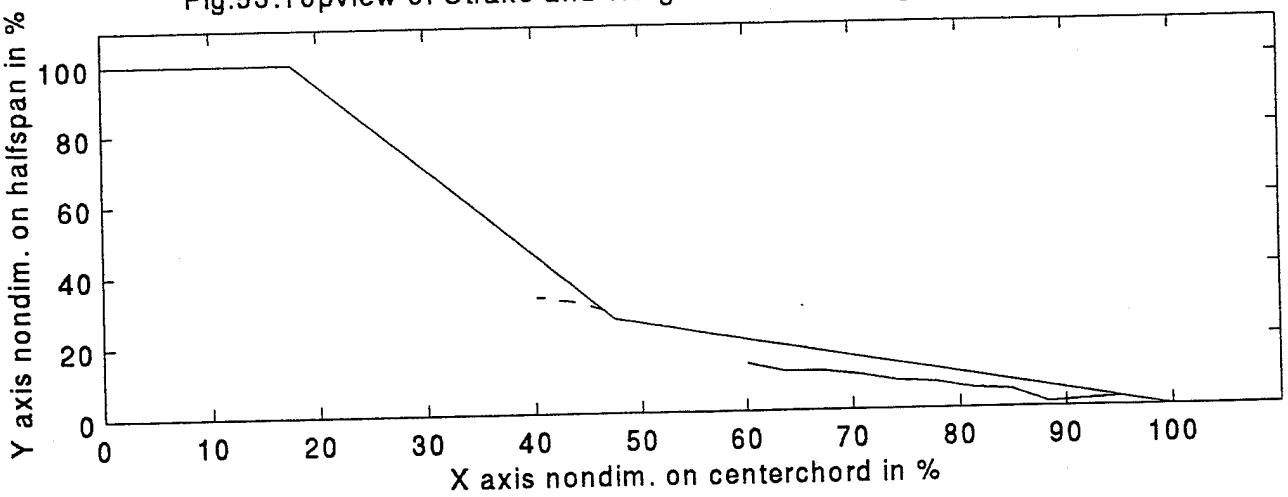

Fig.54:Sideview of Strake and Wing Vortex at 5 deg. AOA and V=0.6 ft/s

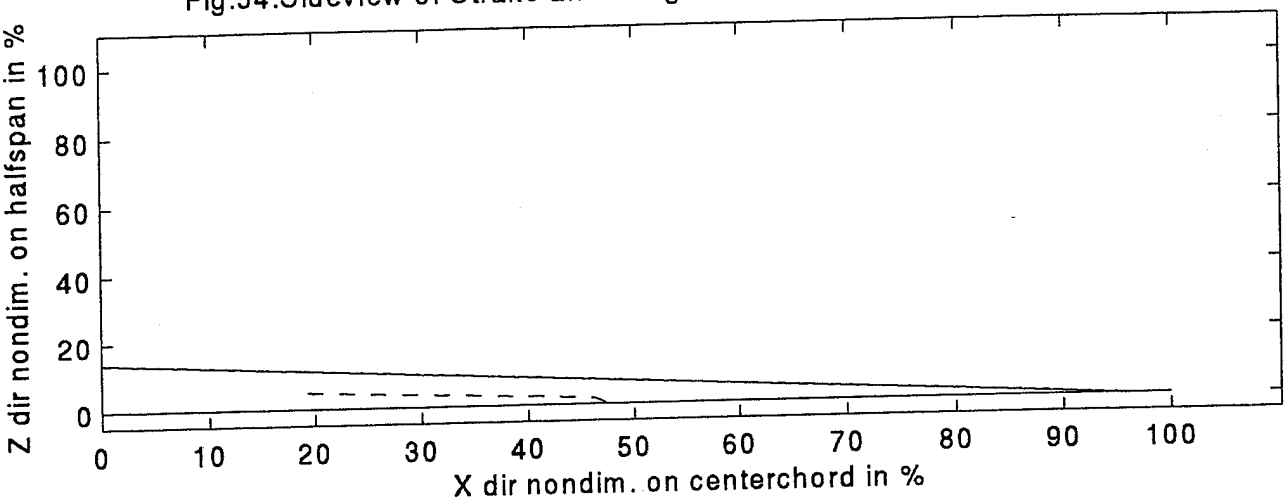

Fig.55:Topview of Strake and Wing Vortex at 5 deg. AOA and V=0.6 ft/s

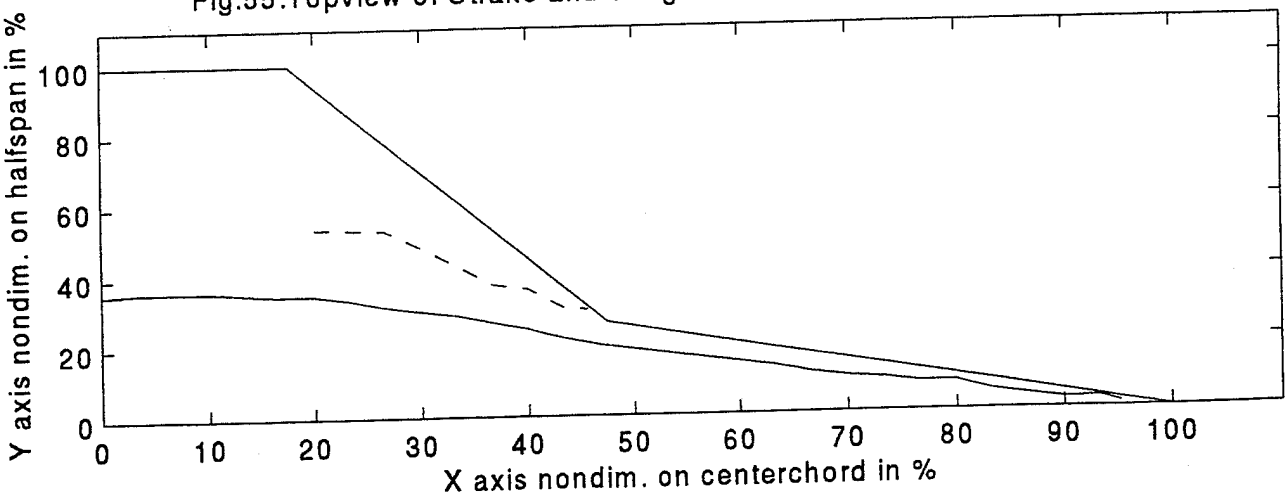

Fig.56:Sideview of Strake and Wing Vortex at 10 deg. AOA and V=0.6 ft/s

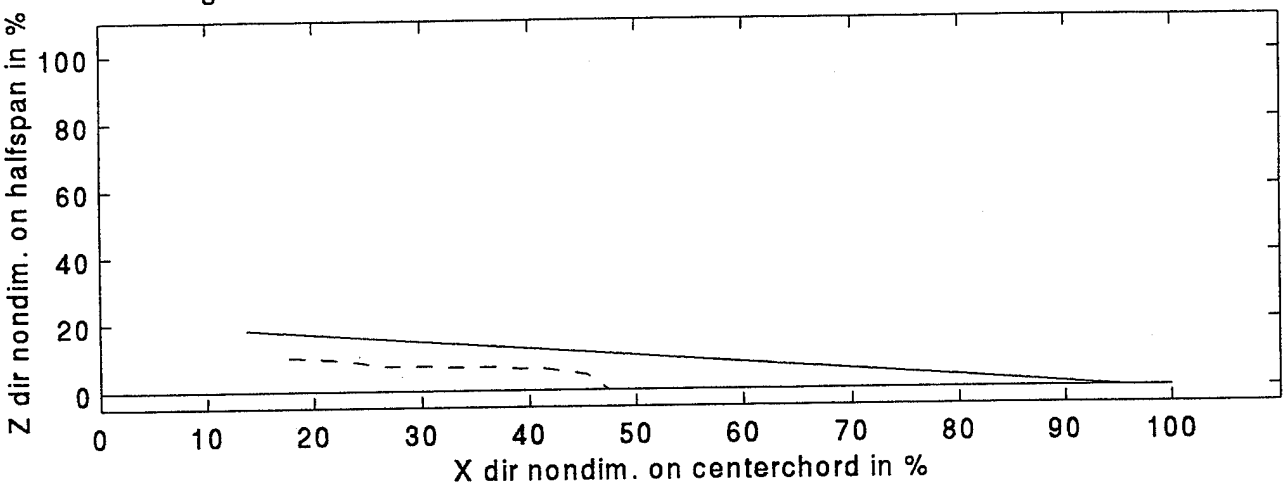

Fig.57:Topview of Strake and Wing Vortex at 10 deg. AOA and V=0.6 ft/s

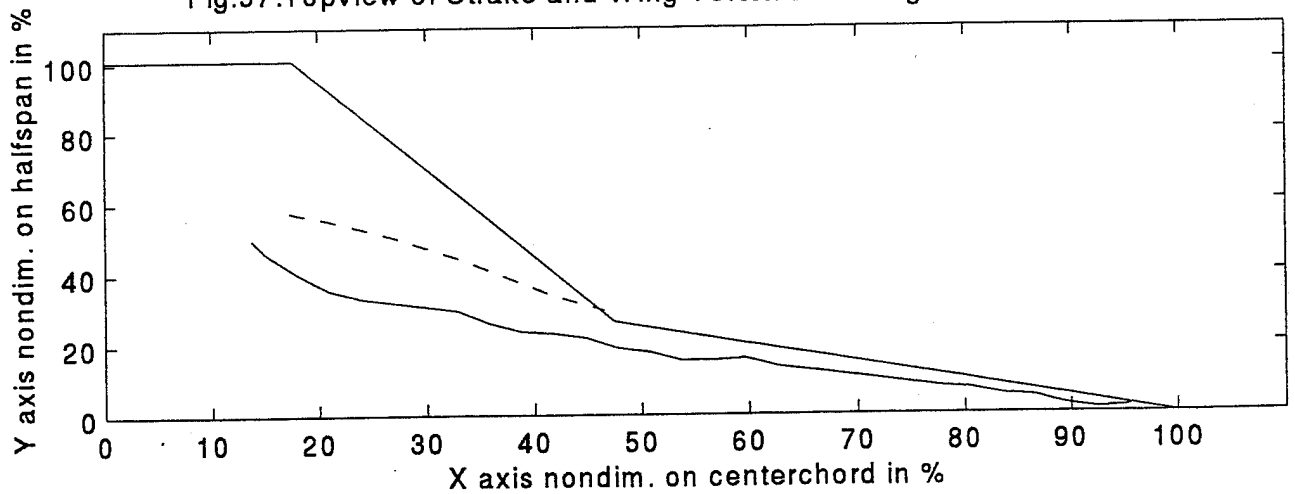

Fig.58:Sideview of Strake and Wing Vortex at 15 deg. AOA and V=0.6 ft/s

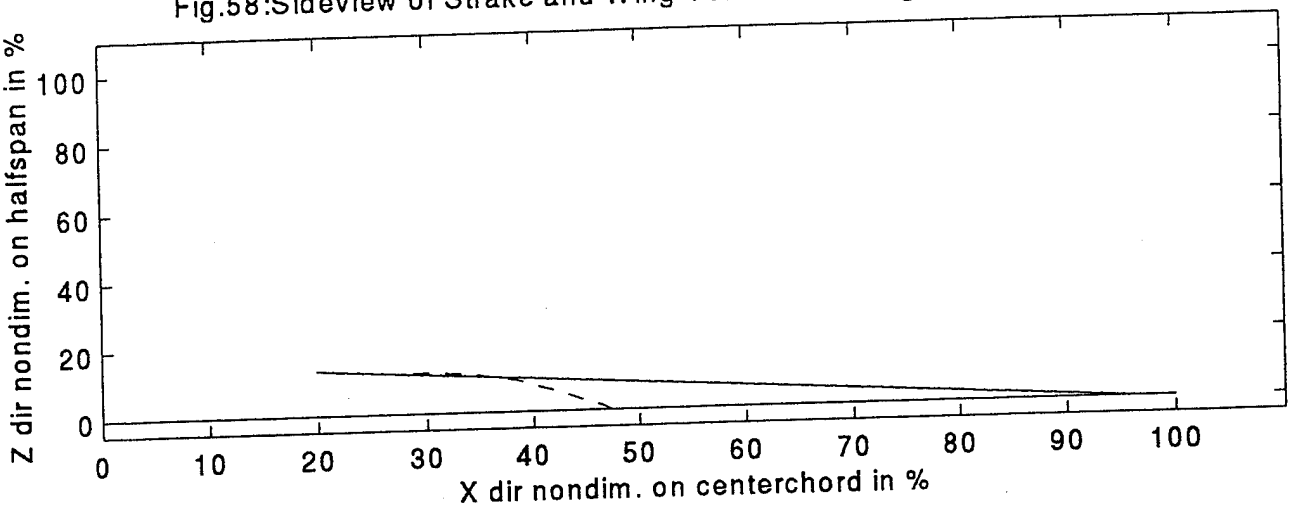

Fig.59:Topview of Strake and Wing Vortex at 15 deg. AOA and V=0.6 ft/s

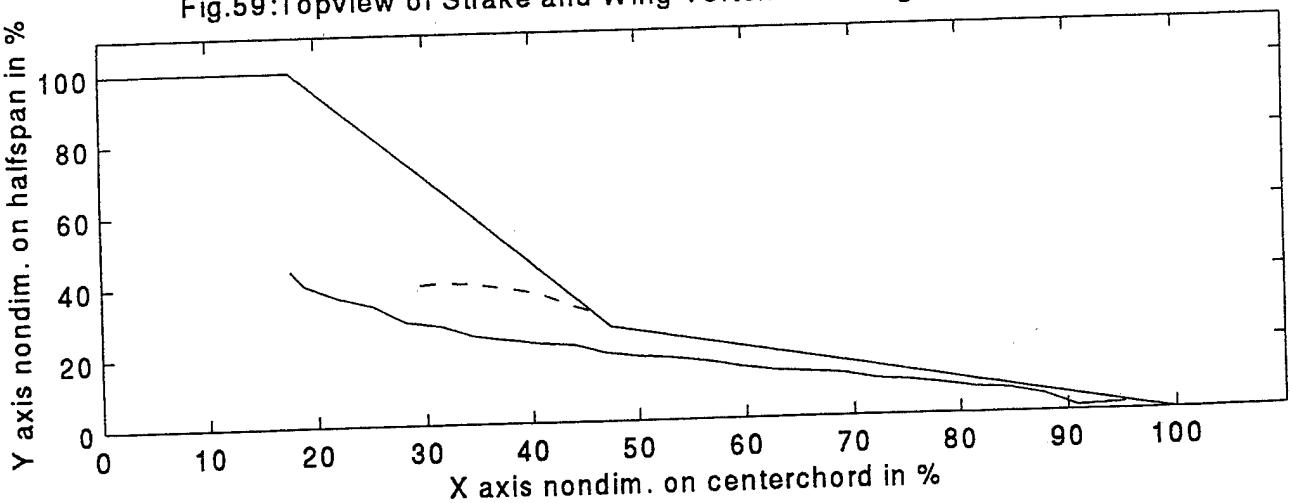

Fig.60:Sideview of Strake and Wing Vortex at 20 deg. AOA and V=0.6 ft/s

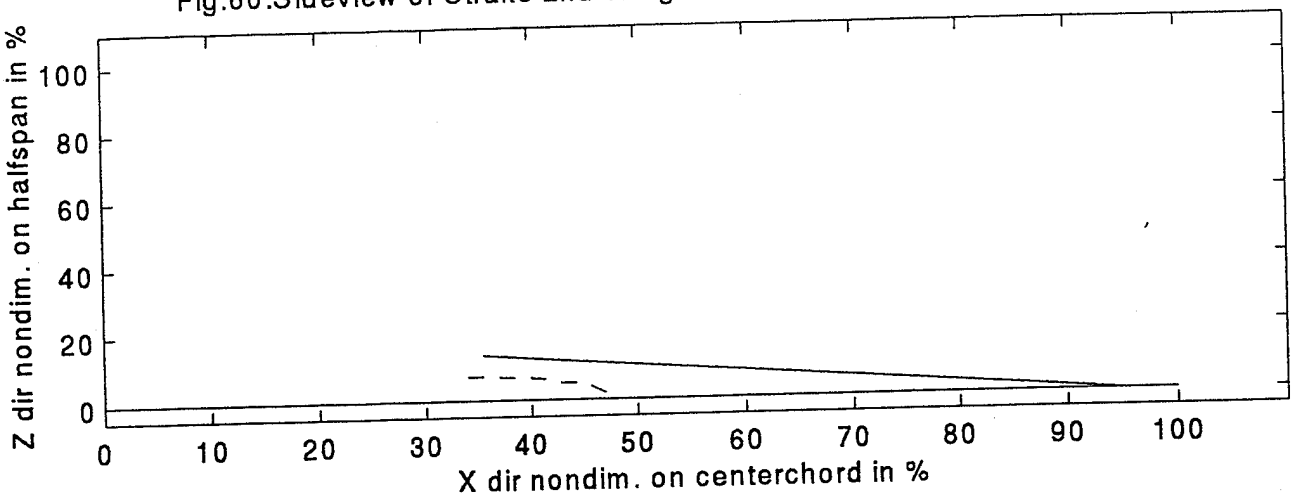

Fig.61:Topview of Strake and Wing Vortex at 20 deg. AOA and V=0.6 ft/s

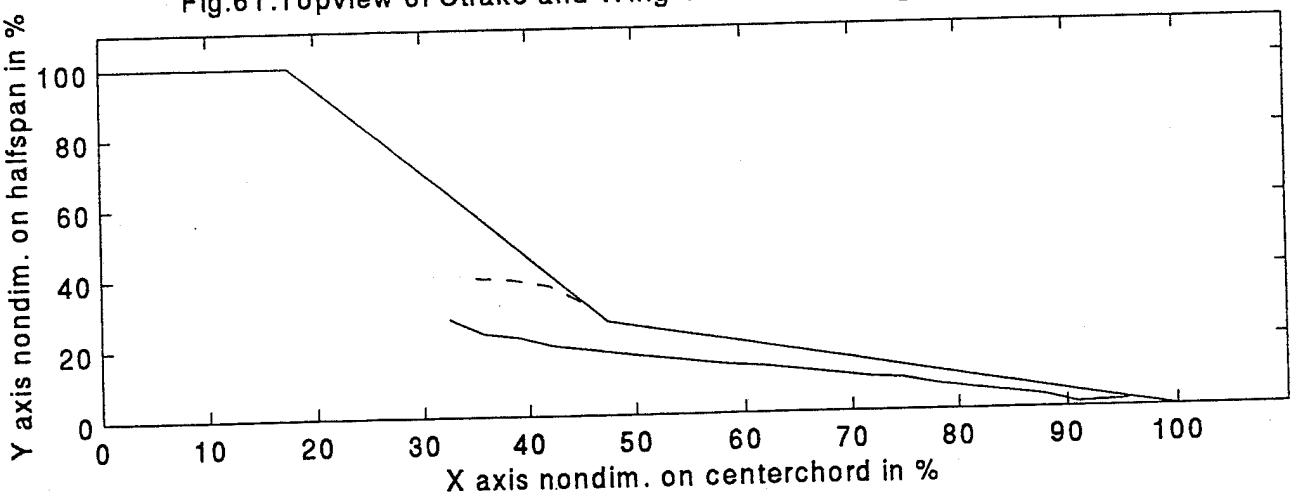

Fig.62:Sideview of Strake and Wing Vortex at 22.5 deg. AOA and V=0.6 ft/s

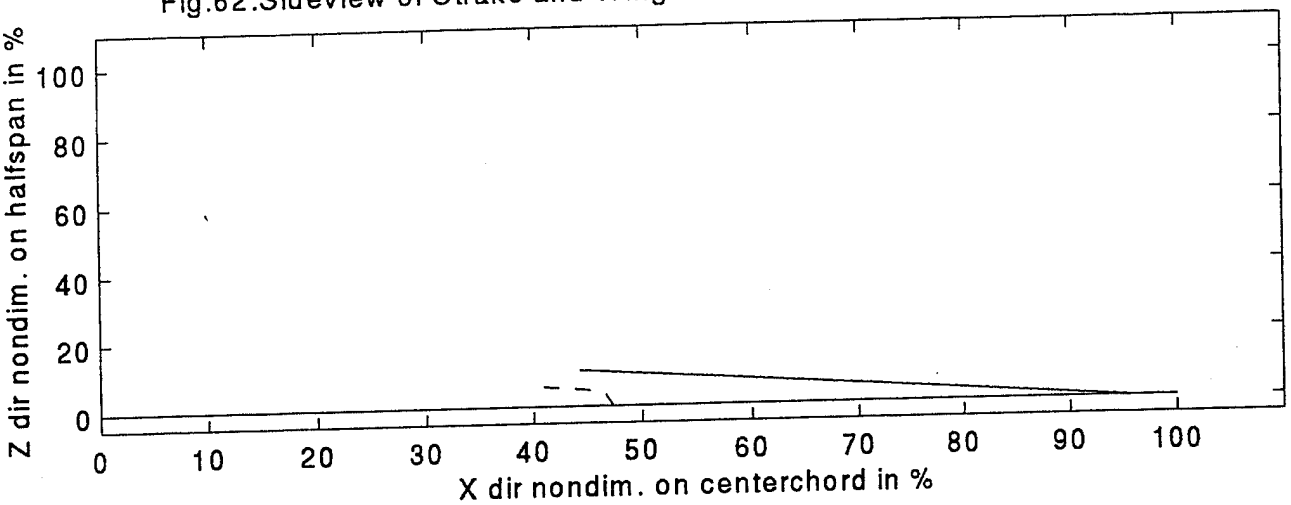

Fig.63:Topview of Strake and Wing Vortex at 22.5 deg. AOA and V=0.6 ft/s

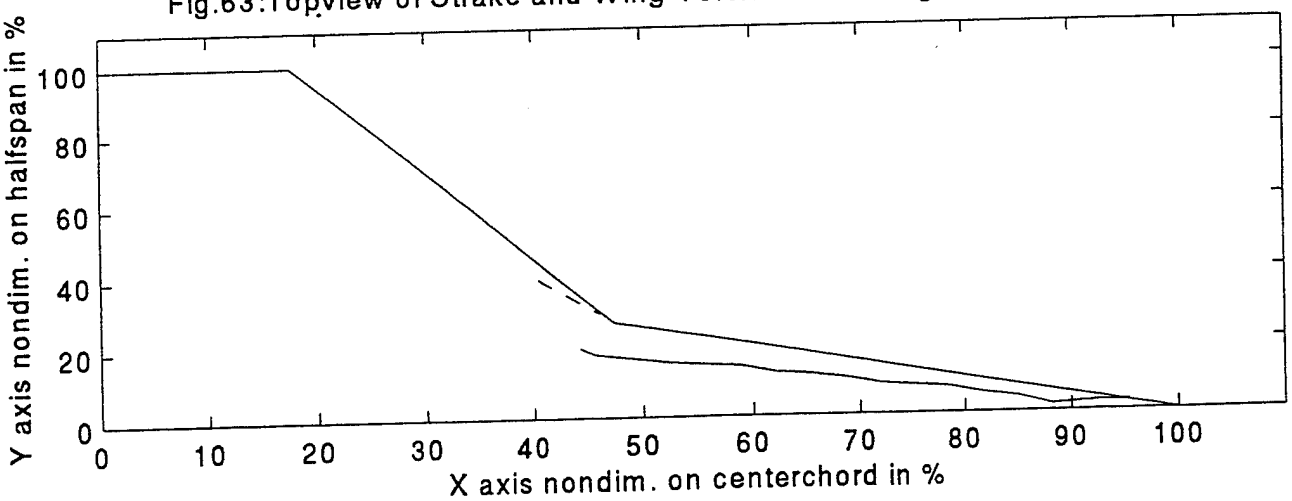

Fig.64:Sideview of Strake and Wing Vortex at 25 deg. AOA and V=0.6 ft/s

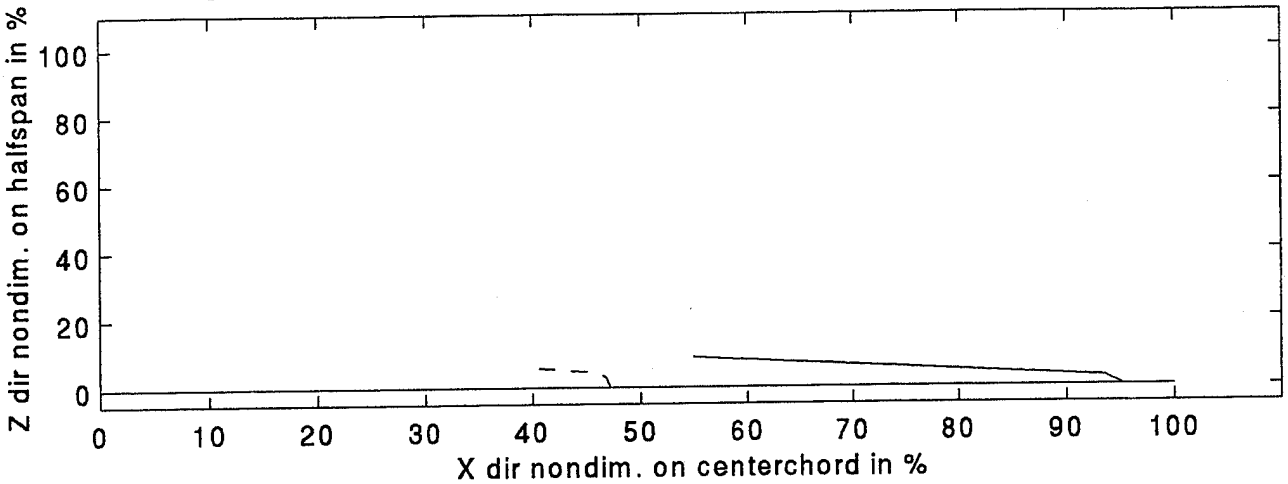

Fig.65:Topview of Strake and Wing Vortex at 25 deg. AOA and V=0.6 ft/s

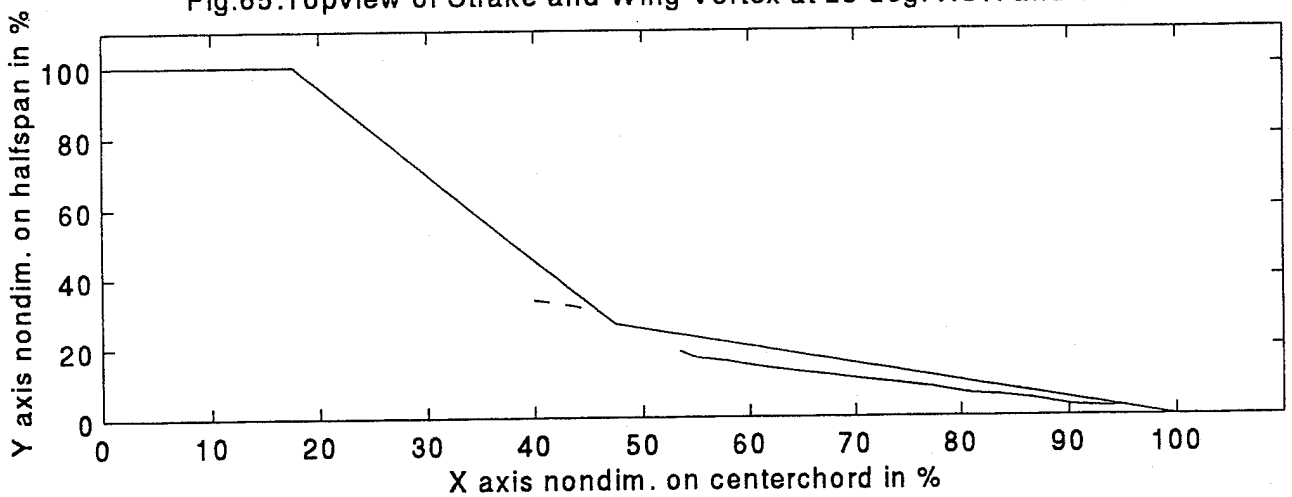

Fig.66:Sideview of Strake and Wing Vortex at 30 deg. AOA and V=0.6 ft/s

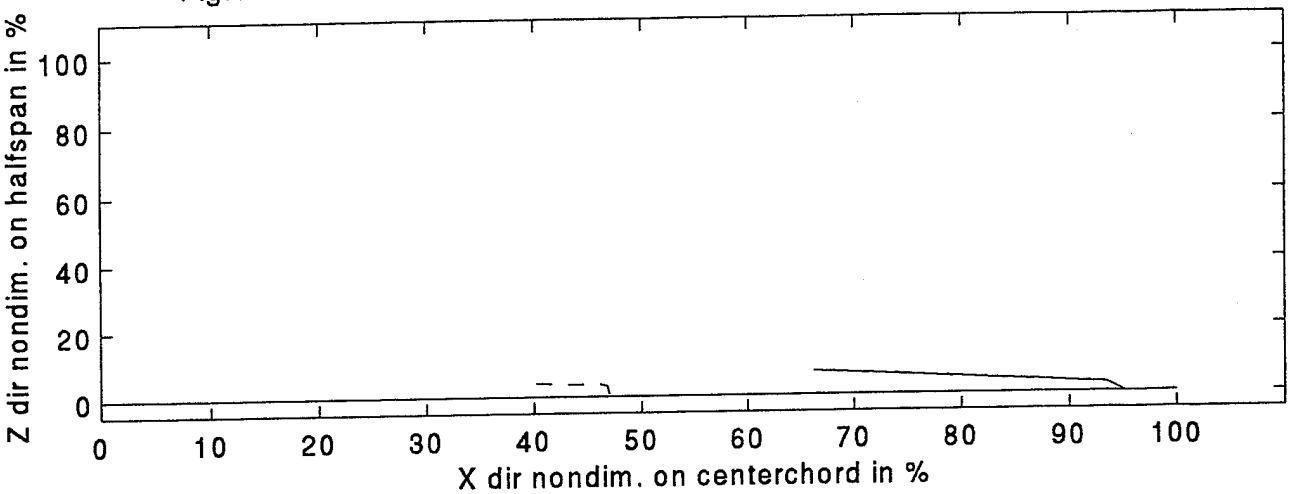

Fig.67:Topview of Strake and Wing Vortex at 30 deg. AOA and V=0.6 ft/s

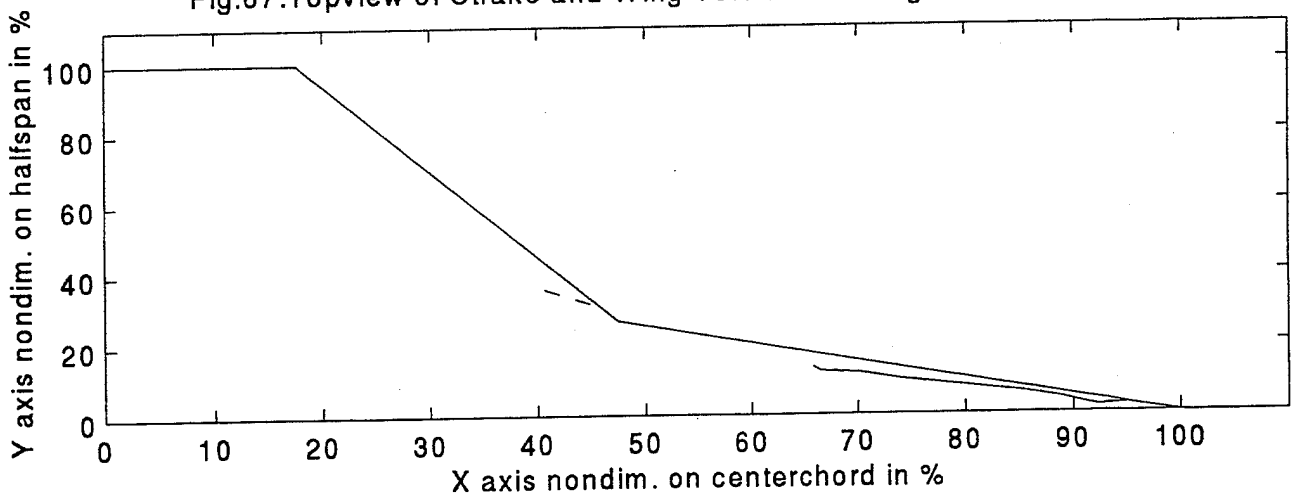

Fig.68:Sideview of Strake and Wing Vortex at 5 deg. AOA and V=1.0 ft/s

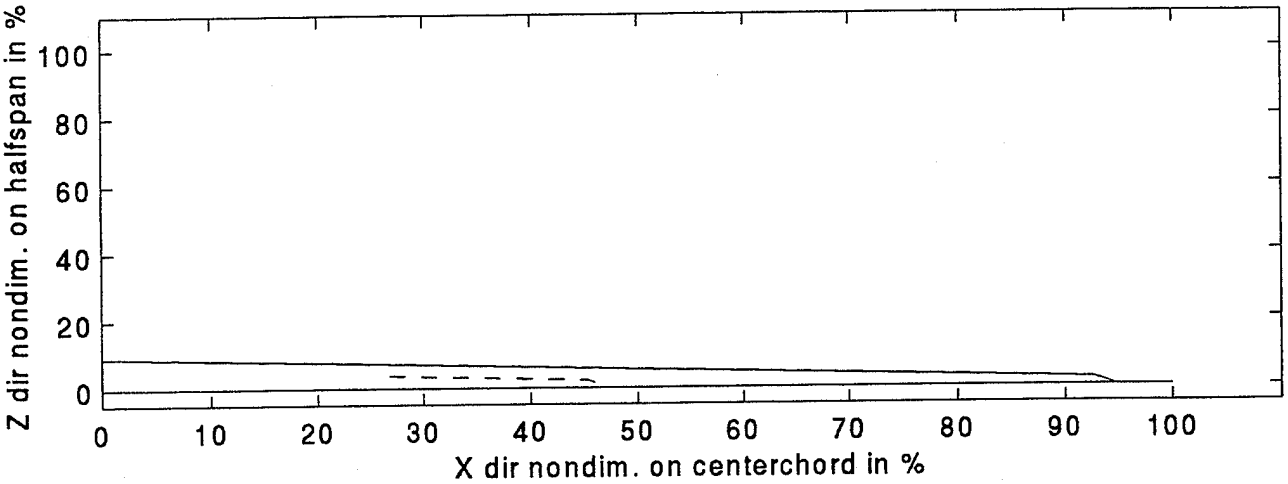

Fig.69:Topview of Strake and Wing Vortex at 5 deg. AOA and V=1.0 ft/s

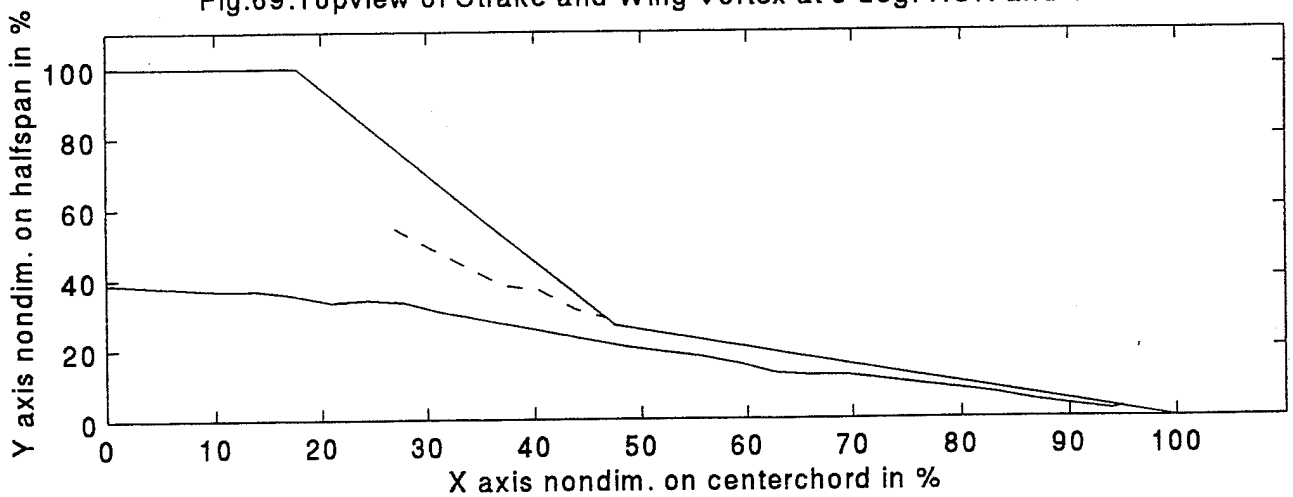

Fig.70:Sideview of Strake and Wing Vortex at 10 deg. AOA and V=1.0 ft/s

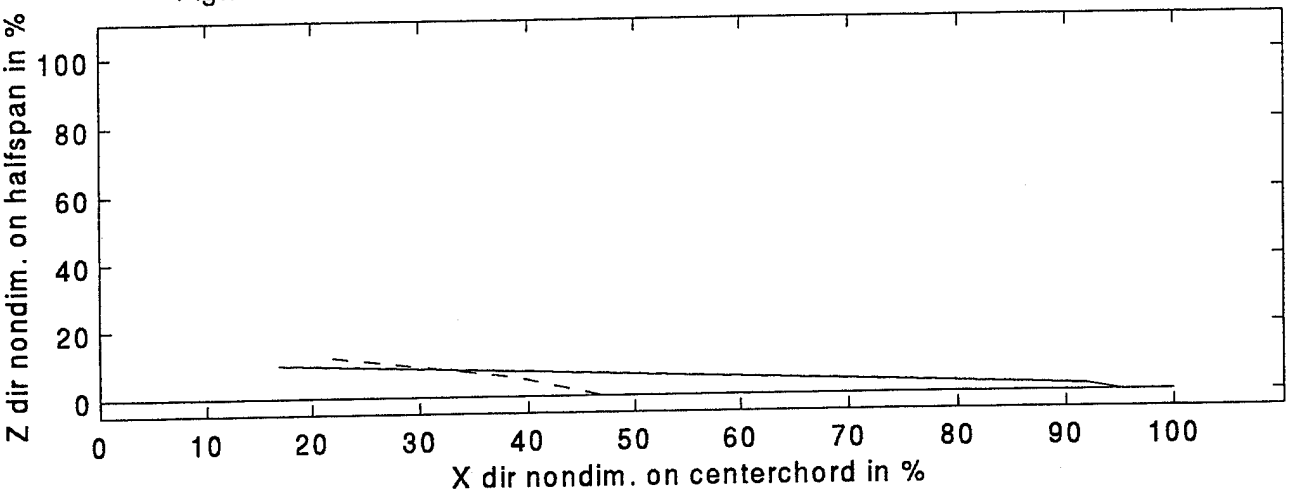

Fig.71:Topview of Strake and Wing Vortex at 10 deg. AOA and V=1.0 ft/s

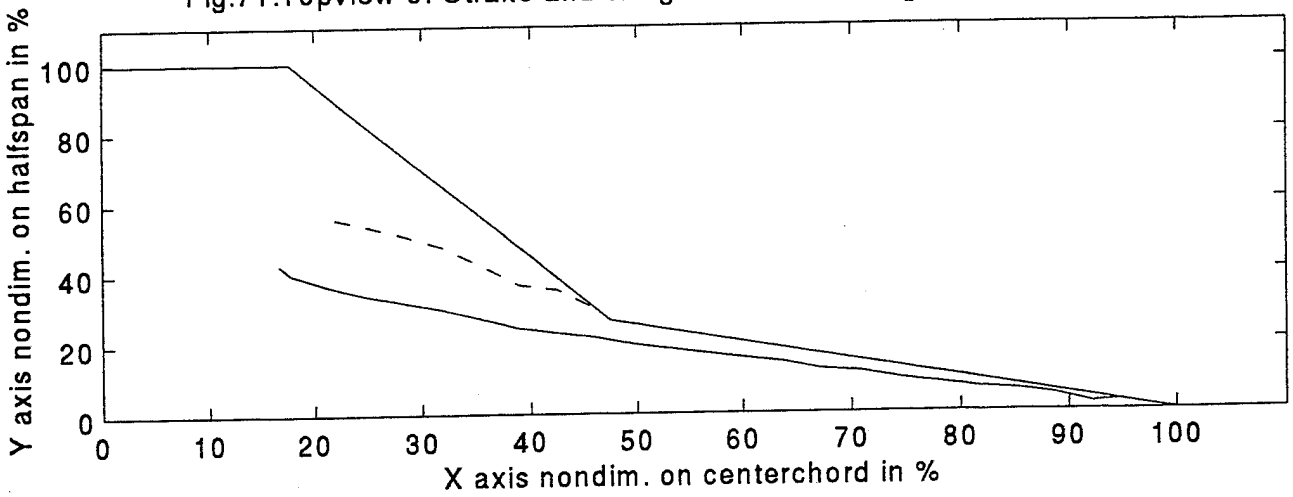

Fig.72:Sideview of Strake and Wing Vortex at 15 deg. AOA and V=1.0 ft/s

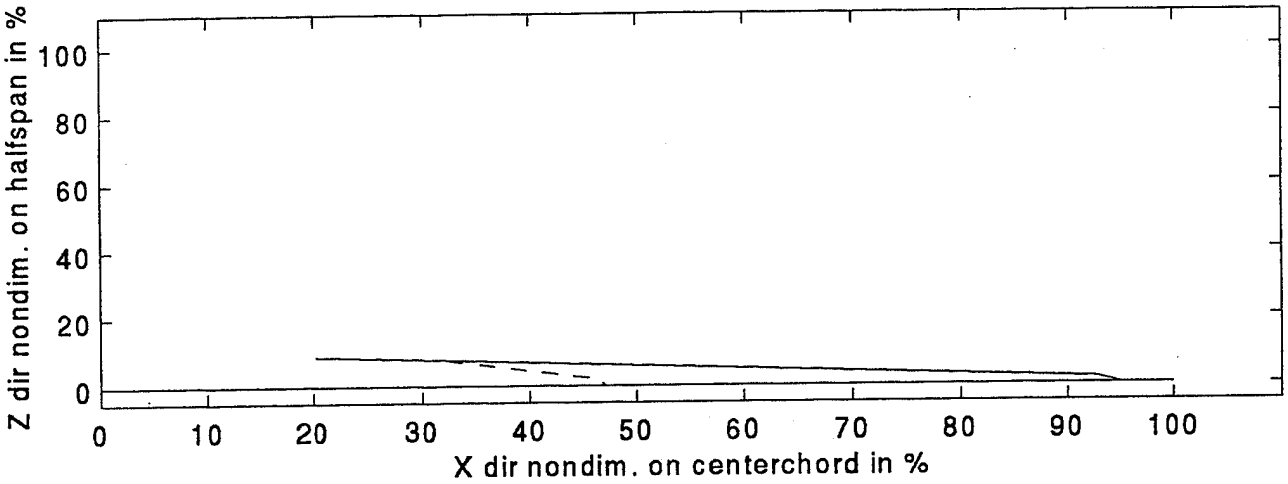

Fig.73:Topview of Strake and Wing Vortex at 15 deg. AOA and V=1.0 ft/s

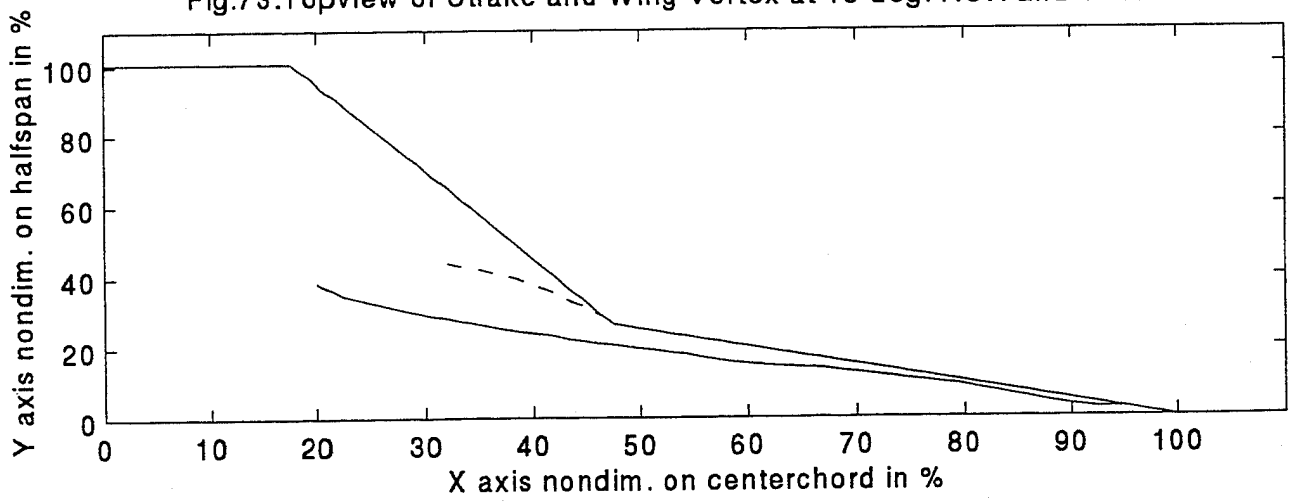

Fig.74:Sideview of Strake and Wing Vortex at 20 deg. AOA and V=1.0 ft/s

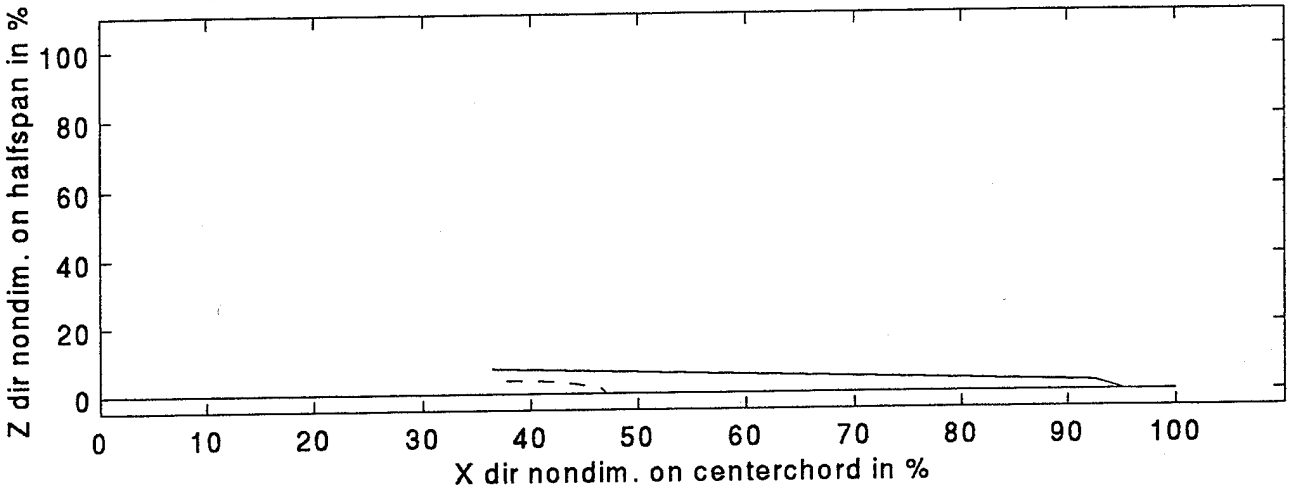

Fig.75:Topview of Strake and Wing Vortex at 20 deg. AOA and V=1.0 ft/s

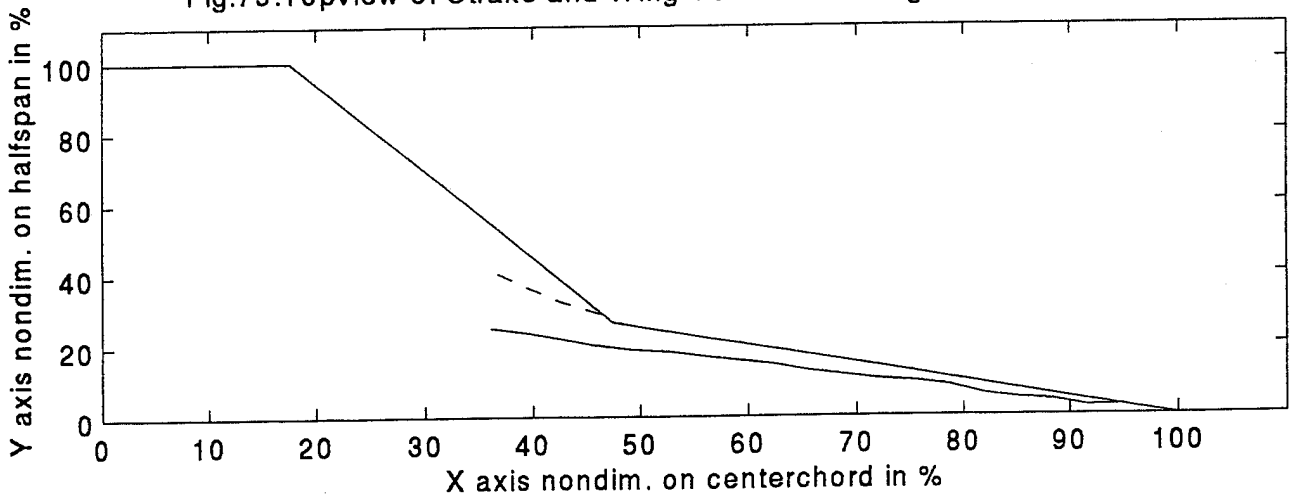

Fig.76:Sideview of Strake and Wing Vortex at 22.5 deg. AOA and V=1.0 ft/s

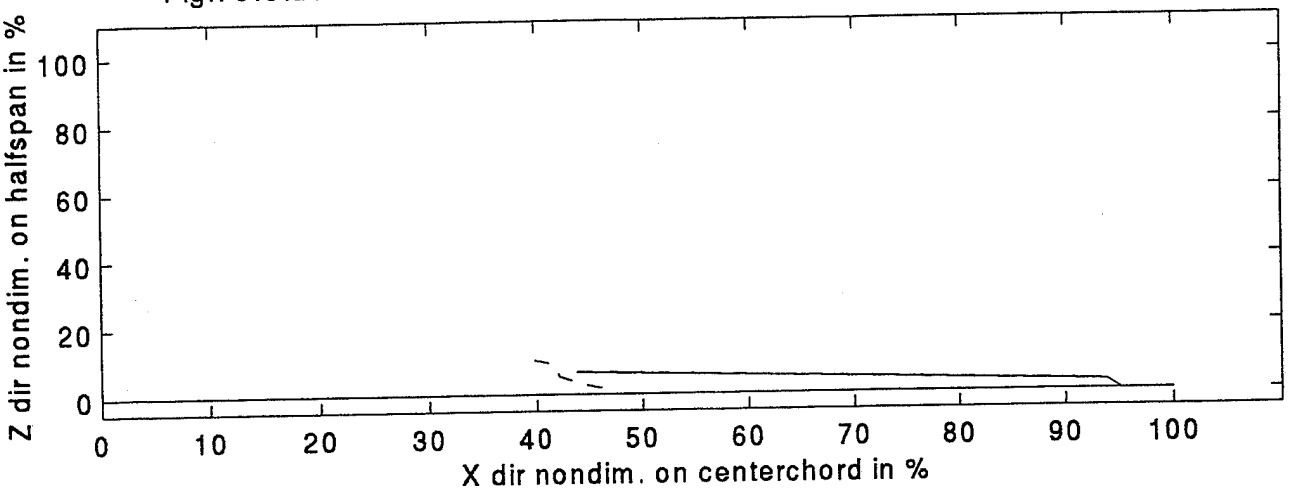

Fig.77:Topview of Strake and Wing Vortex at 22.5 deg. AOA and V=1.0 ft/s

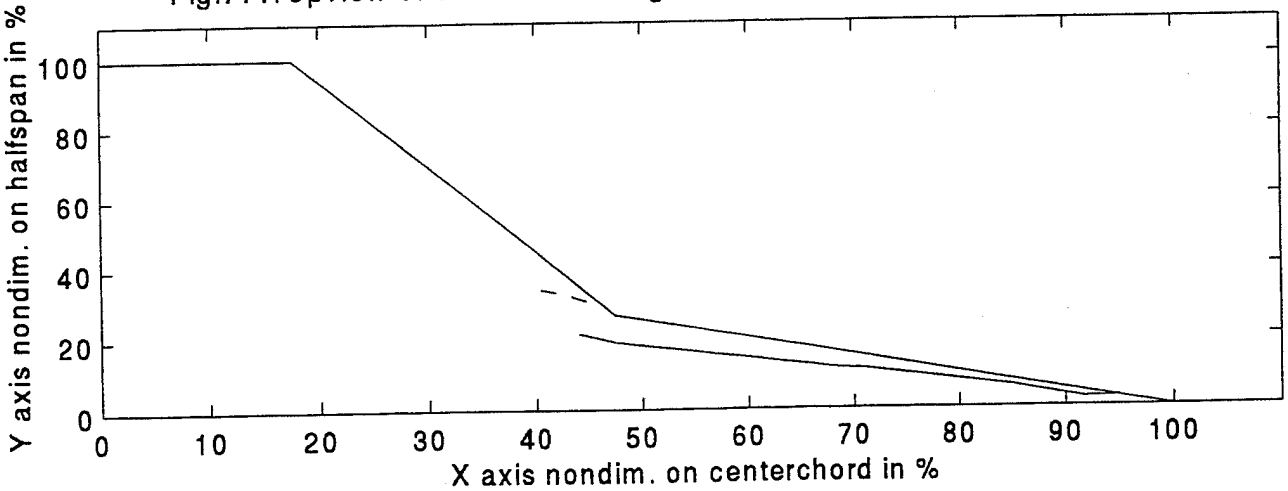

Fig.78:Sideview of Strake and Wing Vortex at 25 deg. AOA and V=1.0 ft/s

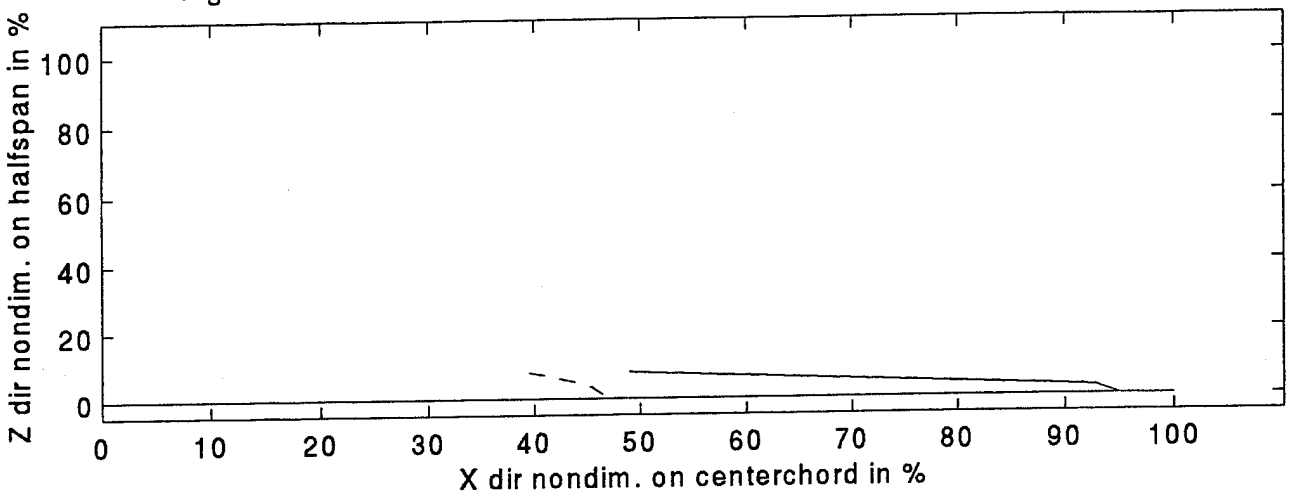

Fig.79:Topview of Strake and Wing Vortex at 25 deg. AOA and V=1.0 ft/s

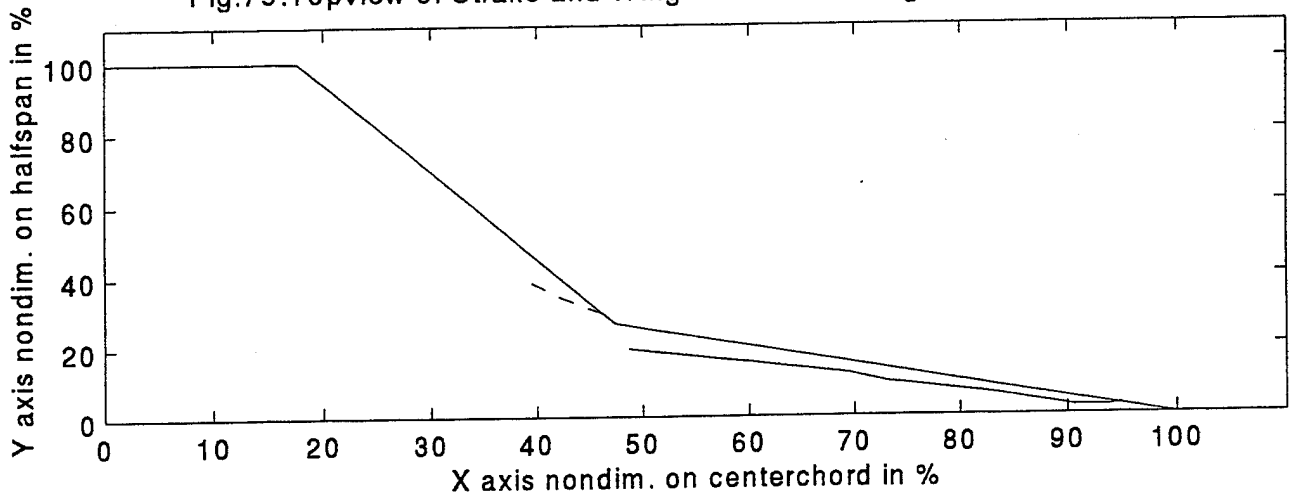

Fig.80:Sideview of Strake and Wing Vortex at 30 deg. AOA and V=1.0 ft/s

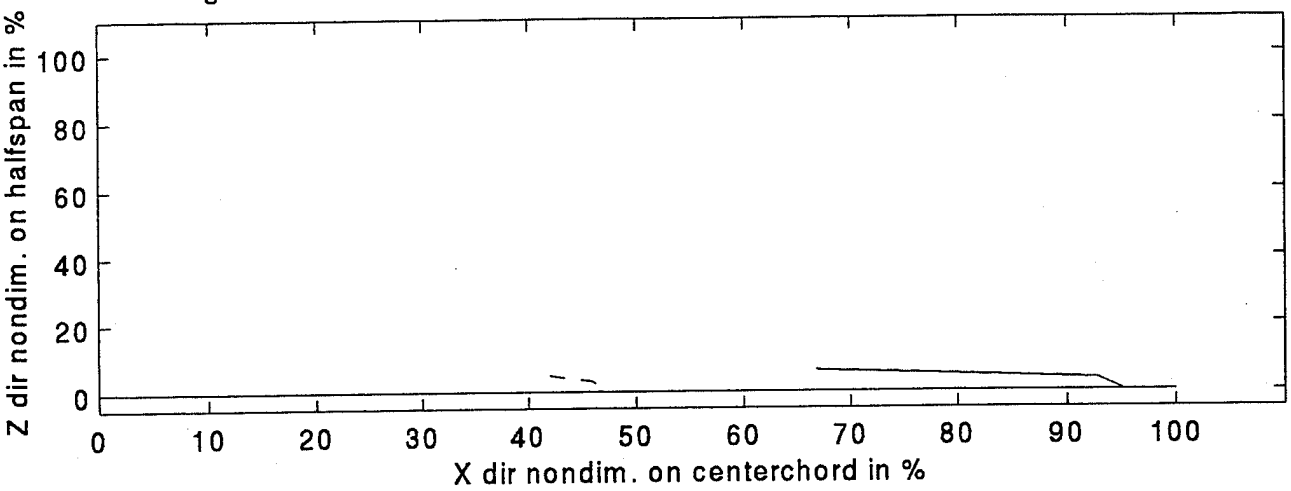

Fig.81:Topview of Strake and Wing Vortex at 30 deg. AOA and V=1.0 ft/s

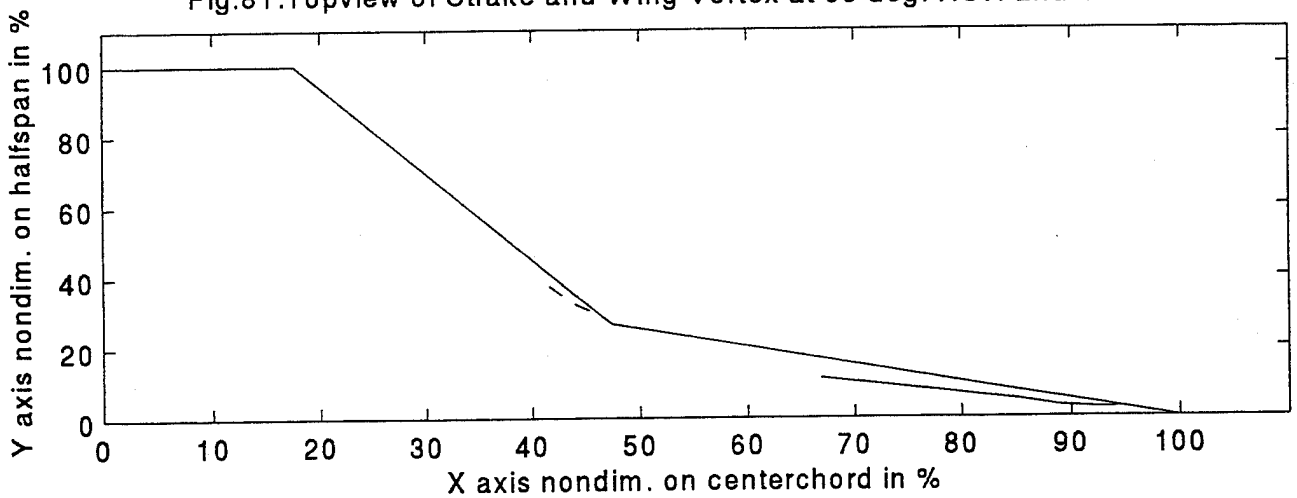

Fig.82:Strake vortex,AOA=5 deg,V=0.2-0.6-1.0 ft/sec

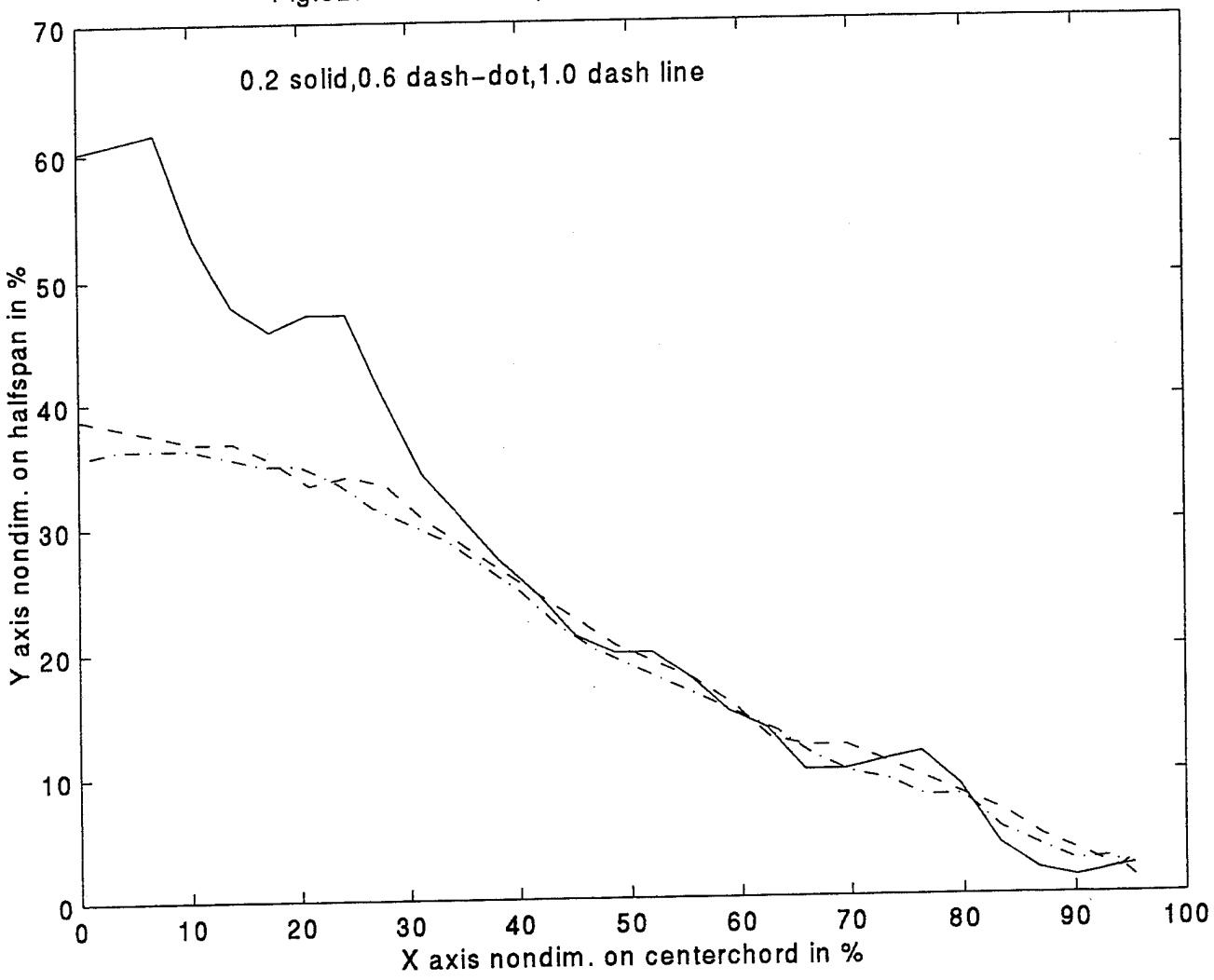

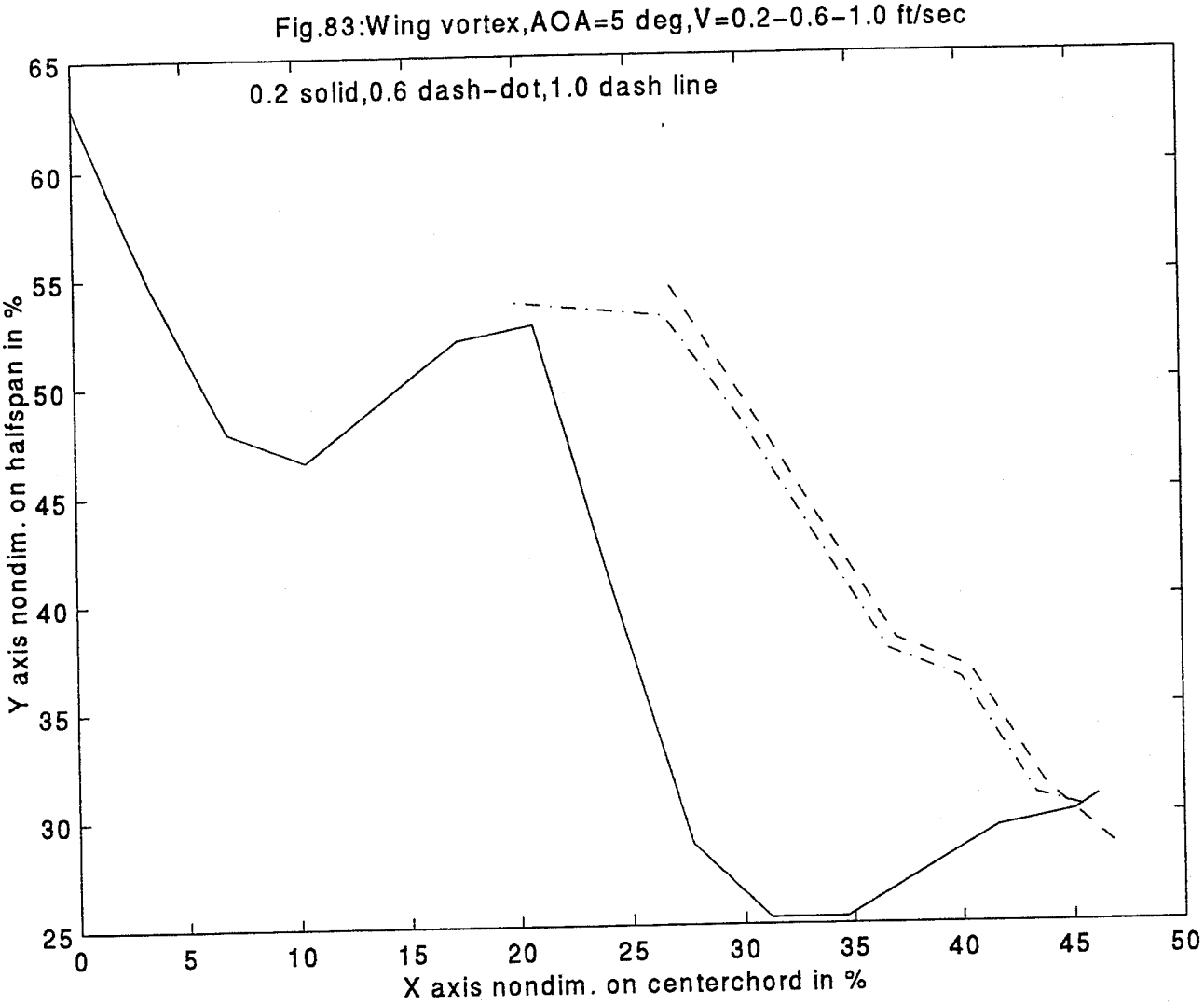
Fig.83:Wing vortex,AOA=5 deg,V=0.2-0.6-1.0 ft/sec
0.2 solid,0.6 dash-dot,1.0 dash line
Y axis nondim. on halfspan in %
X axis nondim. on centerchord in %
65
60
55
50
45
40
35
30
25
0
5
10
15
20
25
30
35
40
45
50

Fig.84:Strake vortex,AOA=10 deg,V=0.2-0.6-1.0 ft/sec

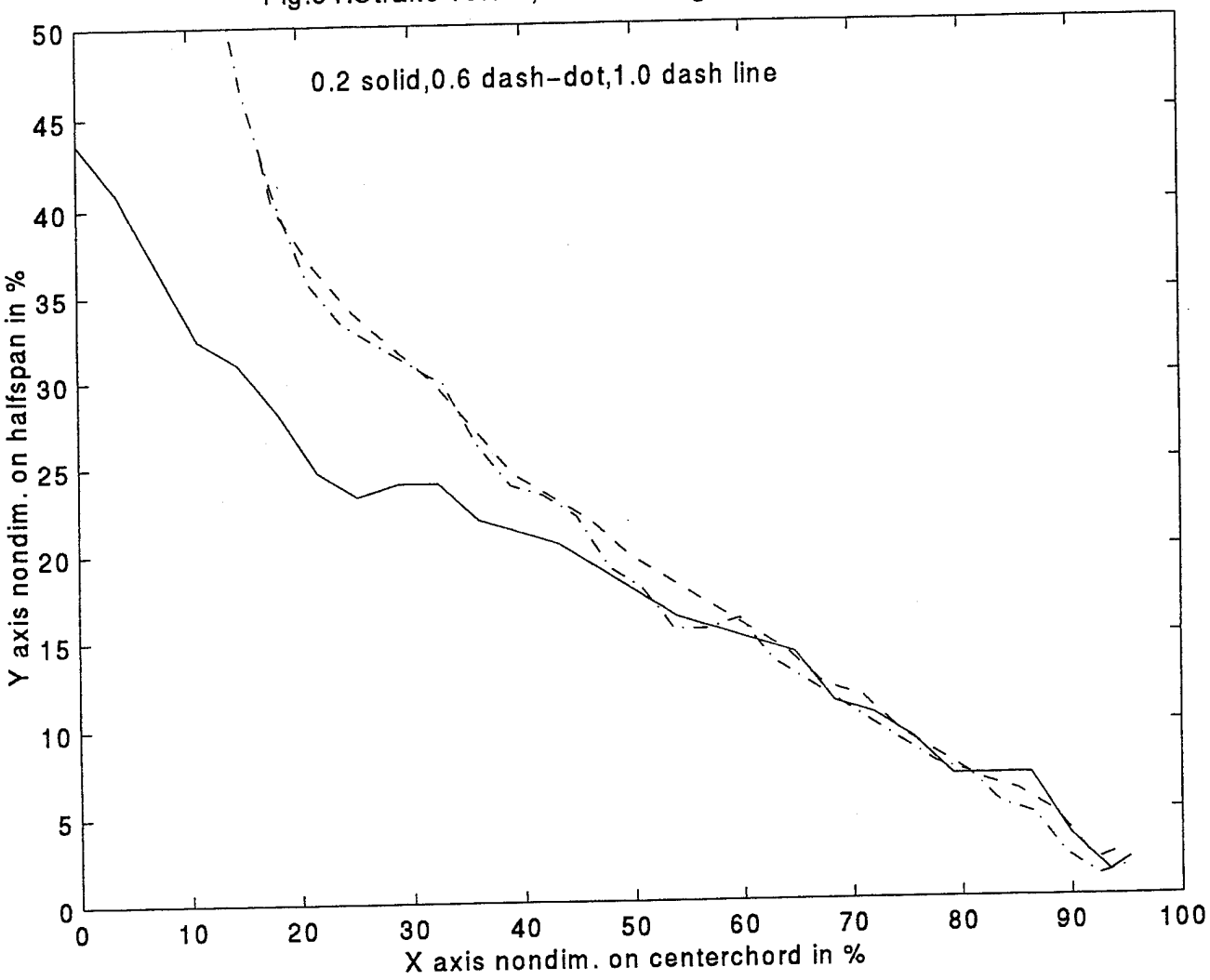

Fig.85:Wing vortex,AOA=10 deg,V=0.2-0.6-1.0 ft/sec

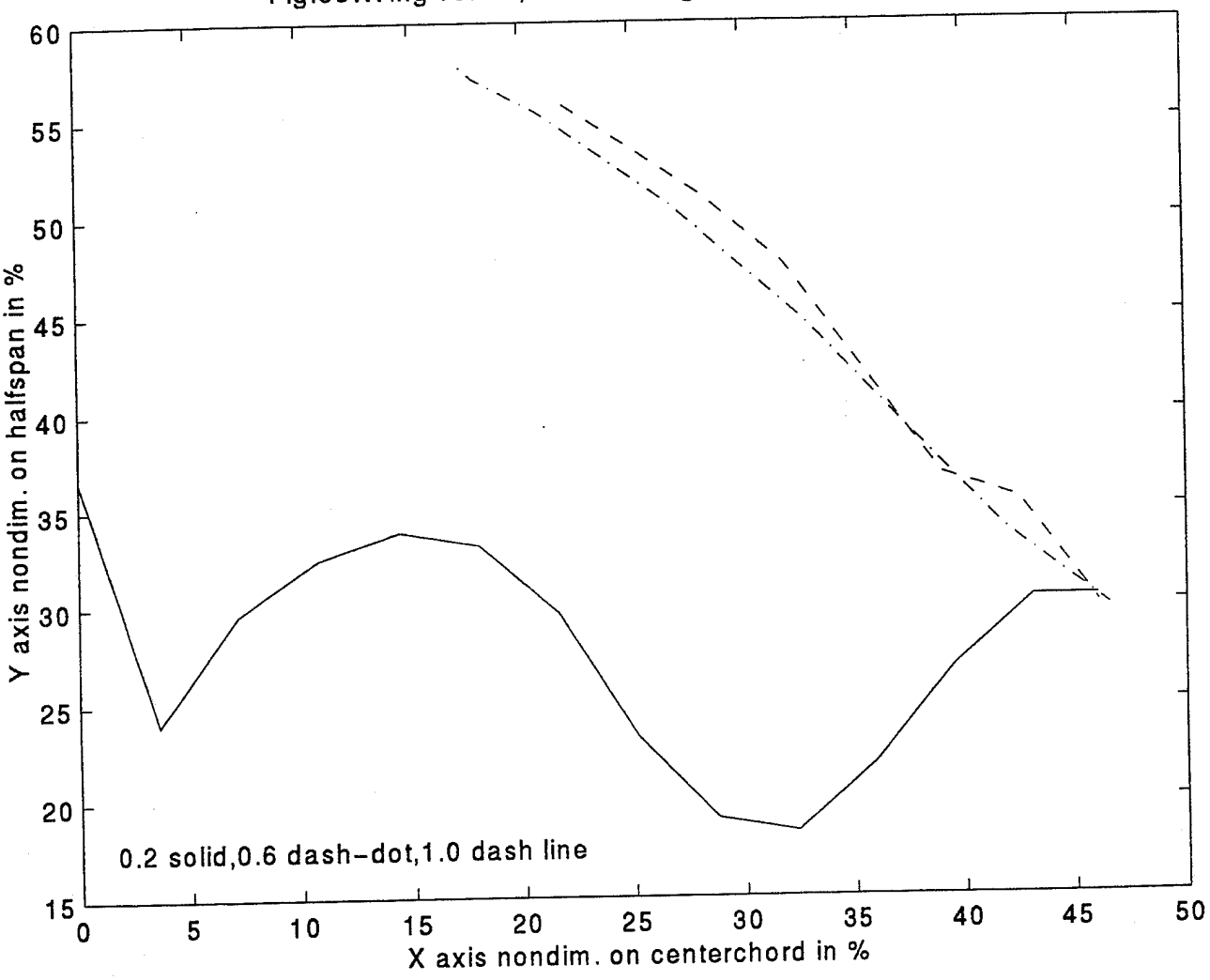

Fig.86:Strake vortex,AOA=15 deg,V=0.2-0.6-1.0 ft/sec

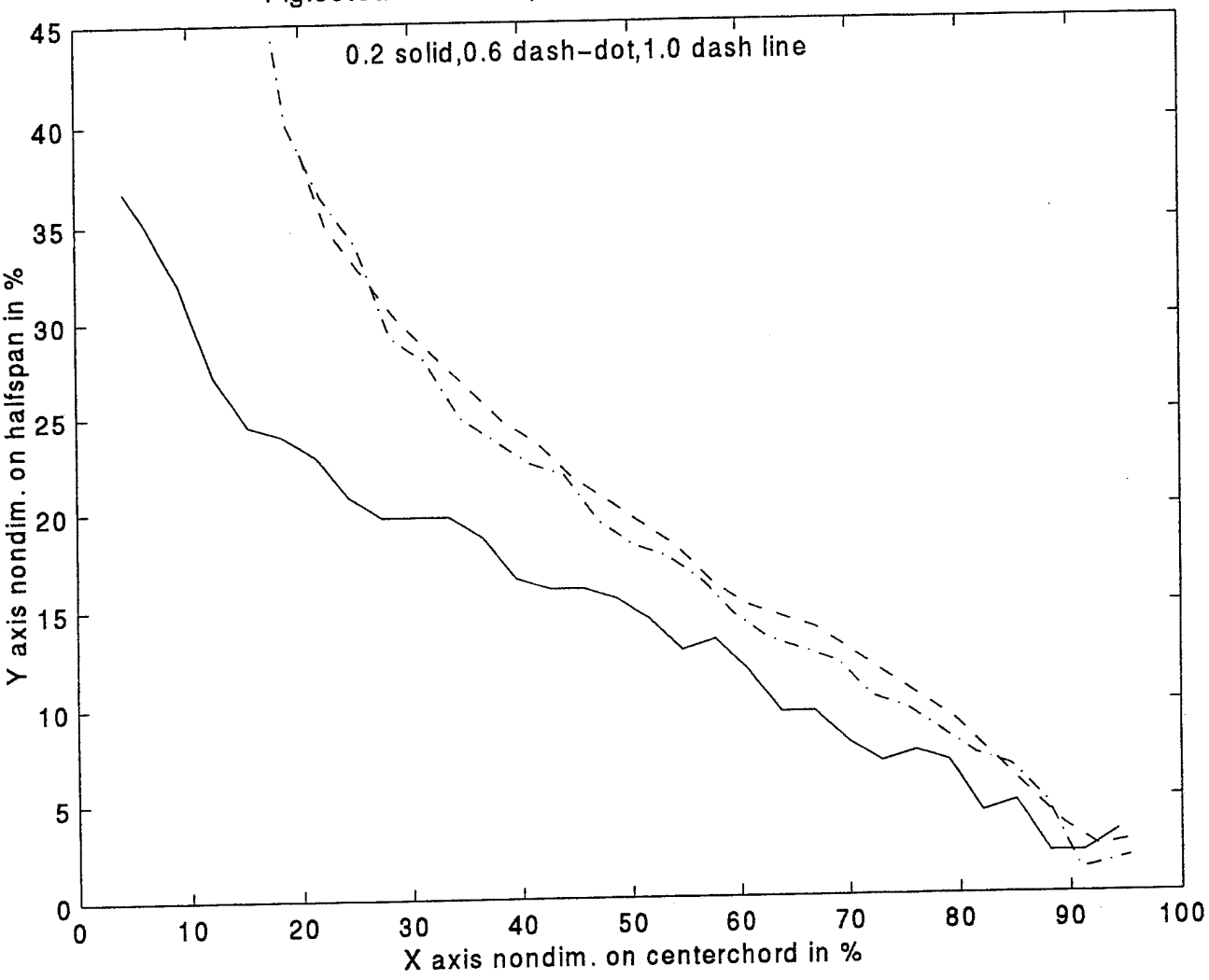

Fig.87:Wing vortex,AOA=15 deg,V=0.2-0.6-1.0 ft/sec

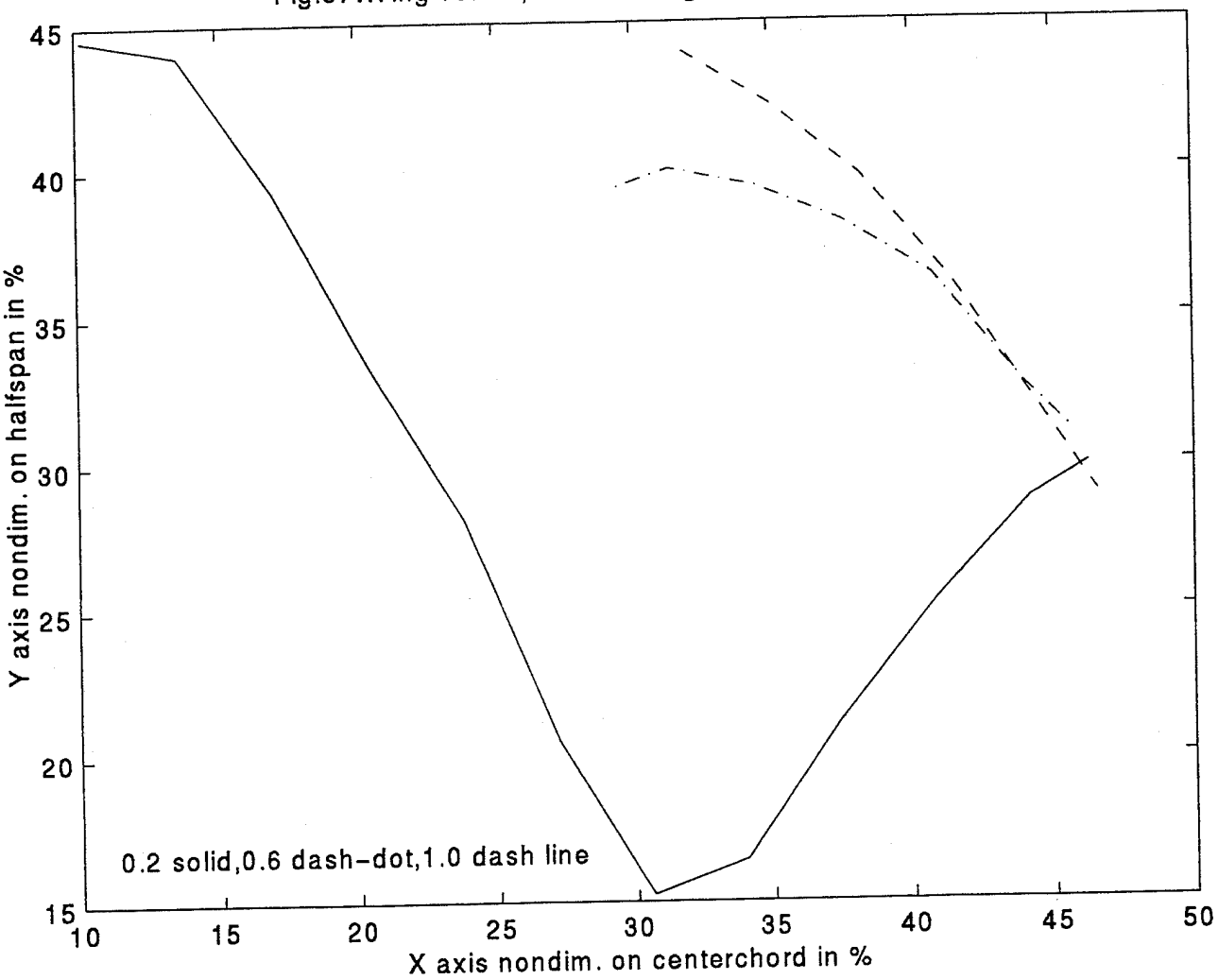

Fig.88:Strake vortex,AOA=20 deg,V=0.2-0.6-1.0 ft/sec

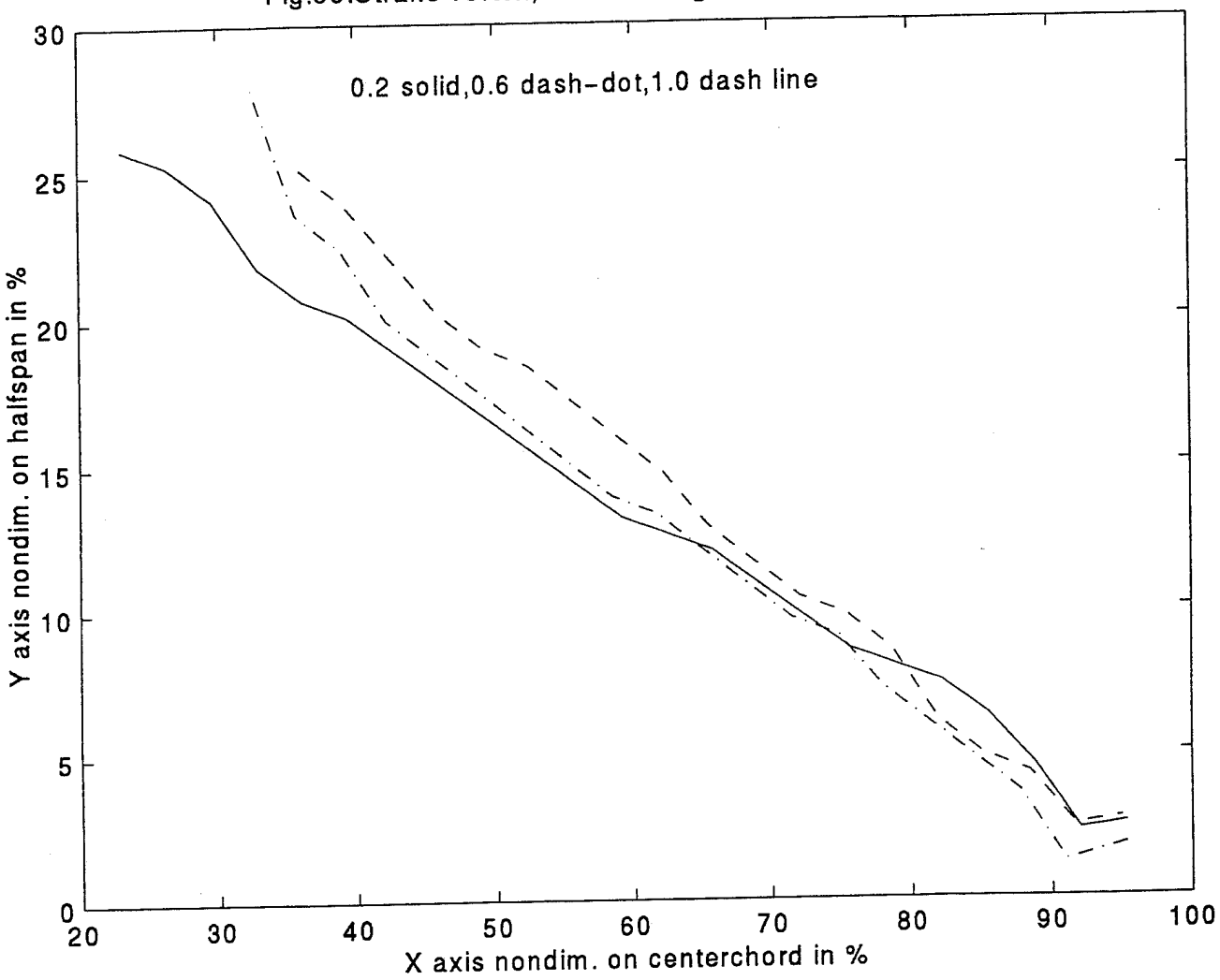

Fig.89:Wing vortex,AOA=20 deg,V=0.2-0.6-1.0 ft/sec

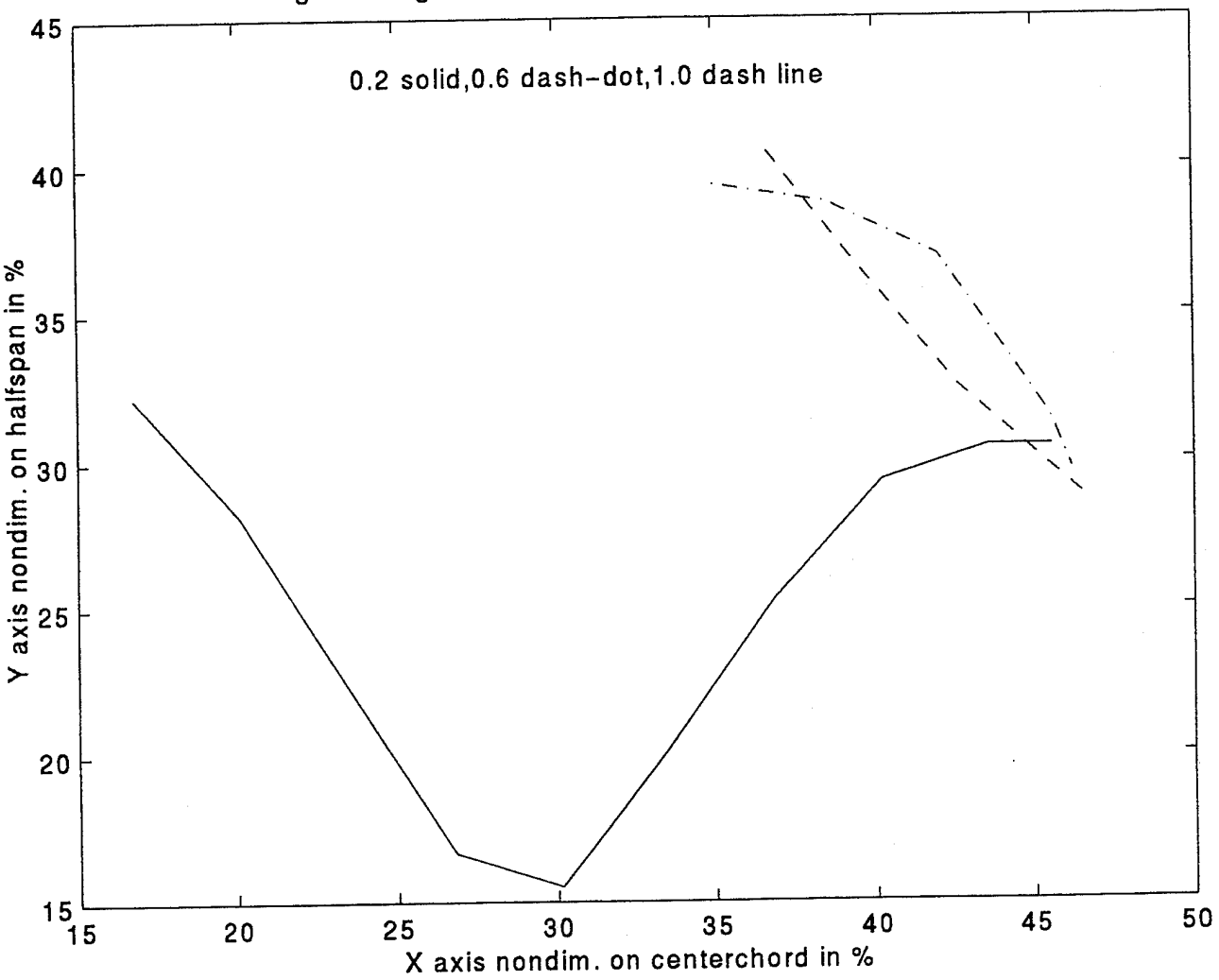

Fig.90:Strake vortex,AOA=22.5 deg,V=0.2-0.6-1.0 ft/sec

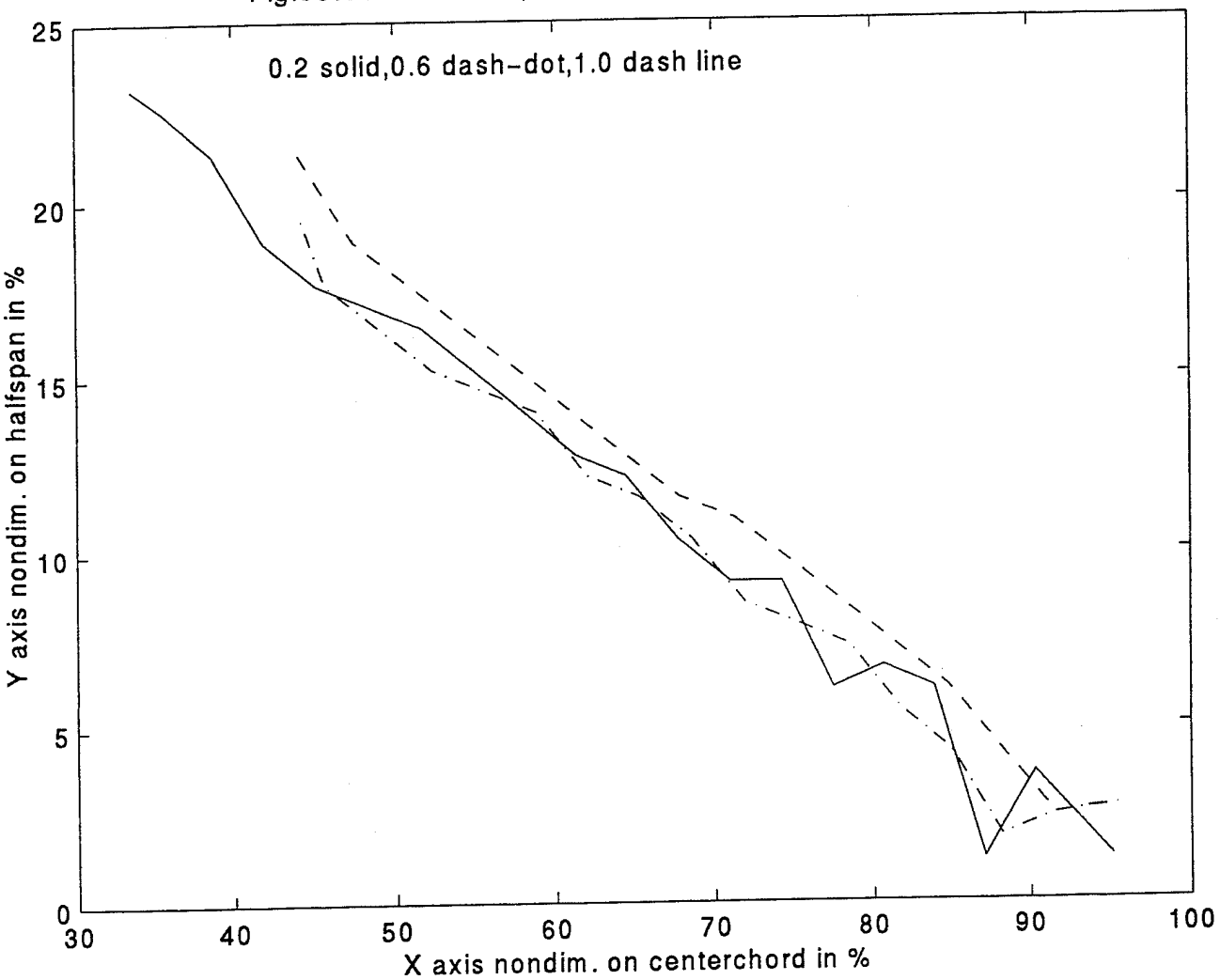

Fig.91:Strake vortex,AOA=22.5 deg,V=0.2-0.6-1.0 ft/sec

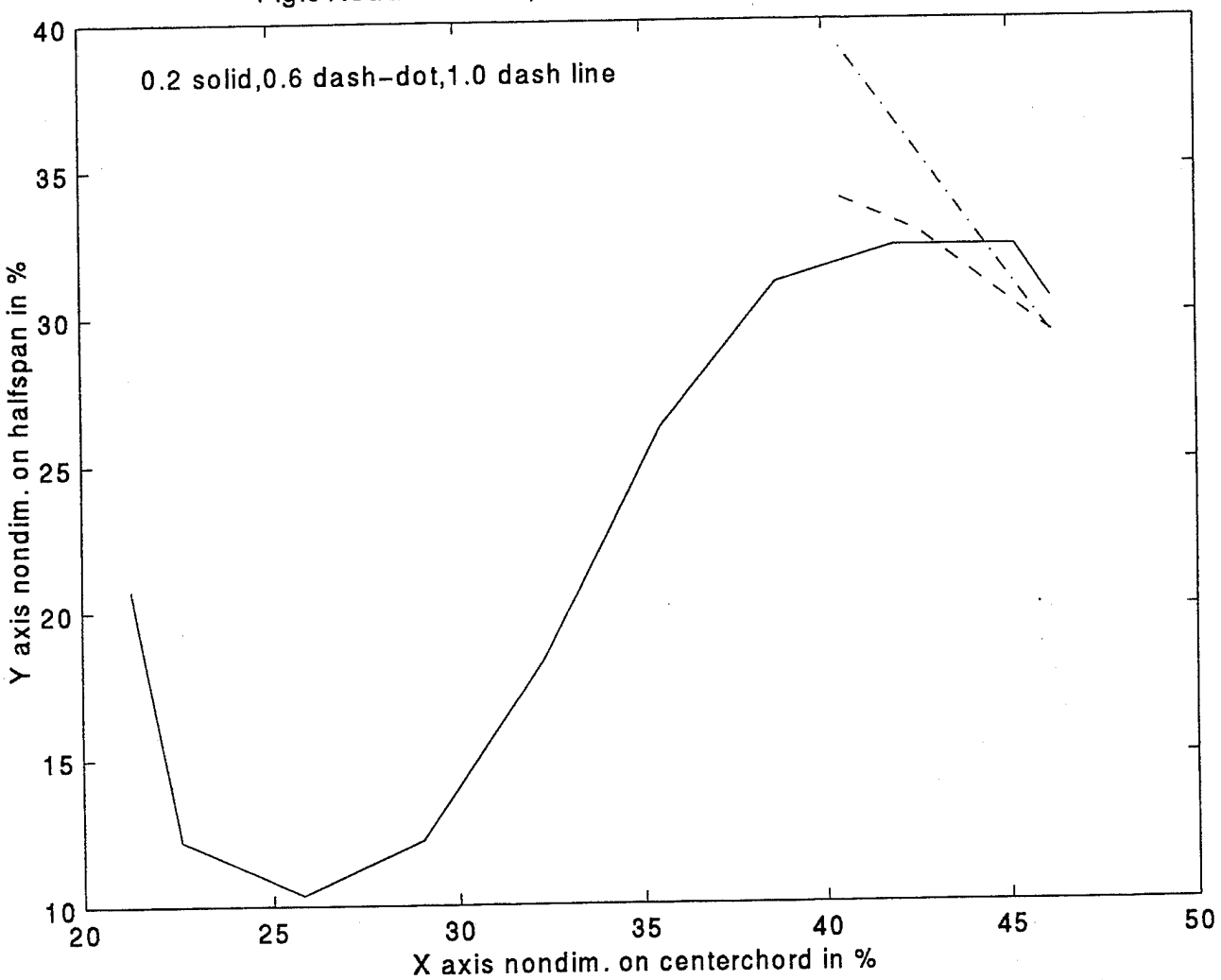

Fig.92:Strake vortex,AOA=25 deg,V=0.2-0.6-1.0 ft/sec

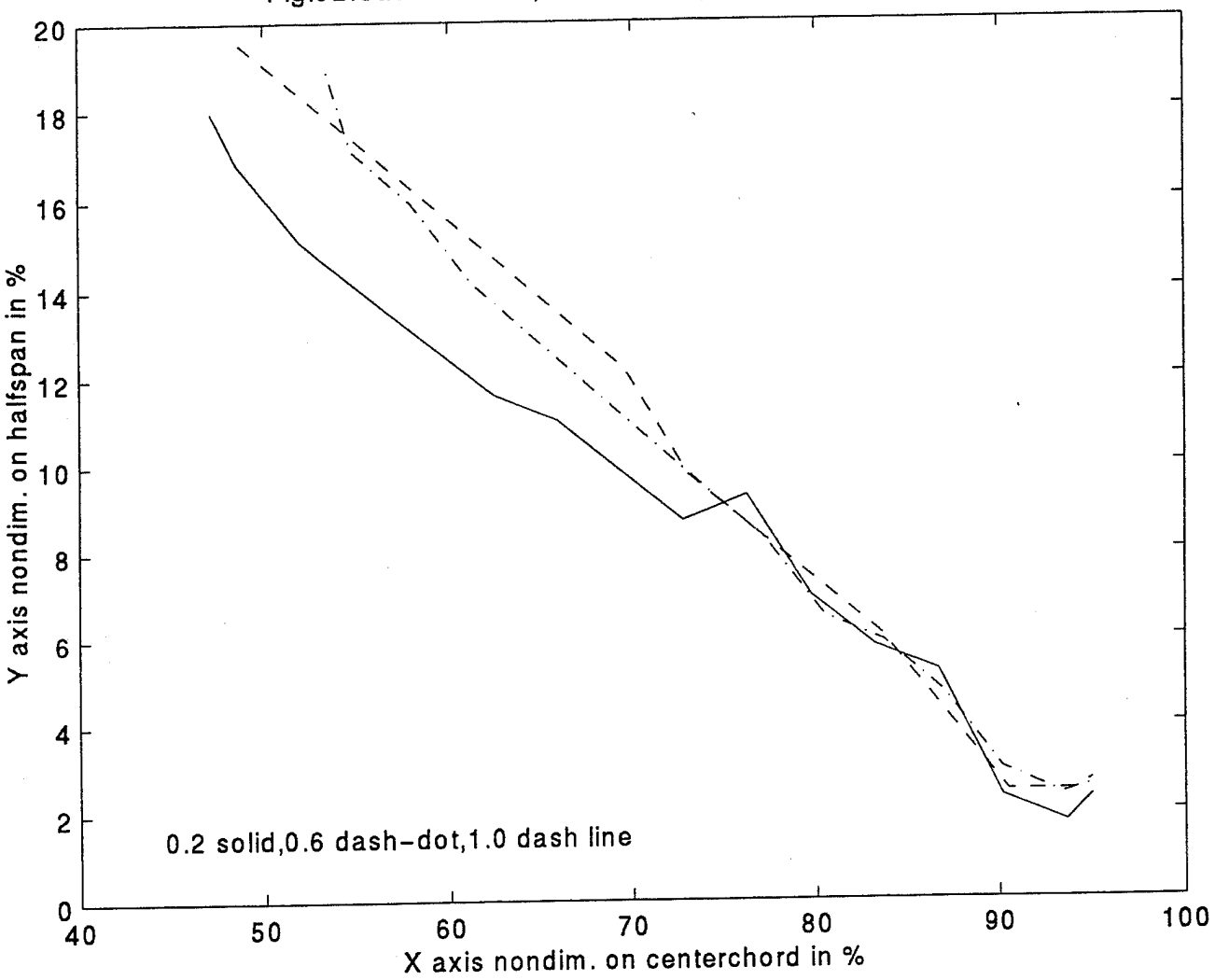

Fig.93:Wing vortex,AOA=25 deg,V=0.2-0.6-1.0 ft/sec

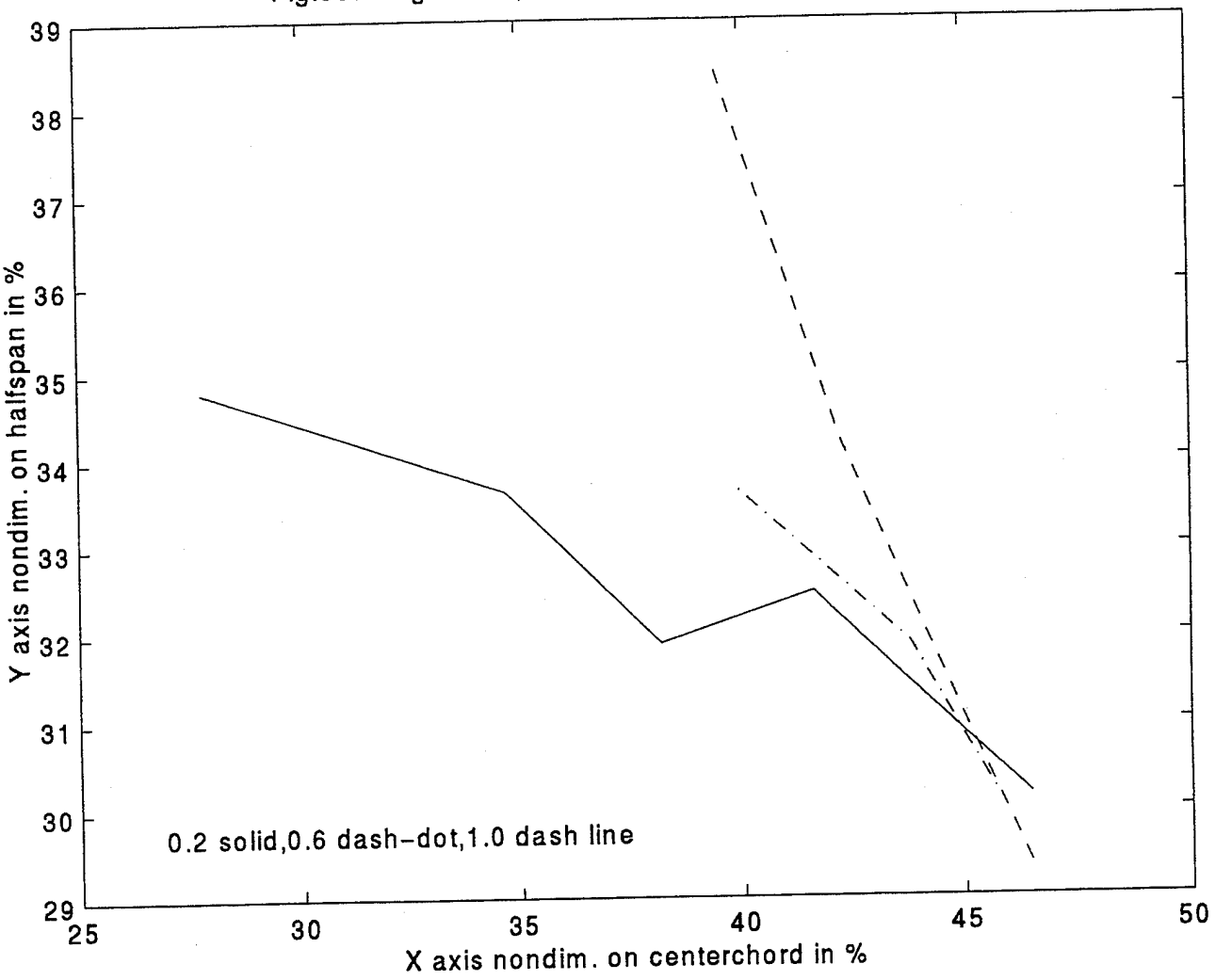

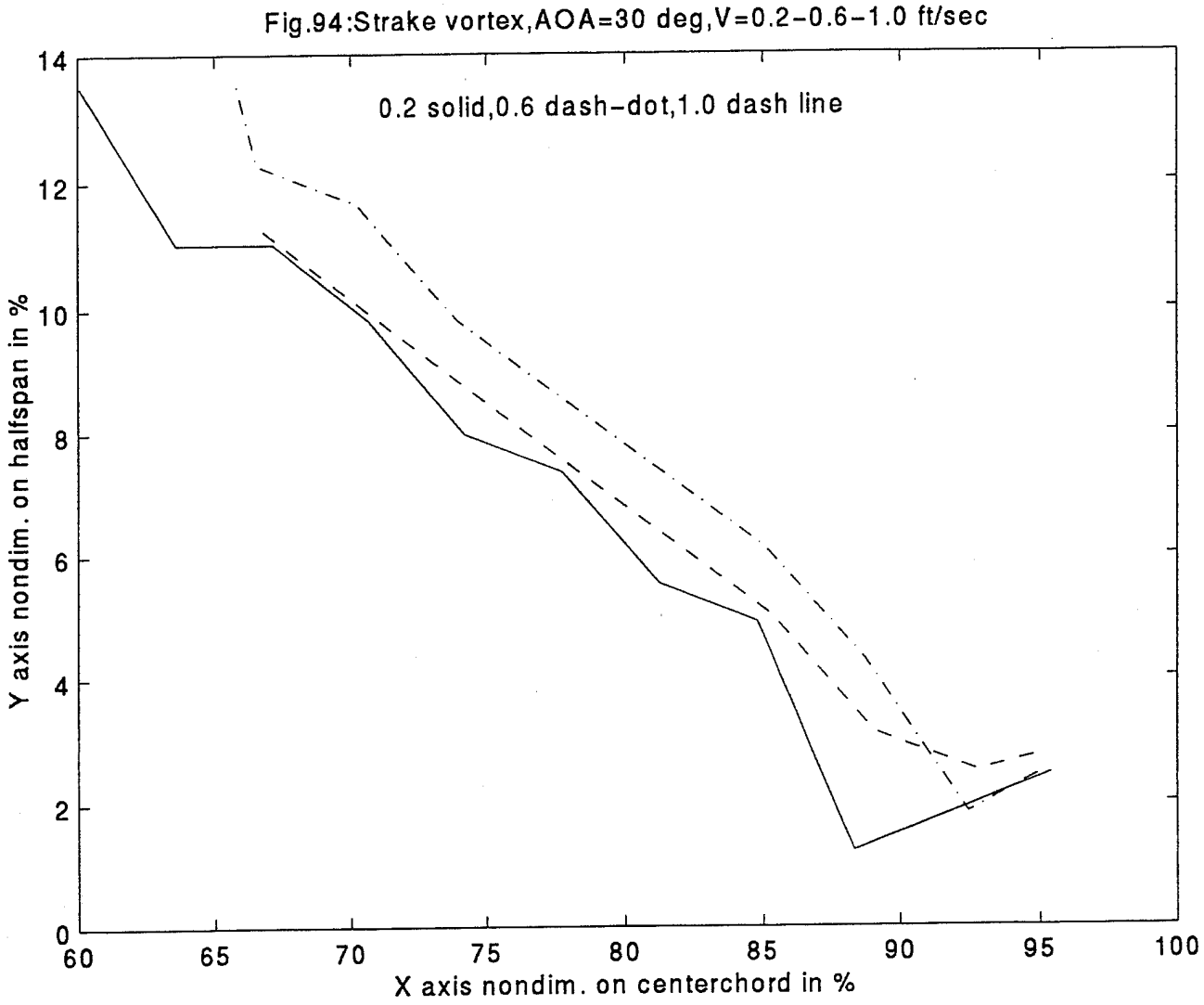
Fig.94:Strake vortex,AOA=30 deg,V=0.2-0.6-1.0 ft/sec
0.2 solid,0.6 dash-dot,1.0 dash line
Y axis nondim. on halfspan in %
X axis nondim. on centerchord in %
0
2
4
6
8
10
12
14
60
65
70
75
80
85
90
95
100

Fig.95:Wing vortex,AOA=30 deg,V=0.2-0.6-1.0 ft/sec

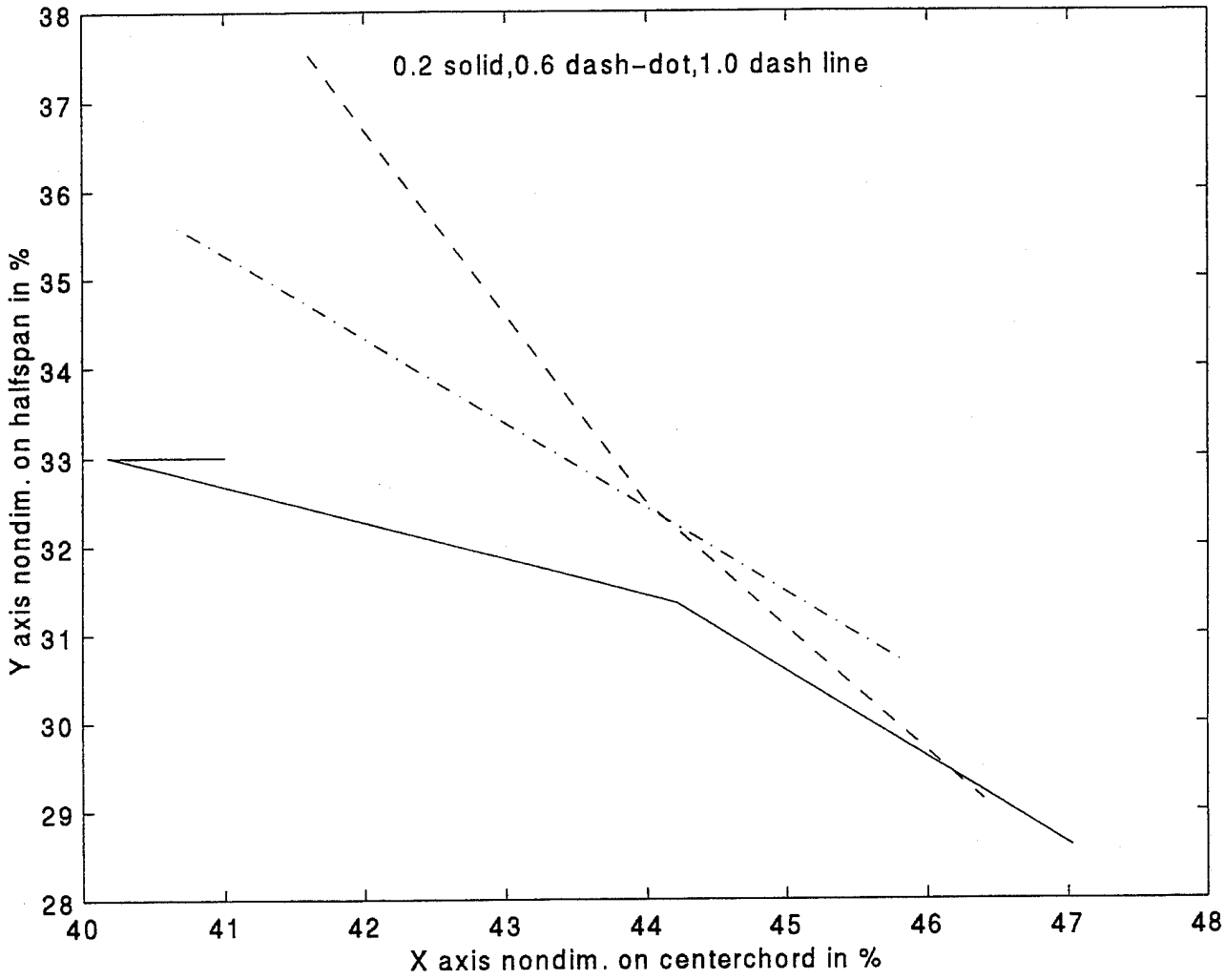

APPENDIX - C

EXPERIMENTAL RESULTS

(L. D. V. MEASUREMENTS)

Table 45 : LDV Measurements at X = 62.73 % , V = 0.6 ft/sec - AOA = 15 deg .

X/C in %	Y/S in %	Z in mm	VELOCITY	TURB.	STAND.DEV.
62.73	19,06 (100)	0,35	0,190	0,019	0
62.73	18,23 (95,65)	0,35	0,191	0,494	0,001
62.73	17,41 (91,3)	0,35	0,193	0,482	0,001
62.73	16,58 (86,96)	0,35	0,193	0,490	0,001
62.73	15,75 (82,6)	0,35	0,195	0,483	0,001
62.73	14,92 (78,26)	0,35	0,197	0,476	0,001
62.73	14,09 (73,91)	0,35	0,145	1,027	0,001
62.73	13,26 (69,56)	0,35	0,128	0,020	0
62.73	12,43 (65,22)	0,35	0,127	1,628	0,002
62.73	11,60 (60,87)	0,35	0,169	1,190	0,002
62.73	10,77 (56,52)	0,35	0,219	0,007	0
62.73	9,95 (52,17)	0,35	0,212	0,354	0,001
62.73	9,12 (47,83)	0,35	0,201	0,017	0
62.73	8,29 (43,48)	0,35	0,195	0,397	0,001
62.73	7,46 (39,13)	0,35	0,192	0,029	0
62.73	6,63 (34,78)	0,35	0,193	0,002	0
62.73	5,8 (30,43)	0,35	0,197	0,391	0,001
62.73	4,97 (26,09)	0,35	0,205	0,369	0,001
62.73	4,14 (21,74)	0,35	0,207	0,019	0
62.73	3,31 (17,39)	0,35	0,208	0,453	0,001
62.73	2,49 (13,04)	0,35	0,211	0,017	0
62.73	1,66 (8,69)	0,35	0,213	0,016	0
62.73	0,0083 (4,35)	0,35	0,214	0,440	0,001
62.73	0	0,35	----0,214----	----0,443----	----0,001----
62.73	-0,0083	0,35	0,214	0,439	0,001
62.73	-1,66	0,35	0,214	0,442	0,001
62.73	-2,49	0,35	0,212	0,443	0,001
62.73	-3,31	0,35	0,210	0,449	0,001
62.73	-4,14	0,35	0,208	0,455	0,001
62.73	-4,97	0,35	0,204	0,464	0,001
62.73	-5,8	0,35	0,201	0,472	0,001
62.73	-6,63	0,35	0,198	0,010	0

X/C in %	Y/S in %	Z in mm	VELOCITY	TURB.	STAND.DEV.
62.73	-7,46	0,35	0,194	0,015	0
62.73	-8,29	0,35	0,192	0,021	0
62.73	-9,12	0,35	0,193	0,490	0,001
62.73	-9,95	0,35	0,201	0,444	0,001
62.73	-10,77	0,35	0,201	0,470	0,001
62.73	-11,60	0,35	0,141	1,790	0,003
62.73	-12,43	0,35	0,082	0,003	0
62.73	-13,26	0,35	0,135	0,693	0,001
62.73	-14,09	0,35	0,125	1,215	0,002
62.73	-14,92	0,35	0,124	2,140	0,003
62.73	-15,75	0,35	0,190	0,019	0
62.73	-16,58	0,35	0,190	0,022	0
62.73	-17,41	0,35	0,190	0,016	0
62.73	-18,23	0,35	0,188	0,014	0
62.73	-19,06	0,35	0,186	0,012	0
62.73	-19,89	0,35	0,185	0,018	0
---	---	---	---	---	---
62.73	19,06 (100)	2,35	0,191	0,488	0,001
62.73	18,23 (95,65)	2,35	0,193	0,489	0,001
62.73	17,41 (91,3)	2,35	0,202	0,466	0,001
62.73	16,58 (86,96)	2,35	0,202	0,009	0
62.73	15,75 (82,6)	2,35	0,210	0,450	0,001
62.73	14,92 (78,26)	2,35	0,201	1,004	0,002
62.73	14,09 (73,91)	2,35	0,167	1,239	0,002
62.73	13,26 (69,56)	2,35	0,183	1,852	0,003
62.73	12,43 (65,22)	2,35	0,239	0,392	0,001
62.73	11,60 (60,87)	2,35	0,232	0,016	0
62.73	10,77 (56,52)	2,35	0,220	0,431	0,001
62.73	9,95 (52,17)	2,35	0,208	0,428	0,001
62.73	9,12 (47,83)	2,35	0,211	0,015	0
62.73	8,29 (43,48)	2,35	0,192	0,456	0,001
62.73	7,46 (39,13)	2,35	0,181	0,014	0
62.73	6,63 (34,78)	2,35	0,179	0,006	0

X/C in %	Y/C in %	Z in mm	VELOCITY	TURB.	STAND.DEV.
62.73	5,8 (30,43)	2,35	0,191	0,493	0,001
62.73	4,97 (26,09)	2,35	0,193	0,486	0,001
62.73	4,14 (21,74)	2,35	0,199	0,466	0,001
62.73	3,31 (17,39)	2,35	0,204	0,456	0,001
62.73	2,49 (13,04)	2,35	0,207	0,016	0
62.73	1,66 (8,69)	2,35	0,210	0,449	0,001
62.73	0,0083 (4,35)	2,35	0,210	0,442	0,001
62.73	0	2,35	----0,210----	----0,442----	----0,001----
62.73	-0,0083	2,35	0,210	0,450	0,001
62.73	-1,66	2,35	0,209	0,020	0
62.73	-2,49	2,35	0,208	0,453	0,001
62.73	-3,31	2,35	0,203	0,467	0,001
62.73	-4,14	2,35	0,199	0,475	0,001
62.73	-4,97	2,35	0,193	0,490	0,001
62.73	-5,8	2,35	0,191	0,492	0,001
62.73	-6,63	2,35	0,177	0,016	0
62.73	-7,46	2,35	0,182	0,522	0,001
62.73	-8,29	2,35	0,192	0,793	0,002
62.73	-9,12	2,35	0,200	0,834	0,002
62.73	-9,95	2,35	0,210	1,028	0,002
62.73	-10,77	2,35	0,231	0,407	0,001
62.73	-11,60	2,35	0,229	0,413	0,001
62.73	-12,43	2,35	0,158	2,308	0,004
62.73	-13,26	2,35	0,114	1,300	0,001
62.73	-14,09	2,35	0,144	2,278	0,003
62.73	-14,92	2,35	0,204	0,461	0,001
62.73	-15,75	2,35	0,206	0,445	0,001
62.73	-16,58	2,35	0,199	0,477	0,001
62.73	-17,41	2,35	0,199	0,474	0,001
62.73	-18,23	2,35	0,191	0,474	0,001
62.73	-19,06	2,35	0,196	0,015	0
----------	----------	----------	----------	----------	----------
62.73	19,06 (100)	4,35	0,202	0,014	0

X/C in %	Y/C in %	Z in mm	VELOCITY	TURB.	STAND.DEV.
62.73	18,23 (95,65)	4,35	0,204	0,023	0
62.73	17,41 (91,3)	4,35	0,206	0,014	0
62.73	16,58 (86,96)	4,35	0,209	0,018	0
62.73	15,75 (82,6)	4,35	0,211	0,022	0
62.73	14,92 (78,26)	4,35	0,214	0,514	0,001
62.73	14,09 (73,91)	4,35	0,180	0,021	0
62.73	13,26 (69,56)	4,35	0,232	0,987	0,002
62.73	12,43 (65,22)	4,35	0,256	0,431	0,001
62.73	11,60 (60,87)	4,35	0,263	0,418	0,001
62.73	10,77 (56,52)	4,35	0,277	0,020	0
62.73	9,95 (52,17)	4,35	0,290	0,010	0
62.73	9,12 (47,83)	4,35	0,269	0,410	0,001
62.73	8,29 (43,48)	4,35	0,232	0,022	0
62.73	7,46 (39,13)	4,35	0,203	0,018	0
62.73	6,63 (34,78)	4,35	0,188	0,013	0
62.73	5,8 (30,43)	4,35	0,185	0,486	0,001
62.73	4,97 (26,09)	4,35	0,192	0,021	0,001
62.73	4,14 (21,74)	4,35	0,196	0,012	0
62.73	3,31 (17,39)	4,35	0,201	0,469	0,001
62.73	2,49 (13,04)	4,35	0,203	0,465	0,001
62.73	1,66 (8,69)	4,35	0,204	0,448	0,001
62.73	0,0083 (4,35)	4,35	0,206	0,455	0,001
62.73	0	4,35	----0,206----	----0,457----	----0,001----
62.73	-0,0083	4,35	0,206	0,459	0,001
62.73	-1,66	4,35	0,204	0,463	0,001
62.73	-2,49	4,35	0,203	0,465	0,001
62.73	-3,31	4,35	0,201	0,471	0,001
62.73	-4,14	4,35	0,195	0,486	0,001
62.73	-4,97	4,35	0,186	0,020	0
62.73	-5,8	4,35	0,188	0,015	0
62.73	-6,63	4,35	0,195	0,918	0,002
62.73	-7,46	4,35	0,214	1,150	0,002
62.73	-8,29	4,35	0,237	0,770	0,002

X/C in %	Y/S in %	Z in mm	VELOCITY	TURB.	STAND.DEV.
62.73	-9,12	4,35	0,263	1,017	0,003
62.73	-9,95	4,35	0,262	0,681	0,002
62.73	-10,77	4,35	0,250	0,691	0,002
62.73	-11,60	4,35	0,254	0,431	0,001
62.73	-12,43	4,35	0,249	0,443	0,001
62.73	-13,26	4,35	0,199	1,856	0,004
62.73	-14,09	4,35	0,201	1,227	0,002
62.73	-14,92	4,35	0,215	0,015	0
62.73	-15,75	4,35	0,211	0,015	0
62.73	-16,58	4,35	0,204	0,023	0
62.73	-17,41	4,35	0,202	0,014	0
62.73	-18,23	4,35	0,200	0,013	0
62.73	-19,06	4,35	0,198	0,013	0
62.73	-19,89	4,35	0,195	0,007	0
---	---	---	---	---	---
62.73	19,06 (100)	6,35	0,206	0,005	0
62.73	18,23 (95,65)	6,35	0,208	0,010	0
62.73	17,41 (91,3)	6,35	0,211	0,005	0
62.73	16,58 (86,96)	6,35	0,213	0,018	0
62.73	15,75 (82,6)	6,35	0,221	0,021	0
62.73	14,92 (78,26)	6,35	0,228	0,009	0
62.73	14,09 (73,91)	6,35	0,238	0,019	0
62.73	13,26 (69,56)	6,35	0,246	0,017	0
62.73	12,43 (65,22)	6,35	0,269	0,008	0
62.73	11,60 (60,87)	6,35	0,285	0,420	0,001
62.73	10,77 (56,52)	6,35	0,313	0,403	0,001
62.73	9,95 (52,17)	6,35	0,321	0,390	0,001
62.73	9,12 (47,83)	6,35	0,307	0,358	0,001
62.73	8,29 (43,48)	6,35	0,264	0,720	0,002
62.73	7,46 (39,13)	6,35	0,237	0,902	0,002
62.73	6,63 (34,78)	6,35	0,166	1,219	0,002
62.73	5,8 (30,43)	6,35	0,188	0,497	0,001
62.73	4,97 (26,09)	6,35	0,192	0,017	0

X/C in %	Y/C in %	Z in mm	VELOCITY	TURB.	STAND.DEV.
62.73	4,14 (21,74)	6,35	0,197	0,479	0,001
62.73	3,31 (17,39)	6,35	0,199	0,473	0,001
62.73	2,49 (13,04)	6,35	0,203	0,011	0
62.73	1,66 (8,69)	6,35	0,204	0,463	0,001
62.73	0,0083 (4,35)	6,35	0,203	0,010	0
62.73	0	6,35	----0,204----	----0,023----	----0----
62.73	-0,0083	6,35	0,203	0,023	0
62.73	-1,66	6,35	0,203	0,021	0
62.73	-2,49	6,35	0,201	0,011	0
62.73	-3,31	6,35	0,198	0,014	0
62.73	-4,14	6,35	0,196	0,018	0
62.73	-4,97	6,35	0,196	0,011	0
62.73	-5,8	6,35	0,188	0,003	0
62.73	-6,63	6,35	0,187	1,133	0,002
62.73	-7,46	6,35	0,248	0,838	0,002
62.73	-8,29	6,35	0,278	0,454	0,002
62.73	-9,12	6,35	0,317	0,721	0,002
62.73	-9,95	6,35	0,320	0,671	0,002
62.73	-10,77	6,35	0,295	0,425	0,001
62.73	-11,60	6,35	0,277	1,009	0,003
62.73	-12,43	6,35	0,237	1,269	0,003
62.73	-13,26	6,35	0,232	0,542	0,001
62.73	-14,09	6,35	0,223	0,010	0
62.73	-14,92	6,35	0,218	0,014	0
62.73	-15,75	6,35	0,213	0,008	0
62.73	-16,58	6,35	0,211	0,018	0
62.73	-17,41	6,35	0,206	0,022	0
62.73	-18,23	6,35	0,203	0,017	0
62.73	-19,06	6,35	0,210	0,024	0
62,73	-19,89	6,35	0,198	0,012	0
---	---	---	---	---	---
62.73	19,06 (100)	8,35	0,206	0,024	0
62.73	18,23 (95,65)	8,35	0,208	0,003	0

X/C in %	Y/C in %	Z in mm	VELOCITY	TURB.	STAND.DEV.
62.73	17,41 (91,3)	8,35	0,211	0,014	0
62.73	16,58 (86,96)	8,35	0,213	0,030	0
62.73	15,75 (82,6)	8,35	0,218	0,015	0
62.73	14,92 (78,26)	8,35	0,226	0,015	0
62.73	14,09 (73,91)	8,35	0,231	0,010	0
62.73	13,26 (69,56)	8,35	0,233	0,021	0
62.73	12,43 (65,22)	8,35	0,232	1,096	0,003
62.73	11,60 (60,87)	8,35	0,227	1,205	0,003
62.73	10,77 (56,52)	8,35	0,263	1,095	0,003
62.73	9,95 (52,17)	8,35	0,275	0,456	0,001
62.73	9,12 (47,83)	8,35	0,268	0,015	0
62.73	8,29 (43,48)	8,35	0,249	0,418	0,001
62.73	7,46 (39,13)	8,35	0,228	0,879	0,002
62.73	6,63 (34,78)	8,35	0,189	0,500	0,001
62.73	5,8 (30,43)	8,35	0,193	0,487	0,001
62.73	4,97 (26,09)	8,35	0,197	0,480	0,001
62.73	4,14 (21,74)	8,35	0,199	0,474	0,001
62.73	3,31 (17,39)	8,35	0,201	0,472	0,001
62.73	2,49 (13,04)	8,35	0,204	0,462	0,001
62.73	1,66 (8,69)	8,35	0,203	0,465	0,001
62.73	0,0083 (4,35)	8,35	0,205	0,007	0
62.73	0	8,35	----0,204----	----0,014----	----0----
62.73	-0,0083	8,35	0,203	0,019	0
62.73	-1,66	8,35	0,203	0,009	0
62.73	-2,49	8,35	0,201	0,020	0
62.73	-3,31	8,35	0,201	0,005	0
62.73	-4,14	8,35	0,201	0,025	0
62.73	-4,97	8,35	0,198	0,012	0
62.73	-5,8	8,35	0,198	0,027	0
62.73	-6,63	8,35	0,197	0,641	0,001
62.73	-7,46	8,35	0,220	1,359	0,003
62.73	-8,29	8,35	0,256	0,742	0,002
62.73	-9,12	8,35	0,267	1,122	0,003

X/C in %	Y/S in %	Z in mm	VELOCITY	TURB.	STAND.DEV.
62.73	-9,95	8,35	0,280	1,006	0,003
62.73	-10,77	8,35	0,271	1,251	0,003
62.73	-11,60	8,35	0,241	0,882	0,002
62.73	-12,43	8,35	0,235	0,539	0,001
62.73	-13,26	8,35	0,231	0,016	0
62.73	-14,09	8,35	0,226	0,008	0
62.73	-14,92	8,35	0,218	0,009	0
62.73	-15,75	8,35	0,213	0,013	0
62.73	-16,58	8,35	0,211	0,010	0
62.73	-17,41	8,35	0,208	0,021	0
62.73	-18,23	8,35	0,203	0,029	0
62,73	-19,06	8,35	0,203	0,019	0
62,73	-19,89	8,35	0,201	0,018	0
---	---	---	---	---	---
62.73	19,06 (100)	10,35	0,208	0,014	0
62.73	18,23 (95,65)	10,35	0,208	0,021	0
62.73	17,41 (91,3)	10,35	0,211	0,021	0
62.73	16,58 (86,96)	10,35	0,216	0,015	0
62.73	15,75 (82,6)	10,35	0,216	0,002	0
62.73	14,92 (78,26)	10,35	0,223	0,017	0
62.73	14,09 (73,91)	10,35	0,226	0,020	0
62.73	13,26 (69,56)	10,35	0,226	0,013	0
62.73	12,43 (65,22)	10,35	0,223	0,011	0
62.73	11,60 (60,87)	10,35	0,223	0,004	0
62.73	10,77 (56,52)	10,35	0,236	0,022	0
62.73	9,95 (52,17)	10,35	0,244	0,003	0
62.73	9,12 (47,83)	10,35	0,238	0,462	0,001
62.73	8,29 (43,48)	10,35	0,231	0,018	0
62.73	7,46 (39,13)	10,35	0,217	0,635	0,001
62.73	6,63 (34,78)	10,35	0,207	0,018	0
62.73	5,8 (30,43)	10,35	0,203	0,011	0
62.73	4,97 (26,09)	10,35	0,203	0,468	0,001
62.73	4,14 (21,74)	10,35	0,203	0,018	0

X/C in %	Y/S in %	Z in mm	VELOCITY	TURB.	STAND.DEV.
62.73	3,31 (17,39)	10,35	0,203	0,460	0,001
62.73	2,49 (13,04)	10,35	0,203	0,464	0,001
62.73	1,66 (8,69)	10,35	0,203	0,023	0
62.73	0,0083 (4,35)	10,35	0,205	0,022	0
62.73	0	10,35	----0,204----	----0,005----	----0----
62.73	-0,0083	10,35	0,203	0,022	0
62.73	-1,66	10,35	0,203	0,017	0
62.73	-2,49	10,35	0,203	0,029	0
62.73	-3,31	10,35	0,203	0,017	0
62.73	-4,14	10,35	0,203	0,016	0
62.73	-4,97	10,35	0,206	0,022	0
62.73	-5,8	10,35	0,206	0,019	0
62.73	-6,63	10,35	0,208	0,012	0
62.73	-7,46	10,35	0,213	0,008	0
62.73	-8,29	10,35	0,226	0,020	0
62.73	-9,12	10,35	0,228	0,014	0
62.73	-9,95	10,35	0,228	0,028	0
62.73	-10,77	10,35	0,231	0,018	0
62.73	-11,60	10,35	0,228	0,023	0
62.73	-12,43	10,35	0,226	0,022	0
62.73	-13,26	10,35	0,226	0,014	0
62.73	-14,09	10,35	0,218	0,008	0
62.73	-14,92	10,35	0,216	0,015	0
62.73	-15,75	10,35	0,213	0,016	0
62.73	-16,58	10,35	0,211	0,005	0
62.73	-17,41	10,35	0,206	0,004	0
62.73	-18,23	10,35	0,206	0,019	0
62.73	-19,06	10,35	0,203	0,013	0
62,73	-19,89	10,35	0,201	0,010	0
----------	----------	----------	----------	----------	----------
62.73	19,06 (100)	12,35	0,206	0,017	0
62.73	18,23 (95,65)	12,35	0,211	0,017	0
62.73	17,41 (91,3)	12,35	0,211	0,014	0

X/C in %	Y/S in %	Z in mm	VELOCITY	TURB.	STAND.DEV.
62.73	16,58 (86,96)	12,35	0,215	0,021	0
62.73	15,75 (82,6)	12,35	0,219	0,005	0
62.73	14,92 (78,26)	12,35	0,224	0,012	0
62.73	14,09 (73,91)	12,35	0,224	0,026	0
62.73	13,26 (69,56)	12,35	0,228	0,023	0
62.73	12,43 (65,22)	12,35	0,224	0,005	0
62.73	11,60 (60,87)	12,35	0,224	0,019	0
62.73	10,77 (56,52)	12,35	0,228	0,006	0
62.73	9,95 (52,17)	12,35	0,233	0,016	0
62.73	9,12 (47,83)	12,35	0,233	0,025	0
62.73	8,29 (43,48)	12,35	0,224	0,015	0
62.73	7,46 (39,13)	12,35	0,215	0,023	0
62.73	6,63 (34,78)	12,35	0,211	0,014	0
62.73	5,8 (30,43)	12,35	0,206	0,006	0
62.73	4,97 (26,09)	12,35	0,206	0,018	0
62.73	4,14 (21,74)	12,35	0,202	0,018	0
62.73	3,31 (17,39)	12,35	0,202	0,018	0
62.73	2,49 (13,04)	12,35	0,206	0,012	0
62.73	1,66 (8,69)	12,35	0,202	0,017	0
62.73	0,0083 (4,35)	12,35	0,202	0,026	0
62.73	0	12,35	----0,206----	----0,011----	----0----
62.73	-0,0083	12,35	0,206	0,018	0
62.73	-1,66	12,35	0,206	0,021	0
62.73	-2,49	12,35	0,202	0,022	0
62.73	-3,31	12,35	0,202	0,013	0
62.73	-4,14	12,35	0,206	0,002	0
62.73	-4,97	12,35	0,206	0,012	0
62.73	-5,8	12,35	0,211	0,006	0
62.73	-6,63	12,35	0,211	0,023	0
62.73	-7,46	12,35	0,219	0,018	0
62.73	-8,29	12,35	0,224	0,011	0
62.73	-9,12	12,35	0,224	0,015	0
62.73	-9,95	12,35	0,228	0,022	0

X/C in %	Y/S in %	Z in mm	VELOCITY	TURB.	STAND.DEV.
62.73	-10,77	12,35	0,228	0,006	0
62.73	-11,60	12,35	0,224	0,013	0
62.73	-12,43	12,35	0,224	0,024	0
62.73	-13,26	12,35	0,219	0,012	0
62.73	-14,09	12,35	0,219	0,026	0
62.73	-14,92	12,35	0,215	0,011	0
62.73	-15,75	12,35	0,211	0,013	0
62.73	-16,58	12,35	0,211	0,021	0
62.73	-17,41	12,35	0,206	0,012	0
62.73	-18,23	12,35	0,206	0,011	0
62,73	-19,06	12,35	0,202	0,022	0
---	---	---	---	---	---
62.73	19,06 (100)	14,35	0,206	0,010	0
62.73	18,23 (95,65)	14,35	0,206	0,019	0
62.73	17,41 (91,3)	14,35	0,211	0,011	0
62.73	16,58 (86,96)	14,35	0,215	0,012	0
62.73	15,75 (82,6)	14,35	0,219	0,023	0
62.73	14,92 (78,26)	14,35	0,215	0,004	0
62.73	14,09 (73,91)	14,35	0,219	0,009	0
62.73	13,26 (69,56)	14,35	0,224	0,022	0
62.73	12,43 (65,22)	14,35	0,224	0,024	0
62.73	11,60 (60,87)	14,35	0,224	0,019	0
62.73	10,77 (56,52)	14,35	0,224	0,021	0
62.73	9,95 (52,17)	14,35	0,224	0,019	0
62.73	9,12 (47,83)	14,35	0,224	0,021	0
62.73	8,29 (43,48)	14,35	0,215	0,019	0
62.73	7,46 (39,13)	14,35	0,215	0,009	0
62.73	6,63 (34,78)	14,35	0,211	0,017	0
62.73	5,8 (30,43)	14,35	0,211	0,006	0
62.73	4,97 (26,09)	14,35	0,206	0,019	0
62.73	4,14 (21,74)	14,35	0,206	0,009	0
62.73	3,31 (17,39)	14,35	0,206	0,021	0
62.73	2,49 (13,04)	14,35	0,206	0,008	0

X/C in %	Y/S in %	Z in mm	VELOCITY	TURB.	STAND.DEV.
62.73	1,66 (8,69)	14,35	0,202	0,019	0
62.73	0,0083 (4,35)	14,35	0,206	0,017	0
62.73	0	14,35	----0,206----	----0,012----	0
62.73	-0,0083	14,35	0,206	0,012	0
62.73	-1,66	14,35	0,202	0,009	0
62.73	-2,49	14,35	0,206	0,012	0
62.73	-3,31	14,35	0,206	0,011	0
62.73	-4,14	14,35	0,206	0,021	0
62.73	-4,97	14,35	0,206	0,011	0
62.73	-5,8	14,35	0,211	0,008	0
62.73	-6,63	14,35	0,211	0,011	0
62.73	-7,46	14,35	0,215	0,018	0
62.73	-8,29	14,35	0,219	0,005	0
62.73	-9,12	14,35	0,219	0,004	0
62.73	-9,95	14,35	0,224	0,018	0
62.73	-10,77	14,35	0,224	0,017	0
62.73	-11,60	14,35	0,219	0,019	0
62.73	-12,43	14,35	0,219	0,024	0
62.73	-13,26	14,35	0,215	0,011	0
62.73	-14,09	14,35	0,215	0,022	0
62.73	-14,92	14,35	0,215	0,025	0
62.73	-15,75	14,35	0,211	0,020	0
62.73	-16,58	14,35	0,206	0,017	0
62.73	-17,41	14,35	0,206	0,015	0
62.73	-18,23	14,35	0,202	0,020	0
62,73	-19,06	14,35	0,202	0,026	0

Table 46 : LDV Measurements at X = 38.62 % , V = 0.6 ft/sec - AOA = 15 deg .

X/C in %	Y/S in %	Z in mm	VELOCITY	TURB.	STAND.DEV.
38,62	0	0,73	0,202	0,020	0
38,62	0,0083 (1,79)	0,73	0,200	0,022	0
38,62	1,66 (3,57)	0,73	0,204	0,008	0
38,62	2,49 (5,36)	0,73	0,200	0,022	0
38,62	3,31 (7,14)	0,73	0,204	0,014	0
38,62	4,14 (8,93)	0,73	0,202	0,021	0
38,62	4,97 (10,71)	0,73	0,195	0,002	0
38,62	5,8 (12,5)	0,73	0,202	0,014	0
38,62	6,63 (14,29)	0,73	0,198	0,022	0
38,62	7,46 (16,07)	0,73	0,193	0,020	0
38,62	8,29 (17,86)	0,73	0,187	0,003	0
38,62	9,12 (19,64)	0,73	0,187	0,020	0
38,62	9,95 (21,43)	0,73	0,189	0,012	0
38,62	10,77 (23,21)	0,73	0,184	0,013	0
38,62	11,60 (25)	0,73	0,180	0,010	0
38,62	12,43 (26,78)	0,73	0,169	0,019	0
38,62	13,26 (28,57)	0,73	0,171	0,021	0
38,62	14,09 (30,36)	0,73	0,169	0,014	0
38,62	14,92 (32,14)	0,73	0,171	0,021	0
38,62	15,75 (33,93)	0,73	0,169	0,019	0
38,62	16,58 (35,71)	0,73	0,172	0,023	0
38,62	17,41 (37,5)	0,73	0,172	0,025	0
38,62	18,23 (39,29)	0,73	0,185	0,015	0
38,62	19,06 (41,07)	0,73	0,191	0,014	0
38,62	19,89 (42,86)	0,73	0,185	0,015	0
38,62	20,72 (44,64)	0,73	0,181	1,452	0,003
38,62	21,55 (46,43)	0,73	0,139	3,570	0,005
38,62	22,38 (48,21)	0,73	0,092	5,667	0,005
38,62	23,21 (50)	0,73	0,025	14,382	0,004
38,62	24,04 (51,78)	0,73	-0,028	7,754	0,002
38,62	24,86 (53,57)	0,73	-0,046	7,123	0,003
38,62	25,69 (55,36)	0,73	0,013	236,510	0,031

X/C in %	Y/S in %	Z in mm	VELOCITY	TURB.	STAND.DEV.
38,62	26,52 (57,14)	0,73	0,008	365.99	0,028
38,62	27,35 (58,93)	0,73	0,053	3,96	0,002
38,62	28,18 (60,71)	0,73	0,008	0,021	0
38,62	29,01 (62,5)	0,73	0,010	90,91	0,009
38,62	29,83 (64,29)	0,73	0,036	9,837	0,004
38,62	30,67 (66,07)	0,73	0,047	3,309	0,002
38,62	31,5 (67,86)	0,73	0,015	172,84	0,026
38,62	32,32 (69,64)	0,73	0,003	951,54	0,025
38,62	33,15 (71,43)	0,73	0,027	0,018	0
38,62	33,98 (73,21)	0,73	-0,046	0,008	0
38,62	34,81 (75)	0,73	-0,071	3,975	0,003
38,62	35,64 (76,78)	0,73	-0,064	3,322	0,002
38,62	36,47 (78,57)	0,73	-0,060	2,632	0,002
38,62	37,3 (80,36)	0,73	0,172	0,010	0,010
38,62	38,13 (82,14)	0,73	0,162	0,016	0
38,62	38,95 (83,93)	0,73	0,159	0,007	0
---	---	---	---	---	---
38,62	0	3,73	0,202	0,022	0
38,62	0,0083 (1,79)	3,73	0,200	0,028	0
38,62	1,66 (3,57)	3,73	0,202	0,014	0
38,62	2,49 (5,36)	3,73	0,198	0,022	0
38,62	3,31 (7,14)	3,73	0,200	0,016	0
38,62	4,14 (8,93)	3,73	0,198	0,019	0
38,62	4,97 (10,71)	3,73	0,195	0,007	0
38,62	5,8 (12,5)	3,73	0,193	0,017	0
38,62	6,63 (14,29)	3,73	0,193	0,003	0
38,62	7,46 (16,07)	3,73	0,189	0,015	0
38,62	8,29 (17,86)	3,73	0,187	0,015	0
38,62	9,12 (19,64)	3,73	0,182	0,008	0
38,62	9,95 (21,43)	3,73	0,180	0,014	0
38,62	10,77 (23,21)	3,73	0,173	0,018	0
38,62	11,60 (25)	3,73	0,168	0,656	0,001
38,62	12,43 (26,78)	3,73	0,166	0,667	0,001

X/C in %	Y/S in %	Z in mm	VELOCITY	TURB.	STAND.DEV.
38,62	13,26 (28,57)	3,73	0,166	0,666	0,001
38,62	14,09 (30,36)	3,73	0,167	1,218	0,002
38,62	14,92 (32,14)	3,73	0,180	1,058	0,002
38,62	15,75 (33,93)	3,73	0,174	0,771	0,001
38,62	16,58 (35,71)	3,73	0,187	0,756	0,001
38,62	17,41 (37,5)	3,73	0,193	0,728	0,001
38,62	18,23 (39,29)	3,73	0,193	0,744	0,001
38,62	19,06 (41,07)	3,73	0,199	0,755	0,002
38,62	19,89 (42,86)	3,73	0,203	0,026	0
38,62	20,72 (44,64)	3,73	0,207	0,009	0
38,62	21,55 (46,43)	3,73	0,213	0,020	0
38,62	22,38 (48,21)	3,73	0,222	0,026	0
38,62	23,21 (50)	3,73	0,213	0,019	0
38,62	24,04 (51,78)	3,73	0,206	0,955	0,002
38,62	24,86 (53,57)	3,73	0,175	2,401	0,004
38,62	25,69 (55,36)	3,73	0,136	8,717	0,012
38,62	26,52 (57,14)	3,73	0,127	5,639	0,007
38,62	27,35 (58,93)	3,73	0,046	9,375	0,004
38,62	28,18 (60,71)	3,73	0,136	2,294	0,003
38,62	29,01 (62,5)	3,73	0,089	3,932	0,004
38,62	29,83 (64,29)	3,73	0,079	3,973	0,003
38,62	30,67 (66,07)	3,73	0,089	4,198	0,004
38,62	31,5 (67,86)	3,73	0,080	0,017	0
38,62	32,32 (69,64)	3,73	0,062	0,014	0
38,62	33,15 (71,43)	3,73	-0,011	66,571	0,007
38,62	33,98 (73,21)	3,73	-0,041	3,768	0,002
38,62	34,81 (75)	3,73	0,132	2,982	0,004
38,62	35,64 (76,78)	3,73	0,232	0,012	0
38,62	36,47 (78,57)	3,73	0,219	0,014	0
38,62	37,3 (80,36)	3,73	0,210	0,017	0
38,62	38,13 (82,14)	3,73	0,197	0,010	0
38,62	38,95 (83,93)	3,73	0,191	0,015	0
---	---	---	---	---	---

X/C in %	Y/S in %	Z in mm	VELOCITY	TURB.	STAND.DEV.
38,62	0	6,73	0,197	0,025	0
38,62	0,0083 (1,79)	6,73	0,198	0,018	0
38,62	1,66 (3,57)	6,73	0,195	0,007	0
38,62	2,49 (5,36)	6,73	0,200	0,016	0
38,62	3,31 (7,14)	6,73	0,193	0,017	0
38,62	4,14 (8,93)	6,73	0,198	0,022	0
38,62	4,97 (10,71)	6,73	0,193	0,017	0
38,62	5,8 (12,5)	6,73	0,193	0,013	0
38,62	6,63 (14,29)	6,73	0,191	0,017	0
38,62	7,46 (16,07)	6,73	0,184	0,024	0
38,62	8,29 (17,86)	6,73	0,180	0,010	0
38,62	9,12 (19,64)	6,73	0,180	0,025	0
38,62	9,95 (21,43)	6,73	0,176	0,021	0
38,62	10,77 (23,21)	6,73	0,171	0,009	0
38,62	11,60 (25)	6,73	0,187	1,443	0,003
38,62	12,43 (26,78)	6,73	0,189	1,184	0,002
38,62	13,26 (28,57)	6,73	0,203	1,151	0,002
38,62	14,09 (30,36)	6,73	0,205	0,533	0,001
38,62	14,92 (32,14)	6,73	0,201	0,914	0,002
38,62	15,75 (33,93)	6,73	0,220	0,019	0
38,62	16,58 (35,71)	6,73	0,223	0,006	0
38,62	17,41 (37,5)	6,73	0,247	1,099	0,003
38,62	18,23 (39,29)	6,73	0,249	1,577	0,004
38,62	19,06 (41,07)	6,73	0,265	0,593	0,002
38,62	19,89 (42,86)	6,73	0,248	1,213	0,003
38,62	20,72 (44,64)	6,73	0,249	0,631	0,002
38,62	21,55 (46,43)	6,73	0,251	0,016	0
38,62	22,38 (48,21)	6,73	0,244	0,019	0
38,62	23,21 (50)	6,73	0,251	0,012	0
38,62	24,04 (51,78)	6,73	0,244	0,012	0
38,62	24,86 (53,57)	6,73	0,222	1,421	0,003
38,62	25,69 (55,36)	6,73	0,201	0,739	0,001
38,62	26,52 (57,14)	6,73	0,147	2,355	0,003

X/C in %	Y/S in %	Z in mm	VELOCITY	TURB.	STAND.DEV.
38,62	27,35 (58,93)	6,73	0,104	2,942	0,003
38,62	28,18 (60,71)	6,73	0,114	2,671	0,003
38,62	29,01 (62,5)	6,73	0,113	4,883	0,006
38,62	29,83 (64,29)	6,73	0,123	2,622	0,003
38,62	30,67 (66,07)	6,73	0,132	2,941	0,004
38,62	31,5 (67,86)	6,73	0,189	2,394	0,005
38,62	32,32 (69,64)	6,73	0,251	0,996	0,003
38,62	33,15 (71,43)	6,73	0,244	0,012	0
38,62	33,98 (73,21)	6,73	0,244	0,022	0
38,62	34,81 (75)	6,73	0,235	0,017	0
38,62	35,64 (76,78)	6,73	0,229	0,016	0
38,62	36,47 (78,57)	6,73	0,219	0,009	0
38,62	37,3 (80,36)	6,73	0,213	0,021	0
38,62	38,13 (82,14)	6,73	0,207	0,017	0
38,62	38,95 (83,93)	6,73	0,203	0,004	0
---	---	---	---	---	---
38,62	0	9,73	0,197	0,017	0
38,62	0,0083 (1,79)	9,73	0,200	0,015	0
38,62	1,66 (3,57)	9,73	0,200	0,024	0
38,62	2,49 (5,36)	9,73	0,200	0,013	0
38,62	3,31 (7,14)	9,73	0,195	0,007	0
38,62	4,14 (8,93)	9,73	0,195	0,019	0
38,62	4,97 (10,71)	9,73	0,193	0,020	0
38,62	5,8 (12,5)	9,73	0,191	0,013	0
38,62	6,63 (14,29)	9,73	0,191	0,015	0
38,62	7,46 (16,07)	9,73	0,187	0,014	0
38,62	8,29 (17,86)	9,73	0,182	0,018	0
38,62	9,12 (19,64)	9,73	0,183	0,599	0,001
38,62	9,95 (21,43)	9,73	0,187	0,024	0
38,62	10,77 (23,21)	9,73	0,188	0,977	0,002
38,62	11,60 (25)	9,73	0,194	1,209	0,002
38,62	12,43 (26,78)	9,73	0,218	1,327	0,003
38,62	13,26 (28,57)	9,73	0,227	1,216	0,003

X/C in %	Y/S in %	Z in mm	VELOCITY	TURB.	STAND.DEV.
38,62	14,09 (30,36)	9,73	0,244	1,012	0,002
38,62	14,92 (32,14)	9,73	0,265	0,853	0,002
38,62	15,75 (33,93)	9,73	0,319	0,618	0,002
38,62	16,58 (35,71)	9,73	0,369	0,892	0,003
38,62	17,41 (37,5)	9,73	0,363	0,429	0,002
38,62	18,23 (39,29)	9,73	0,344	0,441	0,002
38,62	19,06 (41,07)	9,73	0,328	0,770	0,003
38,62	19,89 (42,86)	9,73	0,311	0,005	0
38,62	20,72 (44,64)	9,73	0,300	0,514	0,002
38,62	21,55 (46,43)	9,73	0,284	0,552	0,002
38,62	22,38 (48,21)	9,73	0,280	0,516	0,001
38,62	23,21 (50)	9,73	0,279	0,986	0,003
38,62	24,04 (51,78)	9,73	0,255	1,205	0,003
38,62	24,86 (53,57)	9,73	0,267	0,858	0,002
38,62	25,69 (55,36)	9,73	0,194	1,624	0,003
38,62	26,52 (57,14)	9,73	0,157	1,892	0,003
38,62	27,35 (58,93)	9,73	0,152	1,034	0,002
38,62	28,18 (60,71)	9,73	0,202	2,278	0,005
38,62	29,01 (62,5)	9,73	0,251	1,284	0,003
38,62	29,83 (64,29)	9,73	0,254	0,005	0
38,62	30,67 (66,07)	9,73	0,254	0,010	0
38,62	31,5 (67,86)	9,73	0,251	0,023	0
38,62	32,32 (69,64)	9,73	0,244	0,024	0
38,62	33,15 (71,43)	9,73	0,238	0,016	0
38,62	33,98 (73,21)	9,73	0,235	0,025	0
38,62	34,81 (75)	9,73	0,229	0,016	0
38,62	35,64 (76,78)	9,73	0,226	0,006	0
38,62	36,47 (78,57)	9,73	0,219	0,011	0
38,62	37,3 (80,36)	9,73	0,216	0,015	0
38,62	38,13 (82,14)	9,73	0,210	0,021	0
38,62	38,95 (83,93)	9,73	0,207	0,009	0
---	---	---	---	---	---
38,62	0	12,73	0,197	0,017	0

X/C in %	Y/S in %	Z in mm	VELOCITY	TURB.	STAND.DEV.
38,62	0,0083 (1,79)	12,73	0,200	0,016	0
38,62	1,66 (3,57)	12,73	0,196	0,536	0,001
38,62	2,49 (5,36)	12,73	0,195	0,006	0
38,62	3,31 (7,14)	12,73	0,198	0,019	0
38,62	4,14 (8,93)	12,73	0,195	0,021	0
38,62	4,97 (10,71)	12,73	0,195	0,001	0
38,62	5,8 (12,5)	12,73	0,195	0,006	0
38,62	6,63 (14,29)	12,73	0,195	0,001	0
38,62	7,46 (16,07)	12,73	0,191	0,013	0
38,62	8,29 (17,86)	12,73	0,189	0,008	0
38,62	9,12 (19,64)	12,73	0,189	0,024	0
38,62	9,95 (21,43)	12,73	0,190	0,705	0,001
38,62	10,77 (23,21)	12,73	0,207	1,083	0,002
38,62	11,60 (25)	12,73	0,214	1,385	0,003
38,62	12,43 (26,78)	12,73	0,246	1,587	0,004
38,62	13,26 (28,57)	12,73	0,261	1,489	0,004
38,62	14,09 (30,36)	12,73	0,295	1,168	0,003
38,62	14,92 (32,14)	12,73	0,305	0,852	0,003
38,62	15,75 (33,93)	12,73	0,325	0,724	0,002
38,62	16,58 (35,71)	12,73	0,353	0,620	0,002
38,62	17,41 (37,5)	12,73	0,369	0,426	0,002
38,62	18,23 (39,29)	12,73	0,343	0,810	0,003
38,62	19,06 (41,07)	12,73	0,347	0,445	0,002
38,62	19,89 (42,86)	12,73	0,335	0,454	0,002
38,62	20,72 (44,64)	12,73	0,310	1,186	0,004
38,62	21,55 (46,43)	12,73	0,297	0,500	0,001
38,62	22,38 (48,21)	12,73	0,277	1,331	0,004
38,62	23,21 (50)	12,73	0,287	1,228	0,004
38,62	24,04 (51,78)	12,73	0,268	0,564	0,002
38,62	24,86 (53,57)	12,73	0,279	0,023	0
38,62	25,69 (55,36)	12,73	0,270	0,014	0
38,62	26,52 (57,14)	12,73	0,268	0,894	0,002
38,62	27,35 (58,93)	12,73	0,260	0,015	0

X/C in %	Y/S in %	Z in mm	VELOCITY	TURB.	STAND.DEV.
38,62	28,18 (60,71)	12,73	0,260	0,008	0
38,62	29,01 (62,5)	12,73	0,254	0,016	0
38,62	29,83 (64,29)	12,73	0,248	0,025	0
38,62	30,67 (66,07)	12,73	0,244	0,017	0
38,62	31,5 (67,86)	12,73	0,238	0,016	0
38,62	32,32 (69,64)	12,73	0,235	0,006	0
38,62	33,15 (71,43)	12,73	0,232	0,011	0
38,62	33,98 (73,21)	12,73	0,229	0,018	0
38,62	34,81 (75)	12,73	0,226	0,009	0
38,62	35,64 (76,78)	12,73	0,219	0,019	0
38,62	36,47 (78,57)	12,73	0,216	0,009	0
38,62	37,3 (80,36)	12,73	0,213	0,013	0
38,62	38,13 (82,14)	12,73	0,213	0,013	0
38,62	38,95 (83,93)	12,73	0,210	0,004	0
---	---	---	---	---	---
38,62	0	15,73	0,197	0,007	0
38,62	0,0083 (1,79)	15,73	0,200	0,022	0
38,62	1,66 (3,57)	15,73	0,198	0,015	0
38,62	2,49 (5,36)	15,73	0,200	0,013	0
38,62	3,31 (7,14)	15,73	0,200	0,015	0
38,62	4,14 (8,93)	15,73	0,200	0,024	0
38,62	4,97 (10,71)	15,73	0,200	0,483	0,001
38,62	5,8 (12,5)	15,73	0,200	0,020	0
38,62	6,63 (14,29)	15,73	0,195	0,021	0
38,62	7,46 (16,07)	15,73	0,198	0,009	0
38,62	8,29 (17,86)	15,73	0,198	0,009	0
38,62	9,12 (19,64)	15,73	0,198	0,010	0
38,62	9,95 (21,43)	15,73	0,200	0,028	0
38,62	10,77 (23,21)	15,73	0,202	0,879	0,002
38,62	11,60 (25)	15,73	0,213	0,655	0,001
38,62	12,43 (26,78)	15,73	0,241	0,908	0,002
38,62	13,26 (28,57)	15,73	0,244	1,459	0,004
38,62	14,09 (30,36)	15,73	0,268	0,645	0,002

X/C in %	Y/S in %	Z in mm	VELOCITY	TURB.	STAND.DEV.
38,62	14,92 (32,14)	15,73	0,283	1,343	0,004
38,62	15,75 (33,93)	15,73	0,289	0,793	0,002
38,62	16,58 (35,71)	15,73	0,319	0,706	0,002
38,62	17,41 (37,5)	15,73	0,299	1,082	0,003
38,62	18,23 (39,29)	15,73	0,329	0,862	0,003
38,62	19,06 (41,07)	15,73	0,291	1,514	0,004
38,62	19,89 (42,86)	15,73	0,277	1,322	0,004
38,62	20,72 (44,64)	15,73	0,274	0,881	0,003
38,62	21,55 (46,43)	15,73	0,261	0,466	0,001
38,62	22,38 (48,21)	15,73	0,262	0,602	0,002
38,62	23,21 (50)	15,73	0,263	0,009	0
38,62	24,04 (51,78)	15,73	0,263	0,016	0
38,62	24,86 (53,57)	15,73	0,260	0,017	0
38,62	25,69 (55,36)	15,73	0,257	0,019	0
38,62	26,52 (57,14)	15,73	0,257	0,010	0
38,62	27,35 (58,93)	15,73	0,251	0,013	0
38,62	28,18 (60,71)	15,73	0,248	0,013	0
38,62	29,01 (62,5)	15,73	0,246	0,642	0,002
38,62	29,83 (64,29)	15,73	0,241	0,001	0
38,62	30,67 (66,07)	15,73	0,240	0,658	0,002
38,62	31,5 (67,86)	15,73	0,235	0,019	0
38,62	32,32 (69,64)	15,73	0,232	0,023	0
38,62	33,15 (71,43)	15,73	0,229	0,028	0
38,62	33,98 (73,21)	15,73	0,226	0,015	0
38,62	34,81 (75)	15,73	0,219	0,022	0
38,62	35,64 (76,78)	15,73	0,222	0,017	0
38,62	36,47 (78,57)	15,73	0,219	0,007	0
38,62	37,3 (80,36)	15,73	0,216	0,014	0
38,62	38,13 (82,14)	15,73	0,213	0,012	0
38,62	38,95 (83,93)	15,73	0,210	0,010	0
---	---	---	---	---	---
38,62	0	18,73	0,202	0,026	0
38,62	0,0083 (1,79)	18,73	0,203	0,545	0,001

X/C in %	Y/S in %	Z in mm	VELOCITY	TURB.	STAND.DEV.
38,62	1,66 (3,57)	18,73	0,200	0,024	0
38,62	2,49 (5,36)	18,73	0,202	0,022	0
38,62	3,31 (7,14)	18,73	0,202	0,018	0
38,62	4,14 (8,93)	18,73	0,202	0,022	0
38,62	4,97 (10,71)	18,73	0,202	0,018	0
38,62	5,8 (12,5)	18,73	0,202	0,014	0
38,62	6,63 (14,29)	18,73	0,202	0,022	0
38,62	7,46 (16,07)	18,73	0,202	0,021	0
38,62	8,29 (17,86)	18,73	0,202	0,014	0
38,62	9,12 (19,64)	18,73	0,206	0,014	0
38,62	9,95 (21,43)	18,73	0,206	0,014	0
38,62	10,77 (23,21)	18,73	0,209	0,009	0
38,62	11,60 (25)	18,73	0,219	0,504	0,001
38,62	12,43 (26,78)	18,73	0,219	0,505	0,001
38,62	13,26 (28,57)	18,73	0,231	0,827	0,002
38,62	14,09 (30,36)	18,73	0,247	0,783	0,002
38,62	14,92 (32,14)	18,73	0,256	0,551	0,001
38,62	15,75 (33,93)	18,73	0,265	0,825	0,002
38,62	16,58 (35,71)	18,73	0,255	0,519	0,001
38,62	17,41 (37,5)	18,73	0,269	0,489	0,001
38,62	18,23 (39,29)	18,73	0,263	0,013	0
38,62	19,06 (41,07)	18,73	0,263	0,020	0
38,62	19,89 (42,86)	18,73	0,263	0,023	0
38,62	20,72 (44,64)	18,73	0,257	0,019	0
38,62	21,55 (46,43)	18,73	0,254	0,005	0
38,62	22,38 (48,21)	18,73	0,254	0,010	0
38,62	23,21 (50)	18,73	0,254	0,021	0
38,62	24,04 (51,78)	18,73	0,251	0,023	0
38,62	24,86 (53,57)	18,73	0,251	0,023	0
38,62	25,69 (55,36)	18,73	0,248	0,024	0
38,62	26,52 (57,14)	18,73	0,248	0,016	0
38,62	27,35 (58,93)	18,73	0,244	0,019	0
38,62	28,18 (60,71)	18,73	0,241	0,001	0

X/C in %	Y/S in %	Z in mm	VELOCITY	TURB.	STAND.DEV.
38,62	29,01 (62,5)	18,73	0,241	0,001	0
38,62	29,83 (64,29)	18,73	0,235	0,019	0
38,62	30,67 (66,07)	18,73	0,235	0,011	0
38,62	31,5 (67,86)	18,73	0,229	0,006	0
38,62	32,32 (69,64)	18,73	0,229	0,024	0
38,62	33,15 (71,43)	18,73	0,229	0,010	0
38,62	33,98 (73,21)	18,73	0,226	0,022	0
38,62	34,81 (75)	18,73	0,219	0,014	0
38,62	35,64 (76,78)	18,73	0,219	0,022	0
38,62	36,47 (78,57)	18,73	0,216	0,012	0
38,62	37,3 (80,36)	18,73	0,216	0,008	0
38,62	38,13 (82,14)	18,73	0,213	0,020	0
38,62	38,95 (83,93)	18,73	0,210	0,004	0
---	---	---	---	---	---
38,62	0	21,73	0,202	0,025	0
38,62	0,0083 (1,79)	21,73	0,202	0,018	0
38,62	1,66 (3,57)	21,73	0,204	0,017	0
38,62	2,49 (5,36)	21,73	0,202	0,005	0
38,62	3,31 (7,14)	21,73	0,201	0,475	0,001
38,62	4,14 (8,93)	21,73	0,206	0,014	0
38,62	4,97 (10,71)	21,73	0,206	0,014	0
38,62	5,8 (12,5)	21,73	0,206	0,014	0
38,62	6,63 (14,29)	21,73	0,204	0,017	0
38,62	7,46 (16,07)	21,73	0,204	0,017	0
38,62	8,29 (17,86)	21,73	0,209	0,021	0
38,62	9,12 (19,64)	21,73	0,211	0,003	0
38,62	9,95 (21,43)	21,73	0,209	0,016	0
38,62	10,77 (23,21)	21,73	0,215	0,011	0
38,62	11,60 (25)	21,73	0,217	0,480	0,001
38,62	12,43 (26,78)	21,73	0,224	0,007	0
38,62	13,26 (28,57)	21,73	0,227	0,485	0,001
38,62	14,09 (30,36)	21,73	0,232	0,473	0,001
38,62	14,92 (32,14)	21,73	0,234	0,022	0

X/C in %	Y/S in %	Z in mm	VELOCITY	TURB.	STAND.DEV.
38,62	15,75 (33,93)	21,73	0,237	0,008	0
38,62	16,58 (35,71)	21,73	0,243	0,020	0
38,62	17,41 (37,5)	21,73	0,248	0,020	0
38,62	18,23 (39,29)	21,73	0,248	0,010	0
38,62	19,06 (41,07)	21,73	0,248	0,029	0
38,62	19,89 (42,86)	21,73	0,251	0,018	0
38,62	20,72 (44,64)	21,73	0,248	0,016	0
38,62	21,55 (46,43)	21,73	0,248	0,025	0
38,62	22,38 (48,21)	21,73	0,246	0,642	0,002
38,62	23,21 (50)	21,73	0,244	0,028	0
38,62	24,04 (51,78)	21,73	0,244	0,012	0
38,62	24,86 (53,57)	21,73	0,244	0,024	0
38,62	25,69 (55,36)	21,73	0,241	0,024	0
38,62	26,52 (57,14)	21,73	0,244	0,019	0
38,62	27,35 (58,93)	21,73	0,238	0,009	0
38,62	28,18 (60,71)	21,73	0,238	0,011	0
38,62	29,01 (62,5)	21,73	0,235	0,016	0
38,62	29,83 (64,29)	21,73	0,232	0,020	0
38,62	30,67 (66,07)	21,73	0,229	0,024	0
38,62	31,5 (67,86)	21,73	0,229	0,016	0
38,62	32,32 (69,64)	21,73	0,226	0,018	0
38,62	33,15 (71,43)	21,73	0,222	0,017	0
38,62	33,98 (73,21)	21,73	0,219	0,009	0
38,62	34,81 (75)	21,73	0,222	0,023	0
38,62	35,64 (76,78)	21,73	0,219	0,009	0
38,62	36,47 (78,57)	21,73	0,213	0,013	0
38,62	37,3 (80,36)	21,73	0,216	0,015	0
38,62	38,13 (82,14)	21,73	0,213	0,020	0
38,62	38,95 (83,93)	21,73	0,210	0,017	0
---	---	---	---	---	---
38,62	0	24,73	0,202	0,026	0
38,62	0,0083 (1,79)	24,73	0,206	0,491	0,001
38,62	1,66 (3,57)	24,73	0,206	0,014	0

X/C in %	Y/S in %	Z in mm	VELOCITY	TURB.	STAND.DEV.
38,62	2,49 (5,36)	24,73	0,204	0,024	0
38,62	3,31 (7,14)	24,73	0,204	0,023	0
38,62	4,14 (8,93)	24,73	0,204	0,017	0
38,62	4,97 (10,71)	24,73	0,204	0,017	0
38,62	5,8 (12,5)	24,73	0,206	0,014	0
38,62	6,63 (14,29)	24,73	0,211	0,027	0
38,62	7,46 (16,07)	24,73	0,209	0,028	0
38,62	8,29 (17,86)	24,73	0,211	0,004	0
38,62	9,12 (19,64)	24,73	0,215	0,017	0
38,62	9,95 (21,43)	24,73	0,216	0,481	0,001
38,62	10,77 (23,21)	24,73	0,216	0,510	0,001
38,62	11,60 (25)	24,73	0,221	0,437	0,001
38,62	12,43 (26,78)	24,73	0,220	0,023	0
38,62	13,26 (28,57)	24,73	0,225	0,486	0,001
38,62	14,09 (30,36)	24,73	0,227	0,487	0,001
38,62	14,92 (32,14)	24,73	0,231	0,012	0
38,62	15,75 (33,93)	24,73	0,234	0,012	0
38,62	16,58 (35,71)	24,73	0,234	0,018	0
38,62	17,41 (37,5)	24,73	0,237	0,019	0
38,62	18,23 (39,29)	24,73	0,238	0,010	0
38,62	19,06 (41,07)	24,73	0,241	0,017	0
38,62	19,89 (42,86)	24,73	0,238	0,011	0
38,62	20,72 (44,64)	24,73	0,238	0,016	0
38,62	21,55 (46,43)	24,73	0,238	0,015	0
38,62	22,38 (48,21)	24,73	0,235	0,017	0
38,62	23,21 (50)	24,73	0,235	0,018	0
38,62	24,04 (51,78)	24,73	0,235	0,006	0
38,62	24,86 (53,57)	24,73	0,235	0,012	0
38,62	25,69 (55,36)	24,73	0,238	0,019	0
38,62	26,52 (57,14)	24,73	0,238	0,011	0
38,62	27,35 (58,93)	24,73	0,232	0,020	0
38,62	28,18 (60,71)	24,73	0,232	0,015	0
38,62	29,01 (62,5)	24,73	0,229	0,025	0

X/C in %	Y/S in %	Z in mm	VELOCITY	TURB.	STAND.DEV.
38,62	29,83 (64,29)	24,73	0,226	0,003	0
38,62	30,67 (66,07)	24,73	0,226	0,003	0
38,62	31,5 (67,86)	24,73	0,222	0,012	0
38,62	32,32 (69,64)	24,73	0,226	0,006	0
38,62	33,15 (71,43)	24,73	0,222	0,009	0
38,62	33,98 (73,21)	24,73	0,219	0,017	0
38,62	34,81 (75)	24,73	0,216	0,019	0
38,62	35,64 (76,78)	24,73	0,216	0,013	0
38,62	36,47 (78,57)	24,73	0,216	0,015	0
38,62	37,3 (80,36)	24,73	0,213	0,014	0
38,62	38,13 (82,14)	24,73	0,213	0,013	0
38,62	38,95 (83,93)	24,73	0,210	0,021	0
---	---	---	---	---	---
38,62	0	27,73	0,206	0,018	0
38,62	0,0083 (1,79)	27,73	0,206	0,023	0
38,62	1,66 (3,57)	27,73	0,206	0,023	0
38,62	2,49 (5,36)	27,73	0,206	0,019	0
38,62	3,31 (7,14)	27,73	0,206	0,014	0
38,62	4,14 (8,93)	27,73	0,206	0,014	0
38,62	4,97 (10,71)	27,73	0,209	0,009	0
38,62	5,8 (12,5)	27,73	0,209	0,028	0
38,62	6,63 (14,29)	27,73	0,206	0,007	0
38,62	7,46 (16,07)	27,73	0,209	0,012	0
38,62	8,29 (17,86)	27,73	0,212	0,485	0,001
38,62	9,12 (19,64)	27,73	0,213	0,027	0
38,62	9,95 (21,43)	27,73	0,215	0,007	0
38,62	10,77 (23,21)	27,73	0,216	0,499	0,001
38,62	11,60 (25)	27,73	0,216	0,510	0,001
38,62	12,43 (26,78)	27,73	0,222	0,017	0
38,62	13,26 (28,57)	27,73	0,223	0,495	0,001
38,62	14,09 (30,36)	27,73	0,226	0,462	0,001
38,62	14,92 (32,14)	27,73	0,226	0,027	0
38,62	15,75 (33,93)	27,73	0,226	0,018	0

X/C in %	Y/S in %	Z in mm	VELOCITY	TURB.	STAND.DEV.
38,62	16,58 (35,71)	27,73	0,229	0,011	0
38,62	17,41 (37,5)	27,73	0,231	0,016	0
38,62	18,23 (39,29)	27,73	0,229	0,025	0
38,62	19,06 (41,07)	27,73	0,229	0,006	0
38,62	19,89 (42,86)	27,73	0,232	0,010	0
38,62	20,72 (44,64)	27,73	0,235	0,003	0
38,62	21,55 (46,43)	27,73	0,229	0,016	0
38,62	22,38 (48,21)	27,73	0,229	0,008	0
38,62	23,21 (50)	27,73	0,232	0,012	0
38,62	24,04 (51,78)	27,73	0,232	0,020	0
38,62	24,86 (53,57)	27,73	0,229	0,028	0
38,62	25,69 (55,36)	27,73	0,229	0,018	0
38,62	26,52 (57,14)	27,73	0,229	0,025	0
38,62	27,35 (58,93)	27,73	0,229	0,025	0
38,62	28,18 (60,71)	27,73	0,229	0,006	0
38,62	29,01 (62,5)	27,73	0,229	0,008	0
38,62	29,83 (64,29)	27,73	0,222	0,005	0
38,62	30,67 (66,07)	27,73	0,222	0,020	0
38,62	31,5 (67,86)	27,73	0,219	0,022	0
38,62	32,32 (69,64)	27,73	0,219	0,022	0
38,62	33,15 (71,43)	27,73	0,216	0,008	0
38,62	33,98 (73,21)	27,73	0,216	0,019	0
38,62	34,81 (75)	27,73	0,216	0,017	0
38,62	35,64 (76,78)	27,73	0,213	0,014	0
38,62	36,47 (78,57)	27,73	0,213	0,013	0
38,62	37,3 (80,36)	27,73	0,213	0,014	0
38,62	38,13 (82,14)	27,73	0,210	0,017	0
38,62	38,95 (83,93)	27,73	0,207	0,026	0
---	---	---	---	---	---
38,62	0	30,73	0,206	0,016	0
38,62	0,0083 (1,79)	30,73	0,206	0,016	0
38,62	1,66 (3,57)	30,73	0,206	0,014	0
38,62	2,49 (5,36)	30,73	0,206	0,014	0

X/C in %	Y/S in %	Z in mm	VELOCITY	TURB.	STAND.DEV.
38,62	3,31 (7,14)	30,73	0,206	0,023	0
38,62	4,14 (8,93)	30,73	0,209	0,028	0
38,62	4,97 (10,71)	30,73	0,206	0,019	0
38,62	5,8 (12,5)	30,73	0,206	0,014	0
38,62	6,63 (14,29)	30,73	0,211	0,002	0
38,62	7,46 (16,07)	30,73	0,209	0,016	0
38,62	8,29 (17,86)	30,73	0,211	0,017	0
38,62	9,12 (19,64)	30,73	0,213	0,020	0
38,62	9,95 (21,43)	30,73	0,212	0,496	0,001
38,62	10,77 (23,21)	30,73	0,215	0,017	0
38,62	11,60 (25)	30,73	0,213	0,012	0
38,62	12,43 (26,78)	30,73	0,218	0,022	0
38,62	13,26 (28,57)	30,73	0,218	0,015	0
38,62	14,09 (30,36)	30,73	0,221	0,493	0,001
38,62	14,92 (32,14)	30,73	0,223	0,012	0
38,62	15,75 (33,93)	30,73	0,223	0,006	0
38,62	16,58 (35,71)	30,73	0,226	0,012	0
38,62	17,41 (37,5)	30,73	0,223	0,005	0
38,62	18,23 (39,29)	30,73	0,226	0,009	0
38,62	19,06 (41,07)	30,73	0,226	0,027	0
38,62	19,89 (42,86)	30,73	0,229	0,025	0
38,62	20,72 (44,64)	30,73	0,226	0,005	0
38,62	21,55 (46,43)	30,73	0,229	0,013	0
38,62	22,38 (48,21)	30,73	0,226	0,018	0
38,62	23,21 (50)	30,73	0,229	0,012	0
38,62	24,04 (51,78)	30,73	0,226	0,006	0
38,62	24,86 (53,57)	30,73	0,226	0,022	0
38,62	25,69 (55,36)	30,73	0,226	0,018	0
38,62	26,52 (57,14)	30,73	0,226	0,009	0
38,62	27,35 (58,93)	30,73	0,219	0,022	0
38,62	28,18 (60,71)	30,73	0,219	0,007	0
38,62	29,01 (62,5)	30,73	0,219	0,022	0
38,62	29,83 (64,29)	30,73	0,221	0,714	0,002

X/C in %	Y/S in %	Z in mm	VELOCITY	TURB.	STAND.DEV.
38,62	30,67 (66,07)	30,73	0,219	0,022	0
38,62	31,5 (67,86)	30,73	0,216	0,009	0
38,62	32,32 (69,64)	30,73	0,213	0,014	0
38,62	33,15 (71,43)	30,73	0,216	0,015	0
38,62	33,98 (73,21)	30,73	0,213	0,012	0
38,62	34,81 (75)	30,73	0,213	0,020	0
38,62	35,64 (76,78)	30,73	0,213	0,021	0
38,62	36,47 (78,57)	30,73	0,213	0,021	0
38,62	37,3 (80,36)	30,73	0,213	0,021	0
38,62	38,13 (82,14)	30,73	0,207	0,014	0
38,62	38,95 (83,93)	30,73	0,207	0,013	0

Table 47 : LDV Measurements for identification of stalled wing areas .
(Zero or reverse flow) .

X in mm	Y in mm	Z in mm	VELOCITY	TURB.	STAND.DEV.
225	20	65	0,067	0,024	0
			0,177	0,022	0
			0,293	0,395	0
---	---	---	---	---	---
210	20	60	0,070	0,024	0
			0,172	0,021	0
			0,287	0,475	0,001
---	---	---	---	---	---
195	20	55	0,064	0,014	0
			0,169	0,010	0
			0,268	0,016	0
---	---	---	---	---	---
180	20	51	0,061	0,022	0
			0,160	0,015	0
			0,243	0,015	0
---	---	---	---	---	---
165	20	46,5	0,067	0,010	0
			0,146	0,021	0
			0,217	0,020	0
---	---	---	---	---	---
150	20	42	0,070	0,019	0
			0,163	0,022	0
			0,214	0,007	0
---	---	---	---	---	---
135	20	37,5	0,081	0,015	0
			0,172	0,017	0
			0,248	0,017	0
---	---	---	---	---	---
120	20	33	0,087	0,028	0
			0,231	0,472	0
			0,334	0,021	0

X in mm	Y in mm	Z in mm	VELOCITY	TURB.	STAND.DEV.
225	10	65	0,072	0,009	0
			0,180	0,018	0
			0,297	0,016	0
----------	----------	----------	----------	----------	----------
210	10	60	0,072	0,013	0
			0,180	0,007	0
			0,294	0,017	0
----------	----------	----------	----------	----------	----------
195	10	55	0,072	0,010	0
			0,183	0,022	0
			0,290	0,490	0,001
----------	----------	----------	----------	----------	----------
180	10	51	0,075	0,011	0
			0,183	0,008	0
			0,282	0,011	0
----------	----------	----------	----------	----------	----------
165	10	46,5	0,078	0,014	0
			0,186	0,015	0
			0,278	0,479	0,001
----------	----------	----------	----------	----------	----------
150	10	42	0,081	0,023	0
			0,192	0,023	0
			0,287	0,495	0,001
----------	----------	----------	----------	----------	----------
135	10	37,5	0,084	0,029	0
			0,197	0,020	0
			0,300	0,015	0
----------	----------	----------	----------	----------	----------
120	10	33	0,081	0,019	0
			0,200	0,009	0
			0,310	0,458	0,001
----------	----------	----------	----------	----------	----------

X in mm	Y in mm	Z in mm	VELOCITY	TURB.	STAND.DEV.
225	0	65	0,072	0,022	0
			0,189	0,026	0
			0,294	0,019	0
---	---	---	---	---	---
210	0	60	0,072	0,022	0
			0,180	0,007	0
			0,292	0,480	0,001
---	---	---	---	---	---
195	0	55	0,075	0,017	0
			0,183	0,018	0
			0,288	0,014	0
---	---	---	---	---	---
180	0	51	0,075	0,010	0
			0,189	0,021	0
			0,284	0,497	0,001
---	---	---	---	---	---
165	0	46,5	0,081	0,009	0
			0,194	0,019	0
			0,285	0,017	0
---	---	---	---	---	---
150	0	42	0,084	0,019	0
			0,197	0,029	0
			0,292	0,471	0,001
---	---	---	---	---	---
135	0	37,5	0,087	0,016	0
			0,206	0,013	0
			0,305	0,014	0
---	---	---	---	---	---
120	0	33	0,087	0,028	0
			0,212	0,016	0
			0,318	0,446	0,001
---	---	---	---	---	---

X in mm	Y in mm	Z in mm	VELOCITY	TURB.	STAND.DEV.
225	-10	65	0,072	0,009	0
			0,180	0,008	0
			0,297	0,009	0
----------	----------	----------	----------	----------	----------
210	-10	60	0,070	0,011	0
			0,177	0,015	0
			0,295	0,495	0,001
----------	----------	----------	----------	----------	----------
195	-10	55	0,070	0,011	0
			0,175	0,017	0
			0,284	0,487	0,001
----------	----------	----------	----------	----------	----------
180	-10	51	0,072	0,005	0
			0,172	0,002	0
			0,268	0,024	0
----------	----------	----------	----------	----------	----------
165	-10	46,5	0,075	0,017	0
			0,172	0,005	0
			0,248	0,023	0
----------	----------	----------	----------	----------	----------
150	-10	42	0,081	0,011	0
			0,172	0,006	0
			0,254	0,013	0
----------	----------	----------	----------	----------	----------
135	-10	37,5	0,081	0,027	0
			0,175	0,026	0
			0,268	0,424	0,001
----------	----------	----------	----------	----------	----------
120	-10	33	0,078	0,022	0
			0,189	0,009	0
			0,287	0,488	0,001
----------	----------	----------	----------	----------	----------

X in mm	Y in mm	Z in mm	VELOCITY	TURB.	STAND.DEV.
225	-20	65	0,064	0,021	0
			0,172	0,023	0
			0,294	0,013	0
----------	----------	----------	----------	----------	----------
210	-20	60	0,058	0,016	0
			0,160	0,020	0
			0,282	0,023	0
----------	----------	----------	----------	----------	----------
195	-20	55	0,047	0,018	0
			0,149	0,014	0
			0,253	0,502	0,001
----------	----------	----------	----------	----------	----------
180	-20	51	0,055	0,020	0
			0,126	0,015	0
			0,191	1,061	0,002
----------	----------	----------	----------	----------	----------
165	-20	46,5	0,072	0,009	0
			0,127	1,073	0,001
			0,174	0,727	0,001
----------	----------	----------	----------	----------	----------
150	-20	42	0,089	0,005	0
			0,166	0,015	0
			0,207	0,629	0,001
----------	----------	----------	----------	----------	----------
135	-20	37,5	0,013	0,025	0
			0,223	0,018	0
			0,309	0,459	0,001
----------	----------	----------	----------	----------	----------
120	-20	33	0,035	0,013	0
			0,158	0,016	0
			0,260	0,784	0,002
----------	----------	----------	----------	----------	----------

X in mm	Y in mm	Z in mm	VELOCITY	TURB.	STAND.DEV.
225	-30	65	0,050	0,014	0
			0,154	0,881	0,001
			0,250	2,088	0,005
----------	----------	----------	----------	----------	----------
210	-30	60	0,038	0,007	0
			0,137	1,018	0,001
			0,240	1,972	0,005
----------	----------	----------	----------	----------	----------
195	-30	55	0,038	0,021	0
			0,106	0,007	0
			0,213	1,316	0,003
----------	----------	----------	----------	----------	----------
180	-30	51	0,072	0,009	0
			0,093	2,761	0,003
			0,102	3,056	0,003
----------	----------	----------	----------	----------	----------
165	-30	46,5	0,010	0,014	0
			0,158	0,020	0
			0,172	1,184	0,002
----------	----------	----------	----------	----------	----------
150	-30	42	0,0	2487,8	0,001
			0,027	8,362	0,002
			0,260	0,006	0
----------	----------	----------	----------	----------	----------
135	-30	37,5	0,010	0,030	0
			0,099	4,493	0,004
			0,142	3,763	0,005
----------	----------	----------	----------	----------	----------
----------	----------	----------	----------	----------	----------

X in mm	Y in mm	Z in mm	VELOCITY	TURB.	STAND.DEV.
225	-40	65	0,038	0,009	0
			0,119	1,190	0,001
			0,218	1,608	0,004
---	---	---	---	---	---
210	-40	60	0,038	0,007	0
			0,100	4,132	0,004
			0,158	4,309	0,007
---	---	---	---	---	---
195	-40	55	0,043	3,333	0,001
			0,078	3,765	0,003
			0,175	2,722	0,005
---	---	---	---	---	---
180	-40	51	-0,007	0,013	0
			0,108	1,313	0,001
			0,092	4,394	0,004
---	---	---	---	---	---
165	-40	46,5	-,010	0,009	0
			0,069	4,696	0,003
			0,129	4,164	0,005
---	---	---	---	---	---
150	-40	42	-0,018	0,010	0
			-0,008	26,796	0,002
			0,149	2,212	0,003
---	---	---	---	---	---
---	---	---	---	---	---
225	-50	65	0,041	0,028	0
			0,098	1,883	0,002
			0,170	3,938	0,007
---	---	---	---	---	---
210	-50	60	0,030	0,024	0
			0,082	4,39	0,004
			0,084	5,051	0,004
---	---	---	---	---	---

X in mm	Y in mm	Z in mm	VELOCITY	TURB.	STAND.DEV.
195	-50	55	0,021	0,024	0
			0,078	2,924	0,002
			0,068	15,043	0,010
----------	----------	----------	----------	----------	----------
180	-50	51	-0,011	11,856	0,001
			0,031	16,18	0,005
			0,097	4,302	0,004
----------	----------	----------	----------	----------	----------
165	-50	46,5	-0,016	0,014	0
			0,005	25,721	0,001
			0,121	2,605	0,003
----------	----------	----------	----------	----------	----------
----------	----------	----------	----------	----------	----------
225	-60	65	0,027	0,024	0
			0,064	8,324	0,005
			0,085	6,161	0,005
----------	----------	----------	----------	----------	----------
210	-60	60	0,008	62,2	0,005
			0,052	3,908	0,002
			0,106	3,557	0,004
----------	----------	----------	----------	----------	----------
195	-60	55	0,001	790,9	0,010
			0,069	5,69	0,004
			0,096	4,637	0,004
----------	----------	----------	----------	----------	----------
180	-60	51	-0,027	0,020	0
			0,026	17,07	0,005
			0,115	4,62	0,005
----------	----------	----------	----------	----------	----------
165	-60	46,5	-0,035	0,007	0
			0,043	3,319	0,001
			0,034	3,884	0,001
----------	----------	----------	----------	----------	----------

X in mm	Y in mm	Z in mm	VELOCITY	TURB.	STAND.DEV.
225	-70	65	0,026	5,265	0,001
			0,061	3,723	0,002
			0,059	14,431	0,009
---	---	---	---	---	---
210	-70	60	0,018	6,928	0,001
			0,055	4,687	0,003
			0,015	15,018	0,002
---	---	---	---	---	---
195	-70	55	-0,021	0,017	0
			0,025	12,791	0,003
			0,110	4,713	0,005
---	---	---	---	---	---
180	-70	51	-0,030	0,022	0
			-0,050	0,017	0
			0,105	4,208	0,004
---	---	---	---	---	---
---	---	---	---	---	---
225	-80	65	0,008	16,865	0,001
			0,043	5,439	0,002
			0,034	5,297	0,002
---	---	---	---	---	---
210	-80	60	0,001	239,7	0,002
			0,036	6,388	0,002
			0,138	4,664	0,006
---	---	---	---	---	---
195	-80	55	-0,014	9,931	0,001
			-0,006	27,595	0,002
			0,132	1,74	0,002
---	---	---	---	---	---
---	---	---	---	---	---
---	---	---	---	---	---

Table 48 : Vortex breakdown location based on Flow visualisation and LDV measurements at AOA = 15 deg . - V = 0.2 / 0.6 / 1.0 ft /sec .

FLOW VISUALISATION					
VELOCITY	VORTEX	X in mm	Y in mm	Z in mm	
0,2	STRAKE	227.88	44.09	14.87	
0,2	WING	213.72	53.48	12.75	
---	---	---	---	---	---
0,6	STRAKE	196.23	53.09	12.75	
0,6	WING	167.86	47.27	14.46	
---	---	---	---	---	---
1,0	STRAKE	190.18	46.27	10.46	
1,0	WING	162.12	52.78	8.89	
---	---	---	---	---	---

LDV MEASUREMENTS					
VELOCITY	VORTEX	X in mm	Y in mm	Z in mm	
0,2	STRAKE	226.7	40.61	13.5	
0,2	WING	200	20	7.34	
---	---	---	---	---	---
0,6	STRAKE	215	42	11.4	
0,6	WING	178	45.75	10.85	
---	---	---	---	---	---
1,0	STRAKE	200	38	12.14	
1,0	WING	168	49.88	6.35	
---	---	---	---	---	---

Fig.96:Velocity profile at x=62.73% , z=0.35mm

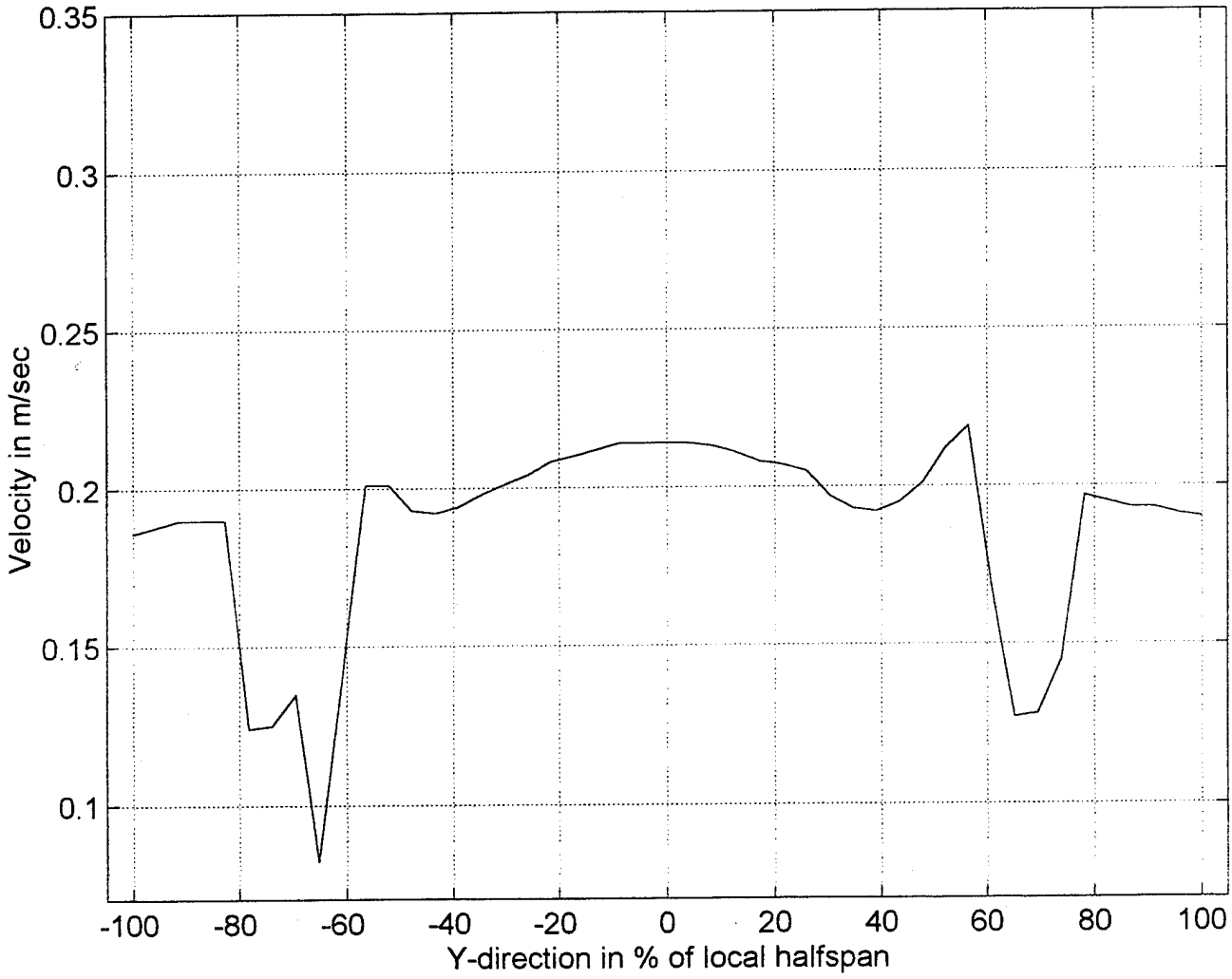

Fig.97:Velocity profile at x=62.73% , z=2.35mm

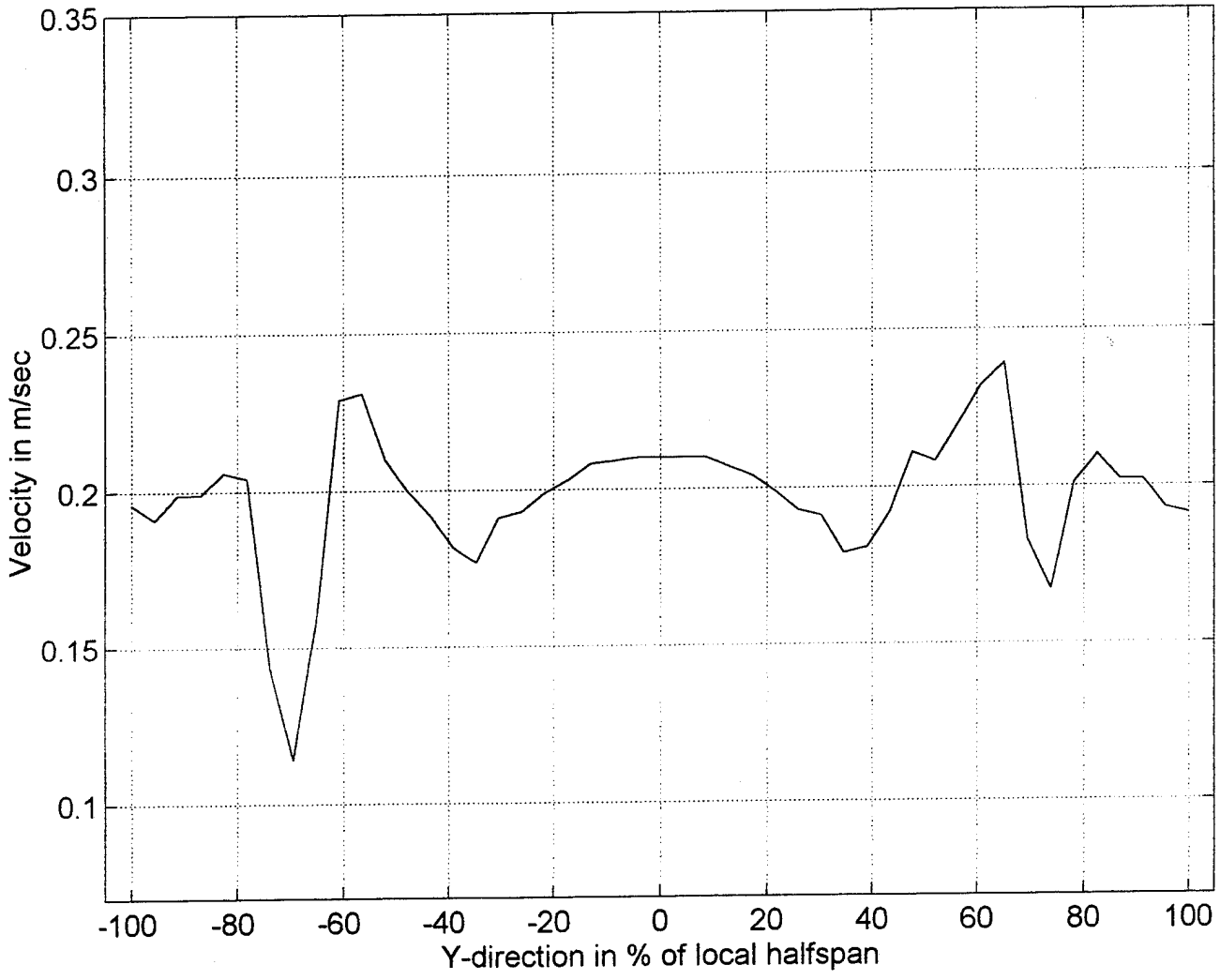

Fig.98:Velocity profile at x=62.73% , z=4.35mm

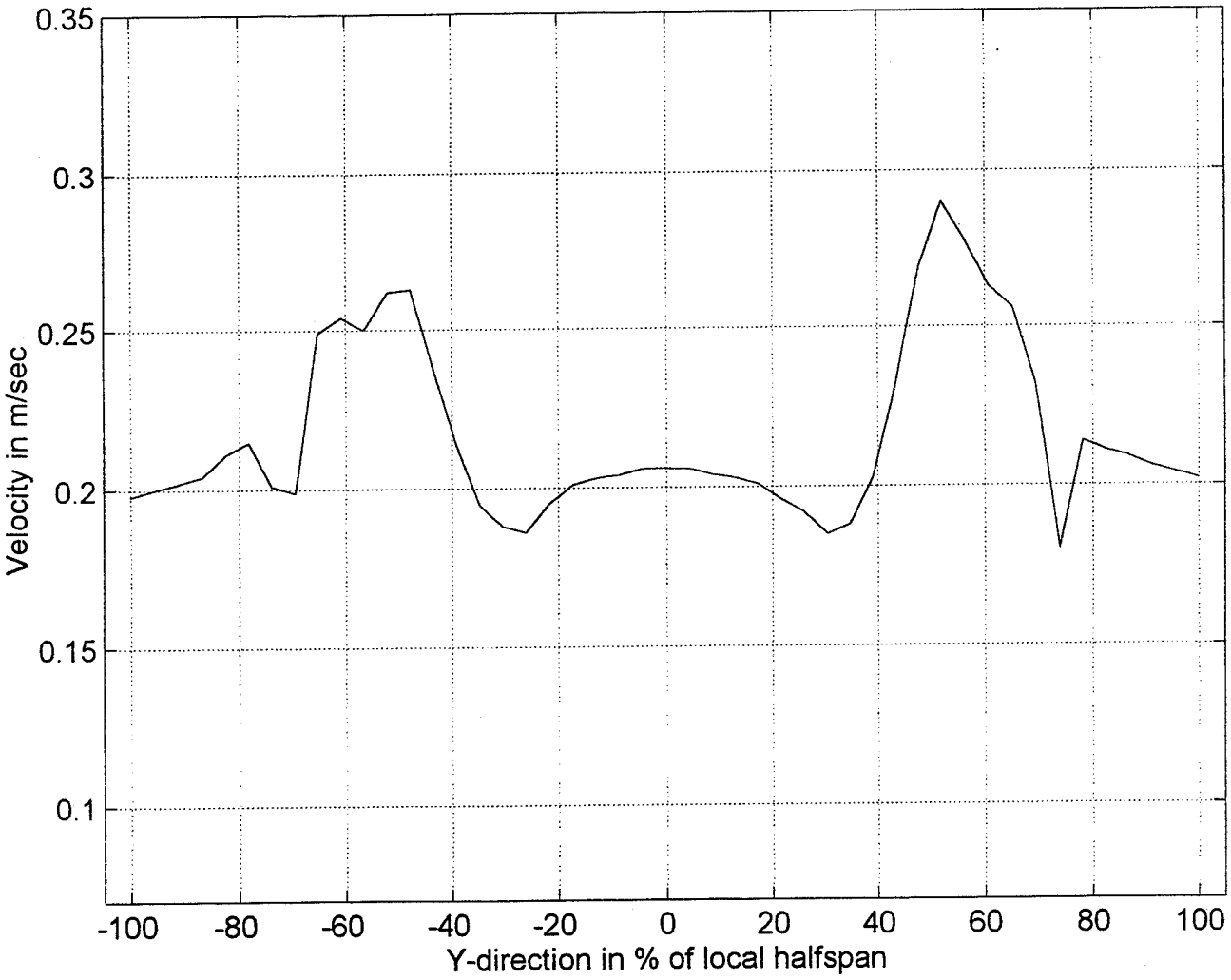

Fig.99:Velocity profile at x=62.73% , z=6.35mm

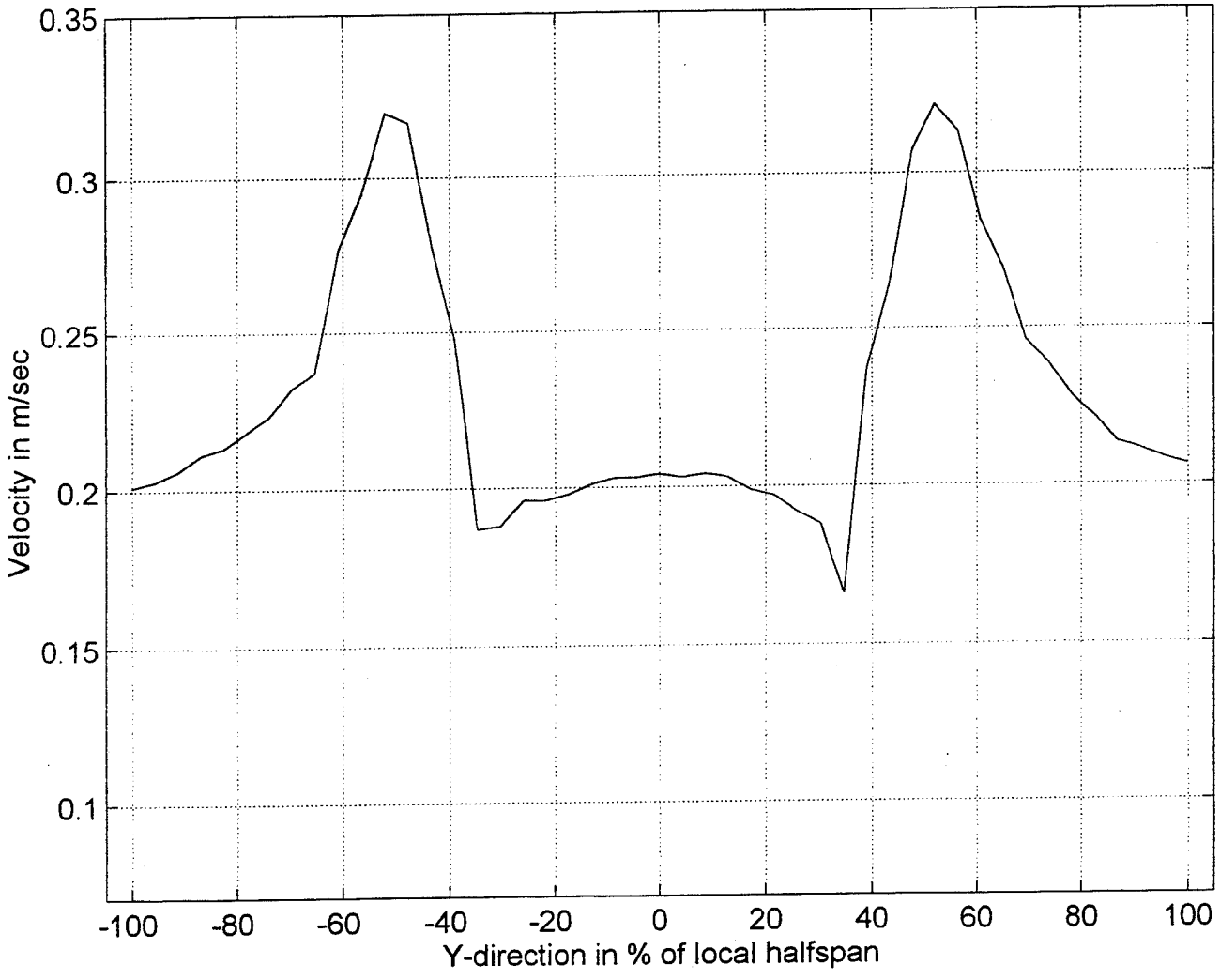

Fig.100:Velocity profile at x=62.73% , z=8.35mm

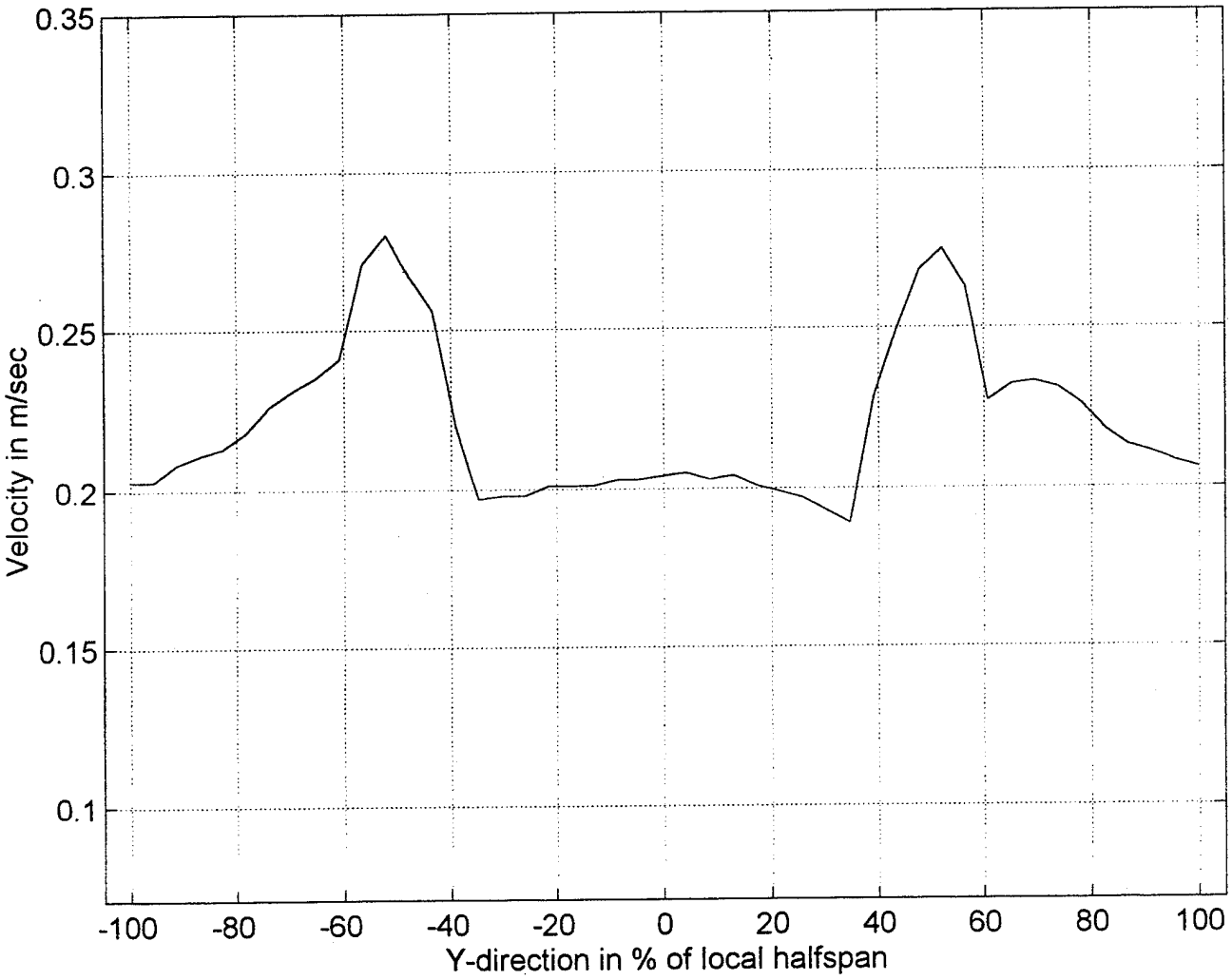

Fig.101:Velocity profile at x=62.73% , z=10.35mm

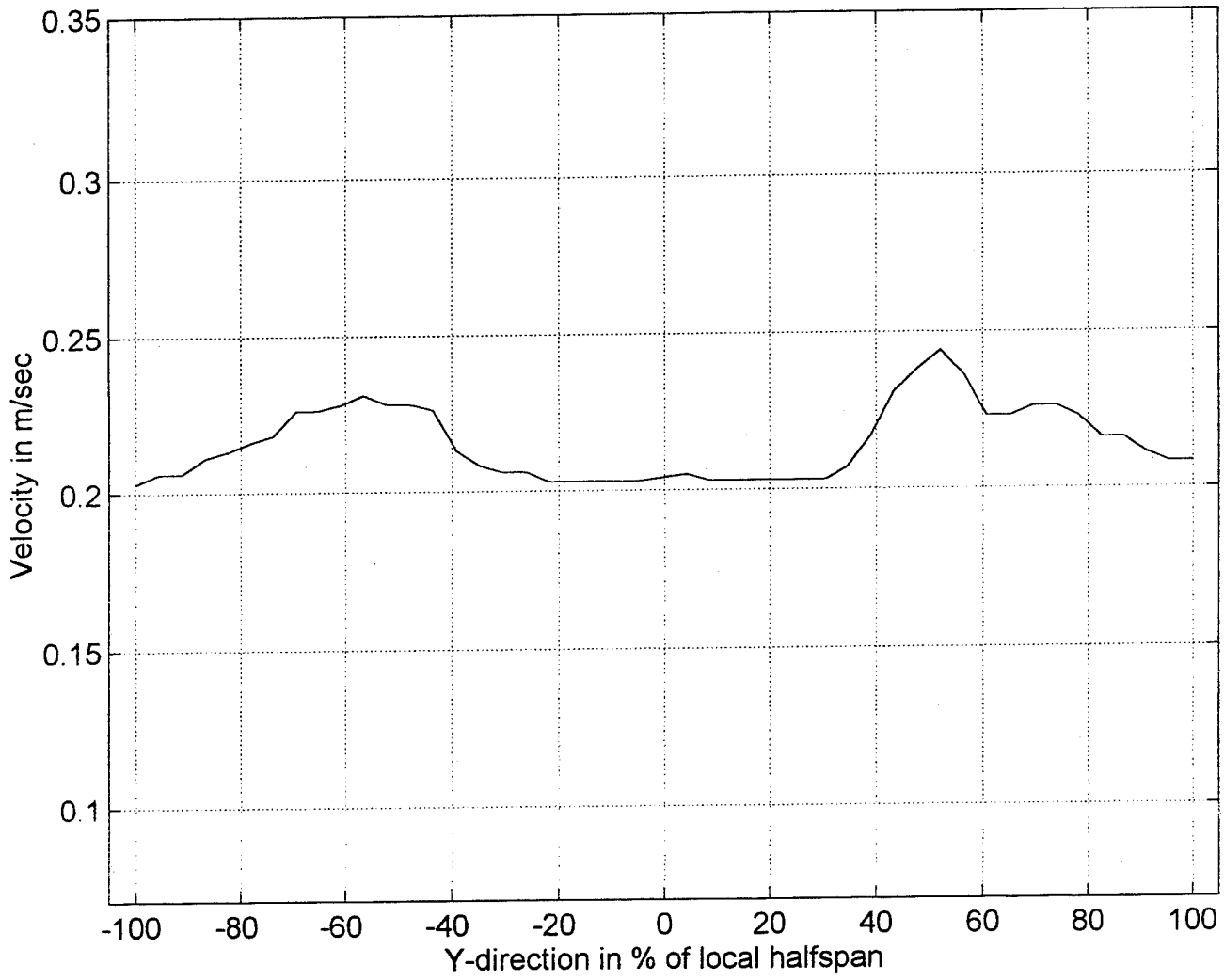

Fig.102:Velocity profile at x=62.73% , z=12.35mm

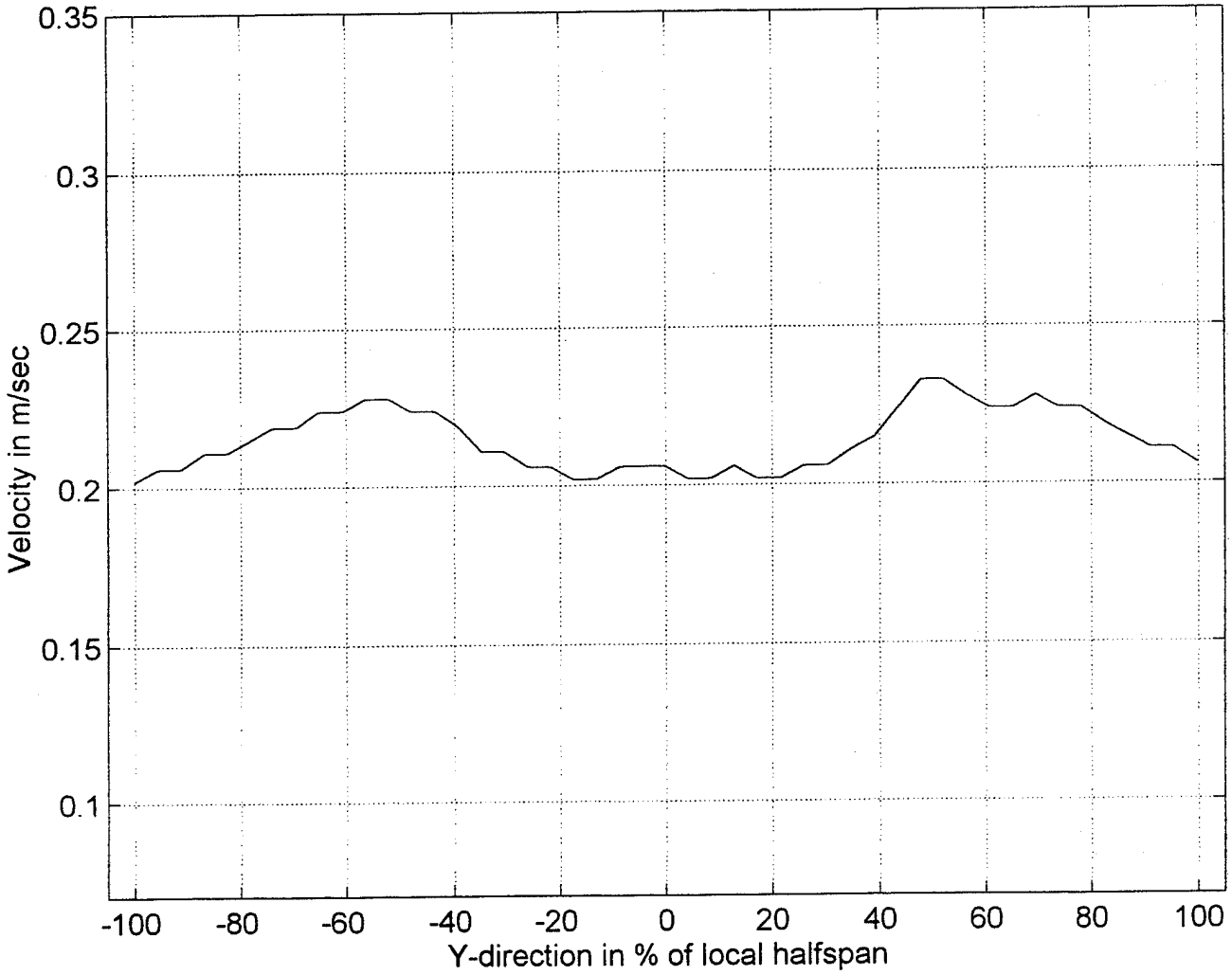

Fig.103:Velocity profile at x=62.73% , z=14.35mm

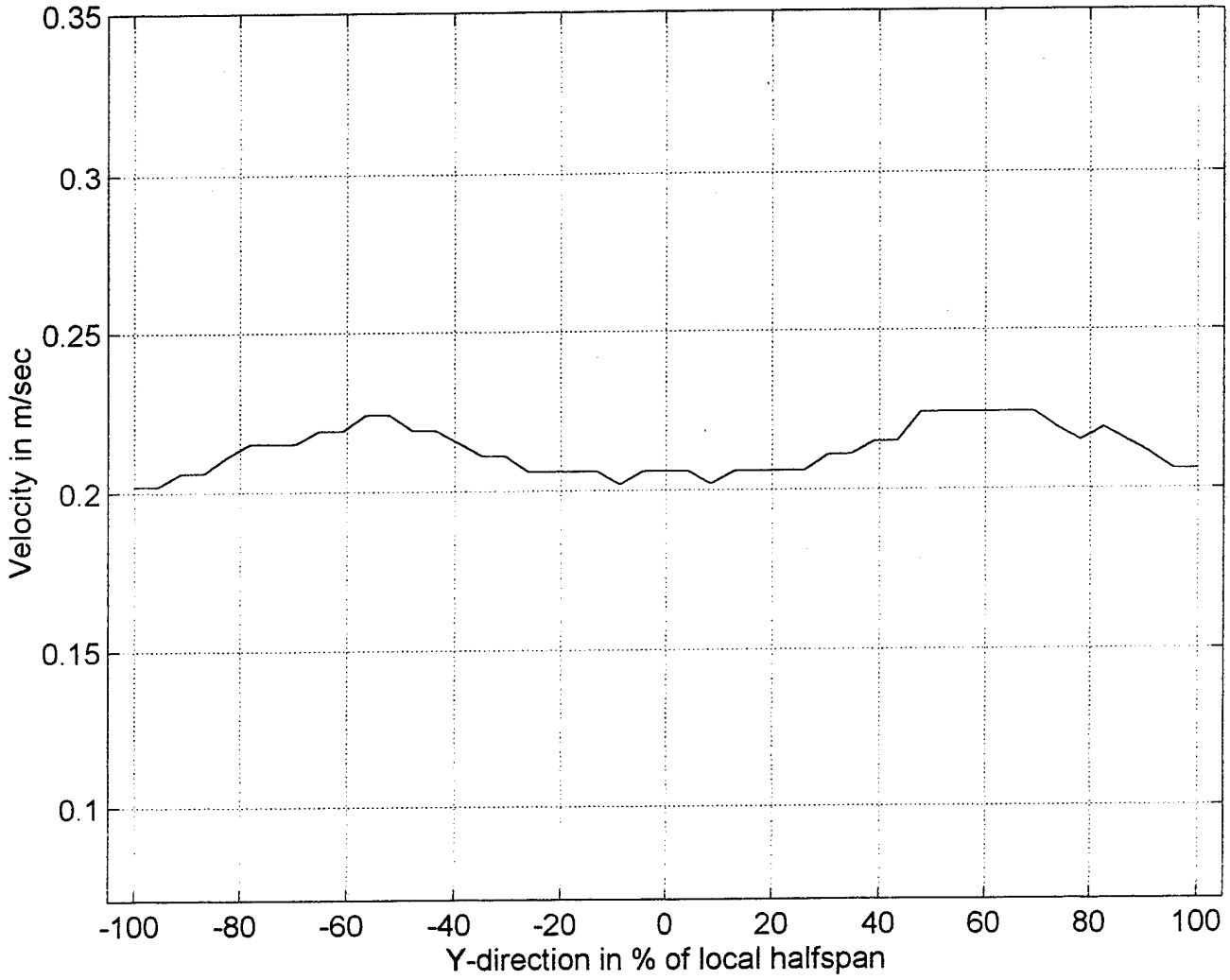

Fig.104:Velocity profile at x=38.62% , z=0.73 mm

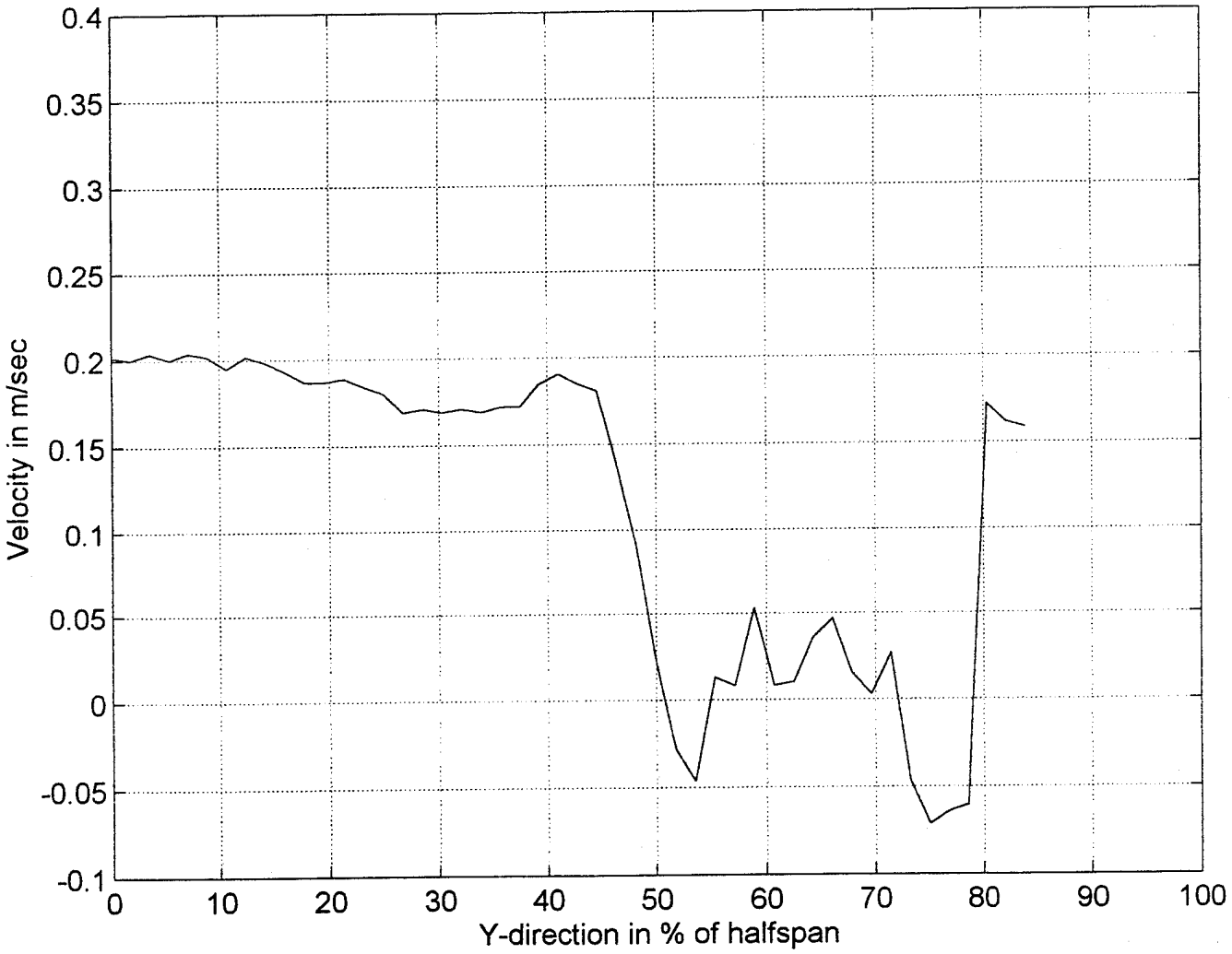

Fig.105:Velocity profile at x=38.62% , z=3.73 mm

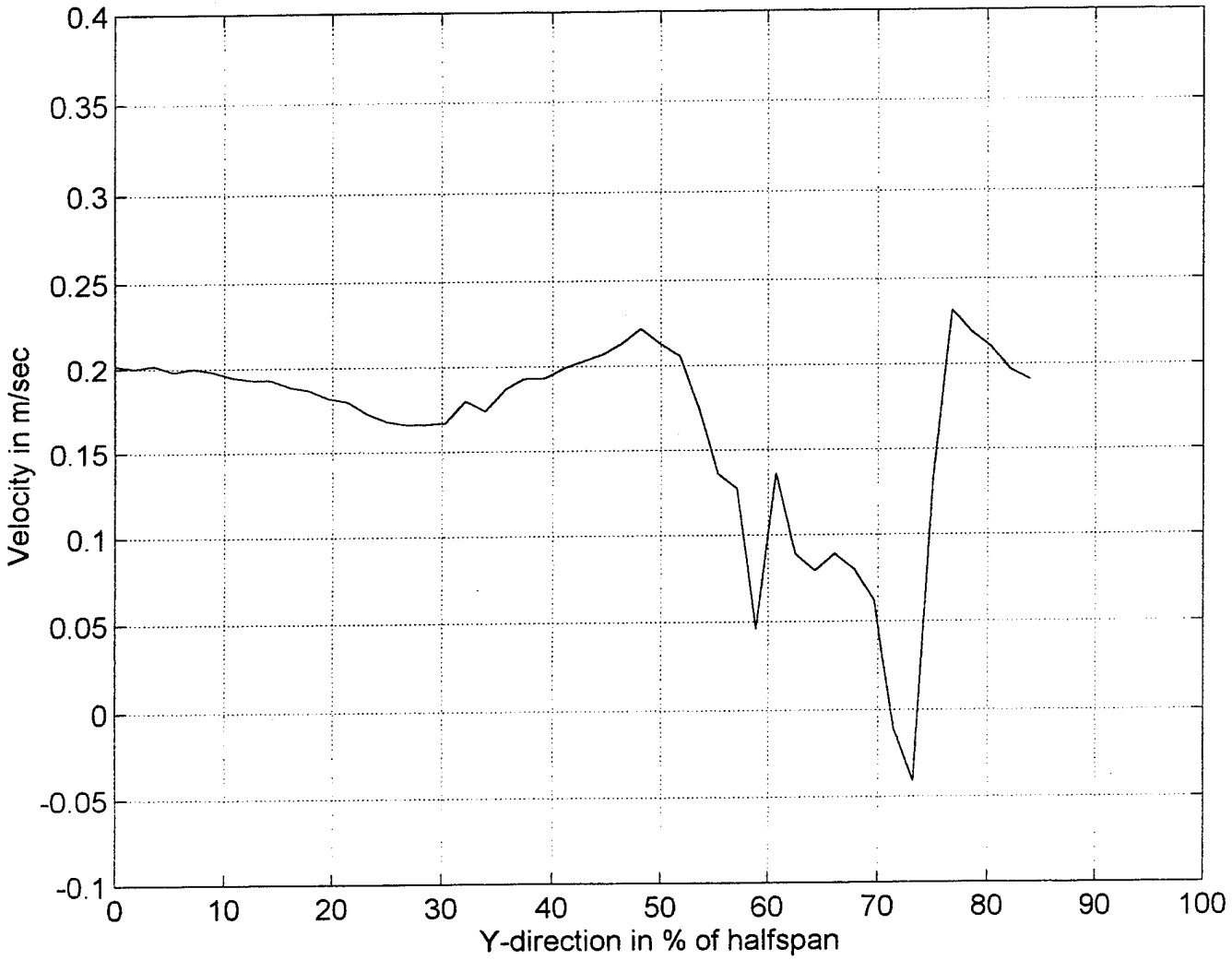

Fig.106:Velocity profile at x=38.62% , z=6.73 mm

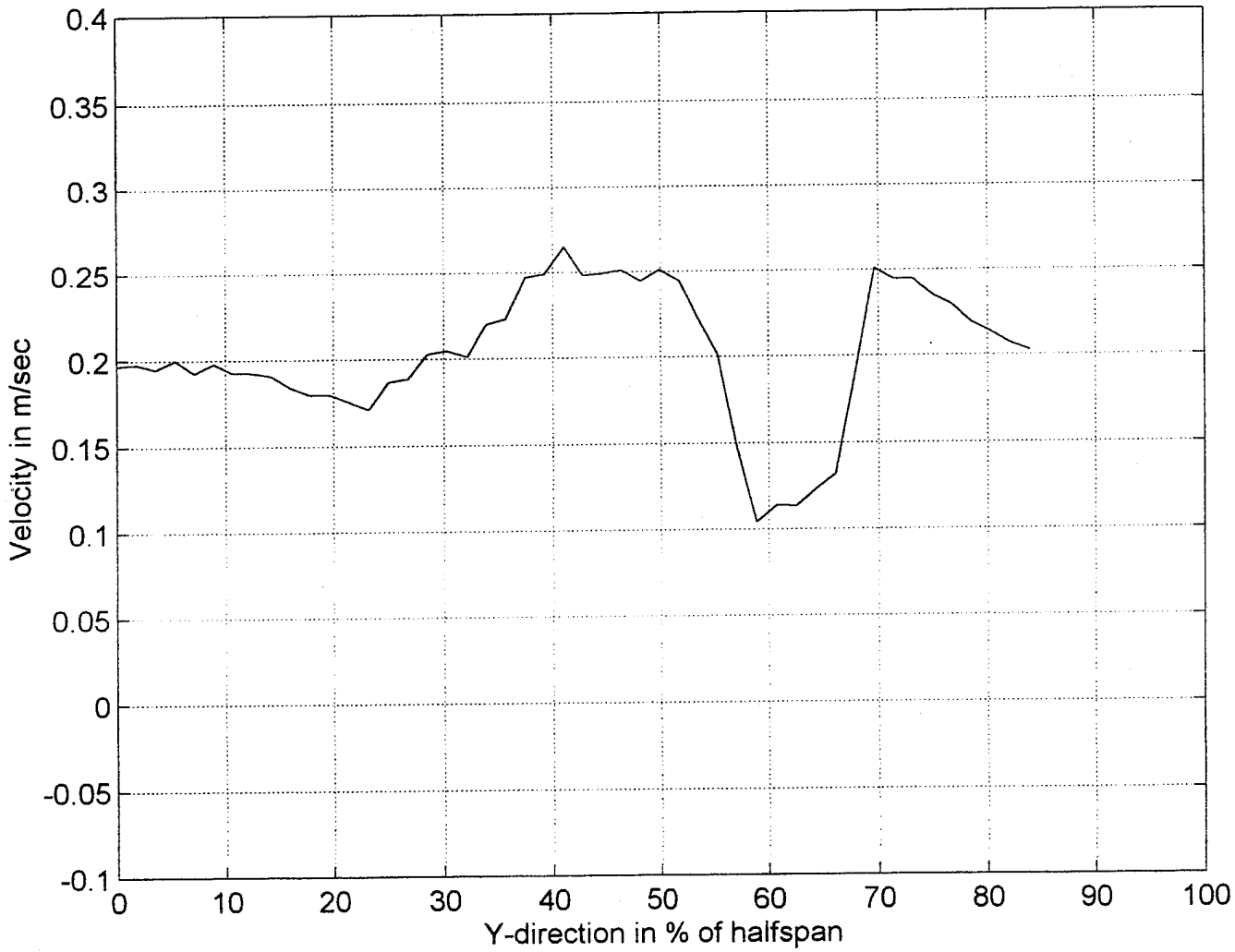

Fig.107:Velocity profile at x=38.62% , z=9.73 mm

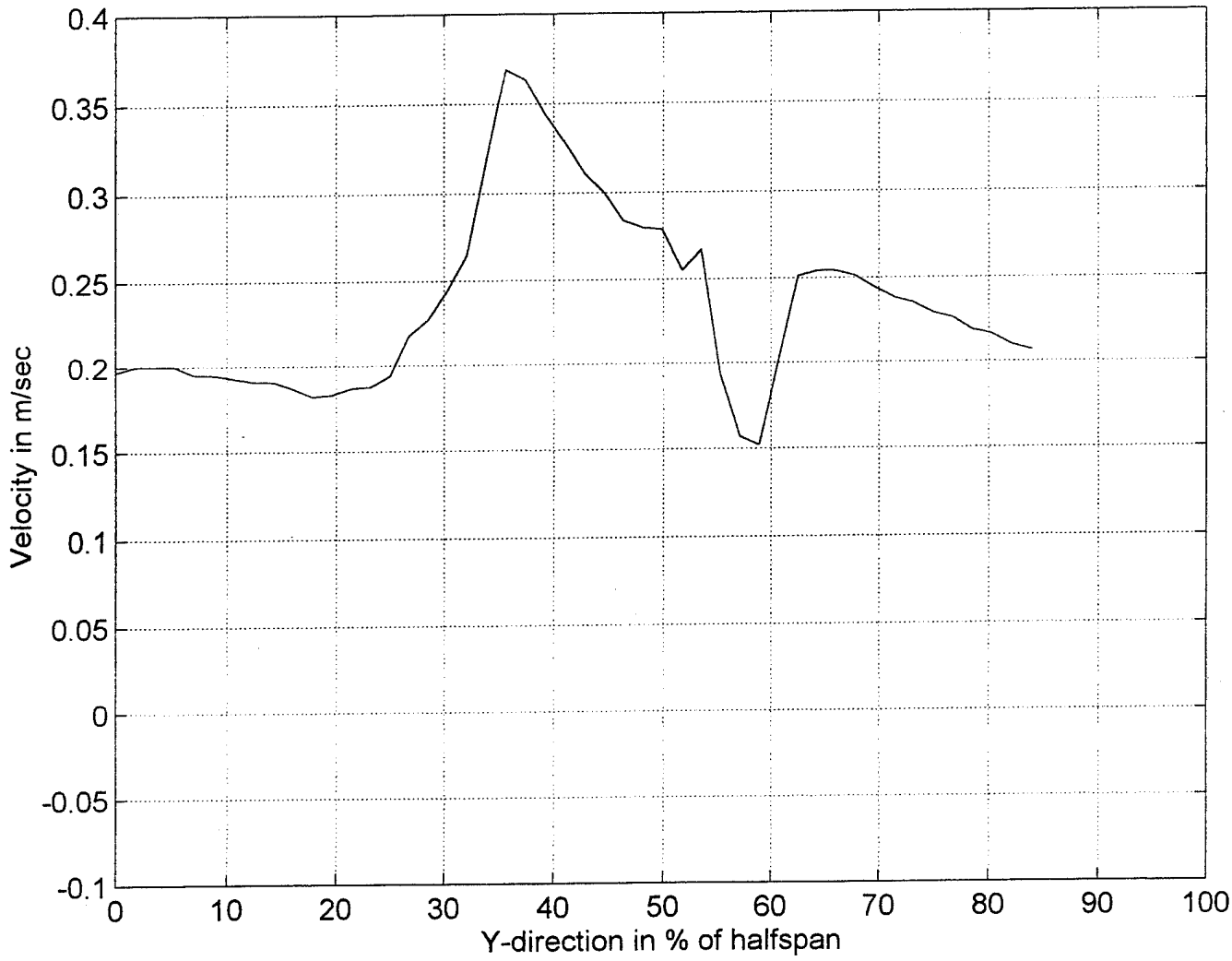

Fig.108:Velocity profile at x=38.62% , z=12.73 mm

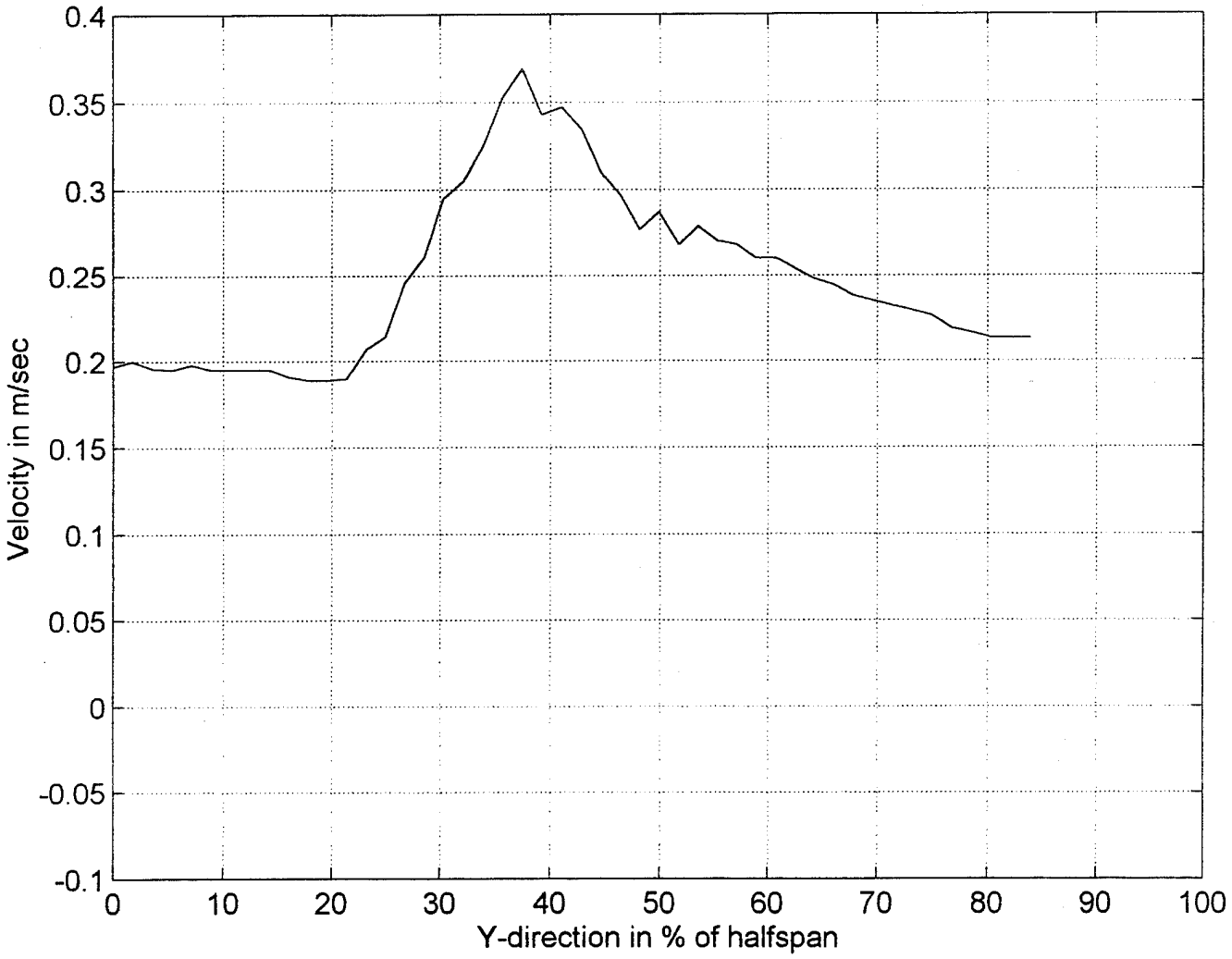

Fig.109:Velocity profile at x=38.62% , z=15.73 mm

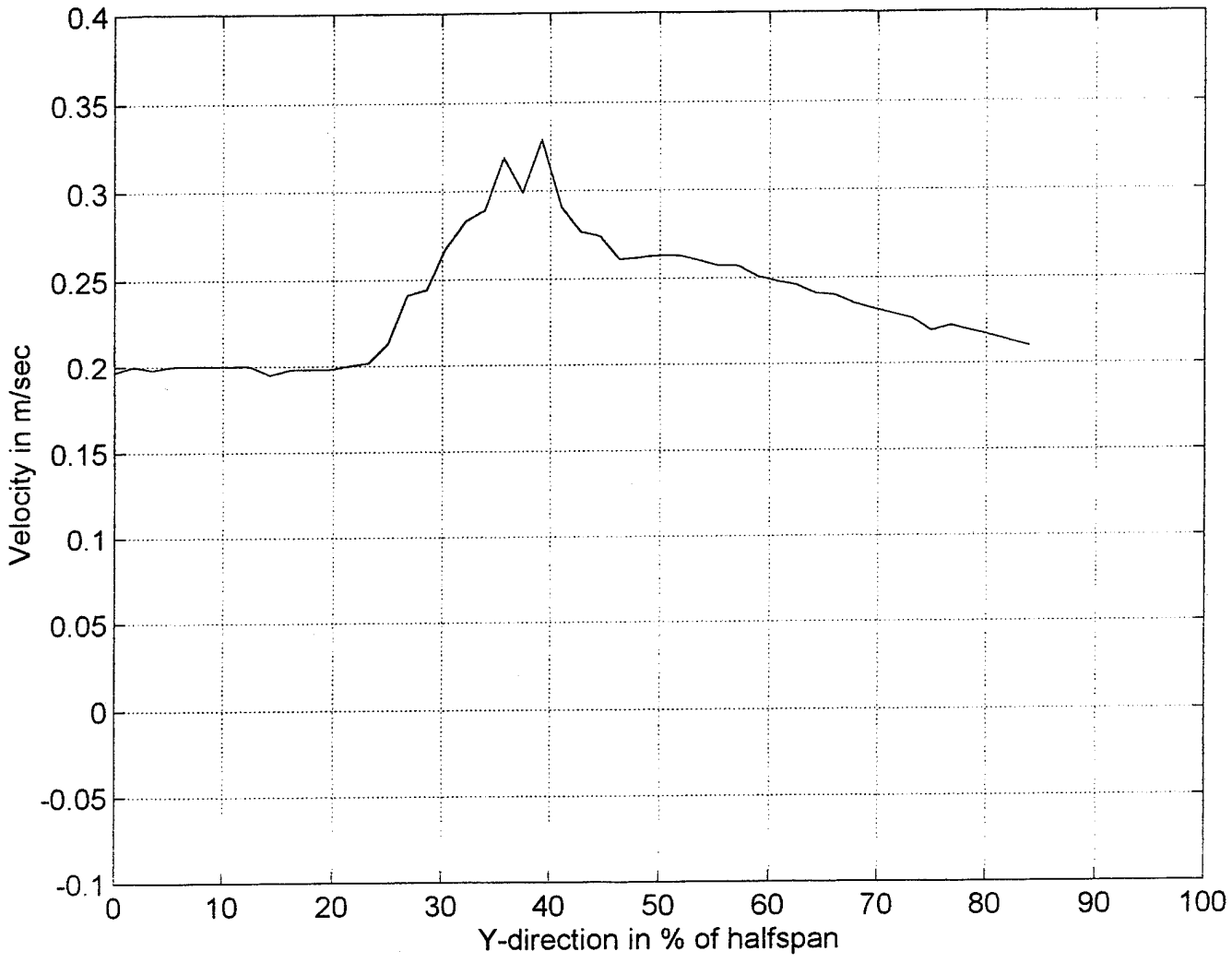

Fig.110:Velocity profile at x=38.62% , z=18.73 mm

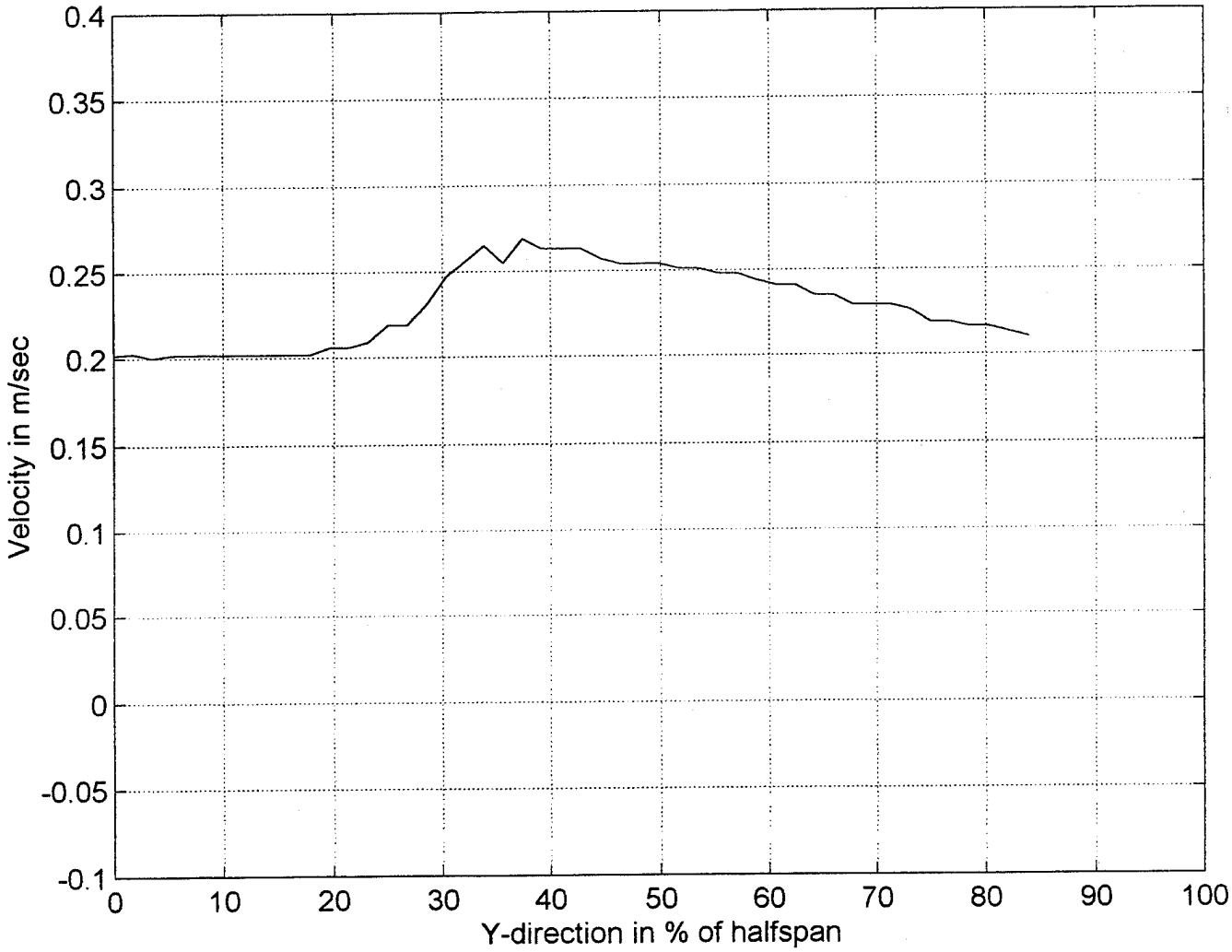

Fig.111:Velocity profile at x=38.62% , z=21.73 mm

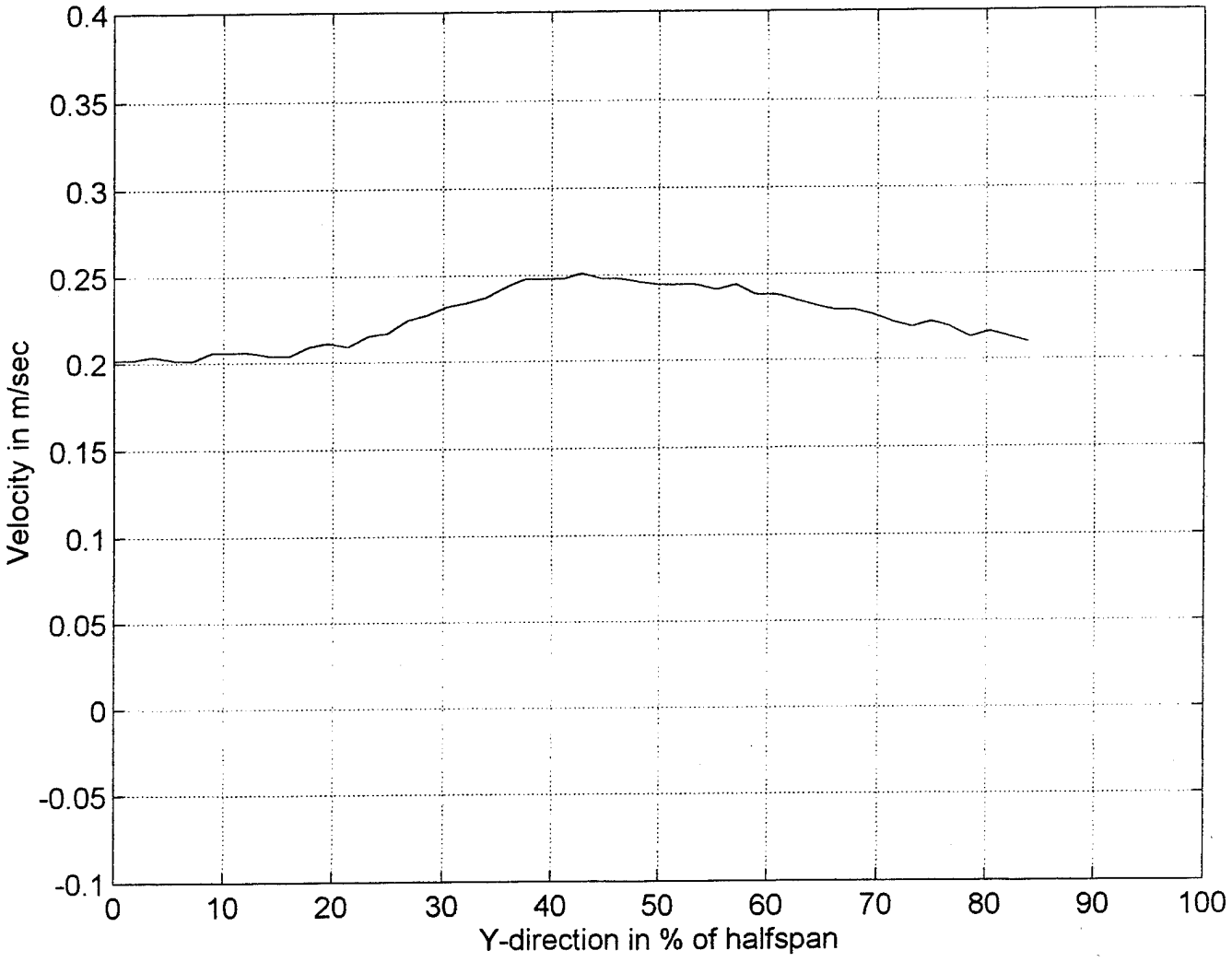

Fig.112:Velocity profile at x=38.62% , z=24.73 mm

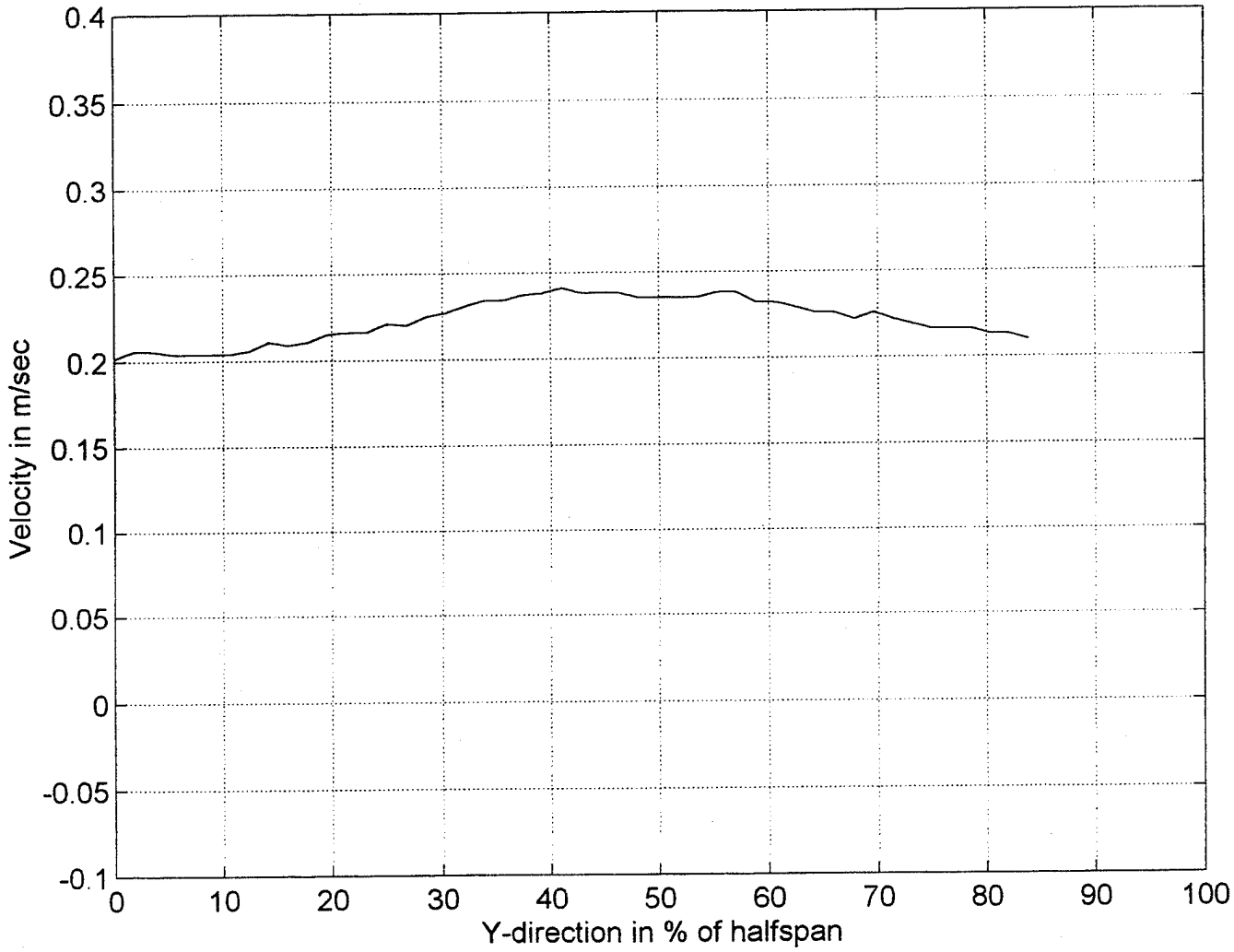

Fig.113:Velocity profile at x=38.62% , z=27.73 mm

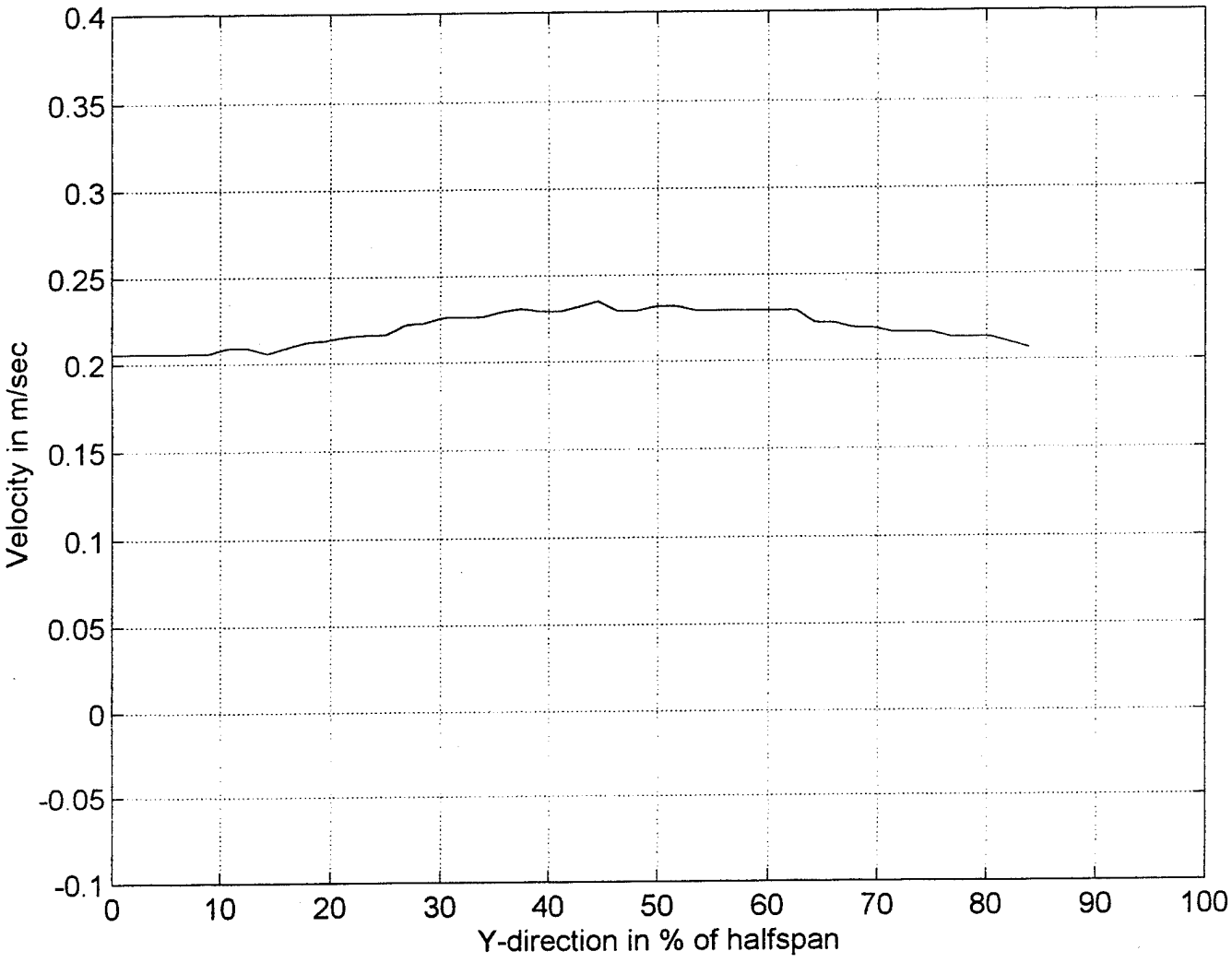

Fig.114:Velocity profile at x=38.62% , z=30.73 mm

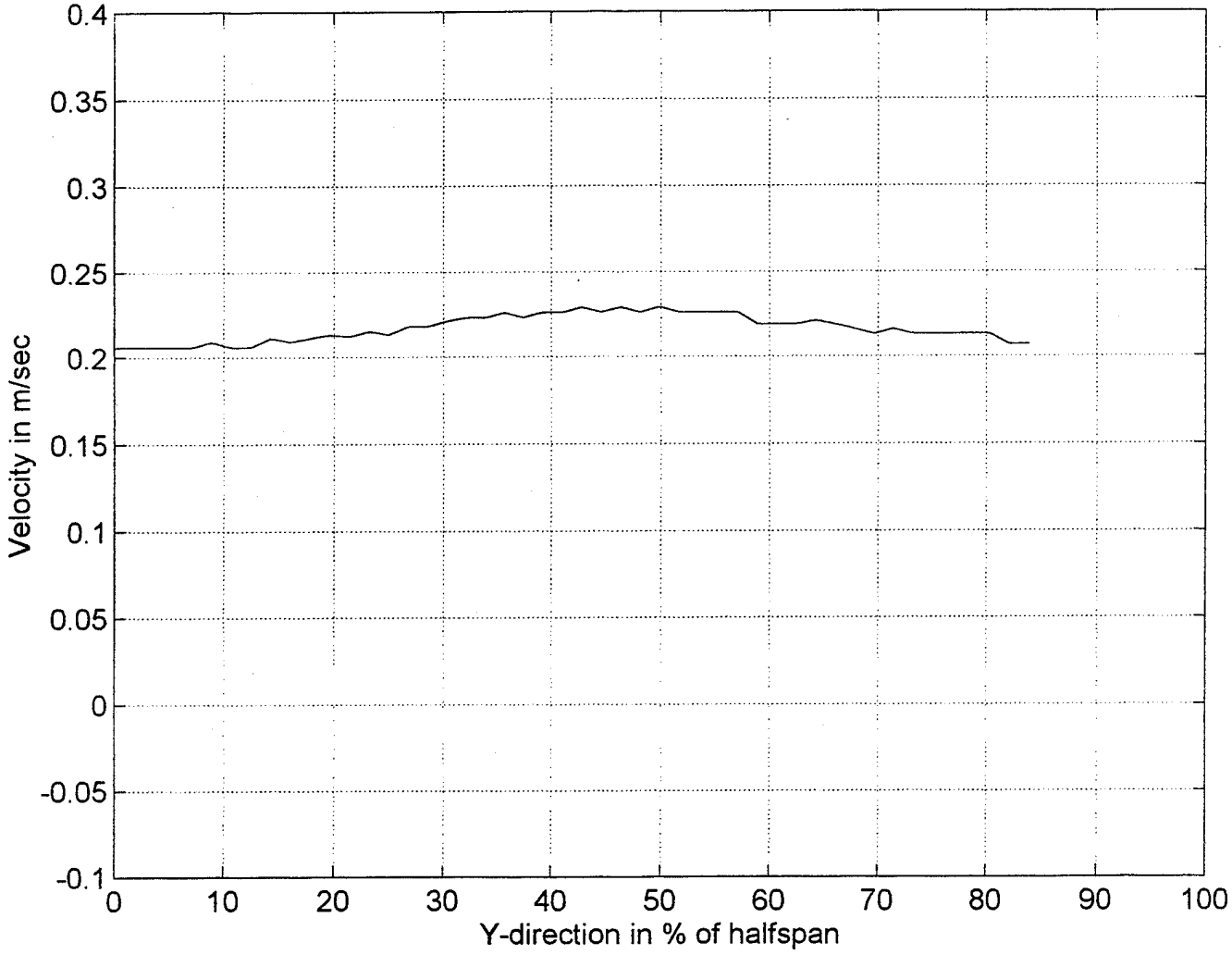

Figure 115:Model diagram showing areas with zero or reverse flow

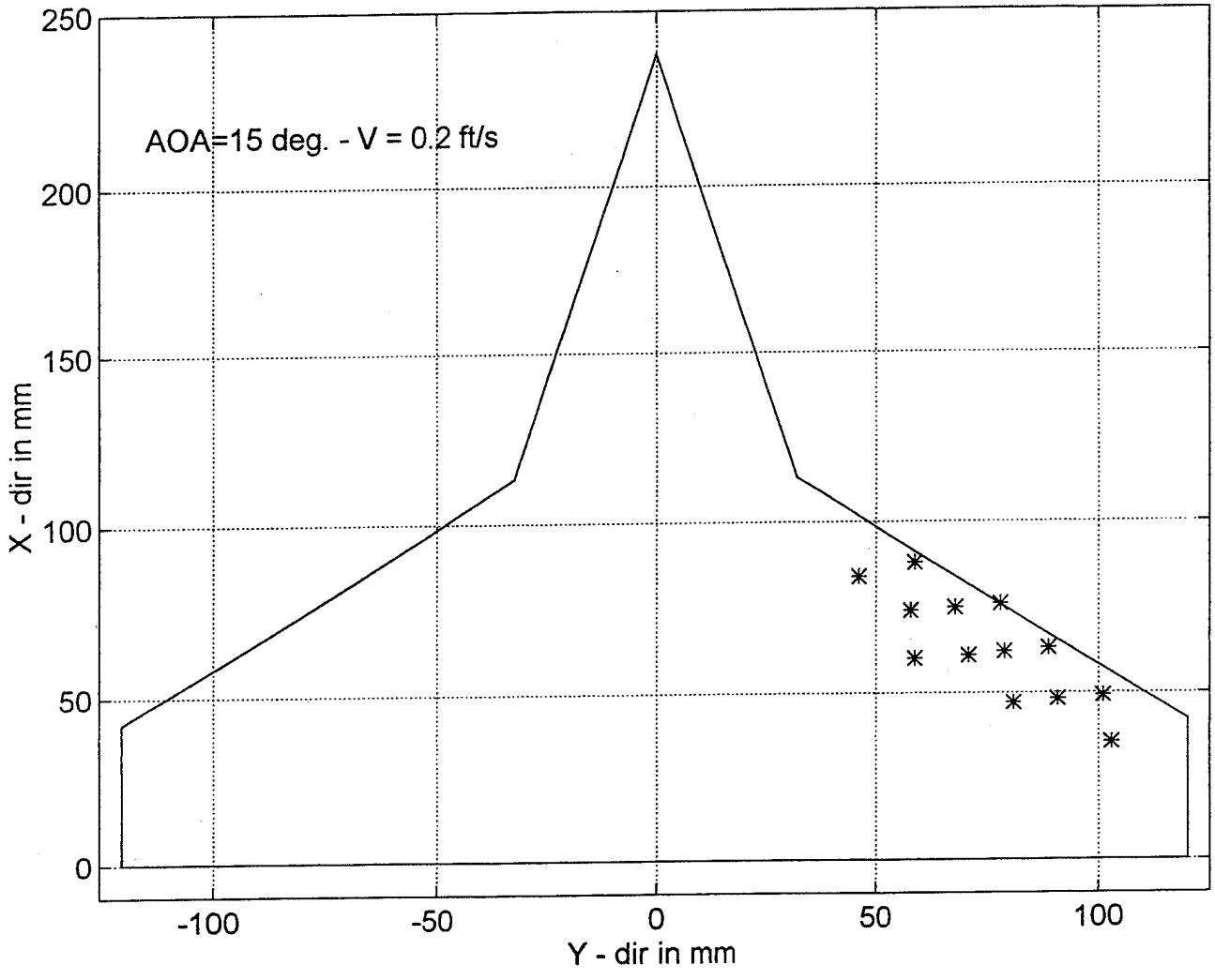

Figure 116:Model diagram showing areas with zero or reverse flow

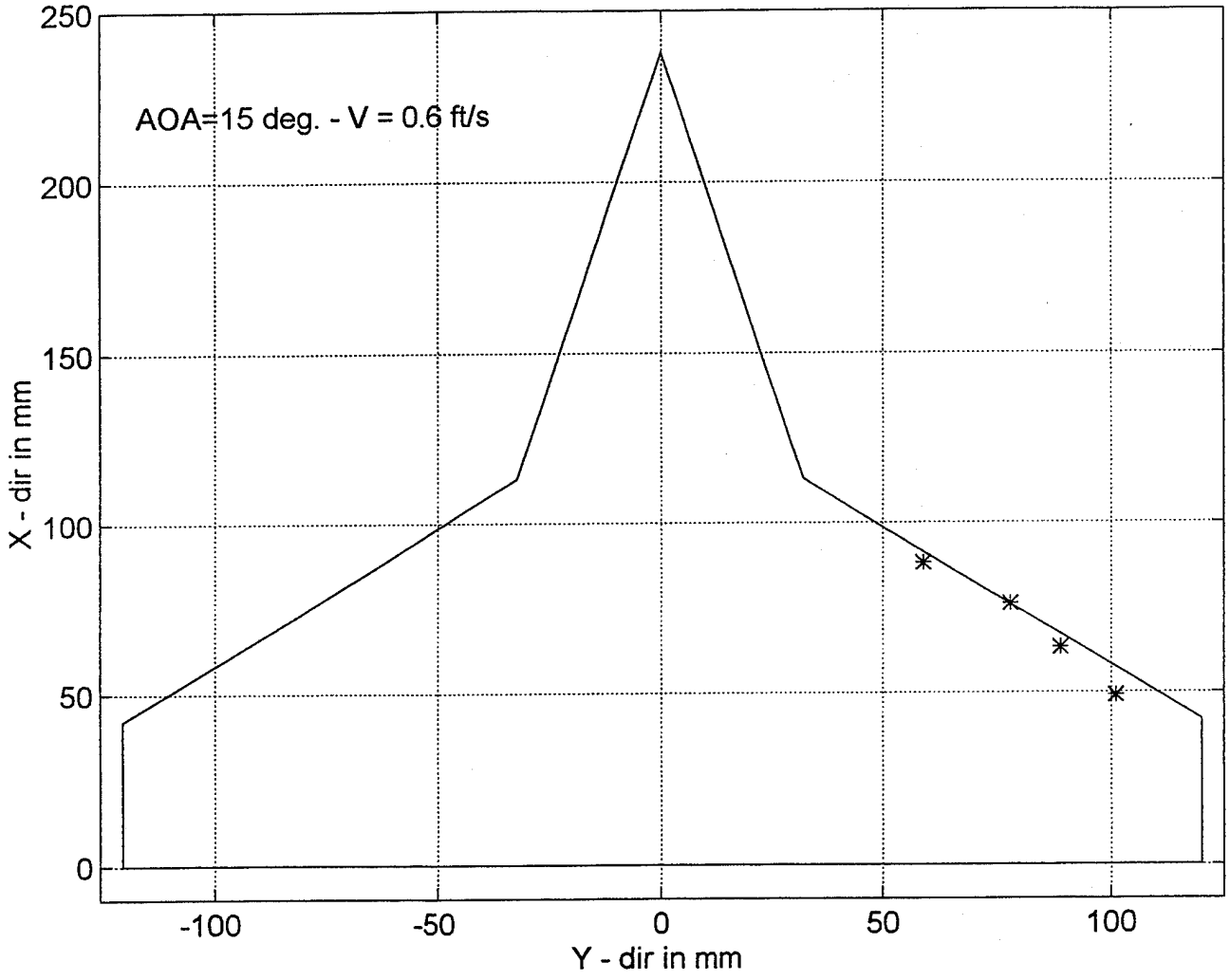

Figure 117:Model diagram showing areas with zero or reverse flow

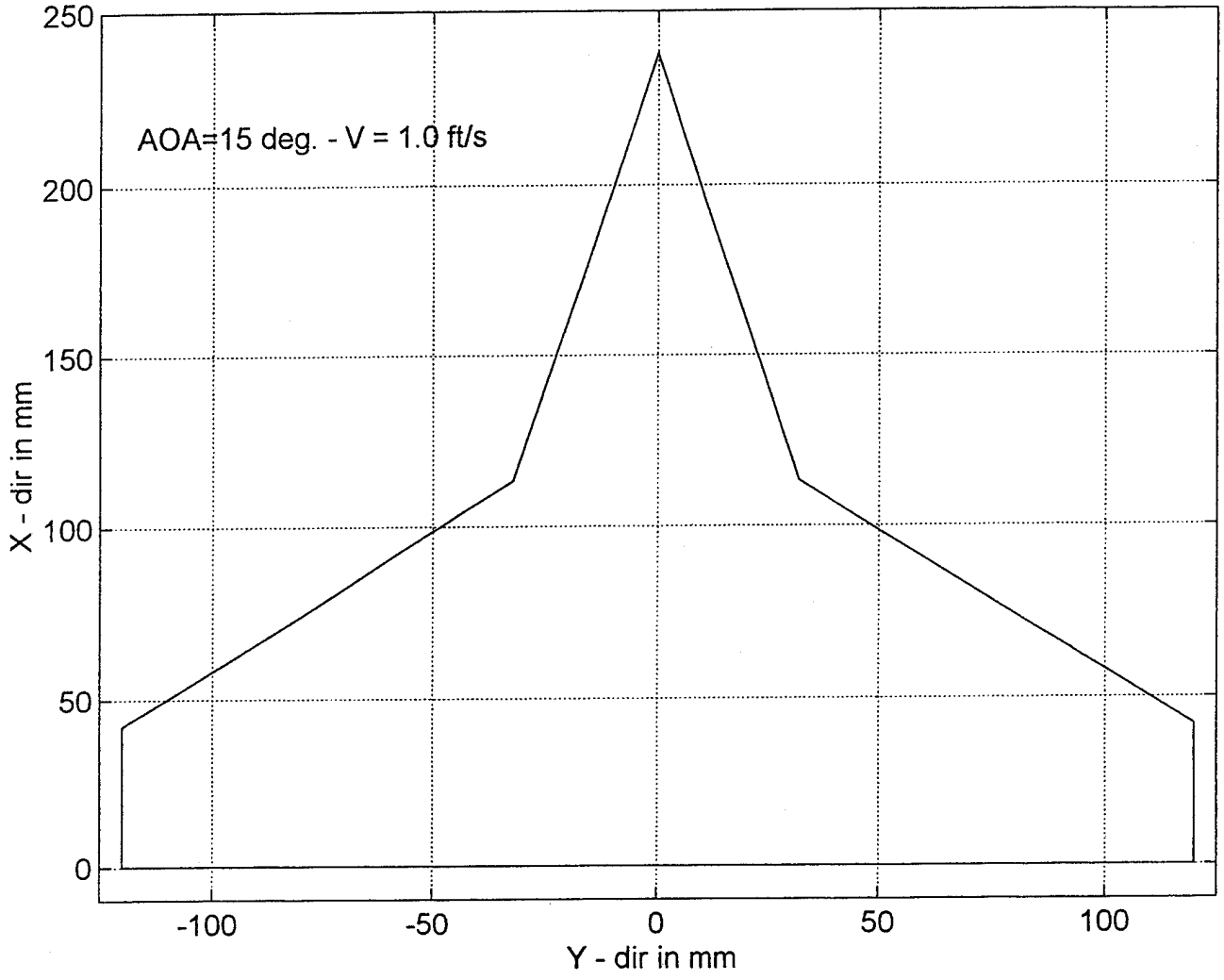

INITIAL DISTRIBUTION LIST

No. of copies

1. Defense Technical Information Center.....2
   8725 John J. Kingman Rd. STE 0944
   Ft. Belvoir, VA 22060 - 6218

2. Dudley Knox Library.....2
   Naval Postgraduate School
   411 Dyer Rd.
   Monterey, CA 93943-5101

3. Professor M.F. Platzer, Code AA/P1.....10
   Naval Postgraduate School
   Monterey, CA 93943-5000

4. Professor S.K. Hebbar.....1
   295 Quebrada Del Mar Rd.
   Marina, CA 93933

5. Marvin Walters.....1
   Naval Air Warfare Center
   Aircraft Division
   Street Road
   Warminster, PA 18974-5000

6. S. Kern.....1
   Naval Air Warfare Center
   Aircraft Division
   Street Road
   Warminster, PA 18974-5000

7. Anastasios Fritzelas.....4
   Makrigianni 8
   Moschato, 18344
   Athens, Greece.